ZooKeys 1085: 1–9 (2022)
doi: 10.3897/zookeys.1085.77900
https://zookeys.pensoft.net

RESEARCH ARTICLE

A peer-reviewed open-access journal
ZooKeys
Launched to accelerate biodiversity research

The genus *Erhaia* (Gastropoda, Truncatelloidea, Amnicolidae), with a new species from Bhutan

Edmund Gittenberger[1,2], Choki Gyeltshen[3], Björn Stelbrink[4]

1 *Naturalis Biodiversity Center, P.O. Box 9517, NL-2300 RA Leiden, Netherlands* **2** *GiMaRIS, Rijksstraatweg 75, NL-2171AK Sassenheim, Netherlands* **3** *National Biodiversity Centre, Serbithang, Thimphu, Bhutan* **4** *Department of Animal Ecology & Systematics, Justus Liebig University Giessen, Heinrich-Buff-Ring 26 (IFZ), D-35392 Giessen, Germany*

Corresponding author: Edmund Gittenberger (egittenberger@yahoo.com)

Academic editor: Eike Neubert | Received 11 November 2021 | Accepted 13 January 2022 | Published 2 February 2022

http://zoobank.org/12FC8134-F5CA-4EA9-97D1-711DB7643E2C

Citation: Gittenberger E, Gyeltshen C, Stelbrink B (2022) The genus *Erhaia* (Gastropoda, Truncatelloidea, Amnicolidae), with a new species from Bhutan. ZooKeys 1085: 1–9. https://doi.org/10.3897/zookeys.1085.77900

Abstract

The distribution of the five *Erhaia* (Gastropoda, Truncatelloidea, Amnicolidae) species that are diagnosed by both morphological and molecular data is combined with several records of less completely diagnosed nominal *Erhaia* species. The resulting distribution pattern is summarized in a map and is discussed herein. *Erhaia norbui* **sp. nov.** is described from Bhutan on the basis of shell morphology and two mitochondrial DNA barcoding markers. A molecular phylogeny is presented for the five *Erhaia* species for which molecular data are available, three of which form a separate clade and are from Bhutan.

Keywords

16S, Bhutan, China, COI, *Erhaia*, India, Nepal, taxonomy

Introduction

The genus *Erhaia* Davis & Kuo, 1985 (Gastropoda, Truncatelloidea, Amnicolidae), as it is accepted in the literature at present (Gittenberger et al. 2020 and literature therein), is distributed over an area covering nearly 3.500 km from west to east, from

northern India and Nepal to eastern China. Comparable to its European counterpart *Bythinella* Moquin-Tandon, 1856 (Gastropoda, Truncatelloidea, Bythinellidae), which is known from an even larger area measuring nearly 4.000 km from west to east, from Spain to western Russia and Ukraine (Boeters 1998; Vinarski and Kantor 2016), it exemplifies a radiation, in which some species occur syntopically, that may have evolved in a non-adaptive fashion (see Gittenberger 1991; Wilke et al. 2010). However, the lack of data does not allow for a more fundamental discussion here.

Both *Erhaia* and *Bythinella* species occur in the clear waters of springs and brooklets. Despite their large ranges, suggesting relatively easy dispersal mechanisms, i.e., low barriers to gene flow, both genera show a high degree of allopatric speciation. This is illustrated by the occurrences in Bhutan, where four species, including the one described as new below, are known only from a single locality. At one locality, two of these species occur syntopically. Three *Erhaia* species are reported from the Latipur and Kavre districts in the province of Bagmati in Nepal (Nesemann et al. 2007); two of them are known from one locality only, where they occur together with the third species, which has been reported from four additional localities, thus from six in total. A taxonomic revision is needed to clarify whether the Chinese species have similar small ranges and syntopic occurrences.

The shells of species in these two genera are more or less slender ovoid and less than 5 mm high. They show a conspicuous transition in height-width ratio from protoconch to teleoconch. The protoconch shell is valvatiform, as for example in fully grown freshwater snails of the species *Valvata cristata* O.F. Müller, 1774 (Gastropoda, Valvatoidea, Valvatidae) (Glöer 2019: 196, fig. 244), whereas the teleoconch is not, therefore the shells have an obliquely flattened apical part. The adaptive significance of this, if any, is unknown. Fully grown valvatiform or planispiral shells occur in several species of minute spring snails (e.g. Hershler and Longley 1986; Beran et al. 2014). Apart from their general shape, shells of *Erhaia* vary more than those of *Bythinella* and may have character states that do not occur in that genus, viz. a spiral microsculpture and one or more lamellae inside the shell.

Material and methods

Using the literature, we compiled distributional records for 22 nominal species (and a single undetermined individual from China) that are currently classified more or less convincingly in *Erhaia* (Fig. 1). Many of these taxa were originally classified in *Bythinella* or *Pseudobythinella* Liu & Zhang, 1979 (Gastropoda, Truncatelloidea, Bythinellidae) (not *Pseudobythinella* Melville, 1956). A taxonomic revision, which is beyond the scope of the present study and is also currently not possible given the lack of molecular data for many species, may indicate that some nominal taxa are synonyms. The original descriptions of all taxa mentioned here are included in the References. Following Davis et al. (1985) and Davis and Rao (1997), we excluded so-called *Bythinella* taxa described from Japan. Coordinates for each species were obtained from the source publication or were estimated based on the locality information provided therein (Table 1). Distribution maps were generated using QGIS 3.10.5 (QGIS Development Team 2000).

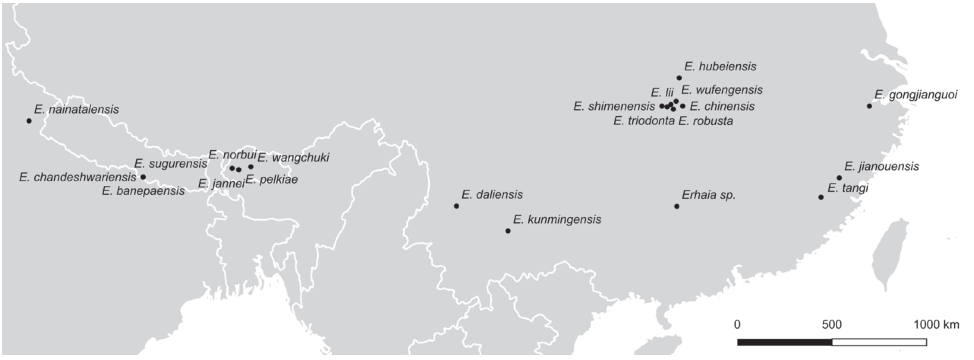

Figure 1. Distribution of *Erhaia* species across Asia.

Table 1. Distribution of *Erhaia* species with coordinates (sorted from west to east) either provided by the source publication or estimated based on the locality information therein.

Species	Coordinates
Bhutan	
E. norbui spec. nov.	27°22'33.0"N, 89°17'15.0"E
E. jannei Gittenberger & Stelbrink in Gittenberger et al., 2020	27°18'43.0"N, 89°36'10.0"E
E. pelkiae Gittenberger & Gyeltshen in Gittenberger et al., 2020	27°18'43.0"N, 89°36'10.0"E
E. wangchuki Gittenberger, Sherub & Stelbrink, 2017	27°26'17.6"N, 90°11'18.9"E
Elsewhere	
E. nainatalensis Davis & Rao, 1997	29°23'00.0"N, 79°30'00.0"E
E. banepaensis Nesemann & S. Sharma in Nesemann et al., 2007	27°00'00.0"N, 85°00'00.0"E
E. chandeshwariensis Nesemann & S. Sharma in Nesemann et al., 2007	27°00'00.0"N, 85°00'00.0"E
E. sugurensis Nesemann, Shah & Tachamo in Nesemann et al., 2007	27°00'00.0"N, 85°00'00.0"E
E. daliensis Davis & Kuo in Davis et al., 1985	25°45'00.0"N, 100°06'00.0"E
E. kunmingensis Davis & Kuo in Davis et al., 1985	24°40'00.0"N, 102°35'00.0"E
E. lii (Kang, 1985) [also in Kang, 1986]	30°00'00.0"N, 110°00'00.0"E
E. shimenensis (Liu, Zhang & Chen, 1982)	30°00'00.0"N, 110°00'00.0"E
E. triodonta (Liu, Wang & Zhang, 1991)	29°58'00.0"N, 110°15'00.0"E
E. wantanensis (Kang, 1983a)	30°04'00.0"N, 110°26'00.0"E
E. robusta (Kang, 1986)	29°52'18.8"N, 110°32'54.5"E
E. wufungensis (Kang, 1983a)	30°12'00.0"N, 110°41'00.0"E
Erhaia sp. [Liu et al. 2014: Table 5]	25°44'16.0"N, 110°43'07.0"E
E. hubeiensis (Liu, Zhang & Wang, 1983)	31°10'00.0"N, 110°50'00.0"E
E. chinensis (Liu & Zhang, 1979)	30°00'00.0"N, 111°00'00.0"E
E. liui (Kang, 1985)	30°00'00.0"N, 111°00'00.0"E
E. tangi (Cheng, Wu, Li & Lin, 2007)	26°08'00.0"N, 117°40'00.0"E
E. jianouensis (Liu & Zhang, 1979)	26°58'00.0"N, 118°33'00.0"E
E. gongjianguoi (Kang, 1983b)	30°00'00.0"N, 120°00'00.0"E

In a spring area in Bhutan (Fig. 2), several specimens of a minute snail species were discovered and collected by Sangay Norbu. Based on this material, *Erhaia norbui* sp. nov. is described here. Photographs of the holotype (Fig. 3) were made using a Wild MS-26 binocular camera set-up. Shells of two paratypes (Figs 4, 5), which were used for a molecular analysis and thus could not be saved, were photographed with a

Keyence VHX-2000 digital microscope system (Keyence Corp., Itasca, IL, USA). Additional paratypes were kept as dry shells.

The DNA lab work and phylogenetic analyses were identical to those described in Gittenberger et al. (2020). For the phylogenetic analyses, a reduced dataset including both mitochondrial markers, COI and 16S rRNA, was used. Uncorrected genetic p-distances for COI and 16S rRNA between the species from Bhutan were calculated using MEGA X 10.1.7 (Kumar et al. 2018).

The following abbreviations are used: B = shell breadth; H = shell height; NBCB = National Biodiversity Centre, Serbithang, Thimphu, Bhutan; RMNH = National Biodiversity Center Naturalis, Leiden, The Netherlands.

Systematics

Superfamily Truncatelloidea Gray, 1840
Family Amnicolidae Tryon, 1863

Genus *Erhaia* Davis & Kuo in Davis et al., 1985

Type species by original designation. *Erhaia daliensis* Davis & Kuo in Davis et al., 1985.

Synonym. *Pseudobythinella* Liu & Zhang, 1979. Not Melville, 1956. Type species by original designation: *Pseudobythinella jianouensis* Liu & Zhang, 1979.

Description. Shell ovoid to elongate ovoid or conical, smooth or with spiral microsculpture on the proto- and/or teleoconch. Apex conspicuously and more or less obliquely flattened. Aperture varying from ovoid-elliptical to circular; its palatal side curved and gradually passing into the basal side. Peristome continuous, attached at the parietal side or more or less protruding. Umbilicus minute or closed. Parietal part of the aperture smooth or with a lamella; columella smooth or with 2 spiral lamellae.

Notes. Molecular data, which are available for only a limited number of the amnicolid species, are inconclusive regarding the status of *Erhaia* versus *Akiyoshia* Kuroda & Habe, 1954 Gastropoda, Truncatelloidea, Amnicolidae) (see also the more comprehensive phylogenetic reconstruction in Gittenberger et al. 2020). No DNA data are known for the type species of these nominal taxa, i.e., *E. daliensis* Davis & Kuo, 1985 and *A. uenoi* Kuroda & Habe, 1954. Furthermore, the species that are generally called *Erhaia jianouensis* (Liu & Zhang, 1979) and *Akiyoshia kobayashii* Kuroda & Habe, 1958 are sister species (Fig. 7) that should be congeneric by definition. At present, their ranges in China and Japan, respectively, have been decisive for the generic classification. Pending additional data that can help solve this problem convincingly, we opted to still use the current, contradictory nomenclature (see also notes under *E. norbui* sp. nov.).

Distribution. The genus *Erhaia* was initially reported from a wide range in southern China, where it has been recorded with various species from the provinces of

Yunnan, Sichuan, Guangxi, Hubei, Hunan, and Fujian (Davis et al. 1985; Davis and Kang 1995; Davis and Rao 1997; Wilke et al. 2000, 2001; Liu et al. 2014). Regarding its occurrence in Japan, see foregoing notes. One species was described from northern India (Davis and Rao 1997), three additional species were described from Nepal (Nesemann et al. 2007), and, most recently, three species were described from Bhutan (Gittenberger et al. 2017, 2020). Here, we describe a fourth species from Bhutan and present, for the first time, a map of all known records of the genus (see Fig. 1 and Table 1). As usual, it is unknown where snails may have been looked for in vain and thus our distribution maps (Figs 1, 6) may represent human sampling activity rather than the real range of *Erhaia*. Contrary to Gittenberger et al. (2020), in the absence of DNA data, we refer to *E. chandeshwariensis* Nesemann & S. Sharma, 2007 as a species closely related to *E. nainatalensis* Davis & Rao, 1997. The shells cannot be distinguished, but the type localities are over 600 km apart, which makes conspecificity unlikely in *Erhaia*. Remarkable facts are the allopatric distribution and diversification in this genus in general, the syntopic occurrence of *E. jannei* Gittenberger & Stelbrink, 2020 and *E. pelkiae* Gittenberger & Gyeltshen, 2020 in Bhutan (Fig. 6), and that of *E. banepaensis* Nesemann & S. Sharma, 2007 with either *E. chandeshwariensis* or *E. sugurensis* Nesemann, Shah & Tachamo, 2007 in Nepal (Fig. 5).

***Erhaia norbui* sp. nov.**
http://zoobank.org/07BF6064-F69D-44FB-BFBA-34E849962BAF
Figs 2–6

Material examined. ***Holotype.*** (Fig. 4) Bhutan • District Haa, Uesu, Naychu, ca. 2700 m a.s.l.; 27°22'33"N 89°17'15"E; Sangay Norbu leg. 2020 (NBCB 1239).

Paratypes. (Figs 5–6) 3 shells (NBCB 1240), 2 shells (RMNH.MOL.511432).

Figure 2. Habitat of *E. norbui* sp. nov. at the type locality. Photo by Mr. Sangay Norbu.

Figures 3–5. *Erhaia norbui* sp. nov. from the type locality, district Haa, Uesu, Naychu, ca. 2700 m a.s.l. **3** holotype, NBCB 1239 (H = 2.3 mm) and paratypes used for DNA analyses (**4** UGSB 25956, H = 1.5 mm **5** UGSB 25957, H = 1.8 mm). Scale bar: 1 mm.

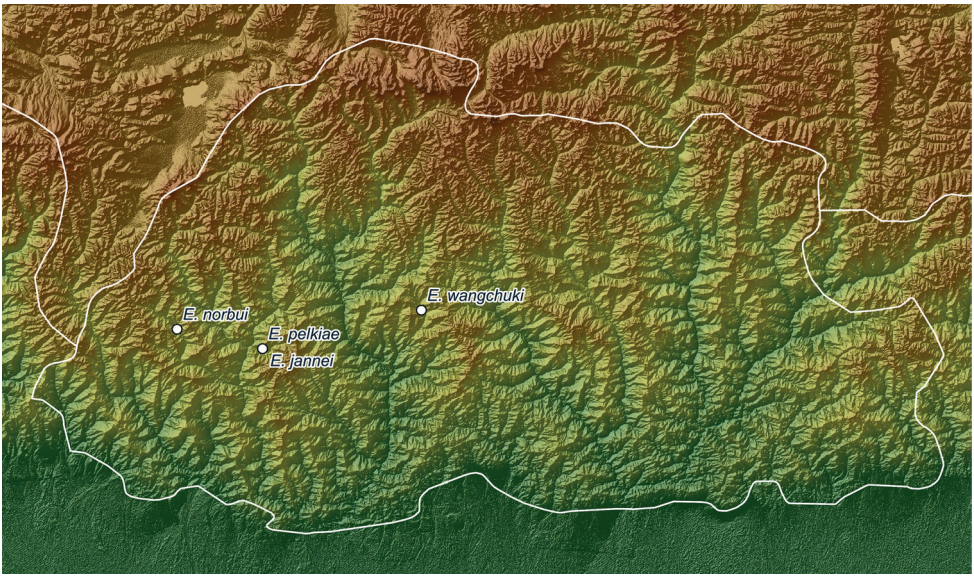

Figure 6. Distribution of *Erhaia* species described for Bhutan. Note that *E. jannei* and *E. pelkiae* were found to occur syntopically.

Diagnosis. Shell pale greyish, large for the genus (H > 2 mm), with a globular body whorl and a roundish aperture.

Description. Shell obliquely ovoid, with 3½–3¾ regularly convex whorls that are separated by a deep suture; clearly higher than broad; pale greyish with fine irregular growth lines and some blackish-brown periostracal ridges, one of which runs from the apertural columellar border into the umbilicus. Aperture nearly circular in fully grown specimens, with a continuous, free peristome that is thickened, not reflected; with a minute umbilicus. Protoconch encrusted in all specimens; teleoconch without spiral sculpture.

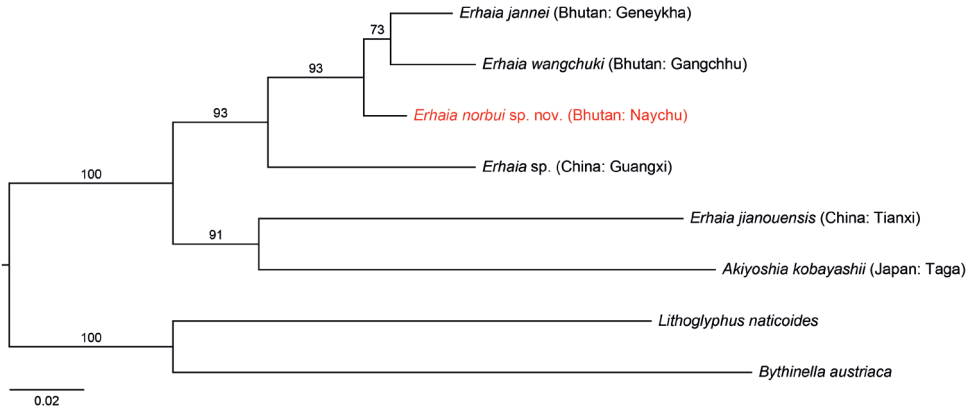

Figure 7. Maximum likelihood tree reconstructed with RAxML BlackBox (Stamatakis et al. 2008; GTR+G substitution model for each partition and 100 bootstrap replicates) based on the COI and 16S rRNA dataset of Liu et al. (2014) and Guan et al. (2008), with new data in red. Numbers on branches denote bootstrap values > 50.

Measurements of shells with thickened apertural border (n = 6): H 2.3–2.6 mm, B 1.6–1.8 mm. Holotype 2.3×1.7 mm.

Shells of *E. jannei*, which are most similar in shape, are yellowish-brown and a little narrower, with the aperture slightly compressed laterally. The other Bhutanese *Erhaia* species known, i.e., *Erhaia pelkiae* and *E. wangchucki* Gittenberger, Sherub & Stelbrink, 2017, are smaller, i.e. H < 2 mm and H < 2.2 mm, respectively; their shells are less pale, of an elongated ovoid shape and with an elliptical aperture in *E. pelkiae*, or conical shape with a piriform aperture in *E. wangchucki*.

Ecology (Fig. 2). The species was found in spring water among abundant watercress. The annual temperature of the water is 9–12 °C, with pH of 7–8.5 and 6.5 mg/l oxygen.

Molecular data (Fig. 7). Both of the individuals (paratypes) that we analyzed genetically shared an identical haplotype for both COI (GenBank acc. no.: OM135616) and 16S rRNA (GenBank acc. no.: OM135244). The uncorrected genetic p-distances between *E. norbui* sp. nov. vs. *E. jannei* and *E. wangchuki* were 3.97% and 5.19%, respectively, for COI, and 1.42% and 1.22%, respectively, for 16S rRNA.

Notes. The three *Erhaia* species from Bhutan form a highly supported clade, with *Erhaia* sp. from China as the sister-group. Interestingly, the species called *E. jianouensis*, from China, and *Akiyoshia kobayashii*, from Japan, form the highly supported sister-group of the remaining *Erhaia* species (see foregoing notes for *Erhaia*). For additional notes regarding the truncatelloidean gastropods of N. India, Nepal, Bhutan, and S. China, in particular the species of *Erhaia*, see also Gittenberger et al. (2020).

Etymology. The epithet *norbui* refers to Mr. Sangay Norbu, who discovered this species.

Acknowledgements

We would like to thank Dr Tashi Y. Dorji, Program Director of the NBC, and Ms Sangay Dema (NBC) for their support and guidance during this project. We are particularly grateful to Mr Sangay Norbu (Manager/Livestock Production Officer, Bhutan Livestock development Corporation, Haa, Bhutan), who discovered and collected the species described here as *E. norbui* sp. nov. We also thank both Jonathan Ablett, The Natural History Museum, London, UK, and Bernhard Hausdorf, Leibniz Institute for the Analysis of Biodiversity Change, Hamburg, Germany, for constructive remarks, and the staff members of the Library of Naturalis Biodiversity Center (Leiden) for their bibliographic assistance.

References

Boeters HD (1998) Mollusca: Gastropoda: Rissooidea. Süsswasserfauna von Mitteleuropa 5 (1–2): i–ix, 1–76.

Cheng Y-Z, Wu X-P, Li L-S, Lin C-X (2007) A new species of *Pseudobythinella* (Mesogastropoda, Pomatiopsidae) from China. Acta Zootaxonomica Sinica 32(4): 896–899.

Davis GM, Kang ZB (1995) Advances in the Systematics of *Erhaia* (Gastropoda: Pomatiopsidae) from the People's Republic of China. Proceedings of the Academy of Natural Sciences of Philadelphia 146: 391–427. http://www.jstor.org/stable/4065020

Davis GM, Rao S (1997) Discovery of *Erhaia* (Gastropoda: Pomatiopsidae) in northern India with description of a new genus of Erhaiini from China. Proceedings of the Academy of Natural Sciences of Philadelphia 148: 273–299. http://www.jstor.org/stable/4065055

Davis GM, Kuo Y-H, Hoagland KE, Chen P-L, Yang H-M, Chen D-J (1985) *Erhaia*, a new genus and new species of Pomatiopsidae from China (Gastropoda: Rissoacea). Proceedings of the Academy of Natural Sciences of Philadelphia 137: 48–78. http://www.jstor.org/stable/4064860

Gittenberger E (1991) What about non-adaptive radiation? Biological Journal of the Linnean Society 43: 263–272. https://doi.org/10.1111/j.1095-8312.1991.tb00598.x

Gittenberger E, Sherub S, Stelbrink B (2017) *Erhaia* Davis & Kuo (Gastropoda, Rissooidea, Amnicolidae) also in Bhutan. ZooKeys 679: 21–28. https://doi.org/10.3897/zookeys.679.13326

Gittenberger E, Leda P, Wangchuck J, Gyeltshen C, Stelbrink B (2020) The genera *Erhaia* and *Tricula* (Gastropoda, Rissooidea, Amnicolidae and Pomatiopsidae) in Bhutan and elsewhere in the eastern Himalaya. ZooKeys 929: 1–17. https://doi.org/10.3897/zookeys.929.49987

Glöer P (2019) The freshwater gastropods of the West-Palaearctis. Volume I. Fresh- and brackish waters except spring and subterranean snails. Identification key, anatomy, ecology, distribution. Published by the author, Hetlingen, Germany, 399 pp.

Hershler R, Longley G (1986) Phreatic hydrobiids (Gastropoda: Prosobranchia) from the Edwards (Balcones fault zone) Aquifer region, south-central Texas. Malacologia 27(1): 127–172.

Kang Z-B (1983a) A new genus and three new species of the family Hydrobiidae (Gastropoda: Prosobranchia) from Hubei province, China. Oceanologia et Limnologia Sinica 14(5): 499–505. [In Chinese and English]

Kang Z-B (1983b) Two new molluscan hosts for *Paragonimus skrjabini*. Oceanologia et Limnologia Sinica 14(6): 536–541. [In Chinese and English]

Kang Z-B (1985) Description of a new species of *Bythinella* from China. Acta Hydrobiologica Sinica 9(1): 84–88. [In Chinese and English]

Kang Z-B (1986) Descriptions of eight new minute freshwater snails and a new and rare species of land snail from China. Archiv für Molluskenkunde 117(1–3): 73–91.

Kumar S, Stecher G, Li M, Knyaz C, Tamura K (2018) MEGA X: Molecular Evolutionary Genetics Analysis across computing platforms. Molecular Biology and Evolution 35(6): 1547–1549. https://doi.org/10.1093/molbev/msy096

Liu L, Huo G-N, He H-B, Zhou B, Attwood SW (2014) A phylogeny for the pomatiopsidae (Gastropoda: Rissooidea): a resource for taxonomic, parasitological and biodiversity studies. BMC Evolutionary Biology 14: e29. https://doi.org/10.1186/1471-2148-14-29

Liu Y-Y, Zhang W-Z (1979) On new genus and species of freshwatersnails harbouring cercariae of lung flukes from China. Acta Zootaxonomica Sinica 4(2): 132–136.

Liu Y-Y, Wang Y-X, Zhang W-Z (1991) On the freshwater molluscs in the area of Sanxia Reservoir. Acta Zootaxonomica Sinica 16(1): 1–14.

Liu Y-Y, Zhang W-Z, Chen C-E (1982) *Pseudobythinella shimenensis*, sp. nov., a new aquatic *Paragonimus* cercariae carrying snail from Hunan province. Acta Zootaxonomica Sinica 7(3): 254–256.

Liu Y-Y, Zhang W-Z, Wang Y-X (1983) On three new freshwater snails from China. Acta Zootaxonomica Sinica 8(4): 366–369.

Nesemann H, Sharma S, Sharma G, Khanal SN, Pradhan B, Shah DN, Tachamo RD (2007) Class Gastropoda. In: Nesemann H, Sharma S, Sharma G, Khanal SN, Pradhan B, Shah DN, Tachamo RD (Eds) Aquatic invertebrates of the Ganga river system (Mollusca, Annelida, Crustacea, 57–102.

QGIS Development Team (2020) QGIS Geographic Information System. Open Source Geospatial Foundation Project. https://www.qgis.org/en/site

Vinarski MV, Kantor YI (2016) Analytical catalogue of fresh and brackish water molluscs of Russia and adjacent countries. A.N. Severtsov Institute of Ecology and Evolution of Russian Academy of Sciences, Moscow, 544 pp.

Wilke T, Davis GM, Gong X, Liu H-X (2000) *Erhaia* (Gastropoda: Rissooidea): phylogenetic relationships and the question of *Paragonimus* coevolution in Asia. The American Journal of Tropical Medicine and Hygiene 62: 453–459. https://doi.org/10.4269/ajtmh.2000.62.453

Wilke T, Benke M, Brändle M, Albrecht C, Bichain JM (2010) The neglected side of the coin: non-adaptive radiations in spring snails (*Bythinella* spp.). In: Glaubrecht M (Ed.) Evolution in action: 551–578. Springer, Berlin, Heidelberg. https://doi.org/10.1007/978-3-642-12425-9_25

Wilke T, Davis GM, Falniowski A, Giusti F, Bodon M, Szarowska M (2001) Molecular systematics of Hydrobiidae (Mollusca: Gastropoda: Rissooidea): testing monophyly and phylogenetic relationships. Proceedings of the Academy of Natural Sciences of Philadelphia 151: 1–21. https://doi.org/10.1635/0097-3157(2001)151[0001:MSOHMG]2.0.CO;2

ZooKeys 1085: 11–27 (2022)
doi: 10.3897/zookeys.1085.76484
https://zookeys.pensoft.net

RESEARCH ARTICLE

A peer-reviewed open-access journal
ZooKeys
Launched to accelerate biodiversity research

Xenos yangi sp. nov.: A new twisted-wing parasite species (Strepsiptera, Xenidae) from Gaoligong Mountains, Southwest China

Zhiwei Dong[1], Xingyue Liu[2], Chuyang Mao[1,3], Jinwu He[1], Xueyan Li[1]

1 *State Key Laboratory of Genetic Resources and Evolution, Kunming Institute of Zoology, Chinese Academy of Sciences, Kunming, Yunnan 650201, China* **2** *Department of Entomology, China Agricultural University, Beijing 100193, China* **3** *Kunming College of Life Science, University of Chinese Academy of Sciences, Kunming, Yunnan 650204, China*

Corresponding author: Xueyan Li (lixy@mail.kiz.ac.cn)

Academic editor: Hans Pohl | Received 14 October 2021 | Accepted 14 January 2022 | Published 2 February 2022

http://zoobank.org/F8153EFB-1CAD-457F-89B2-4D1804CE9A29

Citation: Dong Z, Liu X, Mao C, He J, Li X (2022) *Xenos yangi* sp. nov.: A new twisted-wing parasite species (Strepsiptera, Xenidae) from Gaoligong Mountains, Southwest China. ZooKeys 1085: 11–27. https://doi.org/10.3897/zookeys.1085.76484

Abstract

Here we report a new twisted-wing parasite species of the family Xenidae based on both morphological and molecular evidence. By using nearly complete mitogenomes, we confirmed the twisted-wing parasites on two wasps (*Vespa velutina* and *Vespa bicolor*) (China: Yunnan) as the same species, and associated its neotenic females and alate males. Combining the mitogenomic data (*COI*) and morphological traits, this species was identified to be a new species of the genus *Xenos*, namely *Xenos yangi* Dong, Liu & Li, **sp. nov.** Detailed descriptions and illustrations are provided for the new species.

Keywords

Mitogenome, morphology, new species, taxonomy, wasp endoparasite

Introduction

Strepsiptera are obligate endoparasites of silverfish, cockroaches, mantids, orthopterans, hemipterans, wasps, bees and flies, and they comprise about 630 species in 15 families (Kathirithamby 2018). Among 10 extant families, Xenidae Saunders, 1872 uses wasps as hosts and is the one of the species-rich strepsipteran families with ca 110 described

species in four genera (*Paragioxenos* Ogloblin, 1923; *Paraxenos* Saunders, 1872; *Pseudoxenos* Saunders, 1872; *Xenos* Rossius, 1793) (Pohl and Beutel 2008; Cook 2014; Benda et al. 2019). Benda et al. (2019, 2021) comfirmed the paraphyly of *Pseudoxenos* and polyphyly of the genera *Xenos* and *Paraxenos* using molecular data. The genus *Xenos* is one of the twisted-wing insects parasitic on eusocial wasps (Pohl and Beutel 2008; Kathirithamby 2018) and contains 41 species worldwide (Suppl. material 1: Table S1). About two-third (26 species) of *Xenos* species are distributed in the Americas, while the remaining 15 species are distributed in Africa (five species), Africa/Europe (one species) and Asia (nine species) (Buysson 1903; Kifune and Maeta 1985; Yang 1999; McMahon et al. 2009; Cook 2019; Cook et al. 2020; Kathirithamby 2021) (Suppl. material 1: Table S1). Among nine Asian species, five are recorded in China [*Xenos moutoni* (Buysson, 1903): Yunnan, Anhui, Taiwan; *X. circularis* Kifune & Maeta, 1985, *X. yamaneorum* Kifune & Maeta, 1985 and *X. formosanus* Kifune & Maeta, 1985: Taiwan; *X. dianshuiwengi* Yang, 1999: Fujian], two in Japan [*Xenos vespularum* Kifune & Maeta, 1975 and *Xenos oxyodontes* Nakase & Kato 2013], one in India [*Xenos hebraei* Kinzelbach, 1978] and one in Indonesia [*Xenos provesparum* Kifune, 1986] (Buysson 1903; Kifune and Maeta 1985; Yang 1999; Cook 2019). *Xenos vesparum* Rossius, 1793, which is the type species of both this genus and all strepsipteran insects (Rossius 1793), is a well-studied species with abundant data on its morphology and biology (Kifune and Maeta 1985; Manfredini et al. 2007; Nakase and Kato 2013; Richter et al. 2017).

In December 2019, some wasps (*Vespa velutina* Lepeletier, 1836 and *Vespa bicolor* Fabricius, 1787) were collected by local villagers in southern Gaoligong Mountains (Yunnan, China). We checked these wasp individuals and found some of them parasitized by twisted-wing parasites. We collected male adults (Figs 1–3), cephalotheca of male puparium (Fig. 4), and neotenic females (Fig. 4) of these twisted-wing parasites from the abdomen and nests of their wasp hosts (Fig. 5). We assembled the mitogenome of a neotenic female from a *V. velutina* nest using Next-generation technologies, and found that the mitogenome sequence is similar to that of *X. vesparum* in our previous work (Zhang et al. 2021). In this study, we further make a close morphological examination of males and neotenic females and cephalotheca of male puparium, and further assembled mitogenome of a male from a *V. velutina* nest and another neotenic female from a *V. bicolor* nest to compare them with that of the neotenic female from a *V. velutina* nest (Zhang et al. 2021). Our morphological and molecular results revealed that these adults of different sexes and different hosts are associated with the same species of *Xenos*, and is new to science.

Materials and methods

Specimens

The male and neotenic female specimens of the new species *Xenos yangi* Dong, Liu & Li, sp. nov. were collected from the nests of both *V. velutina* and *V. bicolor* in Gaoligong Mountains, Xiangda Township, Longling County, Yunnan Province in

December, 2019. The type materials of the new species described in this paper are deposited in the Insect Collection of Kunming Institute of Zoology, Chinese Academy of Sciences, Kunming, China (KIZ). Information on the other seven *Xenos* species (*X. oxyodontes*, *X. moutoni*, *X. vespularum*, *X. pecki*, *X. vesparum*, *X. ropalidiae*, *X. minor*) in the phylogenetic analysis was obtained from previous reports (Carapelli et al. 2006; McMahon et al. 2011; Nakase and Kato 2013; Jůzová et al. 2015; Benda et al. 2019, 2021). In detail, male and neotenic females of *X. oxyodontes* (*COI* GenBank accessions number: AB759562–AB759569; JN082805; MK431184; MN914546) were collected from Japan and Korea (McMahon et al. 2011; Nakase and Kato 2013; Benda et al. 2019, 2021); male pupa, males and neotenic females of *X. moutoni* (*COI* GenBank accessions number: AB759570–AB759582, MN914545, MK431183) were collected from China, Japan and Laos (Nakase and Kato 2013; Benda et al. 2019, 2021); two males of *X. vespularum* (*COI* GenBank accessions number: AB759583; MK431222) were collected from Japan (Nakase and Kato 2013; Benda et al. 2021); male and neotenic females of *X. pecki* (*COI* GenBank accessions number: MN914547–MN914549; MK431187) were collected from USA (Benda et al. 2019, 2021); male and neotenic females of *X. vesparum* (*COI* GenBank accessions number: DQ364229.1; KF803535.1; MN914557; JN082806; MN914561; MK431205) were collected from Italy, Czech Republic, Austria (Carapelli et al. 2006; Jůzová et al. 2015; Benda et al. 2019, 2021); two neotenic females of *X. ropalidiae* (*COI* GenBank accessions number: MK431185–MK431186) were collected from Laos and Nepal, and two males of *X. ropalidiae* (*COI* GenBank accessions number: MK431189-MK431190) were collected from Malaysia (Benda et al. 2019); and male and neotenic females of *X. minor* (*COI* GenBank accessions number: MN914559–MN914560; MN914569) were collected from Croatia (Benda et al. 2021).

Morphological description

Images of the living adults were taken using a Canon 70D camera in conjunction with a Canon EF 100 mm f/2.8L IS USM. The habitus images were taken using a stereomicroscope Nikon, SMZ18 equipped with NIS-Elements (Nikon, Japan). Scanning electron microscopes (SEM) images were taken using TM4000 II (Hitachi, Japan). The specimens used for SEM were directly fixed in 70% ethanol, and then dried at the room temperature. Morphological terminology follows those of Kinzelbach (1971), Kifune and Maeta (1985), Kathirithamby and Hughes (2006) and Koeth et al. (2012).

DNA extraction, library construction, sequencing, mitogenome assembling and sequence comparison

Total genomic DNA of one male collected from *V. velutina* nest and one neotenic female collected from *V. bicolo*r nest was extracted using a TIANamp Genomic DNA Kit (TIANGEN, China) based on manual instruction. Library construction, sequencing, mitogenome assembly follows those in our previous work (Zhang et al. 2021),

in which the mitogenome of one neotenic female collected from *V. velutina* was sequenced. We assembled the nearly complete mitogenomes of both male and neotenic female individuals, and compared them with that in our previous work (Zhang et al. 2021). Then the mitogenome sequences of the three individuals were compared in pairs using BLAST in NCBI website.

Phylogenetic analyses

COI is an useful molecular marker for species identification in many insects, including twisted-wing parasites (Nakase and Kato 2013; Jůzová et al. 2015; Benda et al. 2021, 2019). Here, we used the *COI* sequences from the nearly complete mitogenomes of one male and one neotenic female of *Xenos yangi* sp. nov. and another *Xenos* neotenic female individual in our previous work (Zhang et al. 2021) for the association between neotenic female and male adults.

Combined with 45 *COI* sequences of *Xenos* published by others (Carapelli et al. 2006; McMahon et al. 2011; Nakase and Kato 2013; Jůzová et al. 2015; Benda et al. 2021), phylogenetic analyses were performed using maximum likelihood (ML), and maximum parsimony (MP) methods with four strepsipteran species *Stylops ater* Reichert, 1914, *Melittostylops hesperapium* Kinzelbach, 1971, *Halictoxenos tumulorum* Perkins, 1918 and *Crawfordia warnckei* Kinzelbach, 1970 (Stylopidae) (GenBank Accession: GAZM00000000.2, MK431155, KF803415, MK431154) as outgroups (Misof et al. 2014; Jůzová et al. 2015; Benda et al. 2019). Briefly, *COI* sequences were first translated to amino acid sequences with the invertebrate mitochondrial genetic code, and then aligned by codons using the ClustalW algorithm in MEGA-X v10.1.8 (Sudhir et al. 2018). Next, MEGA-X was also used to find the best nucleotide substitution model ("GTR+I") and to reconstruct phylogenetic trees with the default parameters and 1000 bootstrap iterations.

Results

Sequences and phylogenetic analyses

We assembled nearly complete mitogenomes of one male adult collected from a *V. velutina* nest (15324 bp) (GenBank accession number: OK329871) and one neotenic female collected from a *V. bicolo*r nest (14670 bp) (GenBank accession number: OK32987). The mitogenomes of these two individuals in this study and one neotenic female in our previous work (Zhang et al. 2021) contain the same sequence except for the A+T-rich region and a gap between *trnaM* and *trnaI*, suggesting the nature of the same species for these three individuals with different sexes and different host. In this study, the mitogenome of male adult was annotated as 13 protein-coding genes (PCGs), 22 transfer RNA genes (tRNAs) and two ribosomal RNA genes (rRNAs) and an A+T-rich region, while only 36 mitogenomic genes (excl. *trnM*) were annotated in the incomplete mitogenome sequence of the neotenic female.

We further extracted a major fragment (1518 bp) of *COI* sequences from three Chinese *Xenos* individuals (one male and two neotenic females), and combined 45 *COI* sequences of identified species of *Xenos* reported by others to make the dataset for the phylogenetic analyses using ML and MP methods. All phylogenetic trees show that the three Chinese *Xenos* individuals (one male individual from the *V. velutina* nest and two female individuals from the *V. velutina* and *V. bicolo*r nests) cluster together with high bootstrap values (Fig. 6). The genetic divergence among three Chinese *Xenos* individuals varies from 0 to 0.014 (Table 2, Fig. 6), which is equal to that among *X. moutoni* individuals and less than that among *X. oxyodontes* individuals. Especially, one male and one neotenic female from the same host nests (*V. velutina*) showed no genetic divergence, suggesting their conspecific identity. These findings confirm that these male and neotenic female individuals collected from different host populations are the same species. This species can be differentiated from all the other Eurasian species of *Xenos* based on the genetic analyses and further morphological examination, and thus stands as a new species described below.

Taxonomy

Xenidae Saunders, 1872
***Xenos* Rossius, 1793**

***Xenos yangi* Dong, Liu & Li, sp. nov.**
http://zoobank.org/41C69672-2AD0-4E04-8C8B-F1F2352813A9
Chinese name 杨氏胡蜂蝙
Figs 1–5

Type locality. China, Yunnan, Longling County, Xiangda Township.

Type materials. ***Holotype*:** male (KIZ0130767), "Gaoligong Mountains, Xiangda Township, Longling County, Yunnan Province, 24.4441083 N, 98.7239194 E, 1666 m, 20.XII.2019, local villagers leg.", kept in 75% ethanol, [red label]. (KIZ). ***Paratypes*:** four males (KIZ0130768–KIZ0130771), three neotenic females (KIZ0130772–KIZ0130774), same data as holotype (KIZ), kept in 75% ethanol, [yellow label].

Other material examined. One neotenic female, "Gaoligong Mountains, Xiangda Township, Longling County, Yunnan Province, 20. XII. 2019, local villagers leg.", partially used for extracting genomic DNA (accession number MW222190; Zhang et al. 2021). One neotenic female and one male, "Gaoligong Mountains, Xiangda Township, Longling County, Yunnan Province, 20. XII. 2019, local villagers leg.", both partially used for extracting genomic DNA in this study.

Diagnosis. Male. Head transverse. Antenna (Fig. 2B) four-segmented, 1st with distal lateral extension and wider than 2nd, 3rd and 4th flabellate with subequal length. Palpus twice as long as maxilla (Fig. 2C). Mandible (Fig. 2D) slender, widened at base, tapering at tip. Prescutum pentagonal. Scutellum longitudinally elongated, triangular.

Proventrite posteromedially with a small U-shaped notch, forming a pair of small lobes (Fig. 2H). Mesoventrite posteromedially bifurcated into a pair of long digitiform projections (Fig. 2I). Tarsus four-segmented, without claws (Fig. 2E–G). Penis colter-shaped (Fig. 2J). **Cephalotheca of male puparium** (Fig. 4A). Maxillae almost oval, bigger than mandible. Clypeus furrowed and close to mandible. Antenna half size of eye. **Neotenic female** (Fig. 4B–D). Cephalothorax almost rectangular, 3/4 strongly contracted; birth opening, protuberance (Fig. 4C); apex of mandibles straight (Fig. 4D).

Description. Male (Fig. 1). ***Length*** 5.6 mm (holotype), 5.5–8.1 mm (paratypes) (combined length of head, pronotum and abdomen). ***Coloration*** (Fig. 1A, B): head, antenna, maxillary palpus, coxa, and abdomen black; femur, tibia and tarsus brown; hind wing semi-transparent. ***Head*** transverse, 1.44 mm in width. ***Compound eye*** raspberries-like, each composed of about 84 ommatidia, ommatidiaprominent and separated by chitinous bridges covered with micortrichia (Fig. 3A). ***Antenna*** four-segmented (Fig. 2B), scapus wider than pedicellus, scapus with distal lateral extension, pedicellus half as long as scapus, 3rd and 4th flabellate with subequal length, hirsute (Fig. 3B). ***Mandible*** (Fig. 2J) smooth, sword-like, gradually thicker from middle until 3/4, and then sharply tapering at tip. ***Maxillae and palpus*** (Figs 2C, 3B) covered with short hairs, palpus twice half as long as maxillae, palpus narrower. ***Pronotum*** (Fig. 1A) quadrangular with a protuberant apex. ***Acrotergit*** (Fig. 1A) with two ends turned up, central depression. ***Mesonotum*** (Fig. 1A) saddle-shaped, central M-shaped depression, pseudo-haltere on both sides. ***Prescutum*** (Fig. 1A) pentagonal with round

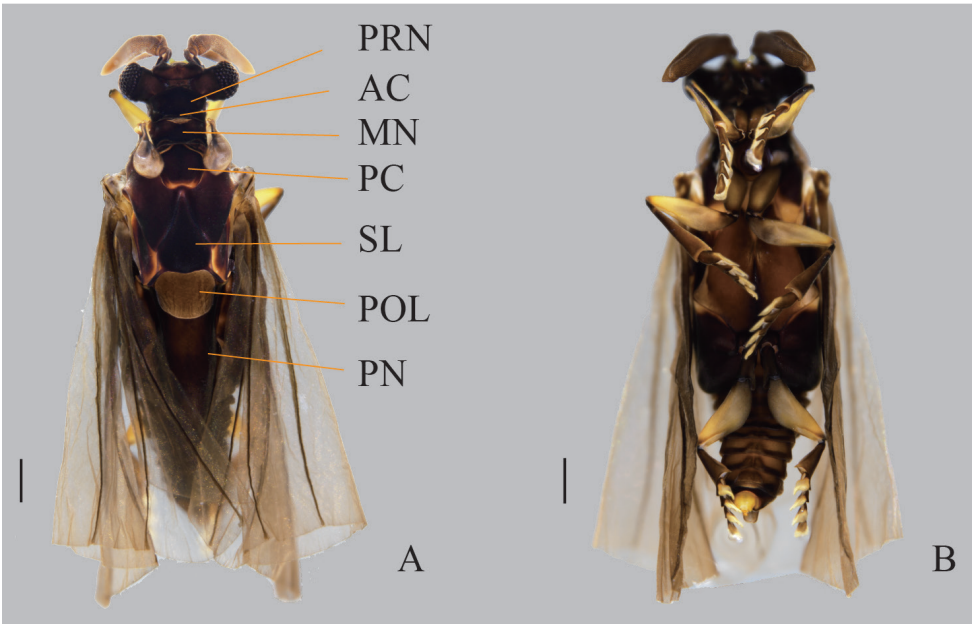

Figure 1. *Xenos yangi* Dong, Liu & Li sp. nov., male adult (holotype) **A** dorsal view (PRN, Pronotum; AC, Acrotergit; MN, Mesonotum; PC, Prescutum; SL, Scutellum; POL, Postlumbium; PN, Postnontum) **B** ventral view. Scale bar: 0.5 mm.

tops. ***Scutellum*** (Fig. 1A) acutely triangular. ***Postlumbium*** (Fig. 1A) broad, generally rounded, but emarginate anteriorly. ***Postnotum*** (Fig. 1A) triangular.

Hind wing sector with nine veins (Fig. 2A). C and Sc fused, half length of costal margin. R1 and R2 veins almost glued together, R2 vein extending from middle to wing apex; R3 vein from middle to outer margin of wing; R4 vein terminated at distal 1/4 of the wing and approximating R5 vein. MA, CuA1, CuA2 and CuP veins present and uninterrupted.

Proventrite laterally with anepisternum angulately curved at middle, and posteromedially with a small U-shaped notch, forming a pair of short lobes (Fig. 2H); ***Mesoventrite***

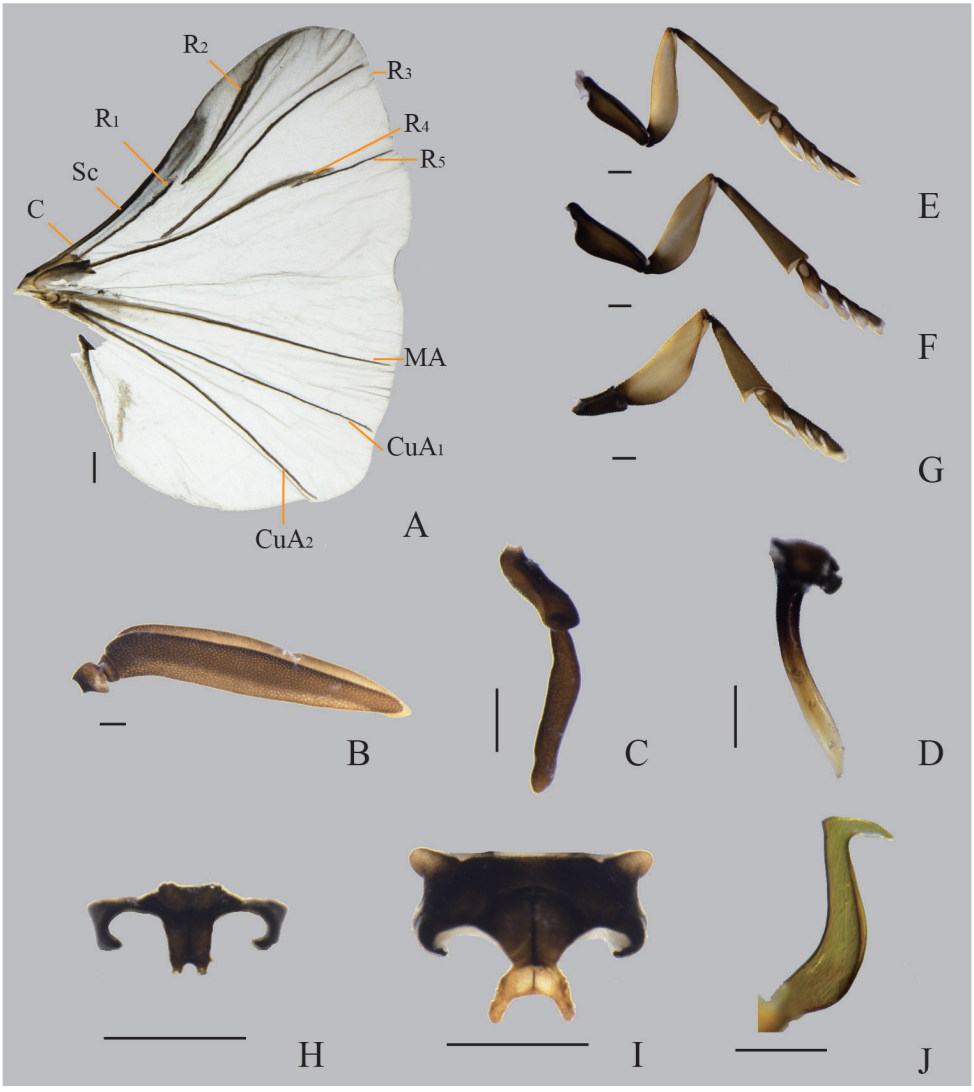

Figure 2. *Xenos yangi* Dong, Liu & Li sp. nov., male adult **A** hind wing **B** right antenna **C** right maxilla and palpus **D** right mandible **E** foreleg (right) **F** midleg (right) **G** hind leg (right) **H** proventrite **I** mesoventrite **J** penis. Scale bars: 0.5 mm. **A, B** dorsal **H, I** ventral **C–J, F** lateral.

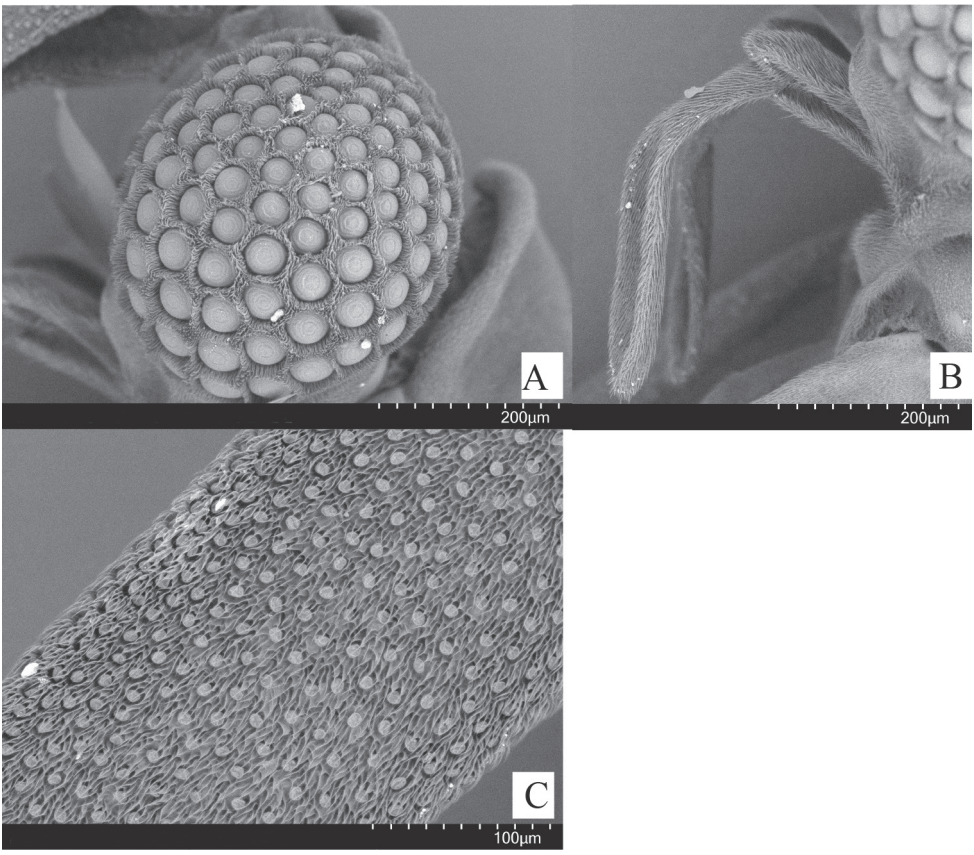

Figure 3. *Xenos yangi* Dong, Liu & Li sp. nov., male adult (SEM micrographs) **A** compound eye (lateral) **B** maxilla and palpus (lateral) **C** fourth antennomer (dorsal).

with basisternum transversely rectangular, anterolaterally roundly prominent, posterolaterally hook-like, sternellum broadly rhombic, posteriorly bifurcated into a pair of long digitiform projections (Fig. 2I). ***Foreleg*** (Fig. 2E) coxa expands, trochanterofemur with a protuberance near coxa, tibia longer than femur, widened near tarsus, tarsus four-segmented, 1st tarsomere with oval pit outside, 4th tarsomer without claws. ***Midleg*** (Fig. 2F) coxa as long as trochanterofemur, other parts similar to those of foreleg. ***Hind leg*** (Fig. 2G) trochanter half length of femur, femur strong. ***Abdomen*** 10-segmented as long as thorax, black; segment I tergites and sternites shrink; segment II–VIII sternites distinctly broader than tergites, segment IX narrower than segment VIII, with caudally elongated subgenital plate; segment X tube-like, curved. Anus flat. Penis colter-shaped (Fig. 2J).

Cephalotheca of male puparium (Fig. 4A). Cephalotheca elliptical. Maxilla almost oval, bigger than mandible. Clypeus furrowed and close to mandible. Antenna half size of eye.

Neotenic female (Fig. 4B–D). Length 11.0–16.0 mm, maximum breadth of abdomen about 4.5–5.0 mm (Fig. 4B); cephalothorax 2.2 mm in length and 1.76 mm

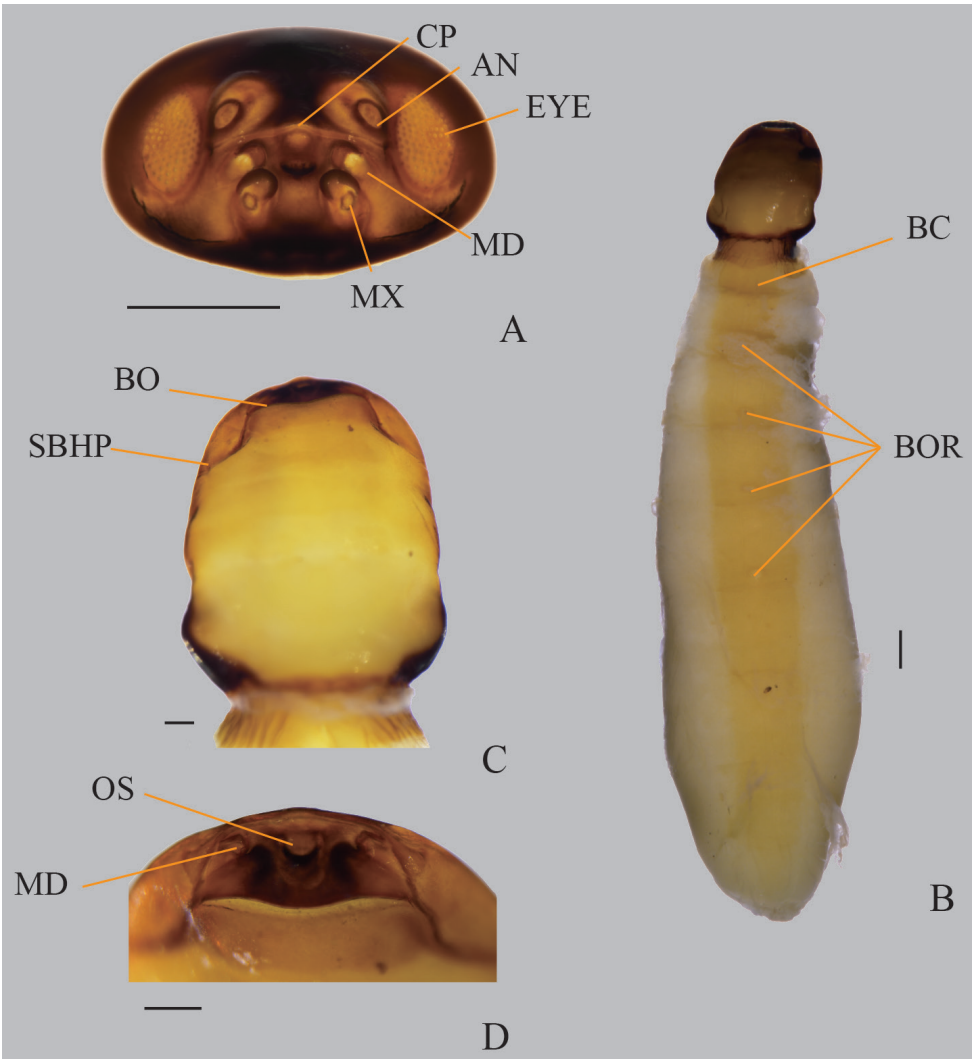

Figure 4. *Xenos yangi* Dong, Liu & Li sp. nov. **A** male cephalotheca frontal view (CP, Clypeus; AN, Antenna; EYE, Eye; MD, Mandible; MX, Maxillae) **B** female ventral view (BC, brood canal; BOR, birth organs) **C, D** female cephalothorax ventral view (BO, birth opening; SBHP, segmental border between head and prothorax; OS, mouth opening; MD, mandible). Scale bar: 0.5 mm.

in width (Fig. 4C, D). Coloration: cephalothorax brownish yellow, abdomen yellow. Cephalothorax almost rectangular, 3/4 strongly contracted; birth opening, protuberance (Fig. 4C); apex of mandible straight (Fig. 4D); abdomen slender, four birth organs.

Comparative notes. Considering the geographic distance and host association of those species of Africa and Americas, we mainly compared the male adult, the cephalotheca of the male papurium, and the neotenic female of this new species with ten described known species distributed in Asia (nine species) and Europe (one species) (Table 1). These species were originally described based on the male adult, the cephalotheca of the male

Table 1. Distribution and described stages of 11 *Xenos* species from Asia and Europe. Literature in which the species was originally described is highlighted in bold.

Species	Distribution	Male	Cephalotheca of male puparium	Neotenic female	Primary larvae
Xenos yangi Dong, Liu & Li sp. nov.	China: Yunnan	This study	This study	This study	NA
Xenos moutoni (Buysson, 1903)	China: Yunnan, Anhui, Taiwan	Kifune & Maeta, 1985	Buysson, 1904	**Buysson, 1903**	NA
Xenos circularis Kifune & Maeta 1985	China: Taiwan	NA	NA	**Kifune & Maeta, 1985**	NA
Xenos yamaneorum Kifune & Maeta, 1985	China: Taiwan	NA	**Kifune & Maeta, 1985**	**Kifune & Maeta, 1985**	NA
Xenos formosanus Kifune & Maeta, 1985	China: Taiwan	**Kifune & Maeta, 1985**	**Kifune & Maeta, 1985**	**Kifune & Maeta, 1985**	NA
Xenos dianshuiwengi Yang, 1999	China: Fujian	**Yang, 1999**	NA	NA	NA
Xenos oxyodontes Yuta & Makoto 2013	Japan	**Yuta & Makoto, 2013**	**Yuta & Makoto, 2013**	**Yuta & Makoto, 2013**	NA
Xenos vespularum Kifune & Maeta, 1975	Japan	**Kifune & Maeta, 1975**	**Kifune & Maeta, 1975**	**Kifune & Maeta, 1975**	NA
Xenos hebraei Kinzelbach, 1978	India	NA	**Kinzelbach, 1978**	**Kinzelbach, 1978**	NA
Xenos provesparum Kifune,1986	Indonesia	**Kifune, 1986**	**Kifune, 1986**	**Kifune, 1986**	NA
Xenos vesparum Rossius, 1793	Europe; Northern Africa	**Rossius, 1793**	**Rossius, 1793**	**Rossius, 1793**	Pohl & Beutel, 2005

NA: Not availabl

Figure 5. *Xenos yangi* Dong, Liu & Li sp. nov. and its host wasp. **A** *Vespa velutina* **B** *Vespa bicolor* **C** wasp host parasitized by the new species (red arrows: male puparium (left), female(right)) **D** living male. (dorsal view).

papurium, and/or the neotenic female (Table 1). The new species can be distinguished from *X. moutoni* (China: Yunnan, Anhui, Taiwan), *X. dianshuiwengi* (China: Fujian), *X. formosanus* (China: Taiwan), *X. provesparum* (Indonesia) and *X. oxyodontes* (Japan) based on the external characters of male adult. The male adult of *X. moutoni* maxilla as long as palpus and the postlumbium is straight anteriorly and posteriorly (Kifune and Maeta 1985). The male adult of *X. oxyodontes* (Japan) has the postlumbium rounded anteriorly and posteriorly (Nakase and Kato 2013). The proventrite is not concaved in *X. dianshuiwengi* (China: Fujian), *X. formosanus* (China: Taiwan) and *X. provesparum* (Indonesia) (Kifune and Maeta 1985; Kifune 1986; Yang 1999).

The new species can be distinguished from *X. circularis* (China: Taiwan), *X. yamaneorum* (China: Taiwan), *X. vespularum* (Japan), *X. hebraei* (India) and *X. vesparum* (Europe; Northern Africa) by the female cephalothorax. It is almost circular or ovoid in *X. yamaneorum*, *X. circularis*, *X. vespularum* and *X. vesparum* (Kifune and Maeta 1975; Kifune and Maeta 1985). The female cephalothorax is slightly wider than long in *X. hebraei*. Besides that, this new species can be also separated from *X. yamaneorum* and *X. vespularum* by the oval maxillae of the male cephalotheca (the two compared species lack the oval maxillae of the male cephalotheca).

Distribution. China (Yunnan).

Biology. The hosts of this new species are *Vespa velutina* (Fig. 5A) and *Vespa bicolor* (Fig. 5B). It parasitizes in the host abdomen. Its body partly protrudes from the portion between the two abdominal segments of the hosts. One wasp can usually carry 1–4 parasite individuals (Fig. 5C). After emergence, male adults fly away from their hosts (Fig. 5D). Neotenic females remain in the host's abdomen with their anterior cephalothorax protruding. When neotenic females are removed from their host abdomen, they can be seen to be covered with larval exuviae.

Etymology. The specific epithet is dedicated to the late famous Chinese entomologist Chi-Kun Yang, who made significant contributions to the studies on Strepsiptera in China.

Discussion

Due to the discovery of *X. yangi* sp. nov., the number of Chinese *Xenos* species increases to six (Fig. 7) while the Asian species add up to ten. In general, the Asian *Xenos* species are endoparasites of Vespinae (yellow jackets and hornets) and Polistinae (paperwasps) (Suppl. material 1: Table S1). *Vespa* (Vespinae) and *Polistes* (Polistinae) are common hosts for most *Xenos* species (Cook 2019). Except two Taiwanese species parasiting on *Polistes*, all other eight Asian species parasite on *Vespa*. Considering the species diversity of Vespinae and Polistinae in China (Carpenter 2011), we confirm the rich *Xenos* species diversity in China.

Among the 10 Asian *Xenos* species, six species (including the new species here) are described based on both males and neotenic females, one species solely based on males, two species are based on neotenic females and the cepholotheca of the male puparium, and one species is solely based on neotenic females (Table 1). This situation

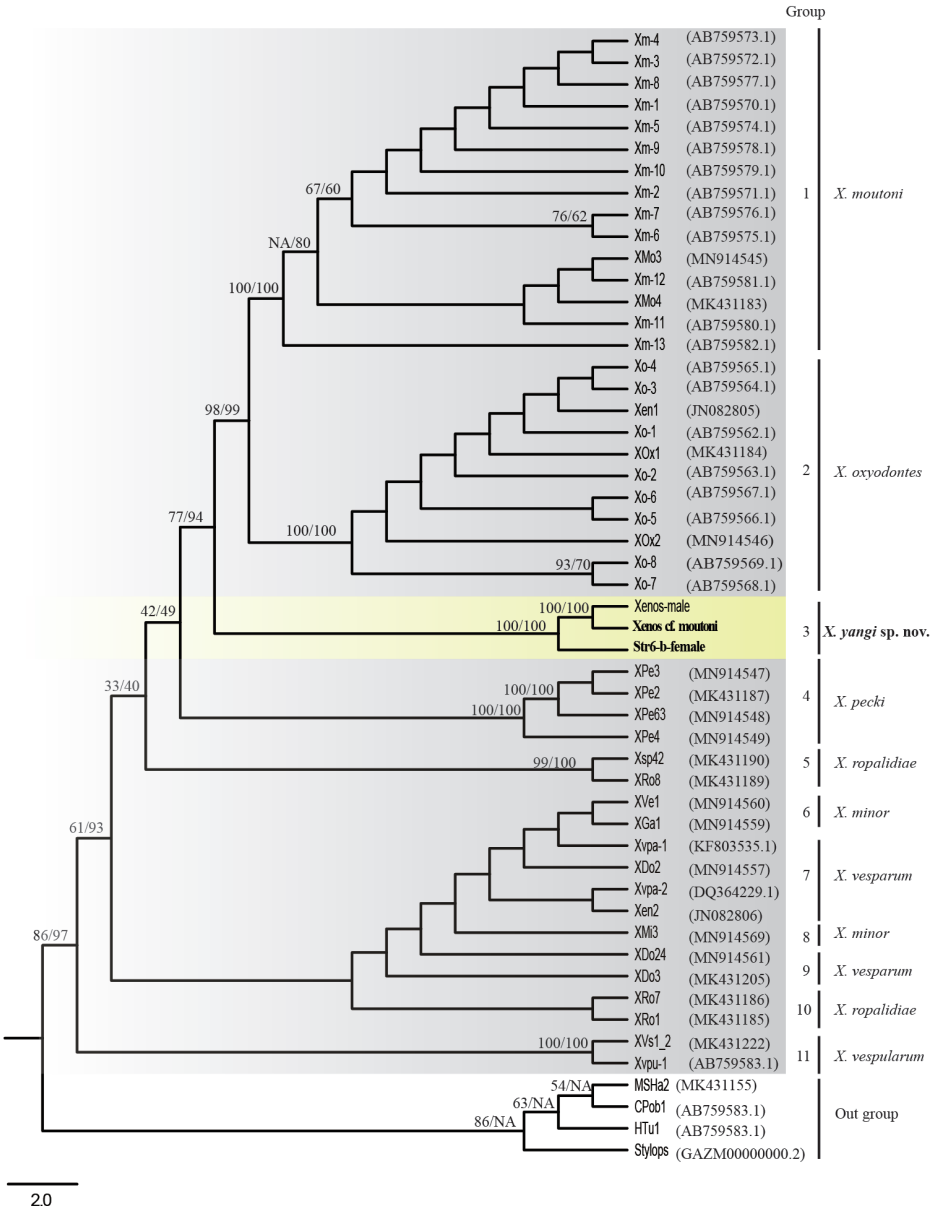

Figure 6. Phylogeny tree of *Xenos* species inferred from mitochondrial cytochrome *c* oxidase subunit 1 (*COI*) using Maximum parsimony method. In total, 48 *COI* sequences of different *Xenos* species were used to investigate their phylogenetic relationships. two sequences (str6-b-female and Xenos-male) were sequenced in this study, and that of *Xenos cf. moutoni* (MW222190.2) was sequenced in Zhang et al. (2021). Other 45 sequences were published by the following studies (Benda et al. 2021; McMahon et al. 2011; Nakase and Kato 2013; Jůzová et al. 2015; Carapelli et al. 2006). *Stylops ater* Reichert, 1914, *Melittostylops hesperapium* Kinzelbach, 1971, *Halictoxenos tumulorum* Perkins, 1918 and *Crawfordia warnckei* Kinzelbach, 1970 (outgroup) were used as outgroups. The phylogenetic trees were constructed using Maximum Parsimony (MP), and Maximum Likelihood (ML). Branch support values are described as Maximum Parsimony (MP)/Maximum Likelihood (ML) in MP tree.

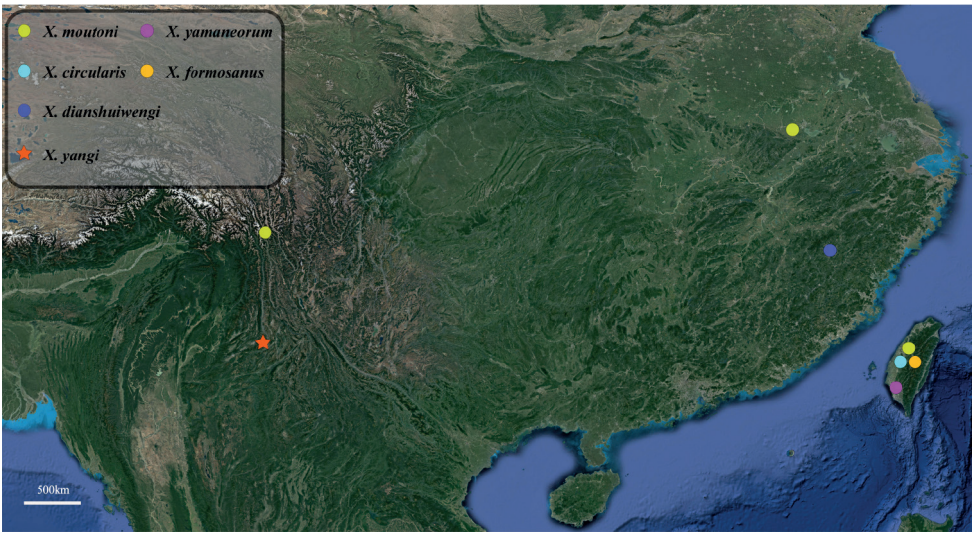

Figure 7. Distribution of the *Xenos* species from China.

Table 2. Summary of pairwise distances based on *COI* sequences among different *Xenos* species.

No.	Species	1	2	3	4	5	6	7	8	9	10	11
1	*X. moutoni*	0–0.014	–	–	–	–	–	–	–	–	–	–
2	*X. oxyodontes*	0.111–0.123	0–0.071	–	–	–	–	–	–	–	–	–
3	*X. yangi* sp. nov.	0.191–0.208	0.269–0.287	0–0.014	–	–	–	–	–	–	–	–
4	*X. pecki*	0.322–0.344	0.369–0.382	0.338–0.361	0–0.036	–	–	–	–	–	–	–
5	*X. ropalidiae*	0.330–0.348	0.308–0.341	0.302–0.333	0.326–0.358	0.089	–	–	–	–	–	–
6	*X. minor*	0.425–0.432	0.451–0.465	0.497–0.508	0.544–0.560	0.367–0.377	0	–	–	–	–	–
7	*X. vesparum*	0.425–0.440	0.451–0.473	0.497–0.516	0.544–0.568	0.367–0.385	0–0.003	0–0.003	–	–	–	–
8	*X. minor*	0.425–0.432	0.451–0.465	0.497–0.508	0.544–0.560	0.367–0.377	0	0–0.003	NA	–	–	–
9	*X. vesparum*	0.411–0.434	0.439–0.475	0.494–0.507	0.526–0.588	0.358–0.393	0.001–0.003	0.001–0.007	0.001–0.003	0.005	–	–
10	*X. ropalidiae*	0.275–0.383	0.329–0.404	0.382–0.433	0.452–0.474	0.368–0.421	0.435–0.517	0.435–0.525	0.435–0.517	0.437–0.552	0.2	–
11	*X. vespularum*	0.481–0.505	0.451–0.478	0.4472–0.478	0.549–0.577	0.458–0.472	0.608–0.612	0.608–0.616	0.608–0.612	0.590–0.608	0.519–0.523	0.001

in describing new species based only on neotenic females is also common in the taxonomy of *Xenos* from Africa and America (Suppl. material 1: Table S1). Considering the sexual dimorphism in twisted-wing parasites it is feasible to describe a new *Xenos* species when both male and female specimens are available. Thus, the association of both sexes and different stages of development in the same species of *Xenos* is crucial for future studies. This study provide an example of associating both sexes using combined biological, morphological and molecular evidence.

Xenos moutoni was originally described by Buysson (1903) based on only neotenic female specimens collected in Anhui (Ngan-hoei = Anhui Prov., Yng-chan = Xuanchen?宣城) and Yunnan (Yun-nam = Yunnan Prov., Tsé-kou = Cigu茨古 (Xu and Qiu 2020). Then, Buysson (1904) recorded its male puparium cephalotheca based on the specimens collected from the type locality. Kifune (1985) redescribed the male adult and cephalotheca of the male puparium of this species from Taiwan. In Buysson's work, the cephalotheca of the male puparium might be the main diagnostic trait to identify Taiwan *X. moutoni*. However, the author did not give a detailed description of the male puparium cephalotheca. According to available male specimens, cephalotheca of the male puparium and the neotenic females of the new species in the present study, we compared the different stages of the new species with the description of a male adult (Taiwan), cephalotheca of the male paparium (type locality), or the neotenic female (type locality) of *X. moutoni*, facilitating the delimitation of these two species both recorded from Yunnan. In addition, our study affirms again that molecular data, e.g., the DNA barcodes, are essential for the association of dimorphic sexes and different developmental stages in twisted-wing parasites taxonomy.

In the molecular data analysis, we noticed that different populations of five monophylic species (*X. moutoni*, *X. oxyodontes*, *X. yangi*, *X. pecki*, and *X. vespularum*) show genetic divergence of less than 0.036 (Table 2). Especially for *X. moutoni*, the genetic divergence among their different populations from Laos, China, Japan is less than 0.014 (Table 2). For the other lineages including specimens identified as *X. minor*, *X. vesparum* and *X. ropalidiae*, we noticed that *X. minor* and *X. vesparum* form a clade including four groups (group 6, 7, 8 and 9) (Fig. 6) and their genetic divergences are less than 0.007 (Table 2), suggesting these specimens may be the same species (Benda et al. 2021). On the other hand, different populations (Laos, Nepal, Malaysia) of *X. ropalidiae* form two separate groups (5 and 10) with a genetic divergence of 0.368–0.421 (Table 2), which may include different species (Benda et al. 2021). These findings suggest that an integrated methodology of molecular, biological, and morphological evidence should be adopted in taxonomy of such endoparasites as twisted-wing insects.

Acknowledgements

We give thanks to those anonymous villagers for helping to collect wasps harboring parasites, Dr Jiangli Tan for helping in wasp identification, Dr Guichun Liu and Ms Ruoping Zhao for helping in DNA extraction, Dr Ru Zhang and Jinwu He for helping in data analysis, Dr Tian-Tian Yu for reading the manuscript. Special thanks are given to Prof. Wen Wang for his courage to perform insect taxonomic work. This work was supported by grants from Yunnan Provincial Science and Technology Department (202105AC160039) and Chinese Academy of Sciences (CAS "Light of West China" Program) to X.L.

References

Benda D, Nakase Y, Straka J (2019) Frozen antarctic path for dispersal initiated parallel host-parasite evolution on different continents. Molecular Phylogenetics and Evolution 135: 67–77. https://doi.org/10.1016/j.ympev.2019.02.023

Benda D, Votýpková K, Nakase Y, Straka J (2021) Unexpected cryptic species diversity of parasites of the family Xenidae (Strepsiptera) with a constant diversification rate over time. Systematic Entomology 46: 252–265. https://doi.org/10.1111/syen.12460

Buysson R (1903) Note pour servir à l'histoire des Strepsiptères. Bulletin de la Société entomologique de France 8(9): 174–175. https://doi.org/10.3406/bsef.1903.23277

Buysson R (1904) Monographie des guêpes ou *Vespa*. Annales de la Societe Entomologique de France 73(3): 85–634.

Carapelli A, Vannini L, Nardi F, Boore JL, Beani L, Dallai R, Frati F (2006) The mitochondrial genome of the entomophagous endoparasite *Xenos vesparum* (Insecta: Strepsiptera). Gene 376(2): 248–259. https://doi.org/10.1016/j.gene.2006.04.005

Carpenter JM, Dvořák L, Kojima J, Nguyen LTP, Perrard A, Pickett KM (2011) Taxonomic notes on the Vespinae of Yunnan (Hymenoptera: Vespidae). American Museum Novitates 3709: 1–10. https://doi.org/10.1206/3709.2

Cook JL (2014) Review of the biology of parasitic insects in the order Strepsiptera. Comparative Parasitology 81(2): 134–151. https://doi.org/10.1654/4723.1

Cook JL (2019) Annotated catalog of the order Strepsiptera of the world. Transactions of the American Entomological Society 145(2): 121–267. https://doi.org/10.3157/061.145.0202

Cook JL, Mayorga-Ch D, Sarmiento CE (2020) A new species of *Xenos* (Strepsiptera: Xenidae) from Colombia, with comments on the neotropical species of the genus. Transactions of the American Entomological Society 146(2): 331–336. https://doi.org/10.3157/061.146.0204

Jůzová K, Nakase Y, Straka J (2015) Host specialization and species diversity in the genus *Stylops* (Strepsiptera: Stylopidae), revealed by molecular phylogenetic analysis. Zoological Journal of the Linnean Society 174(2): 228–243. https://doi.org/10.1111/zoj.12233

Kathirithamby J (2018) Biodiversity of Strepsiptera. In: Foottit RG, Adler PH (Eds) Insect biodiversity: science and society. Vol II. John Wiley & Sons, New York, 673–703. https://doi.org/10.1002/9781118945582.ch22

Kathirithamby J (2021) World Strepsiptera Database. https://strepsiptera.aphia.org [accessed on 2021-08-23]

Kathirithamby J, Hughes DP (2006) Description and biological notes of the first species of *Xenos* (Strepsiptera: Stylopidae) parasitic in *Polistes carnifex* F. (Hymenoptera: Vespidae) in Mexico. Zootaxa 1104(1104): 35–45. https://doi.org/10.11646/zootaxa.1104.1.3

Kinzelbach RK (1971) Morphologische Befunde an Fächerflüglern und ihre phylogenetische Bedeutung (Insecta: Strepsiptera). Zoologica 41(119/126): 1–256.

Kinzelbach RK (1978) Insecta, Fächerflügler (Strepsiptera). Series: Die Tierwelt Deutschlands, vol. 65. G. Fischer Verlag, Jena, 166 pp.

Kifune T, Maeta Y (1975) A New Subgenus and New Species of the Genus *Xenos* (Strepsiptera, Stylopidae) from Japan : Studies on the Japanese Strepsiptera II. Japanese Journal of Entomology 43(4): 446–455.

Kifune T, Maeta Y (1985) Taxonomical studies on the genus *Xenos* (Strepsiptera, Stylopidae) parasitic on *Vespa* and *Polistes* (Hymenoptera, Vespidae) of Taiwan with descriptions of three new species: Notulae Strepsipterologicae XIV. Japanese Journal of Entomology 53: 426–435.

Kifune T (1986) A new species of the genus *Xenos* (Strepsiptera, Stylopidae) parasitic on the genus *Provespa* (Hymenoptera, Vespidae) from West Sumatra, Indonesia. Japanese Journal of Entomology 54: 84–88.

Koeth M, Friedrich F, Pohl H, Beutel RG (2012) The thoracic skeleto-muscular system of *Mengenilla* (Strepsiptera: Mengenillidae) and its phylogenetic implications. Arthropod Structure & Development 41(4): 323–335. https://doi.org/10.1016/j.asd.2012.04.005

Manfredini F, Giusti F, Beani L, Dallai R (2007) Developmental strategy of the endoparasite *Xenos vesparum* (Strepsiptera, Insecta): host invasion and elusion of its defense reactions. Journal of Morphology 268(7): 588–601. https://doi.org/10.1002/jmor.10540

McMahon DP, Hayward A, Kathirithamby J (2009) The mitochondrial genome of the 'twisted-wing parasite' *Mengenilla australiensis* (Insecta, Strepsiptera): a comparative study. BMC Genomics 10: e603. https://doi.org/10.1186/1471-2164-10-603

McMahon DP, Hayward A, Kathirithamby J (2011) The first molecular phylogeny of Strepsiptera (Insecta) reveals an early burst of molecular evolution correlated with the transition to endoparasitism. PLoS ONE 6(6): e21206. https://doi.org/10.1371/journal.pone.0021206

Misof B, Liu S, Meusemann K, Peters RS, Donath A, Mayer C, Frandsen PB, Ware J, Flouri T, Beutel RG, Niehuis O, Petersen M, Izquierdo-Carrasco F, Wappler T, Rust J, Aberer AJ, Aspock U, Aspock H, Bartel D, Blanke A, Berger S, Bohm A, Buckley TR, Calcott B, Chen J, Friedrich F, Fukui M, Fujita M, Greve C, Grobe P, Gu S, Huang Y, Jermiin LS, Kawahara AY, Krogmann L, Kubiak M, Lanfear R, Letsch H, Li Y, Li, Z. Li J, Lu H, Machida R, Mashimo Y, Kapli P, McKenna DD, Meng G, Nakagaki Y, Navarrete-Heredia JL, Ott M, Ou Y, Pass G, Podsiadlowski, L, Pohl H, von Reumont BM, Schutte K, Sekiya K, Shimizu S, Slipinski A, Stamatakis A, Song W, Su X, Szucsich NU, Tan M, Tan X, Tang M, Tang J, Timelthaler G, Tomizuka S, Trautwein M, Tong X, Uchifune T, Walzl MG, Wiegmann BM, Wilbrandt J, Wipfler B, Wong TKF, Wu Q, Wu G, Xie Y, Yang S, Yang Q, Yeates DK, Yoshizawa K, Zhang Q, Zhang R, Zhang W, Zhang Y, Zhao J, Zhou C, Zhou L, Ziesmann T, Zou S, Li Y, Xu X, Zhang Y, Yang H, Wang J, Kjer KM, Zhou X (2014) Phylogenomics resolves the timing and pattern of insect evolution. Science 346: 763–767. https://doi.org/10.1126/science.1257570

Nakase Y, Kato M (2013) Cryptic diversity and host specificity in giant *Xenos* strepsipterans parasitic in large *Vespa* hornets. Zoological Science 30(4): e331. https://doi.org/10.2108/zsj.30.331

Pohl H, Beutel RG (2005) The phylogeny of Strepsiptera (Hexapoda). Cladistics 21(4): 328–374. https://doi.org/10.1111/j.1096-0031.2005.00074.x

Pohl H, Beutel RG (2008) The evolution of Strepsiptera (Hexapoda). Zoology 111(4): 318–338. https://doi.org/10.1016/j.zool.2007.06.008

Richter A, Beutel RG, Pohl H (2017) The female cephalothorax of *Xenos vesparum* Rossi, 1793 (Strepsiptera: Xenidae). Arthropod Systematics and Phylogeny 75(2): 327–347.

Rossius P (1793) Observations de M. Rossi sur un nouveau genre d'insecte, voisin des ichneumons. Bulletin des sciences de la Société Philomathique de Paris 1: e49. [1 plate]

Sudhir K, Glen S, Li M, Christina K, Koichiro T (2018) Mega x: molecular evolutionary genetics analysis across computing platforms. Molecular Biology & Evolution 6: e6.

Xu H, Qiu JY (2020) Three new synonyms within the flower chafer genus *Goliathopsis* Janson, 1881 (Coleoptera: Scarabaeidae: Cetoniinae) from China. Zootaxa 4789(1): 91–131. https://doi.org/10.11646/zootaxa.4789.1.3

Yang CK (1999) Strepsiptera. In: Huang BK (Ed.) Fauna of insect in Fujian porvince of China. Fujian science & technology press, Fujian. Vol. 3, 184–185. [In Chinese]

Zhang R, Li J, Mao CY, Dong ZW, He JW, Liu GC, Zhao RP, Wang W, Li XY (2021) The mitochondrial genome of one 'twisted-wing parasite' *Xenos* cf. *moutoni* (Insecta, Strepsiptera, Xenidae) from Gaoligong Mountains, Southwest of China. Mitochondrial DNA, Part B 6(2): 512–514. https://doi.org/10.1080/23802359.2021.1872443

Supplementary material 1

Table S1

Authors: Zhiwei Dong, Xingyue Liu,Chuyang Mao, Jinwu He, Xueyan Li

Data type: xlsx file

Explanation note: Known species of Xenos and their geographical distribution, type depository and host.

Link: https://doi.org/10.3897/zookeys.1085.76484.suppl1

ZooKeys 1085: 29–49 (2022)
doi: 10.3897/zookeys.1085.77924
https://zookeys.pensoft.net

RESEARCH ARTICLE

A peer-reviewed open-access journal
ZooKeys
Launched to accelerate biodiversity research

Xenia konohana sp. nov. (Cnidaria, Octocorallia, Alcyonacea), a new soft coral species in the family Xeniidae from Miyazaki, Japan

Tatsuki Koido[1,2], Yukimitsu Imahara[2,3,4], Hironobu Fukami[5]

1 *Interdisciplinary Graduate School of Agriculture and Engineering, University of Miyazaki, 1–1 Gakuen-kibanadai-nishi, Miyazaki, Miyazaki 889–2192, Japan* **2** *Kuroshio Biological Research Foundation, 560 Nishidomari, Otsuki, Kochi 788–0333, Japan* **3** *Octocoral Research Laboratory, 300–11 Kire, Wakayama, 640–0351, Japan* **4** *Geological Survey of Japan, National Institute of Advanced Industrial Science and Technology, 1-1-3 Higashi, Tsukuba, Ibaraki 305–8567, Japan* **5** *Department of Marine Biology and Environmental Sciences, Faculty of Agriculture, University of Miyazaki, 1–1 Gakuen-kibanadai-nishi, Miyazaki, Miyazaki 889–2192, Japan*

Corresponding author: Hironobu Fukami (hirofukami@cc.miyazaki-u.ac.jp)

Academic editor: James Reimer | Received 12 November 2021 | Accepted 18 January 2022 | Published 3 February 2022

http://zoobank.org/328695E9-63FE-45B8-ADC2-3DE50DCBBD4E

Citation: Koido T, Imahara Y, Fukami H (2022) *Xenia konohana* sp. nov. (Cnidaria, Octocorallia, Alcyonacea), a new soft coral species in the family Xeniidae from Miyazaki, Japan. ZooKeys 1085: 29–49. https://doi.org/10.3897/zookeys.1085.77924

Abstract

A new soft coral species, *Xenia konohana* **sp. nov.** (Alcyonacea, Xeniidae), is described from Miyazaki in the warm-temperate region of Japan. This new species has conspicuous and unique spindle sclerites in addition to the simple ellipsoid platelet-shaped sclerites typically found in the genus *Xenia*. These unique spindles are a specific key morphological characteristic for this new species and for differentiating this species among congeneric species.

Keywords

Alcyonacea, Cnidaria, Miyazaki, new species, *Xenia*, Xeniidae

Introduction

Species of the family Xeniidae are known as pioneers in tropical coral reefs (Benayahu and Loya 1987), playing an important role for ecological succession in coral reefs. Therefore, knowing how many species of Xeniidae exist, and the range of species diversity will be useful for understanding the coral reef ecosystem.

For species or genus identification of alcyonacean soft corals including xeniids, the shape and arrangement of sclerites are used as key characteristics. Xeniids typically produce minute platelets or corpuscle-like sclerites without tubercular differences among species and genera under light microscopy (Fabricius and Alderslade 2001). The microstructure of sclerites has been shown to be an important character at the genus level of the family Xeniidae. Recently, the type specimens of 21 species in the genus *Xenia* were rechecked and re-described using sclerite microstructure (Halász et al. 2019). Thus, observation of sclerite microstructure is taxonomically useful for species delimitation, at least in some species of *Xenia*.

The genus *Xenia* presently includes 49 valid species (Cordeiro et al. 2021). This genus is characterized by platelet-shaped sclerites with surface microstructure composed of calcite dendritic and sinuous rods (Alderslade 2001; Halász et al. 2019). Koido et al. (2019) reported an undescribed species belonging to *Xenia* (reported as *Xenia* sp. 1) from Oshima Island, Miyazaki, in the warm-temperate region (non-coral reef region) of Japan. This previous work emphasized the high species diversity of Xeniidae in Miyazaki, Japan. This study provides a description of this previously undescribed species (*Xenia* sp. 1) as *Xenia konohana* sp. nov., a new species in the genus.

Materials and methods

All specimens were collected around Oshima Island (31°31.35'N, 131°24.27'E) (Fig. 1), Miyazaki, Japan, by SCUBA diving and snorkeling. A small piece of tissue (5–10 mm) from each specimen was used for molecular analyses and the remainder was preserved in 99% ethanol for morphological analyses as reported by Koido et al. (2019).

Specimens were previously deposited in Miyazaki University, Fisheries Sciences (MUFS) but were subsequently transferred and deposited at the Kuroshio Biological Research Foundation, Kochi, Japan (KBF) in the octocoral collection (OA). Morphological characteristics examined under a stereomicroscope included colony height, length and width of the stalk, presence of branches, length and width of polyps, length and width of tentacles, length and width of pinnules, number of rows of pinnules, and number of pinnules in the aboral row. Sclerites from polyps, and ones from the surface and interior of both stalk and branches of each specimen were examined. Sclerite shape, size, and microstructure were examined with light microscopy and scanning electron microscope (SEM) (HITACHI S-4800 and JEOL JSM-6500F).

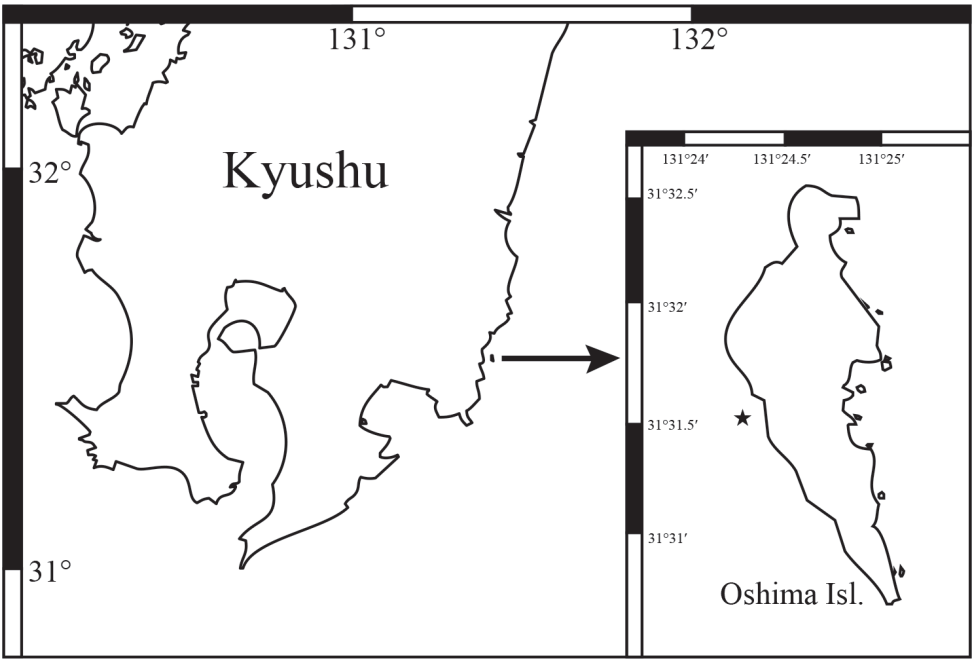

Figure 1. Collection sites of *Xenia konohana* sp. nov. in Miyazaki, Japan.

DNA extraction, amplification, and sequencing

Tissue samples were kept in CHAOS solution for at least a week to dissolve proteins at room temperature as reported by Koido et al. (2019). Total DNA was extracted from CHAOS solutions by conventional phenol/chloroform extraction. The phylogenetic position of *X. konohana* sp. nov. was inferred using three mitochondrial markers (*ND2*, *mtMutS*, *COI*) (16S647F: 5'-ACA CAG CTC GGT TTC TAT CTA CCA-3'; ND21418R: 5' -ACA TCG GGA GCC CAC ATA-3', ND42625F: 5'-TAC GTG GYA CAA TTG CTG-3', Mut-3458R: 5'-TSG AGC AAA AGC CAC TCC-3', COII8068F: 5'-CCA TAA CAG GAC TAG CAG CAT C-3', HC02198: 5'-TAA ACT TCA GGG TGA CCA AAA AAT CA-3') and a nuclear marker (*28S*) (28S-Far: 5'-CAC GAG ACC GAT AGC GAA CAA GTA-3', 28S-Rar: 5'-TCA TTT CGA CCC TAA GAC CTC-3'). PCR reactions for all four markers used 1 μL of DNA solution, 1.6 μL of 2.5 mM dNTP Mixture, 2 μL of 10X Ex Taq buffer, 2 μL of each primer (10 mM), 0.08 μL Ex taq (TaKaRa), and 11.32 μL of sterile distilled water. Amplification of these markers used a GeneQ PCR Thermal Cycler with the following thermal profile; 35 cycles of 90 sec at 94 °C, 60 sec at 58 °C, and 60 sec at 72 °C. Amplicons were checked on 1% agarose gel electrophoresis. All PCR products were treated to remove excess primers and dNTP using Exonuclease I (TaKaRa) and Shrimp Alkaline Phosphatase (TaKaRa). DNA sequences were determined by ABI3000 using a research contract service (Ltd.

FASMAC). DNA sequences of 709 bases for *mtMutS*, 804 for *COI*, 773 for *28S* rDNA, and 673 for *ND2* were obtained in this study. DNA sequences for *mtMutS*, *COI*, and *28S* were combined and analyzed because concatenated DNA sequences using these markers have been recently used for the molecular phylogenetic analyses in the Xeniidae (McFadden et al. 2019; Halász et al. 2019), while sequences for ND2 were analyzed alone because of restricted number of sequences available (McFadden et al. 2006; McFadden and Ofwegen 2012; McFadden et al. 2014b; McFadden et al. 2017). As outgroups for both analyses, we used *Paralemnalia thyrsoides* (Ehrenberg, 1834) (family Nephtheidae), *Rhytisma fulvum* (Forskål, 1775) (family Alcyoniidae) and *Coelogorgia palmosa* Milne Edwards & Haime, 1857 (family Coelogorgiidae), which are all known to be closely related to the Xeniidae (Halász et al. 2019). MEGA6 (Tamura et al. 2013) was used to select appropriate models (T92+G model for the concatenated DNA sequences, including *mtMutS*, *COI*, and *28S*, and T92 model for *ND2*) for maximum likelihood (ML) method and to reconstruct the ML phylogenetic trees with 1000 bootstrap replicates. In Bayesian analysis, the concatenated alignment data was treated as a separate data partition with different models of evolution applied to each of the mitochondrial (*mtMutS* and *COI*: HKY+G) and nuclear (*28S*: GTR+G) markers. MrBayes v. 3.2.1 (Ronquist et al. 2012) was run for 50,000,000 generations (until standard deviation of split partitions < 0.01) with a burn-in of 25% and default Metropolis coupling parameters. For phylogenetic analyses, recently published data for three markers (*mtMutS*, *COI*, and *28S*) from the Xeniidae were also added (Table 1).

Table 1. List of specimens of the family Xeniidae examined in this study and accession numbers for *28S*, *mtMutS*, *COI* and *ND2* markers. The origin of the accession number is shown by asterisk (s) in the reference list for each line if more than one reference exists.

Species	Specimen Catalog #	GenBank accession number				References
		28S	*mtMutS*	*COI*	*ND2*	
Xenia konohana sp. nov.	KBF-OA–00092	LC656679*	LC656674*	LC656676*	LC467035**	*This study **Koido et al. 2019
Xenia konohana sp. nov.	KBF-OA–00093	LC656680*	LC656673*	LC656677*	LC467036**	*This study, **Koido et al. 2019
Xenia konohana sp. nov.	KBF-OA–00094	LC656681*	LC656675*	LC656678*	LC467037**	*This study, **Koido et al. 2019
Anthelia glauca	ZMTAU CO34183	JX203753*	JX203812*	GQ342460**	–	*McFadden and Ofwegen 2012, **Brockman and McFadden 2012
Asterospicularia laurae	CSM-OCDN8971L	KM201433	KM201452	KM201458	–	Janes et al. 2014
Asterospicularia randalli	RMNH:Coel. 41521	KF915316	KF915556	KF955019	–	McFadden et al. 2014a
Heteroxenia mindorensis	CAS:IZ:184566	KJ511300	KJ511339	KJ511379	KJ511421	McFadden et al. 2014b
Heteroxenia mindorensis	CAS:IZ:184574	KJ511381	KJ511341	KJ511302	KJ511423	McFadden et al. 2014b
Ovabunda ainex	ZMTAU:36785	KY442364	KY442323	KY442342	KY442395	McFadden et al. 2017
Ovabunda ainex	ZMTAU:36786	KY442365	KY442324	KY442343	KY442396	McFadden et al. 2017
Ovabunda andamanensis	PMBC:11861	KM201440	KM201455	KM201461	–	Janes et al. 2014
Ovabunda andamanensis	PMBC:11862	KM201439	KM201454	KM201460	–	Janes et al. 2014

Species	Specimen Catalog #	GenBank accession number				References
		28S	***mtMutS***	***COI***	***ND2***	
Ovabunda biseriata	ZMTAU:34876	KY442376	KY442330	KY442349	KY442405	McFadden et al. 2017
Ovabunda biseriata	ZMTAU:34881	KY442378	KY442332	KY442351	KY442407	McFadden et al. 2017
Ovabunda biseriata	ZMTAU:34882	KY442379	KY442333	KY442352	KY442408	McFadden et al. 2017
Ovabunda faraunenesis	ZMTAU:CO 34051	KJ511306**	GU356029*	GU356006*	KJ511427**	*McFadden et al. 2011, **McFadden et al. 2014b
Ovabunda faraunenesis	ZMTAU:34884	KY442380	KY442334	KY442353	KY442412	McFadden et al. 2017
Ovabunda faraunenesis	ZMTAU:34886	KY442381	KY442335	KY442354	KY442413	McFadden et al. 2017
Ovabunda impulsatilla	ZMTAU:34571	KY442374	KY442328	KY442347	KY442418	McFadden et al. 2017
Ovabunda impulsatilla	ZMTAU:34891	KY442383	KY442337	KY442356	KY442419	McFadden et al. 2017
Ovabunda obscuronata	ZMTAU:CO 34077	KJ511307**	GU356027*	GU356004*	KJ511428**	*McFadden et al. 2011, **McFadden et al. 2014b
Sansibia flava	ZMTAU:Co36004	MK400137	MK396681	MK396728	–	McFadden et al. 2019
Sansibia flava	ZMTAU:Co36006	MK030486	MK030380	MK039204	–	McFadden et al. 2019
Sansibia flava	ZMTAU:Co36073	MK030487	MK030381	MK039205	–	McFadden et al. 2019
Sympodium caeruleum	ZMTAU CO34185	JX203758*	JX203815*	GU356009**	KJ511430***	*McFadden and Ofwegen 2012 **McFadden et al. 2011 ***McFadden et al. 2014b
Xenia fisheri	CAS:IZ:184540	KJ511311	KJ511349	KJ511389	KJ511436	McFadden et al. 2014b
Xenia fisheri	CAS:IZ:184541	KJ511312	KJ511350	KJ511390	KJ511437	McFadden et al. 2014b
Xenia kusimotoensis	CAS:IZ:184554	KJ511314	KJ511352	KJ511392	KJ511441	McFadden et al. 2014b
Xenia lepida	CAS:IZ:184535	KJ511316	KJ511354	KJ511394	KJ511443	McFadden et al. 2014b
Xenia lepida	CAS:IZ:184562	KJ511317	KJ511355	KJ511395	KJ511444	McFadden et al. 2014b
Xenia membranacea	CAS:IZ:184536	KJ511308	KJ511345	KJ511385	KJ511432	McFadden et al. 2014b
Xenia membranacea	CAS:IZ:184548	KJ511319	KJ511357	KJ511397	KJ511446	McFadden et al. 2014b
Xenia membranacea	CAS:IZ:184549	KJ511320	KJ511358	KJ511398	KJ511447	McFadden et al. 2014b
Xenia puertogalerae	CAS:IZ:184532	KJ511324	KJ511362	KJ511402	KJ511451	McFadden et al. 2014b
Xenia puertogalerae	CAS:IZ:184539	KJ511325	KJ511363	KJ511403	KJ511452	McFadden et al. 2014b
Xenia puertogalerae	CAS:IZ:184545	KJ511326	KJ511364	KJ511404	KJ511453	McFadden et al. 2014b
Xenia viridis	CAS:IZ:184542	KJ511331	KJ511369	KJ511409	KJ511458	McFadden et al. 2014b
Xenia hicksoni	ZMTAU CO34072	JX203759*	GQ342529**	GQ342463**	KJ511438*	*McFadden and Ofwegen 2012, **Brockman and McFadden 2012
Xenia ternatana	CAS:IZ:184560	KJ511327	KJ511365*	KJ511405*	KJ511454	McFadden et al. 2014b
Xenia umbellata	ZMTAU:36783	KY442362*	KT590452**	KT590435**	KY442431*	*McFadden et al. 2017, **Halász et al. 2019
Xenia umbellata	ZMTAU:36788	KY442367*	KT590457**	KT590438**	KY442432*	*McFadden et al. 2017, **Halász et al. 2019
Xenia umbellata	ZMTAU:36790	KY442369*	KT590458**	KT590439**	–	*McFadden et al. 2017, **Halász et al. 2019
Yamazatum iubatum	ZMTAU:Co35143	MH071864	MK030449	MK039274	–	McFadden et al. 2019
Yamazatum iubatum	ZMTAU:Co35144	MH071865	MH071910	MH071958	–	Benayahu et al. 2018a
Yamazatum iubatum	ZMTAU:Co35741	MK030452	MK030451	MH071955	–	McFadden et al. 2019
Unomia stolonifera	ZMTAU Co38081	MT489336	MT482554	MT487559		Benayahu et al. 2021
Coelogorgia palmosa	NTM C14914	JX203698	DQ302805	GQ342413	DQ302879	McFadden et al. 2006
Rhytisma fulvum	ZMTAU CO34124	JX203728*	GQ342478**	GQ342396**	–	*McFadden and Ofwegen 2012, **Brockman and McFadden 2012
Paralemnalia thyrsoides	ZMTAU:Co36976	MH516907	MH516632	MH516518	–	Benayahu et al. 2018b
Cladiella digitulata	MUFS-COSU14	–	–	–	LC467083	Koido et al. 2019
Cladiella sphaerophora	MUFS-COAK1	–	–	–	LC467084	Koido et al. 2019
Klyxum sp.	MUFS-COMO150	–	–	–	LC467086	Koido et al. 2019
Klyxum sp.	MUFS-COMO164	–	–	–	LC467087	Koido et al. 2019
Klyxum sp.	MUFS-COOTUD8	–	–	–	LC467088	Koido et al. 2019

Results

Taxonomy

Class Anthozoa Ehrenberg, 1831
Subclass Octocorallia Haeckel, 1866
Order Alcyonacea Lamouroux, 1812
Family Xeniidae Ehrenberg, 1828

Genus *Xenia* Lamarck, 1816

Type species. *Xenia umbellata* Lamarck, 1816

Emended diagnosis. (Chiefly after Halász et al. 2019). Colonies are small and soft with cylindrical stalk, undivided or branched, terminating in one or more domed polyp-bearing regions. Polyps are not retractile and are always monomorphic. The dominant sclerites are ellipsoid platelets, usually abundant in all parts of the colony. They are composed of calcite rods, often dendritic or sinuous, mostly radially arranged, at least at the periphery of the sclerites. In addition to ellipsoid platelets, a few species have rods or unique spindles with pointed spear ends.

***Xenia konohana* sp. nov.**
http://zoobank.org/D1BD260D-A55D-4A88-9CF6-823E06AF0504
New Japanese name: konohana-umiazami
Figs 3–10

Synonym. *Xenia* sp. 1 Koido et al. 2019: Table 1, figs 2J–4J.

Materials. ***Holotype*:** KBF-OA-00092 (MUFS-COMO4 in Koido et al. 2019), Oshima Isl., Nichinan City, Miyazaki Prefecture, depth < 5 m, July 2, 2012. ***Paratypes*:** KBF-OA-00093 (MUFS-COMO53 in Koido et al. 2019), Oshima Isl., Nichinan City, Miyazaki Prefecture, depth < 10 m, December 25, 2012; KBF-OA-00094 (One colony with two stems) (MUFS-COMO54 in Koido et al. 2019), Oshima Isl., Nichinan City, Miyazaki Prefecture, depth < 10 m, December 25, 2012.

Descriptions. The holotype (Fig. 2A) displays a typical *Xenia*-style growth form (Alderslade 2001; Benayahu 2010), featuring a distinct cylindrical stalk, 35 mm high and 20 mm wide attached to a rock. The colony possesses three branches 5–7 mm long from a common basal stalk. The whole colony is creamy white in ethanol. Polyps are 4.5–5.0 mm long, excluding tentacles, and 2.0 mm in diameter at their proximal part. Tentacles are 3.0–4.0 mm long and 0.3–0.5 mm wide at their proximal part.

Pinnules are arranged mostly in three rows along each side of the tentacles, leaving free median space along the oral side. This space is not always visible at the distal part of the longest tentacles. The number of rows of pinnules drops to two toward the proximal part of the tentacle, and occasionally, only a single row can be seen (Fig. 3).

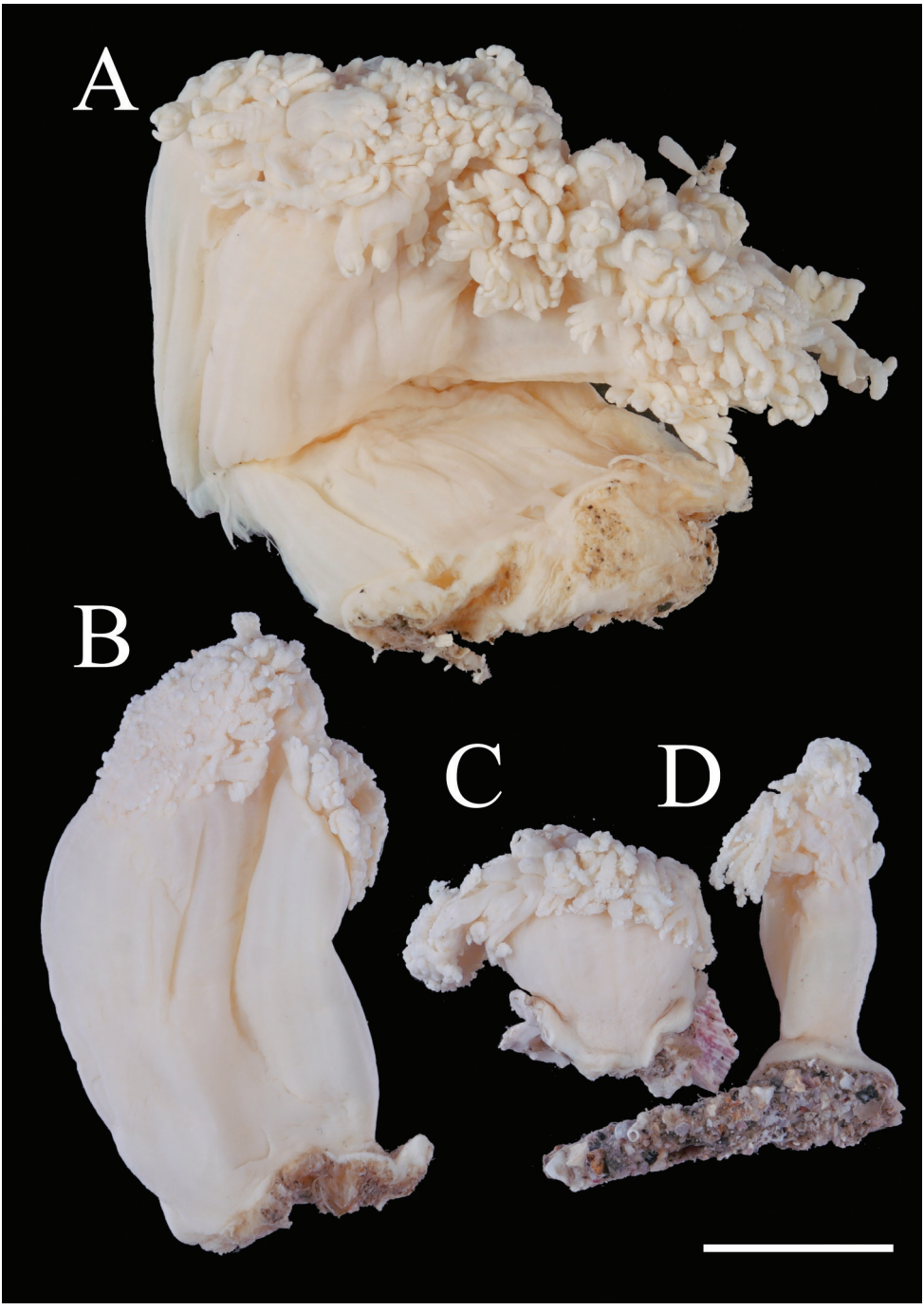

Figure 2. Fixed specimens of *Xenia konohana* sp. nov. **A** holotype BF-OA-00092 **B** paratype KBF-OA-00093 **C, D** paratype KBF-OA-00094. Scale bar: 10 mm.

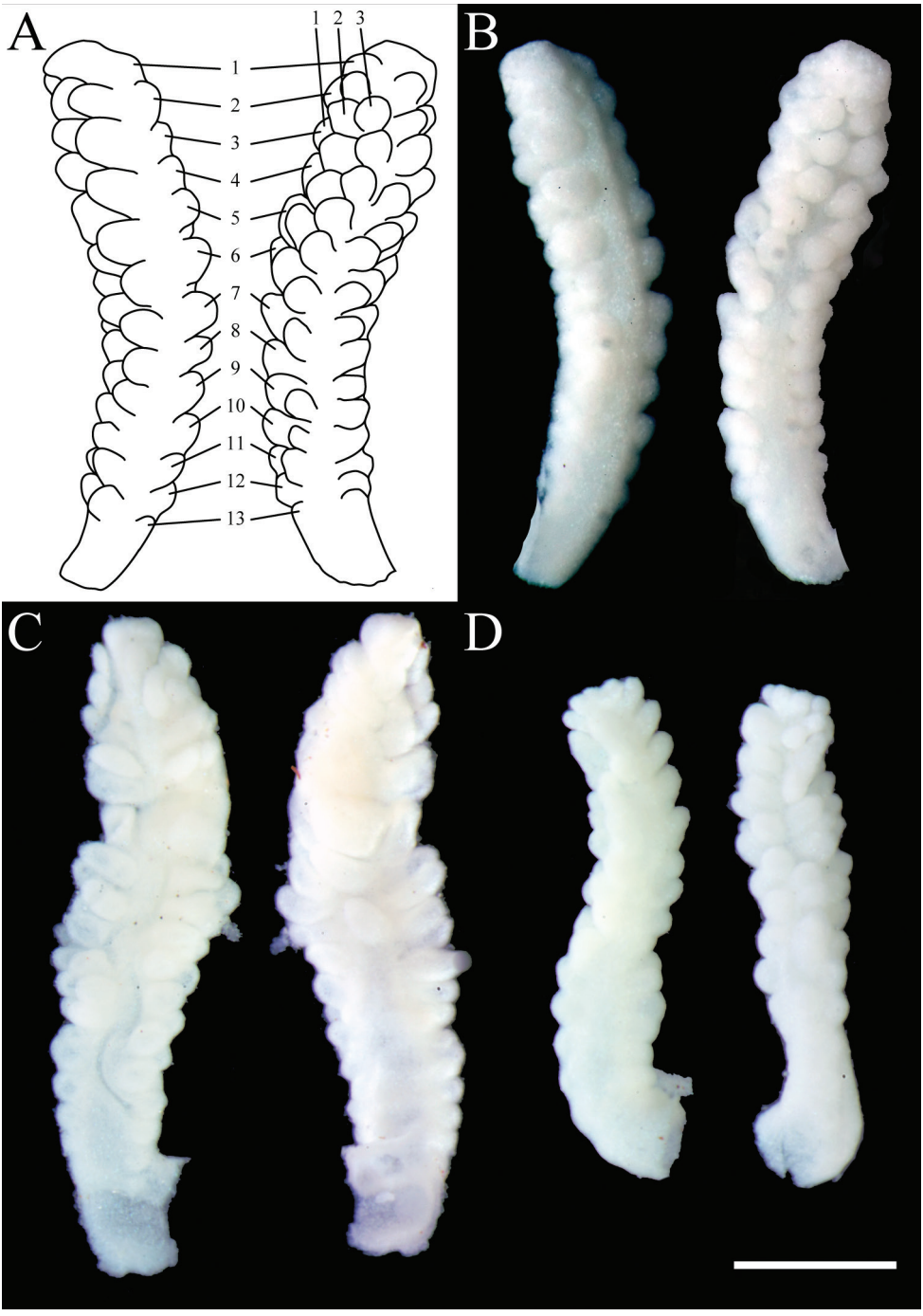

Figure 3. Tentacles of *Xenia konohana* sp. nov. aboral (left) and oral sides (right) **A** schema of holotype KBF-OA-00092: three rows (the number is shown in the upper-right) and 13 pinnules at the outermost row (the number is shown in the center) **B** holotype KBF-OA-00092 **C** paratype KBF-OA-00093 **D** paratype KBF-OA-00094. Scale bar: 1 mm.

The outermost row usually includes 12–16 pinnules each, up to 0.23 mm long and 0.21 mm wide at the proximal part. Typically, no gap between pinnules exists, but in rare cases, a gap of approximately 0.05 mm is observed.

Sclerites are abundant in polyps and surface layers of stalk and branches but absent interior. Under light microscopy, two forms of sclerites are observed – simple platelets (Fig. 4A) and spindles (Fig. 4B). Platelets are brown-red and spindles transparent (Fig. 4) under transmitted illumination. Platelets look pale blue and spindles appear transparent under epi-illumination (Fig. 5).

Polyp sclerites. Two forms of sclerites, simple platelets and spindles, are seen in polyps (Figs 6A, B, 7A, B). Simple platelets are 0.016–0.021 mm long and 0.009–0.011 mm wide. Spindles, 0.035–0.049 mm long and 0.004–0.006 mm wide, display unique ends with pointed spear tips. Sclerite composition in tentacles (n = 124) is 7.3% simple platelets and 92.7% spindles. In the polyp body (n = 83), these proportions are 4.8% and 95.2%, respectively. Thus, the vast majority of sclerites are spindles. Some spindles have thorns on their surface.

Stalk and branch sclerites. Two forms of sclerites, simple platelets and spindles, are also found in stalk and branches (Figs 6C, D, 7C, D). Simple platelets, several with an indistinct median waist, are 0.017–0.021 mm long and 0.009–0.011 mm wide. Spindles are 0.038–0.049 mm long and 0.004–0.006 mm wide. All spindles are more or less bent. Sclerite composition in stalk (n = 104) is 7.7% simple platelets and 92.3% spindles. Thus, the vast majority of sclerites are spindles.

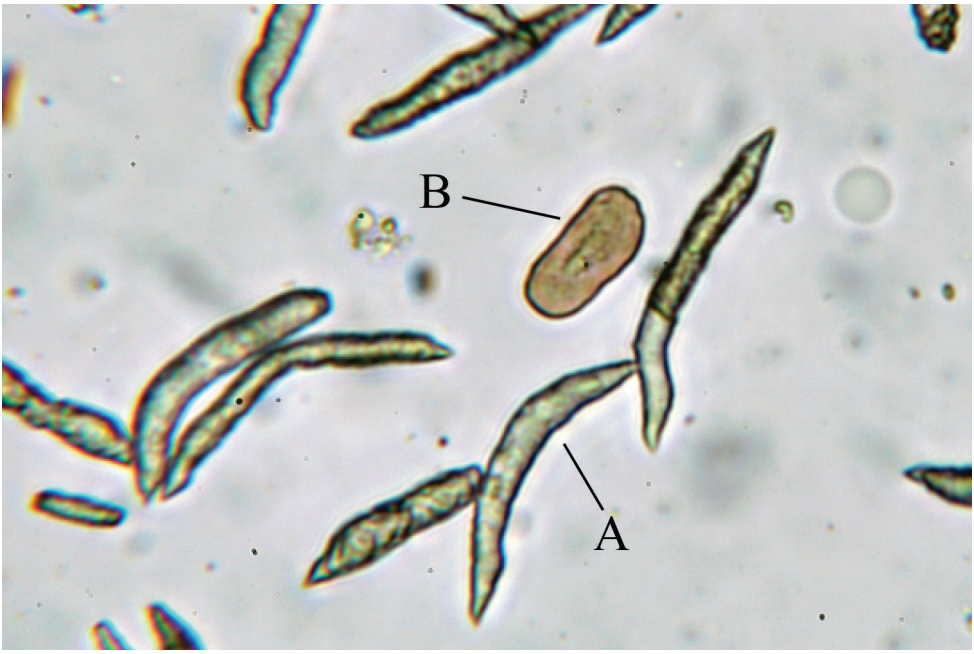

Figure 4. Light microscope images of sclerites in polyps of *Xenia konohana* sp. nov., holotype KBF-OA-00092 **A** spindles **B** simple platelets.

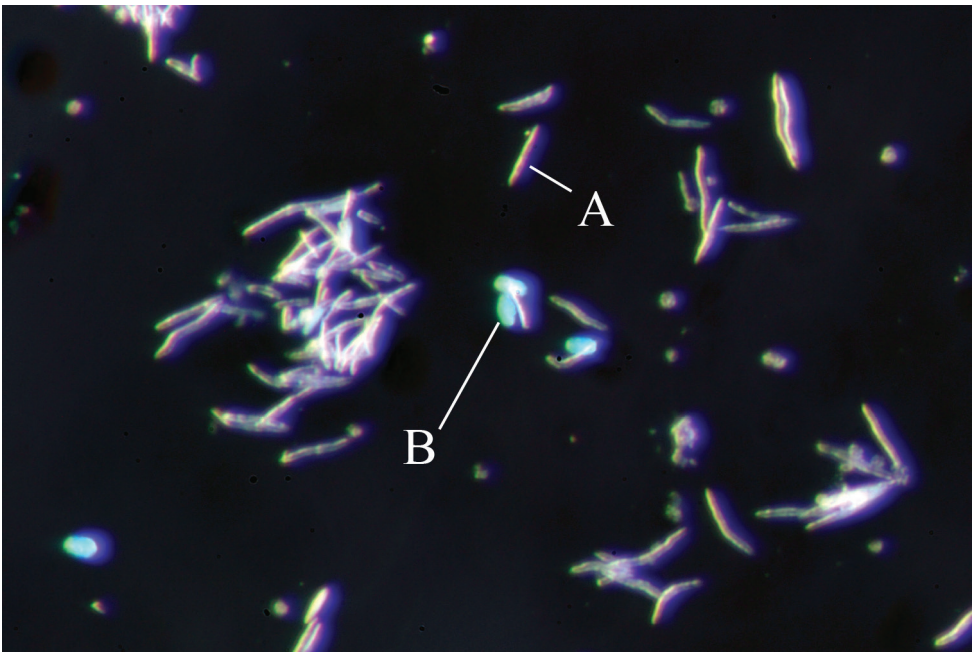

Figure 5. Stereoscopic microscopes images of sclerites in polyps of *Xenia konohana* sp. nov., holotype KBF-OA-00092 **A** spindles **B** simple platelets.

Microstructure of sclerites. The platelets are composed of branched sinuous dendritic rods within the sclerite interior. SEM at 30,000–50,000× magnification shows distal parts of rods that line up almost vertically and parallel to the surface (Fig. 8A, B). The spindles are composed of fused grains with a granular appearance (Fig. 8C, D). Fused grains also exist inside, which can be observed in cross-sections of broken spindles (Fig. 8E, F). Both ends of the spindles are relatively smooth (Fig. 8G). Thorns may form on the surface of spindles (Fig. 7, red arrows indicate the thorn, Fig. 8D shows the thorn expansion).

Variation. Two preserved paratypes (KBF-OA-00093, KBF-OA-00094) differ in size (Fig.2B, C). Both paratypes are smaller than the holotype (30 mm high, 15 mm wide of KBF-OA-00093, and 9–16 mm high, 6–9 mm wide of KBF-OA-00094). One paratype (KBF-OA-00094) does not branch but has two stalks connected at the bottom, although this specimen, accidentally, is broken into two pieces (Fig. 2C, D). Tentacle size is 4.0 mm long and 0.5 mm wide for KBF-OA-00093 and 3.0 mm long and 0.5 mm wide for KBF-OA-00094 (Fig. 3C, D). Paratypes display three rows of pinnules along each side of tentacles, consistent with the holotype. Pinnule numbers in the outermost row are 13–16 for KBF-OA-00093, and 12–14 for KBF-OA-00094, compared to 12–16 for the holotype. All paratypes have the two forms of sclerites as well as holotype (Fig. 9, 10), and are similar in the composition. In all parts of all specimens, the vast majority of sclerites are spindles, with the percentages being approximately 83–94% (Table 2).

Table 2. Sclerite composition of *Xenia konohana* sp. nov.

		Tentacles		Polyp body		Stalk	
		platelets	**spindles**	**platelets**	**spindles**	**platelets**	**spindles**
KBF-OA-00092 (holotype)	Fig. 2A	n = 124		n = 83		n = 104	
		7.3%	92.7%	4.8%	95.2%	7.7%	92.3%
KBF-OA-00093 (paratype)	Fig. 2B	n = 123		n = 132		n = 85	
		5.7%	94.3%	10.6%	89.4%	7.1%	92.9%
KBF-OA-00094 (paratype)	Fig. 2C	n = 138		n = 103		n = 91	
		10.1%	89.9%	5.8%	94.2%	6.6%	93.4%
	Fig. 2D	n = 92		n = 152		n = 96	
		12.0%	88.0%	17.1%	82.9%	7.3%	92.7%

Locality. The species is common in waters around Oshima Island, Miyazaki, Japan, at depths from 5 to 10 m. Specimens exist attached to the surface of rocks or rock debris.

Etymology. Konohana is named after a goddess in Japanese mythology, "Konohanasakuya-hime" ("hime" is "princess" in English). Her shrine is in Miyazaki Prefecture. The present study also proposes a standard Japanese name "konohana-umiazami" for *X. konohana* sp. nov. The specimen KBF-OA-00092 is designated as the standard specimen for this new Japanese name.

Remarks. Most *Xenia* species have only ellipsoid platelets or spheroid sclerites (Halász et al. 2019). Although only two species, *X. membranacea* Schenk, 1896 and *X. depressa* Kükenthal, 1909 have been reported to display rod-shaped sclerites in their original descriptions, this type of sclerite has not been found in the syntype of *X. membranacea* (Halász et al. 2019), and *X. depressa* has never been re-described and the existence of the type materials are unknown. Therefore, we treated the existence of rod-shaped sclerites as either incorrect for *X. membranacea* or unverified for *X. depressa* in this study. On the other hand, *X. konohana* sp. nov. (= *Xenia* sp. 1 by Koido et al. 2019) has unique spindle sclerites in addition to ellipsoid platelets (Figs 4–10). This combination does not occur in other species in the genus. Moreover, it is clear that spindles are the majority sclerites in tentacles, polyp body and stalks for all three specimens (KBF-OA-00092 to KBF-OA-00094).

All three specimens (KBF-OA-00092 to KBF-OA-00094) were nearly identical in sclerite shape, size and composition of two types of sclerite forms (xeniid platelets and unique spindles), number of pinnules, and molecular phylogenetic position. Eight species of *Xenia* (*X. blumi* Schenk, 1896, *X. crassa* Schenk, 1896, *X. cylindrica* Roxas 1933, *X. fisheri* Roxas, 1933, *X. garciae* Bourne, 1895, *X. hicksoni* Ashworth, 1899, *X. ternatana* Schenk, 1896, and *X. viridis* Schenk, 1896), which partly overlap with *X. konohana* sp. nov. in exhibiting platelet sclerites, 3–4 rows of pinnules and 12–23 outermost row of pinnules, are distinguishable by the absence of the specific sclerite form, "unique spindle" (Table 3). A variation of pinnules has been reported in many species in xeniid genera, and the number of pinnules is likely to be unreliable as a character to determine the species boundaries (Halász et al. 2019; McFadden et al. 2017). Therefore, the information on sclerites is more important than ever as a character for identifying species boundaries.

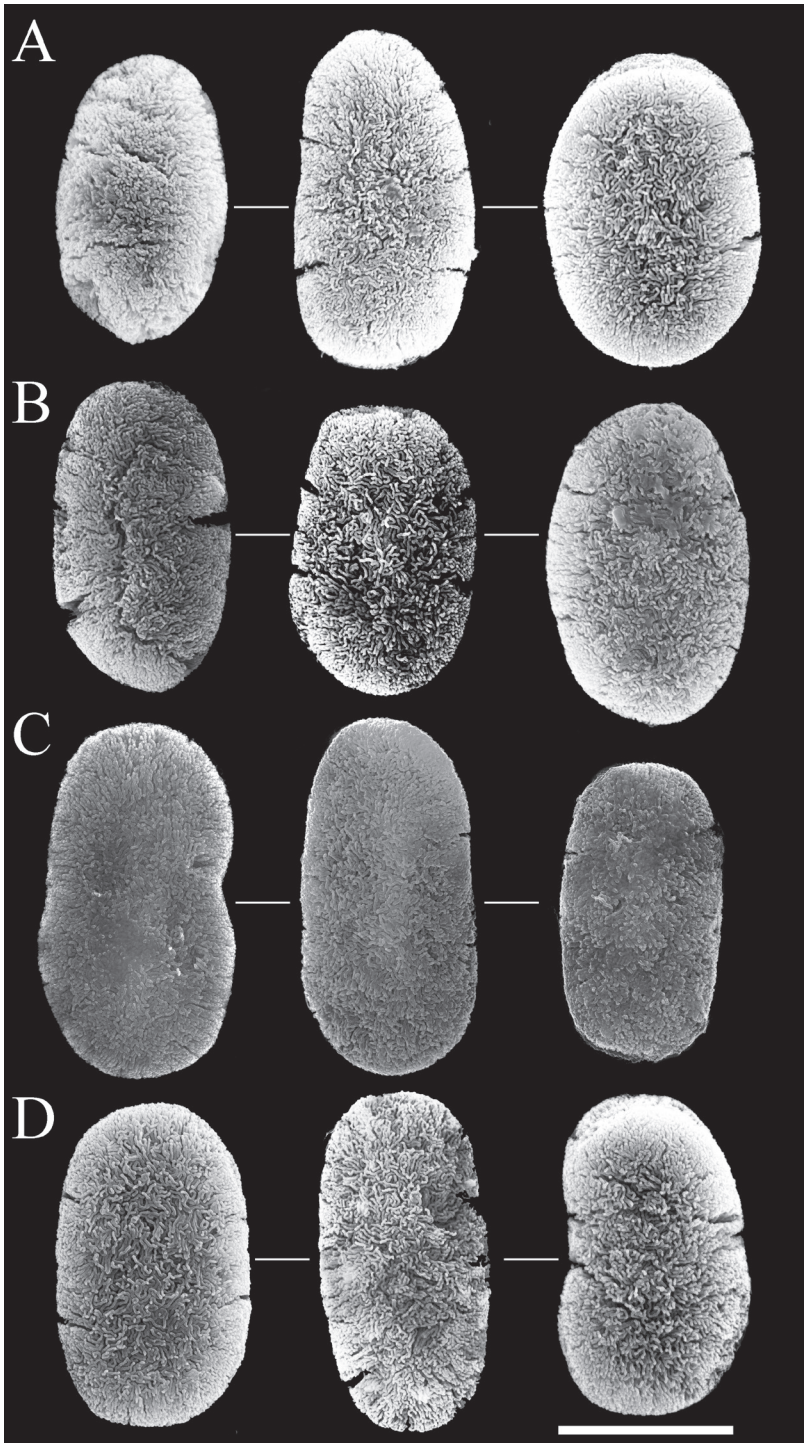

Figure 6. Scanning electron micrographs of platelets of *Xenia konohana* sp. nov., holotype KBF-OA-0009 **A** in tentacles **B** in polyp body **C** in stalk surface **D** in branch surface. Scale bar: 0.010 mm.

Table 3. Morphological comparison with congeneric species. *including oval, round, circles, discs, and biscuit-like shapes. Dashes means absent. Question marks mean unverified. NR means not reported. Note that morphological data were referred from the re-description paper by Halász et al. (2019) rather than the original descriptions for some species.

Species	Rows of pinnules	Pinnules in the outermost row	Sclerites			Crest on the sclerites	Main branch	Secondary branches	References
			platelets*	rods	Spindles				
X. bauiana	4	26–30	present	–	–	–	NR	NR	Halász et al. 2019
X. blumi	3	18–20	present	–	–	–	NR	NR	Halász et al. 2019
X. crassa	3–4	13–18	present	–	–	present	NR	NR	Halász et al. 2019
X. cylindricacy	3	18–20	present	–	–	NR	2	–	Roxas 1933
X. depressa	2	18–26	present	?	–	NR	NR	NR	Kükenthal 1909
X. delicata	3–4	18–23	–	–	–	–	0–5	0–3	Halász et al. 2019
X. elongata	3–4	20–24	present	–	–	NR	2–3	–	Dana 1846, Imahara 1992
X. fimbriata	3	8–15	–	–	–	NR	2–3	present	Utinomi 1955
X. fisheri	3	18–22	present	–	–	NR	–	–	Roxas 1933
X. flexibilis	4	14–32	present	–	–	–	NR	NR	Halász et al. 2019
X. fusca	4(3–5)	14–22	present	–	–	–	NR	NR	Halász et al. 2019
X. garciae	3	16–22	present	–	–	present	–	–	Halász et al. 2019
X. grasshoffi	4	15–24	present	–	–	present	NR	NR	Halász et al. 2019
X. hicksoni	3	12–20	present	–	–	NR	usually branched	2	Ashworth 1899, Utinomi 1950
X. kuekenthali	1	8–10	–	–	–	–	5	0–2	Halász et al. 2019
X. kusimotoensis	2	10–12	present	–	–	NR	2	–	Utinomi 1955
X. lepida	3	28–34	–	–	–	–	present	3rd branches	Halász et al. 2019
X. mayi	5	24–32	present	–	–	NR	single or divided	–	Roxas 1933
X. membranacea	4	20–25	present	–	–	present	8	NR	Halász et al. 2019
X. multipinnata	3–4	40–50	–	–	–	NR	present	–	Tixier-Durivault 1966
X. multispiculata	2–3	26–30	present	–	–	NR	present	–	Kükenthal 1909
X. mucosa	4	30–42	–	–	–	–	2	0–2	Halász et al. 2019
X. novaebritanniae	2	9–10	present	–	–	–	NR	NR	Halász et al. 2019
X. rubens	4(3–5)	12–19	present	–	–	–	2	–	Halász et al. 2019
X. sansibariana	4	26–33	–	–	–	–	NR	NR	Halász et al. 2019
X. stellifera	4–9	<9	present	–	–	NR	present	present	Verseveldt 1977
X. ternatana	3	15–23	present	–	–	present	NR	NR	Halász et al. 2020
X. tripartita	3	5–6	present	–	–	NR	–	–	Roxas 1933
X. tumbatuana	3	NR	–	–	–	NR	present	–	May 1898
X. umbellata	3	19–22	present	–	–	–	–	–	Halász et al. 2019
X. viridis	3	15–22	present	–	–	present	NR	NR	Halász et al. 2019
***X. konohana* sp. nov.**	**3**	**12–18**	**present**	**–**	**Present**	**–**	**2–3**	**–**	**This study**

Molecular phylogenetic results

Molecular phylogenetic trees using the ML and Bayes methods showed very similar topologies. Therefore, in this study, only ML trees are shown (Figs 11, 12). As pointed out in previous studies (Halász et al. 2019; Benayahu et al. 2021), the genus *Xenia* is paraphyletic and polyphyletic with some other taxa, and separated into three clades (clades X1–X3) in the *mtMutS+COI+28S* tree (Fig. 11). All three clades were supported by high bootstrap values (75 to 99%) and posterior probabilities (1). Asides from *Xenia*, clade X1 included

Ovabunda, clade X2 included *Heteroxenia*, and clade X3 included *Sansibia*, *Yamazatum* and *Unomia*. All three specimens of *X. konohana* sp. nov., which had the same DNA sequences for all four markers, belonged to clade X1 forming a sister clade with *Ovabunda* spp., *X. umbellata* and *X. hicksoni*, and united with *X. lepida* Verseveldt, 1971 and *X. viridis* within a strongly supported subclade (bootstrap values: 95%, posterior probability: 1).

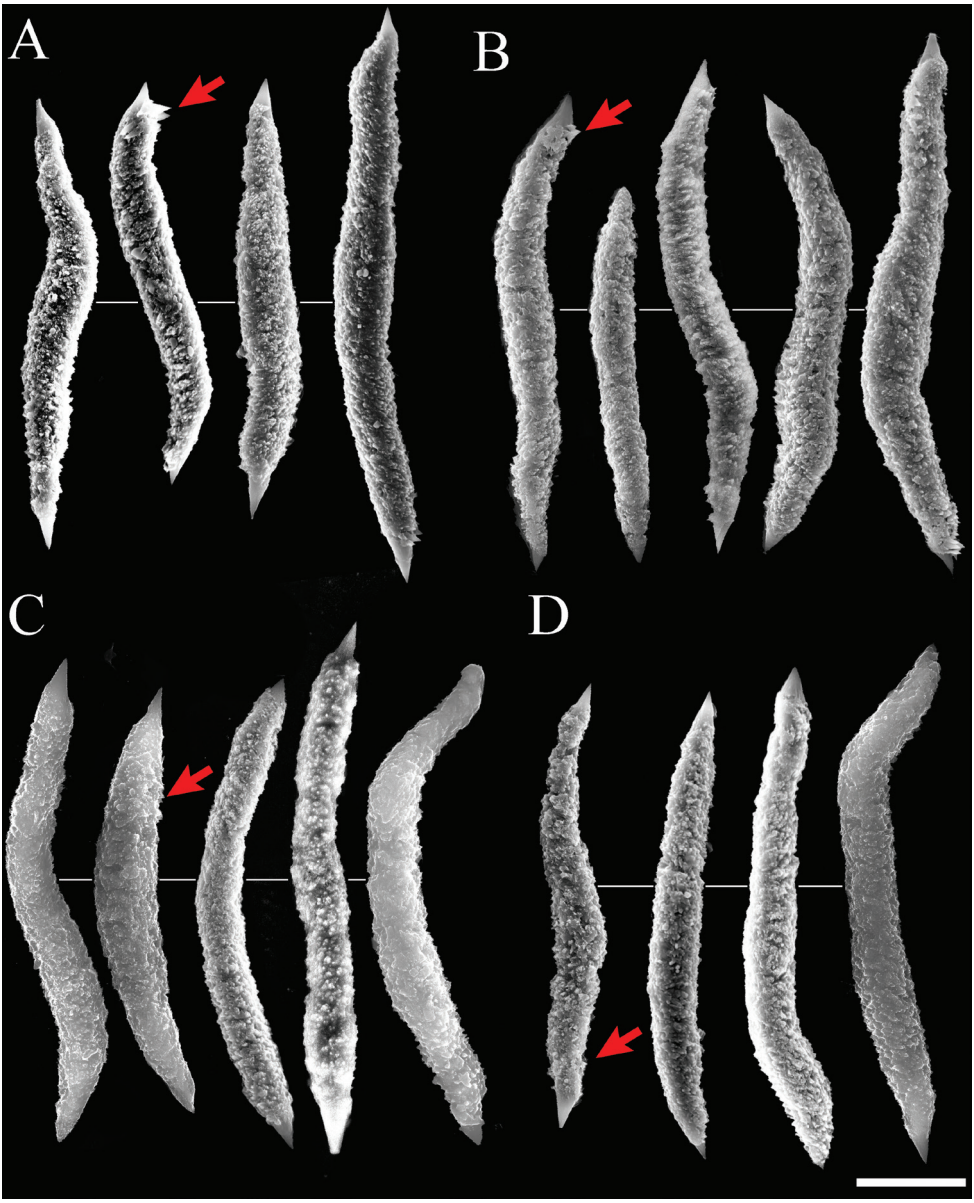

Figure 7. Scanning electron micrographs of spindles of *Xenia konohana* sp. nov., holotype KBF-OA-00092 **A** in tentacles **B** in polyp body **C** in stalk surface **D** in branch surface. Arrow indicates thorns on the surface of spindles. Scale bar: 0.010 mm.

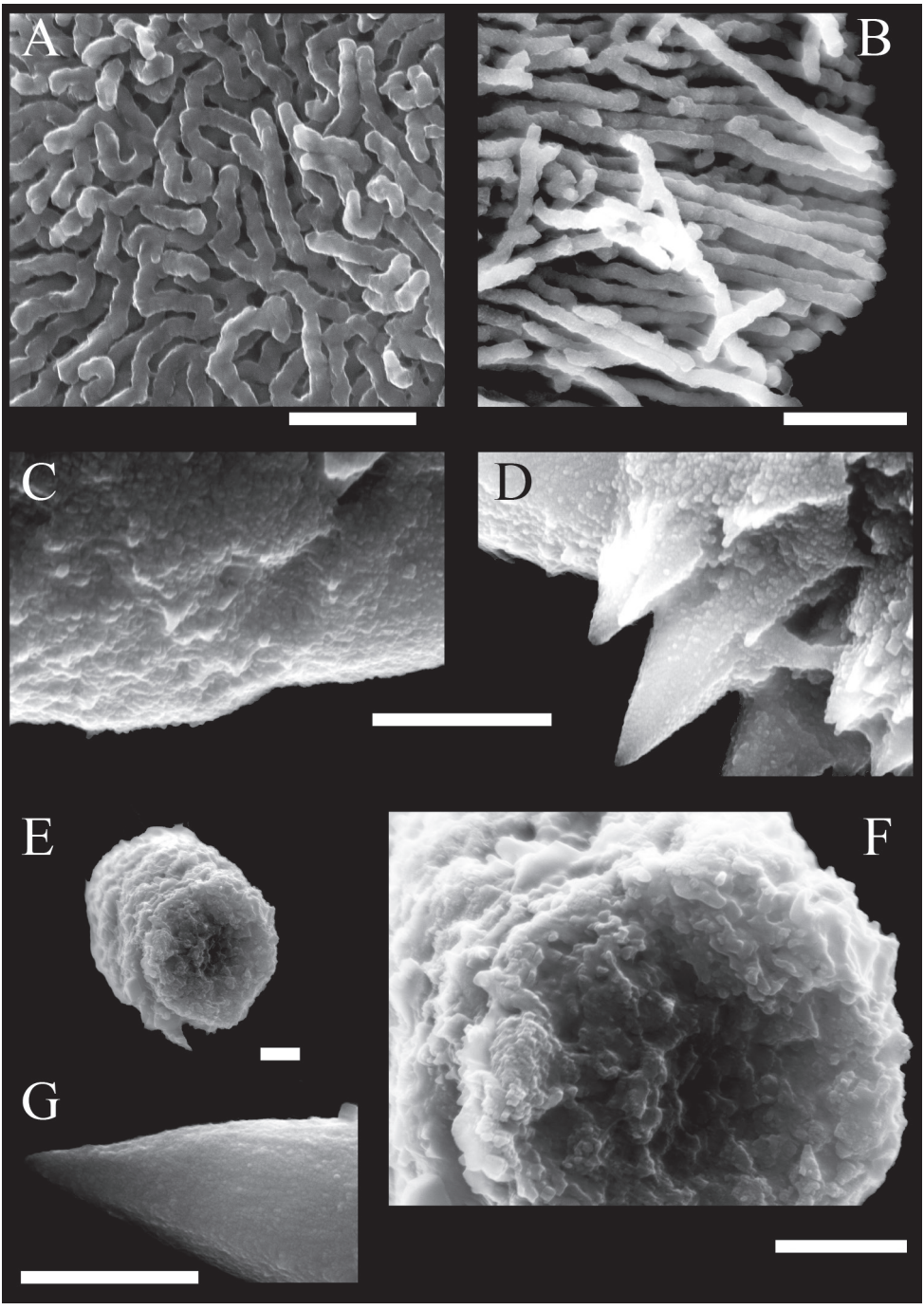

Figure 8. Scanning electron micrographs of the surface of sclerites in tentacles of *Xenia konohana* sp. nov., holotype KBF-OA-00092 **A** surface of platelets covered by minute papillae **B** broken platelets with radial dendritic rods **C** central surface of spindle covered by minute granular **D** thorns on the surface of spindles **E** broken spindle **F** close-up view of a broken spindle with fused grain **G** tip of a spindle. Scale bar: 0.001 mm.

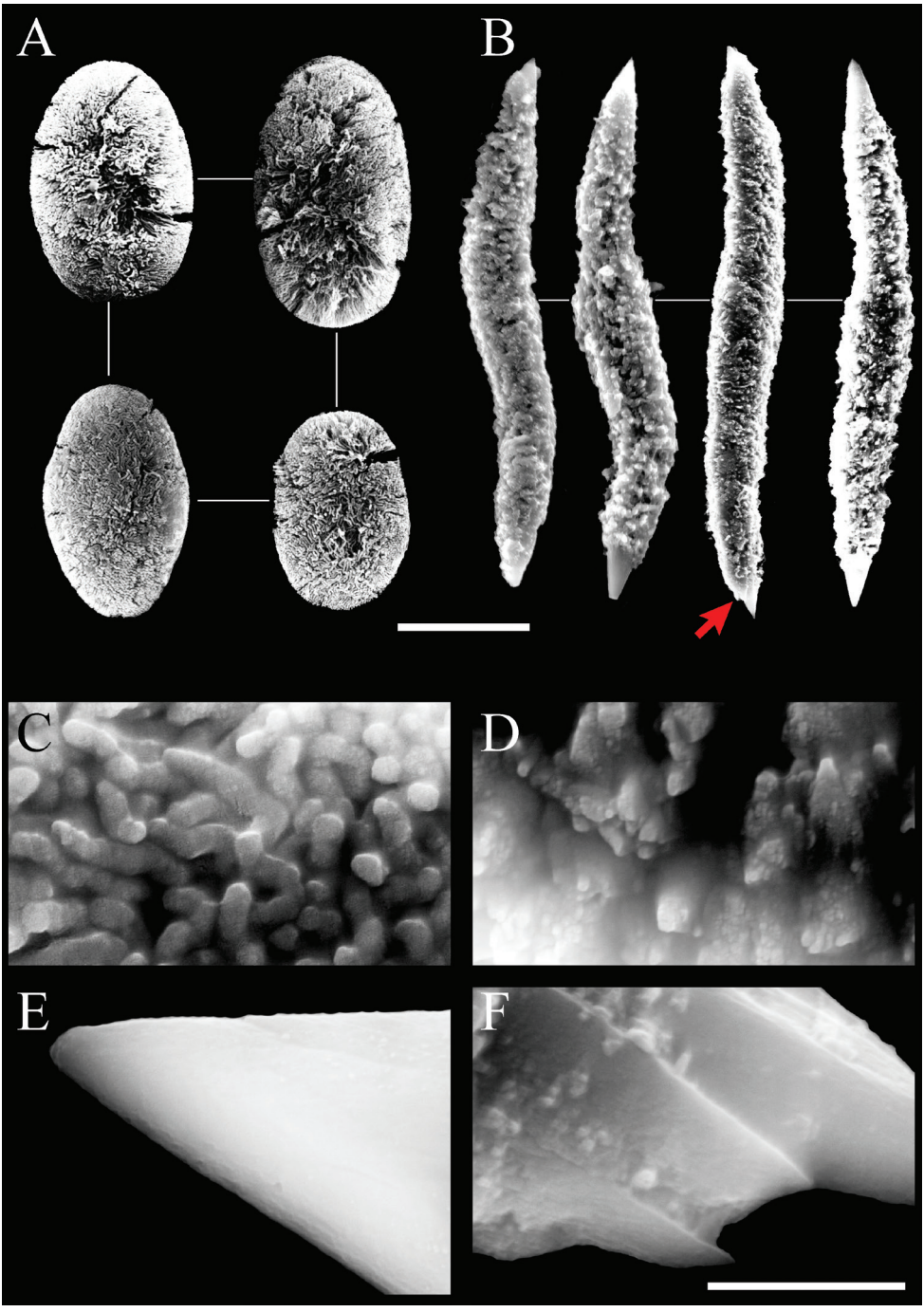

Figure 9. Scanning electron micrographs of paratype (KBF-OA-00093) of *Xenia konohana* sp. nov.: **A** platelets **B** spindles (arrow indicates thorns on the surface of spindles) **C** surface of platelets **D** central surface of spindle **E** tip surface of a spindle **F** thorns on the surface of spindles. Scale bar: 0.01 mm (**A, B**); 0.001 mm (**C–F**).

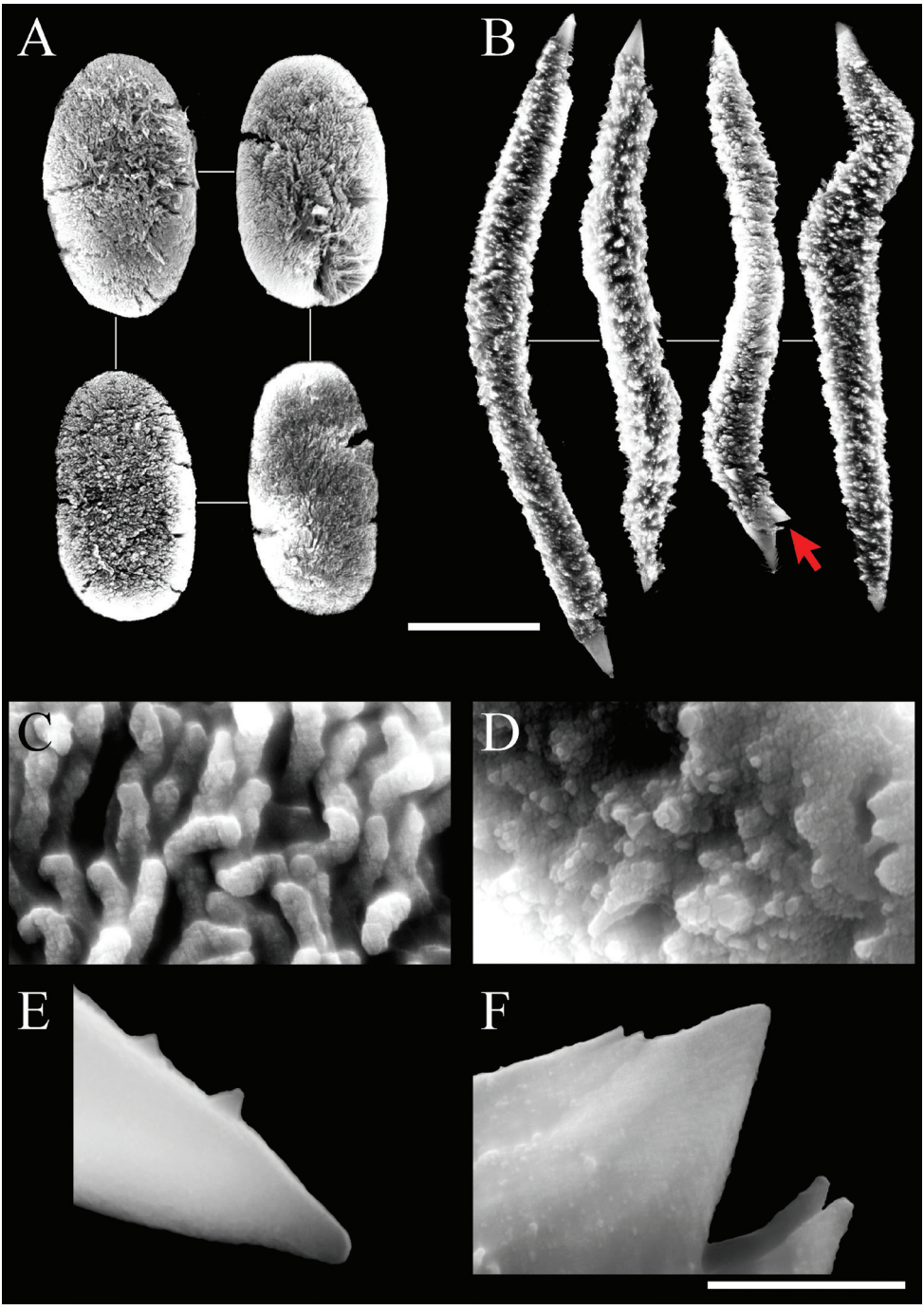

Figure 10. Scanning electron micrographs of paratype (KBF-OA-00094) of *Xenia konohana* sp. nov.: **A** platelets **B** spindles (arrow indicates thorns on the surface of spindles) **C** surface of platelets **D** central surface of spindle **E** tip surface of a spindle **F** thorns on the surface of spindles. Scale bar: 0.01 mm (**A, B**); 0.001 mm (**C–F**).

On the other hand, in the *ND2* tree, *Xenia* was separated into only two clades (XN1 and XN2) (Fig. 12). Clade XN1 was strongly supported by high bootstrap value (100%) and posterior probability (1), and included the same members with all three specimens of *X. konohana* sp. nov. in clade X1 in the *mtMutS+COI+28S* tree. For clade XN2, this clade was not supported by bootstrap values and posterior probabilities, but three *Xenia* species and *Heteroxenia mindorensis* in this clade were genetically identical. Clade XN2 included members belonging to both clades X2 and X3 in the *mtMutS+COI+28S* tree.

Although *X. viridis* was not genetically separated from *X. konohana* sp. nov. in the *ND2* tree (Fig. 12), they were clearly separated from each other in the *mtMutS+COI+28S* tree (Fig. 11). Thus, the molecular phylogenetic tree based on the concatenated DNA sequences of *mtMutS*, *COI*, and *28S*, and the tree based on *ND2* support the phylogenetic position of *X. konohana* sp. nov. in the genus *Xenia* (Figs 11, 12).

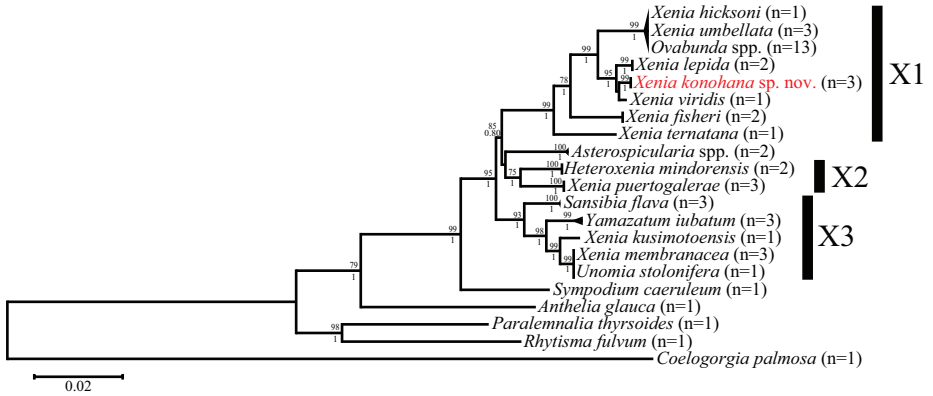

Figure 11. Phylogenetic relationships of species in the Xeniidae based on the concatenated *mtMutS, COI* and *28S* sequences. Numbers above main branches show percentages of bootstrap values (> 50%) in maximum likelihood analysis; numbers below main branches show Bayesian posterior probabilities. X1, X2 and X3 denote clades defined by McFadden et al. (2014b). *Xenia konohana* sp. nov. is shown in red.

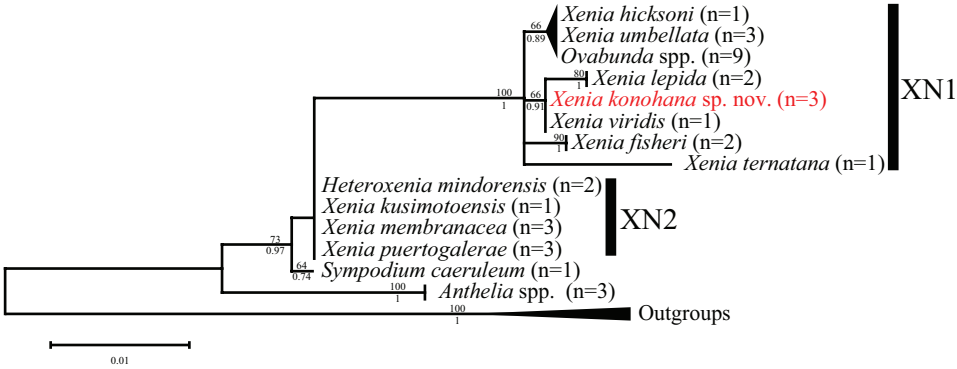

Figure 12. Phylogenetic relationships of species in the Xeniidae based on *ND2* sequences. Numbers above main branches show percentages of bootstrap values (> 50%) in maximum likelihood analysis; numbers below main branches show Bayesian posterior probabilities. *Xenia konohana* sp. nov. is shown in red.

Discussion

The genus *Xenia* is polyphyletic and paraphyletic with other xeniid genera such as *Ovabunda*, *Heteroxenia*, *Sansibia*, *Asterospicularia*, *Unomia*, and *Yamazatum* based on molecular studies (Janes et al. 2014; McFadden et al. 2014b; Benayahu et al. 2018a; Halász et al. 2019; Benayahu et al. 2021). In the present study, *Xenia* was also polyphyletic as well as paraphyletic with some other genera (Figs 11, 12), but *X. konohana* sp. nov. formed a clade with two congeneric species, *X. lepida* and *X. viridis*, and was closely related to a sister clade with *Ovabunda* spp., *X. hicksoni*, and *X. umbellata*. These four *Xenia* species are similar to *X. konohana* sp. nov. in the number of rows and the outermost row of pinnules, but they do not exhibit spindle sclerites. *Ovabunda* exhibits only simple platelets like *Xenia*, but it also displays a corpuscular surface microstructure on platelet surfaces. *Xenia*, including *X. konohana* sp. nov., exhibits a dendritic microstructure on these surfaces of simple platelets. Further taxonomic revision of *Xenia* and related genera such as *Ovabunda*, *Heteroxenia*, *Sansibia*, *Asterospicularia*, *Unomia*, *and Yamazatum* may be necessary due to these phylogenetic relationships. Still, we conclude that *Xenia konohana* sp. nov. is a new member of *Xenia* based on molecular phylogenetic relationships and the presence of unique spindles along with *Xenia*-specific ellipsoid platelets with dendritic surface microstructure.

Acknowledgements

We thank T. Mezaki (Kuroshio Biological Research Foundation) and S. Nakachi (Natural History Lab.) for their assistance with microstructure analyses and sampling. We also thank Y. Oku (Okinawa Churaumi Aquarium) and Coral Lab. of University of Miyazaki for their assistance with sampling; and Y. Goto (Bio-Imaging Lab, University of Miyazaki), K. Arai, T. Matsuzaki and T. Okumura (Center for Advanced Marine Core Research, Kochi University) for assistance with SEM operations. This study was funded by a grant from the Kuroshio Biological Research Foundation to T. Koido, and by JSPS KAKENHI (No.18K06423) to H. Fukami.

References

Alderslade P (2001) Six new genera and six new species of soft corals, and some proposed familial and subfamilial changes within the Alcyonacea (Coelenterata: Octocorallia). Bulletin of the Biological Society of Washington 10: 15–65.

Ashworth JH (1899) The structure of *Xenia hicksoni*, nov. sp., with some observations on *Heteroxenia elizabethae*, Kölliker. Quarterly Journal of Microscopical Science 42(3): 245–304. [pls 23–27] https://doi.org/10.1242/jcs.s2-42.167.245

Benayahu Y, Loya Y (1987) Long-term recruitment of soft-corals (Octocorallia: Alcyonacea) on artificial substrata at Eilat (Red Sea). Marine Ecology Progress Series 38: 161–167. https://doi.org/10.3354/meps038161

Benayahu Y (2010) A new genus of a soft coral of the family Xeniidae (Cnidaria: Octocorallia) from Japan. Galaxea 12: 53–64. https://doi.org/10.3755/galaxea.12.53

Benayahu Y, van Ofwegen LP, McFadden CS (2018a) Evaluating the genus *Cespitularia* Milne Edwards & Haime, 1850, with descriptions of new genera of the family Xeniidae (Octocorallia, Alcyonacea). ZooKeys 754: 63–101. https://doi.org/10.3897/zookeys.754.23368

Benayahu Y, van Ofwegen LP, Dai CF, Jeng MS, Soong K, Shlagman A, Du SW, Hong P, Imam NH, Chung A, Wu T, McFadden CS (2018b) The octocorals of Dongsha Atoll (South China Sea): an iterative approach to species identification using classical taxonomy and molecular barcodes. Zoological Studies 57: e50.

Benayahu Y, Ekins M, McFadden CS (2021) Overview of the genus *Sympodium* Ehrenberg, 1834 (Octocorallia, Alcyonacea, Xeniidae), with the description of new species, revealing regional endemism. Zootaxa 5072(4): 324–350. https://doi.org/10.11646/zootaxa.5072.4.2

Brockman SA, McFadden CS (2012) The mitochondrial genome of *Paraminabea aldersladei* (Cnidaria: Anthozoa: Octocorallia) supports intramolecular recombination as the primary mechanism of gene rearrangement in octocoral mitochondrial genomes. Genome Biology and Evolution 4: 994–1006. https://doi.org/10.1093/gbe/evs074

Cordeiro R, McFadden C, van Ofwegen L, Williams G (2021) World List of Octocorallia. Xeniidae Ehrenberg, 1828. World Register of Marine Species. http://www.marinespecies.org/aphia.php?p=taxdetails&id=125271 [Accessed on 2021–10–20]

Dana JD (1846) Zoophytes. United States Exploring Expedition during the years 1838–1842. Lea and Blanchard, Philadelphia 7: 1–740. [61 pls]

Fabricius K, Alderslade P (2001) Soft Corals and Sea Fans: A Comprehensive Guide to the Tropical Shallow-Water Genera of the Central-West Pacific, the Indian Ocean and the Red Sea. Australian Institute of Marine Science, Townsville, 264 pp.

Halász A, McFadden CS, Toonen R, Benayahu Y (2019) Re-description of type material of *Xenia* Lamarck, 1816 (Octocorallia: Xeniidae). Zootaxa 4652: 201–239. https://doi.org/10.11646/zootaxa.4652.2.1

Imahara Y (1992) Octocorallia (Stolonifera, Telestacea and Alcyonacea). In: Nishimura S (Ed.), Guide to seashore animals of Japan with color pictures and key. Hoikusha Publishing Co. Ltd., Osaka 1: 69–91. [pls 13–19]

Janes MP, McFadden CS, Chanmethakul T (2014) A new species of *Ovabunda* (Octocorallia, Xeniidae) from the Andaman Sea, Thailand with notes on the biogeography of this genus. ZooKeys 431: 1–17. https://doi.org/10.3897/zookeys.431.7751

Koido T, Imahara Y, Fukami H (2019) High species diversity of the soft coral family Xeniidae (Octocorallia, Alcyonacea) in the temperate region of Japan revealed by morphological and molecular analyses. ZooKeys 862: 1–22. https://doi.org/10.3897/zookeys.862.31979

Kükenthal W (1909) Diagnosen neuer Alcyonarien. (7. Mitteilung). Zoologischer Anzeiger 35(1/2): 46–53.

May W (1898) Die von Dr. Stuhlmann im Jahre 1889 gesammelten ostafrikanischen Alcyonaceen des Hamburgers Museums. Jahrbuch der Hamburgischen Wissenschaftlichen Anstalten 15(2): 1–38. https://doi.org/10.5962/bhl.title.23020

McFadden CS, France SC, Sanchez JA, Alderslade P (2006) A molecular phylogenetic analysis of the Octocorallia (Cnidaria: Anthozoa) based on mitochondrial protein-coding

sequences. Molecular Phylogenetics and Evolution 41: 513–527. https://doi.org/10.1016/j.ympev.2006.06.010

McFadden CS, Benayahu Y, Pante E, Thoma JN, Nevarez PA, France SC (2011) Limitations of mitochondrial gene barcoding in Octocorallia. Molecular Ecology Resources 11(1): 19–31. https://doi.org/10.1111/j.1755-0998.2010.02875.x

McFadden CS, van Ofwegen LP (2012) Stoloniferous octocorals (Anthozoa, Octocorallia) from South Africa, with descriptions of a new family of Alcyonacea, a new genus of Clavulariidae, and a new species of *Cornularia* (Cornulariidae). Invertebrate Systematics 26: 331–356. https://doi.org/10.1071/IS12035

McFadden CS, Brown AS, Brayton C, Hunt CB, van Ofwegen LP (2014a) Application of DNA barcoding in biodiversity studies of shallow-water octocorals: Molecular proxies agree with morphological estimates of species richness in Palau. Coral Reefs 33: 275–286. https://doi.org/10.1007/s00338-013-1123-0

McFadden CS, Reynolds AM, Janes MP (2014b) DNA barcoding of xeniid soft corals (Octocorallia: Alcyonacea: Xeniidae) from Indonesia: species richness and phylogenetic relationships. Systematics & Biodiversity 12: 247–257. https://doi.org/10.1080/14772000.2014.902866

McFadden CS, Haverkort-Yeh R, Reynolds AM, Halász A, Quattrini AM, Forsman ZH, Benayahu Y, Toonen RJ (2017) Species boundaries in the absence of morphological, ecological or geographical differentiation in the Red Sea Octocoral genus *Ovabunda* (Alcyonacea: Xeniidae). Molecular Phylogenetics and Evolution 112: 174–184. https://doi.org/10.1016/j.ympev.2017.04.025

McFadden CS, Gonzalez A, Imada R, Shi SS, Hong P, Ekins M, Benayahu Y (2019) Molecular operational taxonomic units reveal restricted geographic ranges and regional endemism in the Indo-Pacific octocoral family Xeniidae. Journal of Biogeography 46: 992–1006. https://doi.org/10.1111/jbi.13543

Ronquist F, Teslenko M, van der Mark P, Ayres D, Darling A, Höhna S, Larget B, Liu L, Suchard MA, Huelsenbeck JP (2012) MrBayes 3.2: Efficient Bayesian phylogenetic inference and model choice across a large model space. Systematic Biology 61: 539–542. https://doi.org/10.1093/sysbio/sys029

Roxas HA (1933) Philippine Alcyonaria. The families Cornulariidae and Xeniidae. The Philippine Journal of Science 50: 49–110.

Tamura K, Stecher G, Peterson D, Filipski A, Kumar S (2013) MEGA6: Molecular Evolutionary Genetics Analysis Version 6.0. Molecular Biology and Evolution 30: 2725–2729. https://doi.org/10.1093/molbev/mst197

Tixier-Durivault A (1966) Quelques Octocoralliaires Australiens. Bulletin de la Museum Nationale d'Histoire naturelle Paris, Ser. 2, 37(4): 705–716.

Utinomi H (1950) Some xeniid alcyonarians from Japan and adjacent localities. Publications of the Seto Marine Biological Laboratory 1(3): 81–91. https://doi.org/10.5134/174440

Utinomi H (1955) Two new species of *Xenia* from Kusimoto (Coelenterata, Alcyonaria). Publications of the Seto Marine Biological Laboratory 4: 105–109.

Verseveldt J (1977) Australian Octocorallia (Coelenterata). Australian Journal of Marine and Freshwater Research 28: 171–240. https://doi.org/10.1071/MF9770171

ZooKeys 1085: 51–68 (2022)
doi: 10.3897/zookeys.1085.75885
https://zookeys.pensoft.net

RESEARCH ARTICLE

A peer-reviewed open-access journal
ZooKeys
Launched to accelerate biodiversity research

The genus *Blepharicera* Macquart, 1843 newly recorded from Sichuan, China with descriptions of three new species (Diptera, Blephariceridae)

Xiao Zhang[1], Zehui Kang[1]

1 *Key Lab of Integrated Crop Pest Management of Shandong Province, College of Plant Health and Medicine, Qingdao Agricultural University, Qingdao 266109, China*

Corresponding author: Zehui Kang (kangzehui1987@163.com)

Academic editor: Gunnar Kvifte | Received 28 September 2021 | Accepted 27 January 2022 | Published 4 February 2022

http://zoobank.org/6CC903FD-C011-4C19-9058-BE0D35172286

Citation: Zhang X, Kang Z (2022) The genus *Blepharicera* Macquart, 1843 newly recorded from Sichuan, China with descriptions of three new species (Diptera, Blephariceridae). ZooKeys 1085: 51–68. https://doi.org/10.3897/zookeys.1085.75885

Abstract

The genus *Blepharicera* Macquart, 1843 is recorded from Sichuan, China for the first time with the following three new species: *B. gengdica* **sp. nov.**, *B. balangshana* **sp. nov.** and *B. kongsica* **sp. nov.**, increasing the number of Chinese *Blepharicera* species to eleven. The new species are distinguished from congeners mainly by their male genitalia. Descriptions and illustrations for the new species and an updated key to Chinese *Blepharicera* species are presented.

Keywords

Blepharicerinae, chinese fauna, net-winged midge, taxonomy

Introduction

Family Blephariceridae, also called the net-winged midge, is a kind of slender delicate fly in lower Diptera. Compound eyes of blepharicerids are transversely divided into dorsal divisions and ventral divisions. Mandibles are absent in males and present in most females. Wings of blepharicerids have a net-like pattern of folds in the wing membrane. Larvae and pupae are often found on rocks in swiftly moving streams or waterfalls (Hogue 1981). Adults are usually found close to the natal stream resting on vegetation or logs (Courtney 2000a).

Blephariceridae is considered a small family with approximately 320 described species in 28 genera (Jacobson et al. 2011). Seven genera of Blephariceridae are known to occur in China (Kitakami 1931, 1950; Mannheims 1938; Kang and Yang 2012, 2014, 2015). *Agathon* Röder, 1890, *Bibiocephala* Osten Sacken, 1874 and *Neohapalothrix* Kitakami, 1938 are found in northeast China, *Apistomyia* Bigot, 1862 in Taiwan, *Horaia* Tonnoir, 1930 in southwest China, and *Philorus* Kellogg, 1903 in three provinces of China (Hebei, Sichuan and Taiwan). *Blepharicera* Macquart, 1843 is the most widely distributed genus of blepharicerids recorded from China, in seven provinces in both south and north China. Eight species of *Blepharicera* are known to occur in China (Kang and Yang 2014): *B. asiatica* (Brodsky, 1930) distributed in Yunnan and Guangxi Provinces, *B. dimorphops* Alexander, 1953 in Fujian, *B. hainana* Kang & Yang, 2014 and *B. macropyga* Zwick, 1990 from Hainan, *B. hebeiensis* Kang & Yang, 2014 in Heibei and Shanxi, *B. taiwanica* Kitakami, 1937 and *B. uenoi* Kitakami, 1937 in Taiwan, and *B. yamasakii* Kitakami, 1950 in Heilongjiang.

Blepharicera can be easily distinguished from other genera of Blephariceridae by the following features: head normally dichoptic in male and subholoptic in female; antennae with 13 flagellomeres; middle coxa of female with setose median outgrowth; base of hind basitarsus with obvious black setae; claws nonsetate dorsally; vein R with 3 branches, veins R_4 and R_5 separate for entire length; absence of cross vein bm-cu, presence of M_2 (Zwick 1990; Courtney 2000b; Jacobson et al. 2011).

Sichuan province is situated in southwestern China; it includes Sichuan Basin, and parts of the Qinghai-Tibetan Plateau and the Hengduan Mountain region, which has been designated as one of the world's biodiversity hotspots (Zhang and Ma 2008; Zhang et al. 2009). As a region of high biodiversity, however, the blepharicerid species in this area has been poorly described. Only one species belonging to *Philorus* was described by Kang and Yang (2012).

Several insect diversity investigations in Sichuan Province were initiated by the authors and other entomologists from 2013 to 2016, and the genus *Blepharicera* was found in Sichuan province for the first time (Fig. 1). In this paper, descriptions and illustrations for three new species from Sichuan, *B. gengdica* sp. nov., *B. balangshana* sp. nov. and *B. kongsica* sp. nov. are provided, and a key to Chinese *Blepharicera* species modified from Kang and Yang (2014) is also presented.

Figure 1. Distribution map of *Blepharicera* from Sichuan.

Material and methods

Adults were collected by insect net and light trap. Type specimens of the new species in this study were deposited in the Entomological Museum of China Agricultural University, Beijing, China (CAU) and the Entomological Museum of Qingdao Agricultural University, Shandong, China (QAU). Studies were based on whole-animal preparations and dissections. Photographs were captured by a Canon EOS 90D digital camera through a macro lens. Genitalia were prepared by immersing the apical portion of the abdomen in warm lactic acid for 0.5–1 hours. Specimens were examined and illustrations prepared by using a ZEISS Stemi 2000-C stereomicroscope. After examination, the removed abdomen was transferred to fresh glycerine and stored in a microvial pinned to the respective specimen. Structural terminology is based primarily on Courtney (2000b).

Taxonomy

Key to adult males of Chinese species of *Blepharicera*

Adult unknown in *B. uenoi* Kitakami

1 Dorsal division of compound eye large, at least 1/2 of ventral division (Fig. 5a, b) **2**

– Dorsal division of compound eye small, at most 1/10 of ventral division (Figs 3a, b, 8a, b) **5**

2 Gonostylus bifurcated **3**

– Gonostylus not bifurcated **4**

3 Ultimate flagellomere shorter than penultimate flagellomere; Rs 1.5 times as long as r-m; ventral branch of gonostylus glabrous (Kitakami 1937: figs 7, 8) ..... ***B. taiwanica*** **(Taiwan)**

– Ultimate flagellomere longer than penultimate flagellomere; Rs as long as or slightly longer than r-m; ventral branch of gonostylus with two tufts of short dense setae (Kang &Yang 2014: figs 23, 24) ..... ***B. macropyga*** **(Hainan)**

4 Dorsal division of compound eye as large as ventral division (Fig. 5a, b); epandrium trapeziform, posterior margin concave; cercus triangular; gonostylus without a semicircular inside lobe near base (Fig. 5a, b) ..... ***B. balangshana*** **sp. nov. (Sichuan)**

– Dorsal division of compound eye 1/2 as large as ventral division; epandrium semicircular, posterior margin rounded; cercus semi-elliptical; gonostylus with a semicircular inside lobe near base (Kang and Yang 2014: figs 14, 15) ..... ***B. hainana*** **(Hainan)**

5 Cercus triangular, posterior margin tapered medially (Figs 3c, 5c, 8c) **6**

– Cercus semicircular or semi-elliptical, posterior margin round medially **8**

6 Outer gonocoxal lobe straight ..... ***B. asiatica*** **(Yunnan, Guangxi; Afghanistan; India; Pakistan; Russia; Sri Lanka)**

– Outer gonocoxal lobe S-shaped 7

7 Ultimate flagellomere shorter than penultimate flagellomere (Fig. 8a); dorsal branch of gonostylus broader than ventral branch (Fig. 8c); inner gonocoxal lobe fusiform (Fig. 8c, d); dorsal carina inapparent (Fig. 8f) ..... ***B. kongsica*** **sp. nov. (Sichuan)**

– Ultimate flagellomere longer than penultimate flagellomere (Fig. 3a); dorsal branch of gonostylus as broad as ventral branch (Fig. 3c); inner gonocoxal lobe digitiform (Fig. 3c, d); dorsal carina apparent (Fig. 3f) ..... ***B. gengdica*** **sp. nov. (Sichuan)**

8 Mid coxa with a conical projection, conical projection about half as long as trochanter and densely with stiff black bristles towards tip (Kitakami 1950: fig. 49) ..... ***B. yamasakii*** **(Heilongjiang)**

– Mid coxa without projection like above **9**

9 Posterior margin of epandrium not distinctly concaved medially; cercus semicircilar; gonostylus bifurcated and strongly notched apically (Kang and Yang 2014: figs 8, 9, 11)..... ***B. dimorphops*** **(Fujian)**

– Posterior margin of epandrium concave medially, V-shaped; cercus semi-elliptical; gonostylus not bifurcated and slightly notched apically (Kang and Yang 2014: figs 18, 19, 20)..... ***B. hebeiensis*** **(Hebei, Shanxi)**

Blepharicera gengdica **sp. nov.**

http://zoobank.org/C46F8572-AFF6-45C0-A8D8-5783D5B8015B

Figs 2, 3

Diagnosis. Compound eye with dorsal division 1/20 as large as ventral division in male. Rs 1.5 times as long as r-m. Cercus triangular. Dorsal branch of gonostylus short; ventral branch longer and broader than dorsal branch, round apically. Outer gonocoxal lobe transparent, S-shaped; inner gonocoxal lobe digitiform. Dorsal carina apparent, tip slightly blunt.

Description. Male. Body length 4.50 mm, wing length 5.75 mm, wing width 2.00 mm.

Head (Figs 2a, 3a, b) pruinose, uniformly brownish black with black hairs. Compound eyes dichoptic, interocular ridge absent; each compound eye divided, callis oculi absent; dorsal division contiguous with ventral division, 1/20 as large as ventral division; dorsal division with 6–7 rows of ommatidia, ommatidia red-orange, larger in diameter, with omatrichia; ventral division black with omatrichia. Ocelli black. Scape and pedicel oval, brown with dark brown hairs; first flagellomere conical, basal 1/2 light brown, apical 1/2 brown, with brownish black hairs; other flagellomeres cylindrical, brown with brownish black hairs; ultimate flagellomere 1.3 times length of penultimate flagellomere. Clypeus oval, brownish black, twice as long as the width; labrum brown; labellum brown with brownish black hairs; proboscis about 0.67 times length of head width. Palpus with five segments, 1st segment almost invisible; 2nd and 3rd segments cylindrical, brownish yellow with brown hairs; 4th segment cylindrical, slightly swollen apically, brownish yellow with brown hairs; 5th segment slender, brownish yellow with brown hairs; relative length of distal four segments as 1.0: 1.2: 1.5: 2.9.

Thorax (Fig. 2b) pruinose. Pronotum and propleuron brown without hairs. Mesonotum dark brown with middle area of posterior margin light brown; scutellum dark brown with middle area light brown, with numerous hairs grouped at posterolateral corner; episternum dark brown; anepimeron light brown, katepimeron dark brown. Relative length of femur, tibiae and 1st to 5th tarsomeres in fore leg as 15: 15: 10.5: 4.3: 2.8: 1.3: 1, in mid leg as 15.5: 14.5: 9.0: 4.0: 2.5: 1: 1, in hind leg as 19.6: 17.6: 7.4: 2.4: 1.6: 1: 1. Fore coxa dark brown with brown hairs; mid and hind coxae pale with brownish black hairs; trochanters pale, anterior margin with black spot apically, with brownish black hairs; fore and mid femora light yellow basally and gradually darkened to dark brown apically, with brownish black hairs; hind femur light yellow

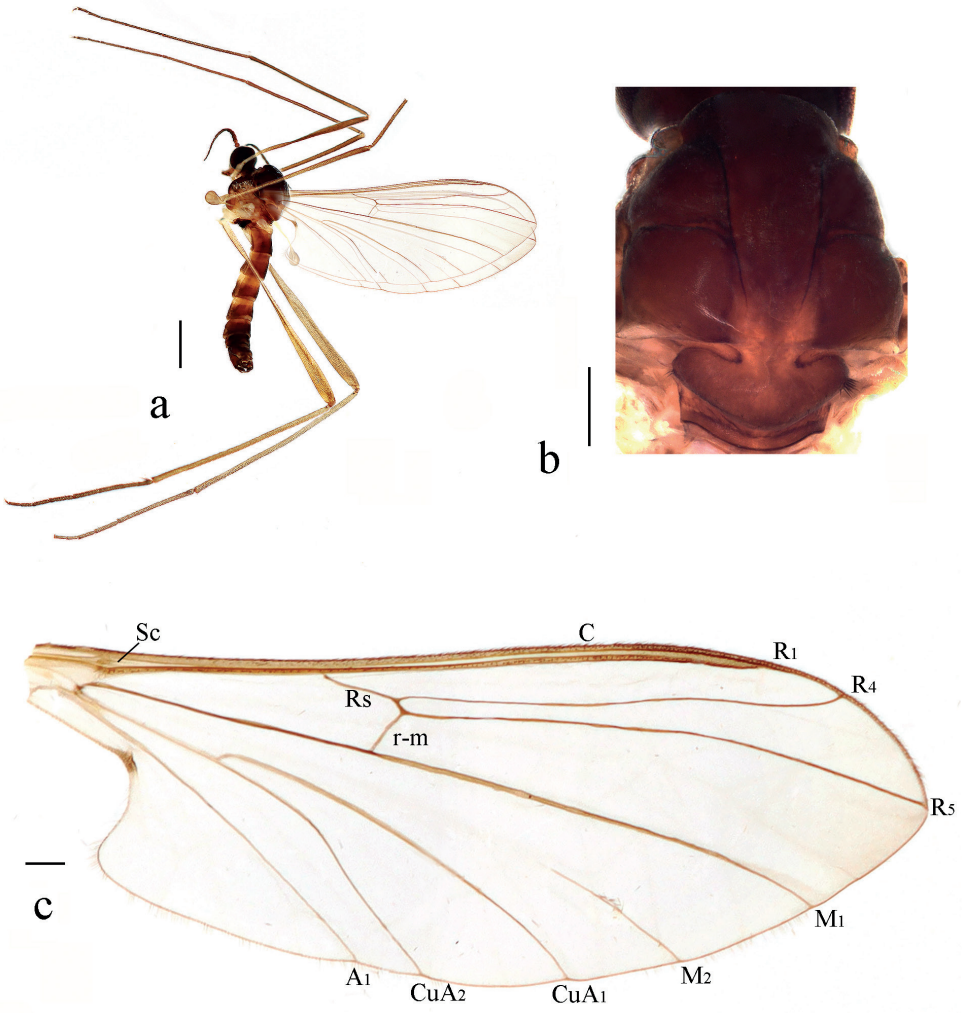

Figure 2. *Blepharicera gengdica* sp. nov. **a** habitus of male, lateral view **b** thorax, dorsal view **c** wing. Scale bars: 1.0 mm (**a**); 0.25 mm (**b, c**).

basally and gradually darkened to brownish yellow apically, with brownish black hairs; fore and mid tibiae dark brown with brownish black hairs; hind tibia brownish yellow with brown hairs; tarsomeres dark brown with brownish black hairs; claw dark brown. Tibial spurs 0–0–0. Wing (Fig. 2c) slightly brown apically, apical 1/3 of sc brown; veins brown. Sc rudimentary, not ending at base of Rs; Rs straight, 1.5 times as long as r-m; R_4 wavy, the length from end of R_1 to end of R_4 shorter than length from end of R_4 to end of R_5; r-m straight, including angle between r-m and Rs less than 90 degrees; the length from end of M_1 to end of M_2 longer than the length from end of M_2 to end of CuA_1. Base of halter pale, apex of halter grey with brownish black hairs.

Abdomen. First tergum dark brown with middle area pale, 2nd tergum dark brown, 3rd to 5th terga dark brown with basal 1/3 brownish yellow, 6th to 8th terga dark brown;

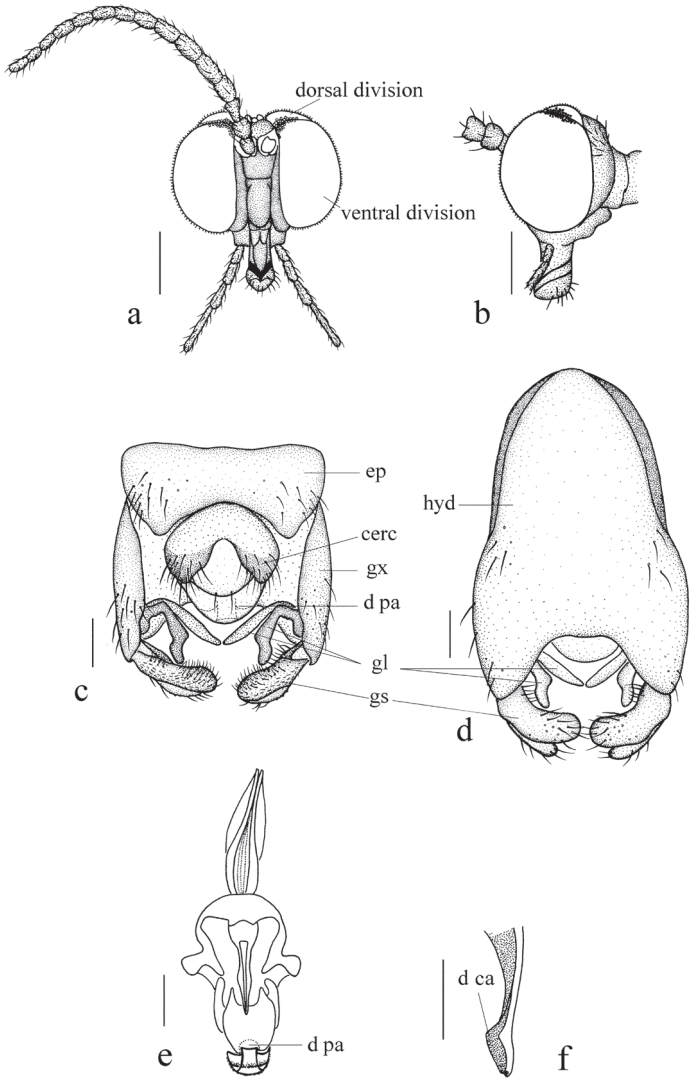

Figure 3. *Blepharicera gengdica* sp. nov. **a** male head, frontal view **b** male head, lateral view **c** male genitalia, dorsal view **d** male genitalia, ventral view **e** aedegal complex, dorsal view **f** tip of dorsal paramere, lateral view. Scale bars: 0.25 mm (**a, b**); 0.10 mm (**c–f**). Abbreviations: cerc = cercus; d ca = dorsal carina; d pa = dorsal paramere; ep = epandrium; gl = gonocoxal lobe; gs = gonostylus; gx = gonocoxite; hyd = hypandrium.

1st to 7th sterna brownish yellow with brownish black stripes laterally; abdomen with brownish black hairs. Male genitalia (Fig. 3c–f) dark brown. Epandrium trapeziform, posterior margin concaved medially, with several brown hairs. Cercus triangular, inner margin bulge, with several brown hairs; anal cone round with two long hairs apically. Gonostylus bifurcated, dorsal branch short, slightly swollen apically, with hairs; ventral branch longer and broader than dorsal branch, round apically, with long hairs. Gonocoxal lobe bifurcated, outer gonocoxal lobe transparent, S-shaped, round apically;

inner gonocoxal lobe digitiform, transparent. Hypandrium nearly triangular, twice as long as the width, round and slightly narrow basally, middle of each lateral margin slightly concave, posterior margin concave, with several brown hairs laterally. Dorsal paramere with posterior margin round; dorsal carina apparent, tip slightly blunt.

Female. Unknown.

Type material. ***Holotype*****:** male (CAU), China: Sichuan Province, Wenchuan County, Gengda, Fuyuan inn (Light trap), 2016.V.24, Zehui Kang.

Distribution. Currently known only from China (Sichuan).

Etymology. The specific name refers to the type locality Gengda.

Remarks. This new species is very similar to *B. parva* Zwick & Arefina, 2005 from the Russian Far East but can be separated by the cercus being tapered posteriorly and the outer gonocoxal lobe being S-shaped. In *B. parva*, the cercus is round, and the outer gonocoxal lobe is digitiform (Zwick and Arefina 2005). This new species is also similar to *B. yamasakii* from China, but it can be separated from the latter by the mid coxa without hairy projection in male, and the triangular cercus. In *B. yamasakii*, the mid coxa has a conical projection in the male which is about half as long as trochanter and has densely stiff black bristles towards tip, and the cercus is semicircular (Kitakami 1950).

Blepharicera balangshana **sp. nov.**

http://zoobank.org/5A4EDC48-D0B5-48B9-819E-A5796ADF6C02

Figs 4–6

Diagnosis. Compound eye with dorsal division as large as ventral division in the male. Scutellum pale brown with anterior margin yellow. Rs as long as r-m. Cercus triangular. Gonostylus slightly swollen and notched apically. Dorsal carina apparent, tip nearly perpendicular. Genital fork X-shaped in female.

Description. Male. Body length 4.50–5.00 mm, wing length 6.00–6.50 mm, wing width 2.00–2.50 mm.

Head (Figs 4a, 5a, b) pruinose, uniformly brown with dark brown hairs. Compound eyes dichoptic, interocular ridge absent; each compound eye divided, callis oculi absent; dorsal division contiguous with ventral division, as large as ventral division; dorsal division with 20 rows of ommatidia, ommatidia red-orange, larger in diameter, with omatrichia; ventral division black with omatrichia. Ocelli brownish yellow. Scape and pedicel oval, brown with brownish black hairs; first flagellomere constricted at base, flared at apex, basal 1/2 brownish yellow, apical 1/2 brownish black, with brownish black hairs; other flagellomeres cylindrical, brownish black with brownish black hairs; ultimate flagellomere 1.6 times length of penultimate flagellomere. Clypeus oval, brownish yellow, twice as long as the width; labrum brownish yellow; labellum brownish yellow with brown hairs; proboscis about 0.63 times length of head width. Palpus with five segments, 1st segment almost invisible; 2nd and 3rd segments cylindrical, yellow with brown hairs; 4th segment cylindrical, slightly swollen apically, basal 1/2 yellow, apical 1/2 brownish black, with brown hairs; 5th segment slender, brownish yellow with brown hairs; relative length of distal four segments as 1.0: 1.0: 1.1: 2.3.

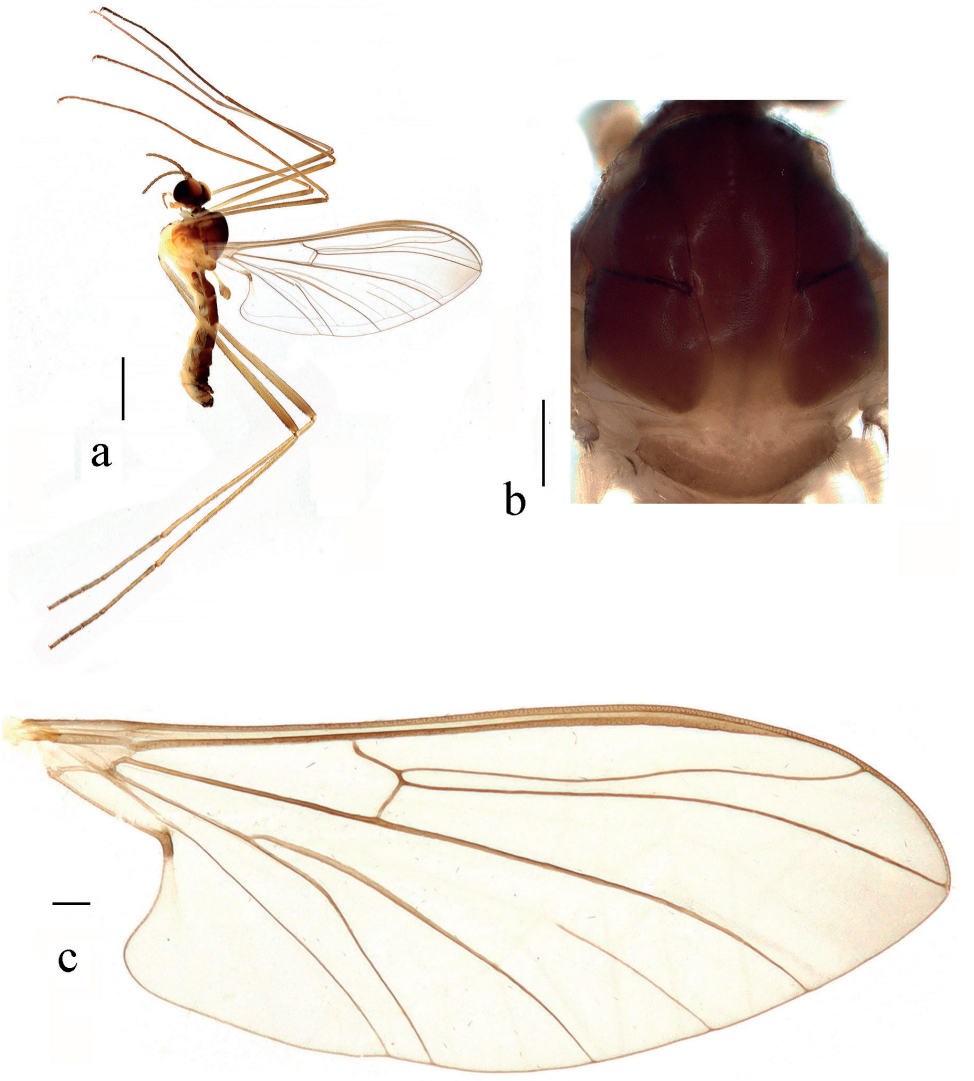

Figure 4. *Blepharicera balangshana* sp. nov. **a** habitus of male, lateral view **b** thorax, dorsal view **c** wing. Scale bars: 1.0 mm (**a**); 0.25 mm (**b, c**).

Thorax (Fig. 4b) pruinose. Pronotum and propleuron brown without hairs. Mesonotum dark brown with middle area of posterior margin yellow; scutellum pale brown with anterior margin yellow, with numerous hairs grouped at posterolateral corner; metanotum brown; episternum brown; epimeron yellow. Relative length of femur, tibiae and 1st to 5th tarsomeres in fore leg as 15: 13: 7.4: 3.4: 2: 1: 1, in mid leg as 15.4: 12.8: 7.4: 2.6: 2.4: 1: 1, in hind leg as 23: 20: 7.2: 2: 1.4: 1: 1. Fore coxa pale with basal margin brownish yellow, with brownish yellow hairs; mid and hind coxae pale with brownish black hairs; trochanters pale, anterior margin with black spot apically, with brownish black hairs; femora yellow basally and gradually darkened apically, with brownish black

hairs; fore and mid tibiae brown with brownish black hairs; hind tibia brownish yellow with brownish black hairs; tarsomeres brown with brownish black hairs; claw brown. Tibial spurs 0–0–0. Wing (Fig. 4c) slightly brown apically, apical 1/3 of sc brown; veins brown. Sc rudimentary, not ending at base of Rs; Rs slightly curved basally, as long as r-m; R_4 wavy, the length from end of R_1 to end of R_4 shorter than length from end of R_4 to end of R_5; r-m straight, included angle between r-m and Rs less than 90 degrees; the length from end of M_1 to end of M_2 as long as the length from end of M_2 to end of CuA_1. Base of halter pale, apex of halter brown with brownish black hairs.

***Abdomen*.** First tergum brown with middle area pale, 2nd tergum brown, 3rd to 5th terga brown with basal 1/3 brown, 6th to 8th terga brown; 1st sternum pale, 2nd to 6th sterna pale with brown stripes laterally, 7th sternum pale; abdomen with brown hairs. Male genitalia (Fig. 5c–f) brown. Epandrium trapeziform, posterior margin concave, with several brown hairs. Cercus triangular, inner margin bulge, with several brown hairs; anal cone round with two long hairs apically. Gonostylus slightly swollen and notched apically, outer side with a wide triangular lobe folded ventrally, with hairs. Gonocoxal lobe bifurcated, outer gonocoxal lobe transparent, rod-shaped, slightly curved; inner gonocoxal lobe transparent, rod-shaped, nearly straight, slenderer than outer gonocoxal lobe. Hypandrium rectangular, twice as long as the width, slightly narrow basally, posterior margin concave, with several brown hairs. Dorsal paramere with posterior margin round; dorsal carina apparent, tip nearly perpendicular.

Female. Body length 6.00 mm, wing length 7.50 mm, wing width 2.75 mm.

Head (Fig. 6a) pruinose. Compound eyes subholoptic, interocular ridge present; each compound eye divided, callis oculi present; dorsal division separated from ventral division, as large as ventral division; dorsal division with about 20 rows of ommatidia, ommatidia red-orange, larger in diameter, with omatrichia; ventral division black with omatrichia. Scape oval, brown with brown hairs; pedicel conical, dark brown with brown hairs; first flagellomere constricted at base, flared at apex, basal 1/2 brownish yellow, apical 1/2 brownish black, with brownish black hairs; other flagellomeres cylindrical, tapering apically, brownish black with brownish black hairs; ultimate flagellomere 1.47 times length of penultimate flagellomere. Labrum brown; labellum pale with brown hairs; mandibles absent; proboscis about 0.74 times length of head width. Palpus with five segments, 1st segment almost invisible, yellow with brownish black hairs; 2nd segment cylindrical, yellow with brownish black hairs; 3rd and 4th segments cylindrical, brownish yellow with brownish black hairs; 5th segment slender, cylindrical, brownish yellow with brownish black hairs; relative length of distal four segments as 1.0: 1.5: 1.5: 2.2. Tibial spurs 0–0–0. Terminalia (Fig. 6b): 8th sternite bilobate, medial depression W-shaped, with six hairs laterally; genital fork X-shaped; hypogynial plate broad basally, bilobate posteriorly, each lobe round apically, intervalvular area U-shaped, with short hairs posteriorly; epiproct with two prominent hairs apically; spermathecae three in number.

Type material. ***Holotype*:** male (CAU), China: Sichuan Province, Xiaojin County, Mount Balangshan, 2013.VII.9, 3281 m, Xiaoyan Liu; ***Paratypes*:** 5 males 1 female (QAU), same data as holotype.

Distribution. Currently known only from China (Sichuan).

Etymology. The specific name refers to the type locality Mount Balangshan.

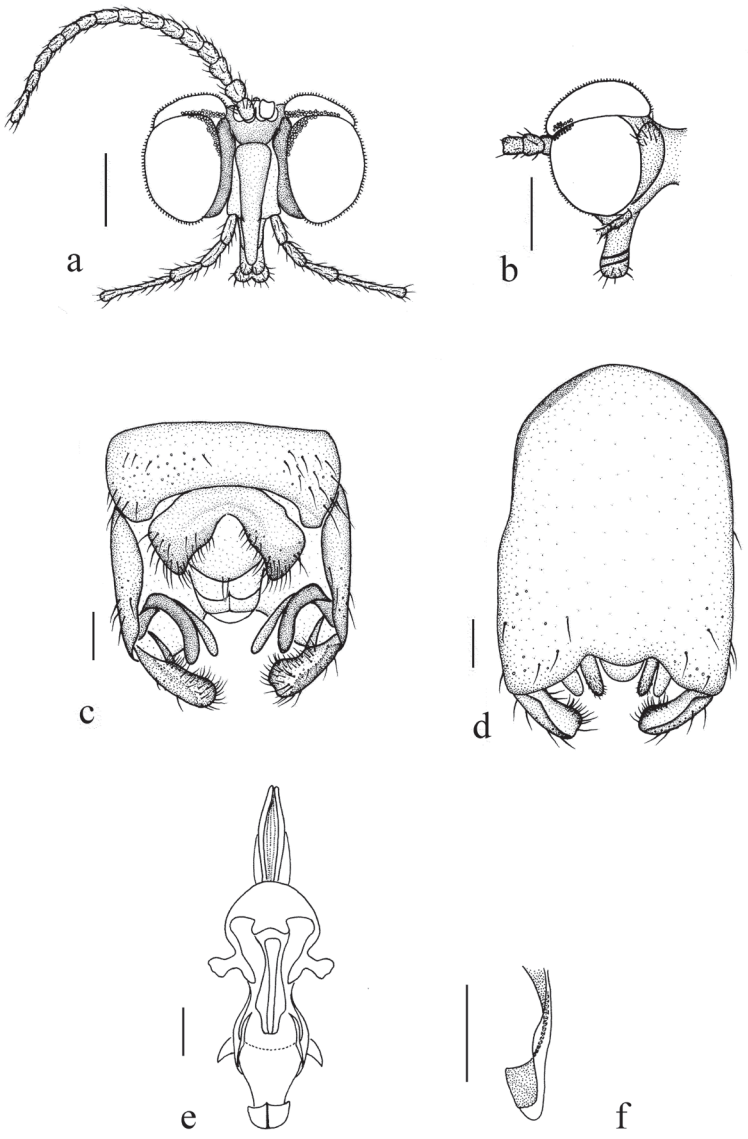

Figure 5. *Blepharicera balangshana* sp. nov. **a** male head, frontal view **b** male head, lateral view **c** male genitalia, dorsal view **d** male genitalia, ventral view **e** aedegal complex, dorsal view **f** tip of dorsal paramere, lateral view. Scale bars: 0.25 mm (**a, b**); 0.10 mm (**c–f**).

Remarks. This new species is very similar to *B. indica* (Brunetti, 1911) from Afghanistan, Pakistan, Sri Lanka and India but can be separated by the apex of the gonostylus being slightly swollen and notched, the dorsal carina being apparent with nearly perpendicular tip. In *B. indica*, the apex of gonostylus is not swollen or notched, and the dorsal carina is inapparent (Zwick 1990). This new species is also similar to *B. asiatica* from Russia, Afghanistan, Pakistan, Sri Lanka and India, but it can be separated

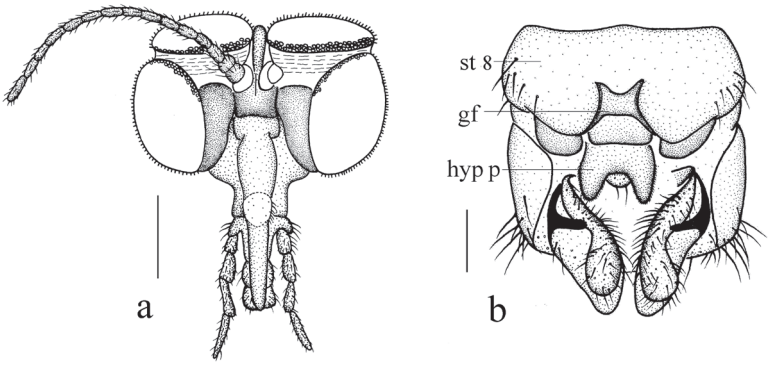

Figure 6. *Blepharicera balangshana* sp. nov. **a** female head, frontal view **b** female terminal, ventral view. Scale bars: 0.25 mm (**a**); 0.10 mm (**b**). Abbreviations: gf = genital fork; hyp p = hypogynial plate; st 8 = eight sternite.

from the latter by the scutellum being pale brown with anterior margin yellow, the sterna of abdomen being mostly pale, and the dorsal carina with nearly perpendicular tip. In *B. asiatica*, the scutellum and the sterna of abdomen are dark brown, the dorsal carina has a very pointed and downcurved tip which is almost parallel to plate sometimes (Zwick 1990).

***Blepharicera kongsica* sp. nov.**

http://zoobank.org/BFAAE688-7006-4834-9F59-67716BDEAAB7

Figs 7–9

Diagnosis. Compound eye with dorsal division 1/15 as large as ventral division in male. Tibial spurs 0–0–2 in female. Rs 1.2 times as long as r-m. Cercus triangular. Dorsal branch of gonostylus short and broad, slightly swollen apically; ventral branch longer and slenderer than dorsal branch. Outer gonocoxal lobe transparent, S-shaped; inner gonocoxal lobe fusiform. Dorsal carina inapparent. Genital fork V-shaped.

Description. Male. Body length 4.00–4.50 mm.

Head (Figs 7a, 8a, b) pruinose, uniformly dark brown with dark brown hairs. Compound eyes dichoptic, interocular ridge absent; each compound eye divided, callis oculi absent; dorsal division contiguous with ventral division, 1/15 as large as ventral division; dorsal division with 7–8 rows of ommatidia, ommatidia red-orange, larger in diameter, with brown omatrichia; ventral division black with omatrichia. Ocelli brownish yellow. Scape and pedicel oval, brown with brownish black hairs; first flagellomere conical, basal 1/2 brownish yellow, apical 1/2 brownish black, with brownish black hairs; other flagellomeres cylindrical, dark brown with dark brown hairs; ultimate flagellomere 1.2 times length of penultimate flagellomere. Clypeus rectangular, basal 1/2 brown, apical 1/2 brownish yellow, twice as long as the width. labrum brownish yellow; labellum brownish yellow with dark brown hairs; proboscis about 0.56 times length of head width. Palpus with five segments, 1st segment almost invisible; 2nd to 4th

segments cylindrical, yellow with brown hairs; 5th segment slender, yellow with dark brown hairs; relative length of distal four segments as 1.0: 1.7: 1.4: 3.2.

Thorax (Fig. 7b) pruinose. Pronotum and propleuron dark brown without hairs. Mesonotum mostly dark brown, except middle area of posterior margin of scutum and middle area of scutellum light brown, scutellum with numerous hairs grouped at posterolateral corner; episternum dark brown; anepimeron yellow, katepimeron light brown. Relative length of femur, tibiae and 1st to 5th tarsomeres in mid leg as 10.0: 9.3: 5.3: 2.1: 1.3: 1: 1.3, in hind leg as 18: 15.8: 6.4: 2: 1.3: 1: 1.3. Fore coxa dark brown with dark brown hairs; mid and hind coxae pale with brownish black hairs; trochanters pale, anterior margin with black spot apically, with brownish black hairs; fore and mid femora brownish yellow basally and gradually darkened to dark brown apically, with dark brown hairs; hind femur yellow basally and gradually darkened to

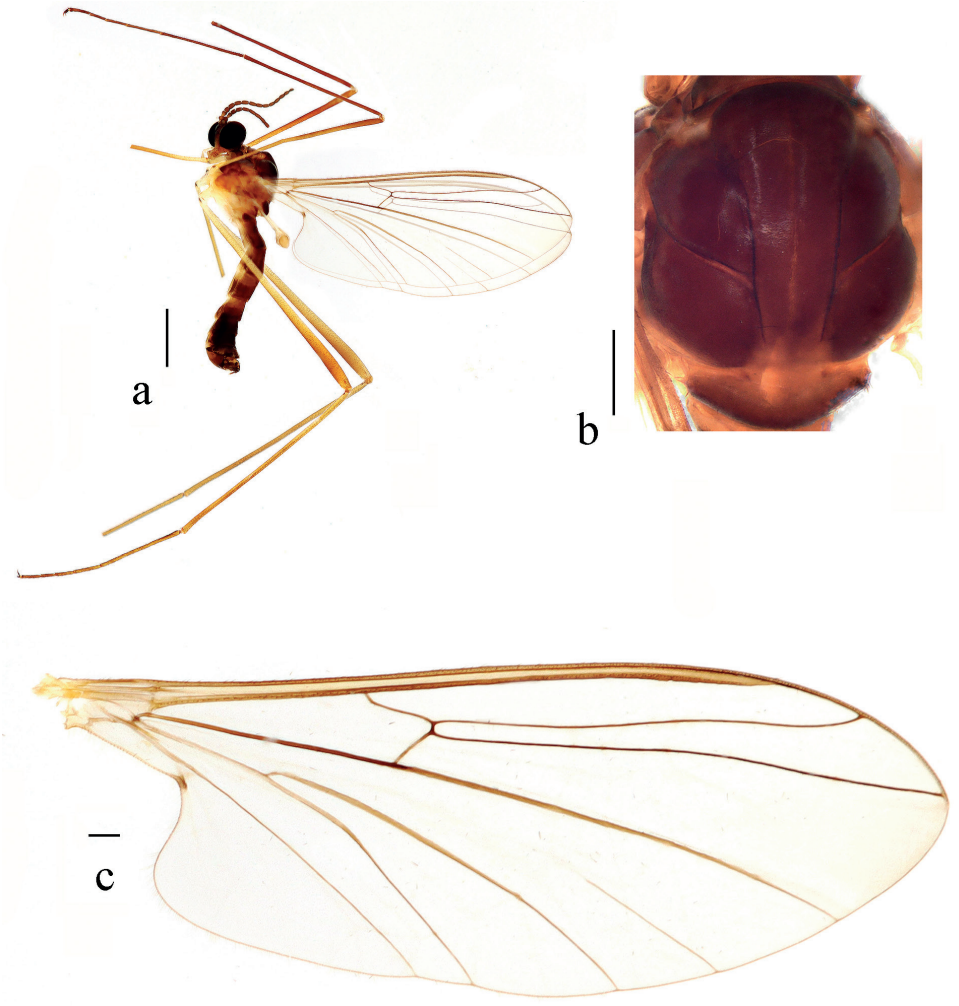

Figure 7. *Blepharicera kongsica* sp. nov. **a** habitus of male, lateral view **b** thorax, dorsal view **c** wing. Scale bars: 1.0 mm (**a**); 0.25 mm (**b, c**).

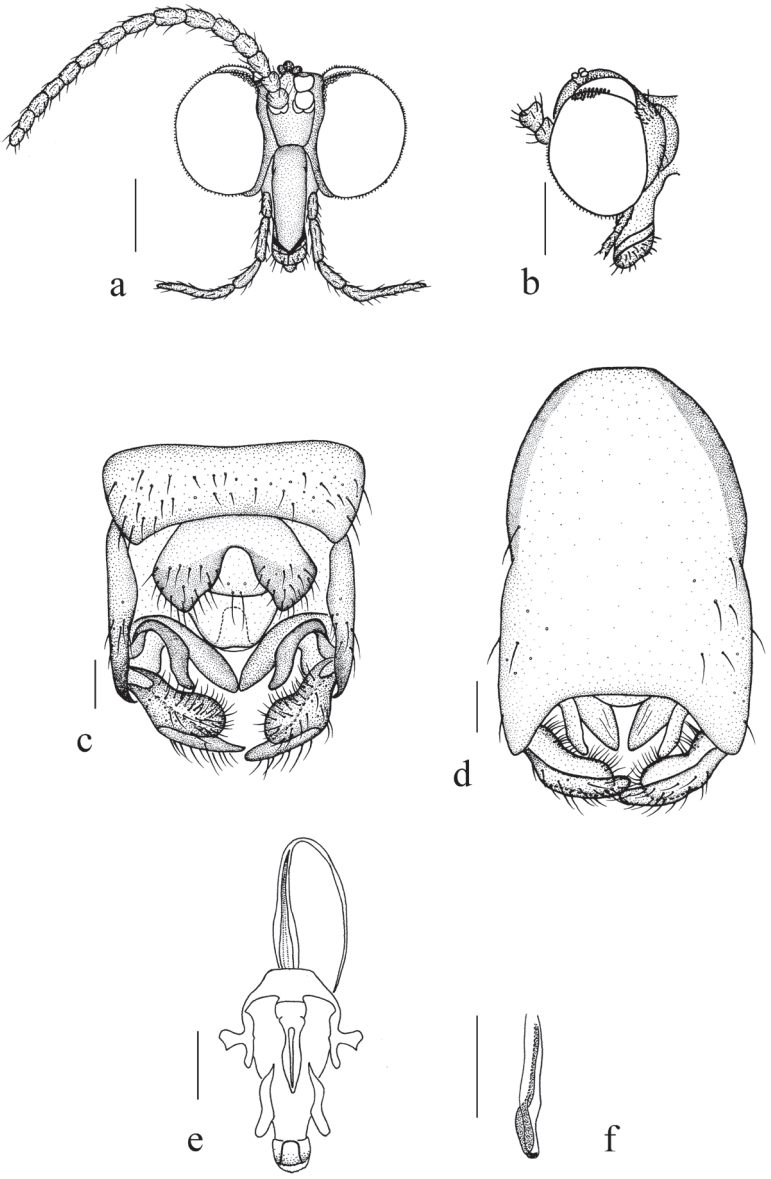

Figure 8. *Blepharicera kongsica* sp. nov. **a** male head, frontal view **b** male head, lateral view **c** male genitalia, dorsal view **d** male genitalia, ventral view **e** aedegal complex, dorsal view **f** tip of dorsal paramere, lateral view. Scale bars: 0.25 mm (**a, b**); 0.10 mm (**c–f**).

dark brown apically, with dark brown hairs; fore and mid tibiae dark brown with dark brown hairs; hind tibia brown with dark brown hairs. Tibial spurs 0–0–0. Wing (Fig. 7c) slightly brown apically; veins brown. Sc rudimentary, not ending at base of Rs; Rs slightly curved basally, 1.2 times as long as r-m; R_4 wavy, the length from end of R_1 to end of R_4 shorter than length from end of R_4 to end of R_5; r-m straight, including

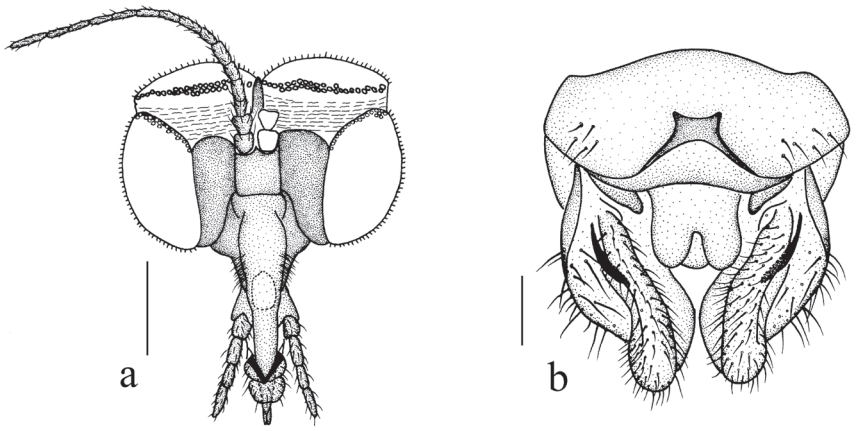

Figure 9. *Blepharicera kongsica* sp. nov. **a** female head, frontal view **b** female terminal, ventral view. Scale bars: 0.25 mm (**a**); 0.10 mm (**b**).

angle between r-m and Rs less than 90 degrees; the length from end of M_1 to end of M_2 longer than the length from end of M_2 to end of CuA_1. Base of halter pale, apex of halter brown with dark brown hairs. Base of halter pale, apex of halter brownish yellow with dark brown hairs.

Abdomen. First tergum brown with middle area pale, 2nd tergum brown, 3rd to 5th terga brown with basal 1/2 light brown, 6th to 8th terga dark brown; 1st sternum pale, 2nd to 7th sterna brown with brownish black stripes laterally; abdomen with dark brown hairs. Male genitalia (Fig. 8c–f) brown. Epandrium trapeziform, posterior margin concaved medially, with several brown hairs. Cercus triangular, inner margin bulge, with several brown hairs; anal cone flat with two long hairs apically. Gonostylus bifurcated, dorsal branch short and broad, slightly swollen apically, with hairs; ventral branch longer and slenderer than dorsal branch, with long hairs. Gonocoxal lobe bifurcated, outer gonocoxal lobe transparent, S-shaped, pointed apically; inner gonocoxal lobe fusiform, transparent. Hypandrium nearly rectangular, 1.5 times as long as the width, slightly narrow basally, posterior margin concave, with several brown hairs laterally. Dorsal paramere with posterior margin round; dorsal carina inapparent.

Female. Body length 5.50–6.00 mm, wing length 6.50–7.00 mm, wing width 2.25–2.50 mm.

Head (Fig. 9a) pruinose. Compound eyes subholoptic, interocular ridge present; each compound eye divided, callis oculi present; dorsal division separated from ventral division, as large as ventral division; dorsal division with about 14 rows of ommatidia, ommatidia red-orange, larger in diameter, with omatrichia; ventral division black with omatrichia. Scape oval, brownish black with brownish black hairs; pedicel conical, brownish black with brownish black hairs; first flagellomere constricted at base, flared at apex, basal 1/2 brown, apical 1/2 brownish black, with brownish black hairs; other flagellomeres cylindrical, tapering apically, brownish black with brownish black hairs; ultimate flagellomere 1.8 times length of penultimate flagellomere. Clypeus brownish black; labrum brown; labellum brownish yellow with brownish black hairs; mandibles

brown; proboscis about 0.8 times length of head width. Palpus with five segments, 1st segment almost invisible, brownish yellow with brownish black hairs; 2nd to 5th segments cylindrical, brownish yellow with brownish black hairs; relative length of distal four segments as 1.0: 1.2: 1.2: 1.5. Fore coxa dark brown with brownish black hairs; mid and hind coxae pale with brownish black hairs; trochanters pale, anterior margin with black spot apically, with brownish black hairs; fore and mid femora brownish yellow basally and gradually darkened to dark brown apically, with dark brown hairs; hind femur yellow basally and gradually darkened to dark brown apically, with dark brown hairs; fore and mid tibiae dark brown with brownish black hairs; hind tibia brown with brownish black hairs. Tibial spurs 0–0–2. Terminalia (Fig. 9b): 8th sternite bilobate, medial depression broadly U-shaped, with several hairs laterally; genital fork V-shaped; hypogynial plate broad basally, bilobate posteriorly, each lobe round apically, intervalvular area U-shaped; spermathecae three in number.

Type material. ***Holotype*****:** male (CAU), China: Sichuan Province, Daofu County, Kongse, 2013.VIII.5, 2976 m, Xiaoyan Liu; ***Paratypes*****:** 1 male 7 females (QAU), same data as holotype.

Distribution. Currently known only from China (Sichuan).

Etymology. The specific name refers to the type locality Kongse.

Remarks. This new species is very similar to *B. japonica* (Kitakami, 1931) from Japan but can be separated by the compound eyes being dichoptic in male and subholoptic in female, the facet of the dorsal division of the compound eye being larger than that of the ventral division, and the dorsal branch of the gonostylus being shorter than the ventral branch. In *B. japonica*, the compound eyes are broadly separated in both sexes, the facet of the dorsal division of the compound eye is smaller than that of the ventral division, and the dorsal branch of the gonostylus is longer than the ventral branch (Kitakami 1931; Zwick 1990). This new species is also similar to *B. fasciata* (Westwood, 1842) from Europe and Asia, but it can be separated from the latter by the dorsal division of the compound eye being contiguous with ventral division in male, the dorsal branch of the gonostylus being shorter than the ventral branch, and the concaved posterior margin of the hypandrium being flat. In *B. fasciata*, the compound eye has a narrow area between the dorsal and ventral divisions in male, the dorsal branch of the gonostylus is as long as the ventral branch, and the concaved posterior margin of the hypandrium is convex medially (Mannheims 1935; Zwick 1990).

Acknowledgements

We express our sincere thanks to Ding Yang (Beijing) for his great help during our study. We are grateful to all the collectors for collecting specimens. The map supporting this study is from https://www.d-maps.com/carte.php?num_car=18064&lang=en. This work was supported by the Shandong Provincial Natural Science Foundation, China [ZR2019BC034], the National Natural Science Foundation of China [41901061 and 32100356], the High-level Talents Funds of Qingdao Agricultural University, China [663-1119008] and the National Animal Collection Resource Center, China.

References

Alexander CP (1953) Undescribed species of Nematocera Diptera. Part III. Bulletin of the Brooklyn Entomological Society 48: 97–103.

Bigot JMF (1862) Diptères nouveaux de la Corse découverts dans la partie montagneuse de cette île par M. E. Bellier de la Chavignerie. Annales de la Société Entomologique de France (Series 4) 2: 109–114.

Brodsky K (1930) Zur Kenntnis der Wirbellosenfauna der Bergströme Mittelasiens. 3. Blepharoceridae. 1. Imagines. Zoologischer Anzeiger 90: 129–146.

Brunetti E (1911) New Oriental Nemocera. Records of the Indian Museum 4: 259–316. https://doi.org/10.5962/bhl.part.10539

Courtney GW (2000a) Revision of the net-winged midges of the genus *Blepharicera* Macquart (Diptera: Blephariceridae) of eastern North America. Memoirs of the Entomological Society of Washington 23: 1–99.

Courtney GW (2000b) A.1. Family Blephariceridae. In: Contributions to a Manual of Palaearctic Diptera. Appendix. Budapest, Science Herald, 7–30.

Hogue CL (1981) Blephariceridae. In: McAlpine JF, Peterson BV, Shewell GE, Teskey HJ, Vockeroth JR, Wood DM (coord.) Manual of Nearctic Diptera. Vol. 1. Agriculture Canada Monograph 27: 191–197.

Jacobson AJ, Curler GR, Courtney GW, Moulton JK (2011) New species of *Blepharicera* Macquart (Diptera: Blephariceridae) from eastern North America, with discussion of the phylogenetic relationships and biogeography of all Nearctic species. Systematic Entomology 36: 768–800. https://doi.org/10.1111/j.1365-3113.2011.00595.x

Kang Z, Yang D (2012) Species of *Philorus* Kellogg from China with description of a new species (Diptera: Blephariceridae). Zootaxa 3311(1): 61–67. https://doi.org/10.11646/zootaxa.3311.1.3

Kang Z, Yang D (2014) Species of *Blepharicera* Macquart from China with descriptions of two new species (Diptera: Blephariceridae). Zootaxa 3866(3): 421–434. https://doi.org/10.11646/zootaxa.3866.3.6

Kang Z, Yang D (2015) New Record of *Horaia* (Diptera: Blephariceridae) in China with Descriptions of Two New Species. Florida Entomologist 98(1): 118–121. https://doi.org/10.1653/024.098.0119

Kellogg VL (1903) The net-winged midges (Blepharoceridae) of North America. Proceedings of the California Academy of Sciences (Series 3) 3: 187–233.

Kitakami S (1931) The Blephariceridae of Japan. Memoirs of the College of Sciences, Kyoto Imperial University 6: 53–108.

Kitakami S (1937) Supplementary notes on the Blephariceridae of Japan. Memoirs of the College of Sciences, Kyoto Imperial University 12: 115–136.

Kitakami S (1938) A new genus and species of Blepharoceridae from Japan. Memoirs of the College of Science, Kyoto Imperial University (Series B) 14(2): 341–352.

Kitakami S (1950) The revision of the Blephariceridae of Japan and adjacent territories. The Journal of Kumamoto Women's University 2: 15–90.

Macquart JM (1843) Description d'un nouveau genre d'insectes Diptères. Annales de la Société Entomologique de France 1(2): 59–63.

Mannheims BJ (1935) Beiträge zur biologie und morphologie der Blepharoceriden (Dipt.). Zoologische Forschungen 2: 1–115. [69 pls.]

Mannheims BJ (1938) Über das vorkommen der gattung *Curupira* in manschukuo nebst beschreibung der entwicklungsstadien zweier neuer Blepharoceriden aus anatolien und Süd-Chile. Arbeiten über morphologische und taxonomische Entomologie aus Berlin-Dahlem 5(4): 328–333.

McAlpine JF (1981) Morphology and terminology, Adults. In: McAlpine JF, Peterson BV, Shewell GE, Teskey HJ, Vockeroth JR, Wood DM (Eds) Manual of Nearctic Diptera (Vol. I). Biosystematic Research Centre, Ottawa, 9–63.

Osten Sacken CR (1874) Report on the Diptera collected by Lieut. W. L. Carpenter in Colorado during the summer of 1873. Annual Report of the United States Geological and Geographical Survey of the Territories for 1873, 7: 561–566.

Tonnoir AL (1930) Notes on Indian blepharocerid larvae and pupae with remarks on the morphology of blepharocerid larvae and pupae in general. Record of the Indian Museum 32(2): 161–214.

von Röder V (1890) Zwei neue nordamerikanische Dipteren. Weiner Entomologische Zeitung 9: 230–232.

Westwood JO (1842) Description de l' *Asthenia fasciata*. Guérin's Magazine of Zoology 12: e94.

Zhang D, Boufford DE, Ree RH, Sun H (2009) The 29°N latitudinal line: an important division in the Hengduan Mountains, a biodiversity hotspot in southwest China. Nordic Journal of Botany 27: 405–412. https://doi.org/10.1111/j.1756-1051.2008.00235.x

Zhang Y, Ma K (2008) Geographic distribution patterns and status assessment of threatened plants in China. Biodiversity and Conservation 17: 1783–1798. https://doi.org/10.1007/s10531-008-9384-6

Zwick P, Arefina T (2005) The net-winged midges (Diptera: Blephariceridae) of the Russian Far East. Bonner Zoologische Beiträge 53(2004): 333–357.

Zwick P (1990) Systematic notes on Holarctic Blephariceridae (Diptera). Bonner Zoologische Beitraege 41: 231–257.

ZooKeys 1085: 69–99 (2022)
doi: 10.3897/zookeys.1085.77966
https://zookeys.pensoft.net

RESEARCH ARTICLE

A peer-reviewed open-access journal
ZooKeys
Launched to accelerate biodiversity research

Taxonomic notes on the genus *Phrynarachne* from China (Araneae, Thomisidae)

Yejie Lin[1], Long Yu[2], Peter Koomen[3], Xunyou Yan[1], Shuqiang Li[4]

1 *Hebei Key Laboratory of Animal Diversity, College of Life Science, Langfang Normal University, Langfang 065000, China* **2** *State Key Laboratory of Biocatalysis and Enzyme Engineering of China & Centre for Behavioural Ecology & Evolution, School of Life Sciences, Hubei University, Wuhan 430062, China* **3** *Natuurmuseum Fryslân, Schoenmakersperk 2, Leeuwarden, 8911 EM, The Netherlands* **4** *Institute of Zoology, Chinese Academy of Sciences, Beijing 100101, China*

Corresponding authors: Xunyou Yan (yanxunyou@163.com), Shuqiang Li (lisq@ioz.ac.cn)

Academic editor: Zhiyuan Yao | Received 13 November 2021 | Accepted 19 January 2022 | Published 4 February 2022

http://zoobank.org/DA1FA04C-FB0F-4325-BDAB-507FF6DEB967

Citation: Lin Y, Yu L, Koomen P, Yan X, Li S (2022) Taxonomic notes on the genus *Phrynarachne* from China (Araneae, Thomisidae). ZooKeys 1085: 69–99. https://doi.org/10.3897/zookeys.1085.77966

Abstract

Four new species of the genus *Phrynarachne* Thorell, 1869 from China are described: *P. dreepy* Lin & S. Li, **sp. nov.** (♂♀), *P. xuxiake* Lin & S. Li, **sp. nov.** (♀), *P. yunhui* Lin & S. Li, **sp. nov.** (♀), and *P. zhengzhongi* Lin & S. Li, **sp. nov.** (♀). The unknown sexes of *P. brevis* Tang & S. Li, 2010 (♂), *P. huangshanensis* Li et al., 1985 (♀), *P. lancea* Tang & S. Li, 2010 (♂), and *P. mammillata* Song, 1990 (♀) are described for the first time. *Phrynarachne sinensis* Peng, Yin & Kim is treated as a nomen dubium.

Keywords

Diagnosis, new species, nomen dubium, type specimens

Introduction

The spider genus *Phrynarachne* Thorell, 1869 currently includes 32 species and subspecies distributed in southern Asia, the Australian region, and sub-Saharan Africa. Only five species are described by both sexes, and 10 species have been studied after their original description. Efforts have been made to find *Phrynarachne* types preserved in well-known European museums, but these endeavors have failed.

Seven *Phrynarachne* species were known from China before the current study; only two species, i.e., *P. ceylonica* (O. Pickard-Cambridge, 1884) and *P. katoi* Chikuni, 1955, are described by both sexes. All endemic Chinese *Phrynarachne* species are only described by few single-sex specimens, and the species in the surrounding areas of China, except Japan, are not well revised and most of them have only initial descriptions (Li et al. 2021; WSC 2021; Yao et al. 2021).

Here, we describe four new and six known *Phrynarachne* species from China. Due to the lost holotype and unknown locality in the original description, we treat *P. sinensis* Peng et al. as *nomen dubium*.

Materials and methods

All specimens were preserved in 80% ethanol. Epigynes were cleared in trypsin enzyme solution to dissolve non-chitinous tissues. Specimens were examined under a LEICA M205C stereomicroscope. Photomicroscopy images were taken with an Olympus C7070 zoom digital camera (7.1 megapixels). Laboratory habitus photographs were taken with a Sony A7RIV digital camera equipped with a Sony FE 90mm Goss lens. Photos were stacked with Helicon Focus (v. 7.6.1) or Zerene Stacker (v. 1.04) and processed in Adobe Photoshop CC2019.

All measurements are in millimeters and were obtained with an Olympus SZX16 stereomicroscope with a Zongyuan CCD industrial camera. Total length is measured without chelicerae. Eye sizes are measured as the maximum diameter from either the dorsal or frontal view. Leg measurements are given as follows: total length (femur, patella, tibia, metatarsus, tarsus). The terminology used in the text and figures follows Ono (1988).

Types of the new species reported here are deposited at the Institute of Zoology, Chinese Academy of Sciences in Beijing.

Abbreviations

ALE anterior lateral eyes;
AME anterior median eyes;
E embolus;
FD fertilization duct;
H hood;
ITA intermediate tibial apophysis;
Mp median plate;
PLE posterior lateral eyes;
PME posterior median eyes;
RTA retrolateral tibial apophysis;
S spermathecae;
VTA ventral tibial apophysis.

Taxonomy

Family Thomisidae Sundevall, 1833

Genus *Phrynarachne* Thorell, 1869

Phrynarachne Thorell, 1869: 37. For the complete list of references see WSC (2021).

Type species. *Thomisus rugosus* Walckenaer, 1805, from Mauritius

Diagnosis. Large or medium-sized, male is much smaller than the female (1:2 or more). Prosoma nearly as long as wide, with granulations. Eyes small, subequal in size. Fovea inconspicuous. Chelicerae with two promarginal and one retromarginal teeth. Labium longer than wide, sternum oval, male palp with VTA, ITA and RTA; tegulum flat, disk-shaped; tegular ridge present; embolus slender. Female epigynum simple, with a media plate, spermathecae strong sclerotized.

Phrynarachne brevis Tang & S. Li, 2010

Figs 1A, 6, 18A, 21

Phrynarachne brevis Tang & Li, 2010: 49, figs 35A–D, 36A, B (♂).

Type material. ***Holotype*:** ♂ (IZCASAr18535), **China:** ***Yunnan:*** Xishuangbanna, Mengla County, Menglun Town, Menglun Nature Reserve, Bamboo plantation near G213 roadside, 21.8940°N, 101.2823°E, 580 m elev., 3.XII.2009, Guo Tang and Zhiyuan Yao leg., examined.

Other material examined. 1♀ (IZCAS-Ar41642), **China:** ***Yunnan*:** Xishuangbanna, Jinghong City, Mengla County, Menglun Town, Menglun Nature Reserve, Bamboo plantation, 21.9008°N, 101.2822°E, 597 m elev., 9.V.2019, Zhigang Chen leg.

Diagnosis. See diagnosis of *P. dreepy* sp. nov.

Description. Female (Figs 1A, 6, 18A). Total length 16.53, carapace 6.62 long, 7.09 wide, yellow brown with brown pattern and granulations dorsally. With large projection between ALE and PLE. Eye sizes and interdistances: ALE 0.26, AME 0.23, PLE 0.25, PME 0.22; ALE–AME 0.51, AME–AME 0.90, PLE–PME 1.62, PME–PME 1.02. Chelicerae brown, with two promarginal and one retromarginal teeth; gnathocoxae, labium dark yellow, labium 1.52 long, 1.18 wide. Sternum yellow. Legs brown, femora I and II with dense, varying-sized tubercles; tibiae and metatarsi I, II with dense asymmetrical ventral spines (I, tibia 12, metatarsus 30; II, tibia 10, metatarsus 30). Leg measurements: I 17.25 (5.74, 6.31, 3.10, 2.10), II 17.61 (5.66, 6.61, 3.30, 2.04), III 12.30 (3.67, 5.74, 1.50, 1.39), IV 10.26 (3.31, 4.12, 1.46, 1.37). Opisthosoma dorsally light yellow, each side with 22 long tubercles, middle with pair of black markings.

Figure 1. *Phrynarachne* spp., live **A** *P. brevis*, adult female **B** *P. xuxiake* sp. nov., juvenile. Photos by Chao Wu (**A**) and Fan Gao (**B**).

Epigyne (Fig. 6) with M-shaped sclerotized margins; median plate obvious, with a posterior hood, anterior edge recurved and posterior edge almost straight, the ratio of length to width is 11:3; copulatory opening obvious; spermathecae kidney-shaped, the ratio of anterior edge to posterior edge length is 1:1. Fertilization duct transverse.

Male. See Tang and Li (2010).
Distribution. China (Yunnan).
Notes. The female is described here for the first time.

***Phrynarachne ceylonica* (O. Pickard-Cambridge, 1884)**
Figs 2, 21

Ornithoscatoides ceylonica O. Pickard-Cambridge, 1884: 201, pl. 15, fig. 3. For the complete list of references see WSC (2021).

Type material. ***Syntypes*** 2♀, "Ceylon, G.H.K. Thwaites leg.", Hope Department of Entomology, Oxford, UK, not examined; *O. nigra* O. Pickard-Cambridge, 1884: ***Syntypes*** 2♂, "Ceylon and India, G.H.K. Thwaites leg.", Hope Department of Entomology, Oxford, UK, not examined.

Figure 2. *Phrynarachne ceylonica* **A** adult male (left) and female (right) **B** male live **C** female live. Photos by Peter Koomen.

Other material examined. 2♂ (IZCAS), Xishuangbanna, Jinghong City, Mengla County, Menglun Town, Menglun Nature Reserve, primary tropical seasonal rain forest, 21.9598°N, 101.2035°E, 822 m elev., 8.VIII.2007, Guo Zheng leg.; 1♂ (IZCAS), Xishuangbanna, Jinghong City, Mengla County, Menglun Town, Menglun Nature Reserve, *Paramichelia baillonii* plantation (about 20 years old), 21.9129°N, 101.2674°E, 556 m elev., 18.VII.2007, Guo Zheng leg.; 2♂ (IZCAS), Xishuangbanna, Jinghong City, Mengla County, Menglun Town, Menglun Nature Reserve, secondary tropical seasonal moist forest, 21.9120°N, 101.2823°E, 645 m elev., 27.VII.2007, Guo Zheng leg.; 1♂ (IZCAS), Xishuangbanna, Jinghong City, Mengla County, Menglun Town, Menglun Nature Reserve, *Anogeissus acuminata* plantation (about 20 yr.), 21.8999°N, 101.2802°E, 611 m elev., 19.VIII.2007, Guo Zheng leg.; 2♀ (IZCAS), Xishuangbanna, Jinghong City, Mengla County, Menglun Town, Menglun Nature Reserve, secondary tropical seasonal moist forest, 21.9065°N, 101.2802°E, 612 m elev., 10.VIII.2007, Guo Zheng leg.

Distribution. Asia: from India and Sri Lanka to Japan, south to Indonesia. In China is known from Guangxi, Taiwan, and Yunnan.

***Phrynarachne dreepy* Lin & S. Li, sp. nov.**

http://zoobank.org/E0BC4600-8F1E-403A-BBDD-C37EDE540845

Figs 3, 7, 8, 18C, D, 21

Type material. ***Holotype*:** ♂ (IZCAS-Ar41643), **China: *Yunnan*:** Xishuangbanna, Jinghong City, Mengla County, Menglun Town, Menglun Nature Reserve, 21.9768°N, 101.2010°E, 814 m elev., 17.VIII.2011, Guo Zheng leg.; ***Paratypes*:** 2♀ (IZCAS-Ar41644, Ar41645), **China: *Yunnan*:** Xishuangbanna, Jinghong City, Mengla County, Menglun Town, Menglun Nature Reserve, Xishuangbanna Tropical Botanic Garden, 21.9277°N, 101.2622°E, 552 m elev., VIII.2019, Long Yu leg.; 1♂ (IZCAS-Ar41646), same data as holotype, but 21.9502°N, 101.2010°E, 814 m elev., 18.VIII.2011; 2♂ (IZCAS-Ar41647, Ar41648), Xishuangbanna, Jinghong City, Guanping Town, Shiwudui, 22.2280°N, 100.8894°E, 888 m elev., 20.VII.2012, Qingyuan Zhao and Zhigang Chen leg.

Etymology. The species is named after *Dreepy*, a fictional character from Pokémon Sword and Shield, who has a triangular head that is reminiscent of the opisthosoma of the new species; noun (name) in apposition.

Diagnosis. *Phrynarachne dreepy* sp. nov. is similar to *P. brevis* in that males have a long RTA; in females the epigyne has sclerotized margins and the posterior edge of the median plate has a depression. However, males of *P. dreepy* sp. nov. can be easily distinguished by the long VTA (vs short VTA in *P. brevis*), the length of embolus to the length of the embolus base (7:1 vs 18:1 in *P. brevis*), and the embolus separate from the tegulum (vs close to the tegulum in *P. brevis*). Females can be separated from *P. brevis* by the short, triangular tubercles on the abdomen (vs long, slender tubercles

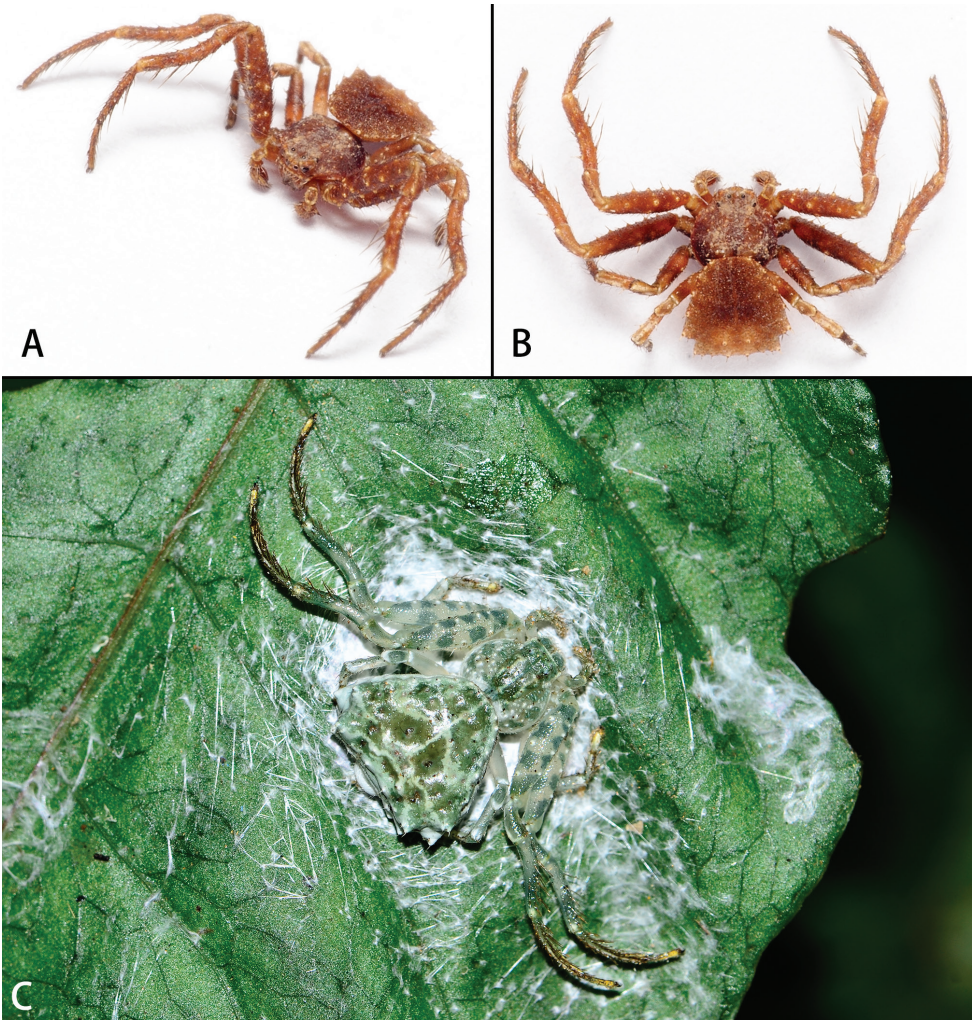

Figure 3. *Phrynarachne dreepy* sp. nov. **A, B** male **C** female life. Photos by Peter Koomen (**A, B**) and Chao Wu (**C**).

in *P. brevis*), the straight anterior edge of median plate (vs recurved in *P. brevis*), and the procurved posterior edge of the median plate (vs almost straight in *P. brevis*).

Description. Male (Figs 3A, B, 7, 18C), ***holotype*:** total length 2.26, carapace 1.04 long, 1.02 wide, yellow-brown, with white tubercles. Eye sizes and interdistances: ALE 0.09, AME 0.07, PLE 0.07, PME 0.06; ALE–AME 0.05, AME–AME 0.07, PLE–PME 0.09, PME–PME 0.11. Chelicerae brown, with two promarginal teeth and one retromarginal tooth; gnathocoxae, yellow-brown, labium brown, 0.23 long, 0.18 wide. Sternum yellow-brown. Legs yellow-brown, femora I ang II with dense, varying-sized tubercles; tibiae and metatarsi I, II with pairs of ventral spines (I, tibia

6, metatarsus 8; II, tibia 6, metatarsus 6). Leg measurements: I 3.85 (1.21, 1.38, 0.76, 0.50), II 3.78 (1.22, 1.34, 0.73, 0.49), III 1.72 (0.55, 0.60, 0.27, 0.30), IV 1.52 (0.51, 0.52, 0.23, 0.26). Leg formula: 1234. Opisthosoma dark brown, each side with 18 tubercles, each with a clavate seta.

Male palp (Fig. 3A, B). Tibia brown, VTA club-shaped; RTA long, the length of VTA to the length of RTA is 3:1. Cymbium brown. Tegulum flat, disk-shaped, with a tegular ridge. Embolus spiraled, thin, separated from tegulum; the length of embolus to the length of embolus base 7:1.

Female (Figs 3C, 8, 18D) one ***paratype***: total length 8.45, carapace 3.77 long, 4.02 wide, pale yellow, green when alive. Eye sizes and interdistances: ALE 0.22, AME 0.12, PLE 0.20, PME 0.15; ALE–AME 0.18, AME–AME 0.24, PLE–PME 0.28, PME–PME 1.02. Chelicerae brown, with two promarginal teeth and one retromarginal tooth; gnathocoxae, labium yellow, labium 0.86 long, 0.63 wide. Sternum yellow. Legs pale yellow, femora I and II with dense, varying-sized tubercles; tibiae and metatarsi I, II with dense asymmetrical ventral spines (I, tibia 25, metatarsus 102; II, tibia 20, metatarsus 83). Leg measurements: I 13.87 (4.26, 4.94, 3.10, 1.57), II 13.99 (4.40, 4.81, 3.16, 1.62), III 7.17 (2.36, 2.67, 1.12, 1.02), IV 6.74 (2.49, 2.57, 0.82, 0.86). Leg formula: 2134. Opisthosoma pale green, each side with 13 triangular tubercles, each with a clavate seta.

Epigyne (Fig. 8) with sclerotized margins; median plate almost rectangular, hood absent, anterior edge straight, posterior edge slightly recurved, the ratio of length to width is 4:1; copulatory opening inconspicuous; spermathecae kidney-shaped, the ratio of anterior edge to posterior edge length is 2:1. Fertilization duct transverse.

Distribution. Known only from the type locality.

Phrynarachne huangshanensis Li, Chen & Song, 1985

Figs 5, 9, 10, 17A, C, 18B, 21

Phrynarachne huangshanensis Li et al., 1985: 73, figs 1, 2. For the complete list of references see WSC (2021).

Type material. ***Holotype*****:** ♀ (IZCAS-Ar41649), **China:** ***Anhui*****:** Huangshan City, Huangshan District, Zhaixi Village, 30.0580°N, 118.1664°E, 423 m elev., 14.VI.1982, Youcai Li, Fayang Chen and Daxiang Song leg., examined.

Other material examined. 1♂(IZCAS-Ar416450), **China:** ***Anhui*****:** Huangshan City, Tangkou Town, Houyuan, ravine, 30.0735°N, 118.1522°E, 470 m elev., IX.2018, Long Yu leg.; 2♂(IZCAS-Ar41651, Ar41652), **China:** ***Anhui*****:** Huangshan City, Tangkou town, Fangcunxin Village, ravine, shrub with broad leaves, 30.0457°N, 118.1606°E, 430±8 m elev., 5.IX.2019, Long Yu leg.; 3♂ (IZCAS-Ar41653–Ar41655), **China:** ***Anhui*****:** Huangshan City, Tangkou town, Fangcun Village, shrub with broad leaves, 30.0302°N, 118.1822°E, 356±6 m elev., 5.IX.2019, Long Yu leg; 5♀(IZCAS-Ar41656–Ar41660), **China:** ***Anhui*****:** Huangshan City,

Tangkou Town, Fangcunxin Village, ravine, 30.0501°N, 118.1854°E, 450 m elev., IX.2018, Long Yu leg.

Diagnosis. Males of *Phrynarachne huangshanensis* can be distinguished from those of *P. mammillata* by the ratio of the length of the embolus to the length of the embolus base (7:1 in *P. huangshanensis* vs 10:1 in *P. mammillata*), and the ratio of the length of the RTA to the length of the VTA (3:1 in *P. huangshanensis* vs 2:1 in *P. mammillata*). Females can be differentiated by the length to width ratio of the median plate (3:1 in *P. huangshanensis* vs 5:1 in *P. mammillata*), and the V-shaped median plate (vs M-shaped in *P. mammillata*).

Description. Male (Figs 5A, 9, 18B): total length 2.45, carapace 1.10 long, 1.14 wide, dark brown with long setae. Opisthosoma brown in middle, with some tubercles, each with a clavate seta. A pair of white lines from PLE to fovea. Eye sizes and interdistances: ALE 0.09, AME 0.06, PLE 0.07, PME 0.04; ALE–AME 0.05, AME–AME 0.11, PLE–PME 0.13, PME–PME 0.15. Chelicerae brown, with two promarginal teeth and one retromarginal tooth; gnathocoxae, labium dark brown, labium 0.20 long, 0.21 wide. Sternum black. Legs black, femora I and II with dense, varying-sized tubercles, tibiae and metatarsi I, II with pairs of ventral spines (I, tibia 6, metatarsus 6; II, tibia 6, metatarsus 6); femora III, IV with white stripe. Leg measurements: I 3.54 (1.13, 1.23, 0.66, 0.52), II 3.50 (1.18, 1.22, 0.60, 0.50), III 1.69 (0.55, 0.56, 0.26, 0.32), IV 2.08 (0.73, 0.72, 0.28, 0.35). Leg formula: 1234. Opisthosoma dorsally dark brown, each side with 17 tubercles, each with a clavate seta, center with a pair of yellow markings.

Male palp (Fig. 9). Tibia brown, VTA club-shaped; RTA long, the length ratio of VTA to RTA is 3:1. Cymbium black. Tegulum flat, disk-shaped, with a tegular ridge. Embolus spiral, thin, the length ratio of the embolus to the embolus base is 7:1.

Female. See Li et al. (1985).

Distribution. China (Anhui).

Notes. The male is described for the first time here.

Phrynarachne katoi **Chikuni, 1955**

Figs 4, 21

Phrynarachne katoi Chikuni, 1955: 35, figs 4A–G, pl. 1. For the complete list of references see WSC (2021).

Type material. ***Holotype*** 1♀ (Collection of Kyukichi Kishida, Tokyo), from Tojigami, Daisan-ku, Kawajimura, Iida-shi, Shimoina-gun, Nagano Pref., 470 m elev., 7.IX.1953, S. Sekigawa leg., not examined.

Other material examined. 1♂1♀ (IZCAS), **China: *Anhui*:** Huangshan City, Xiuning County, Mount Qiyun, 29.8186°N, 118.0294°E, 24.X.2021, Fan Gao leg.

Distribution. China, Korea, and Japan. In China it is known from Anhui, Zhejiang.

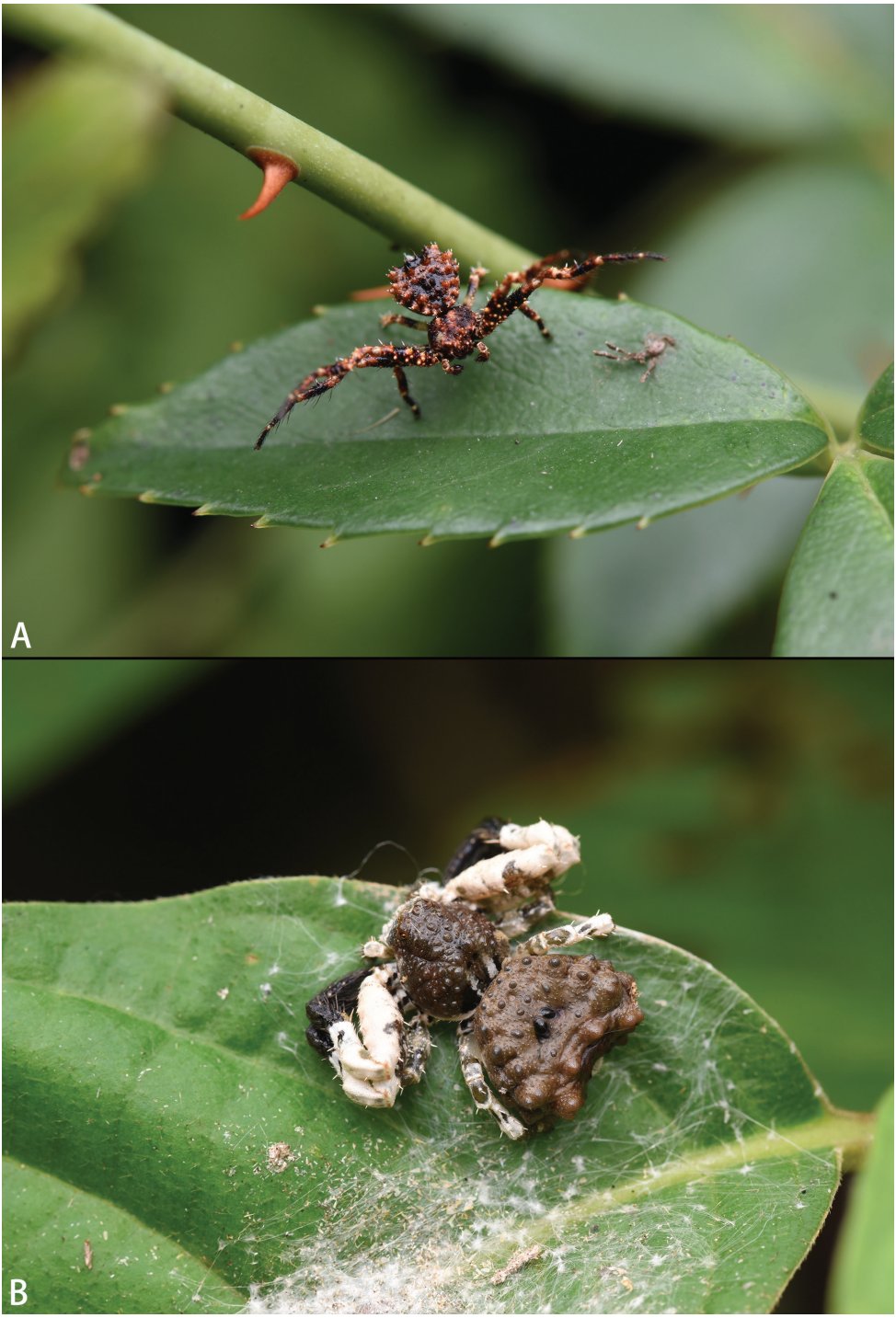

Figure 4. *Phrynarachne katoi*, live **A** male **B** female. Photos by Fan Gao.

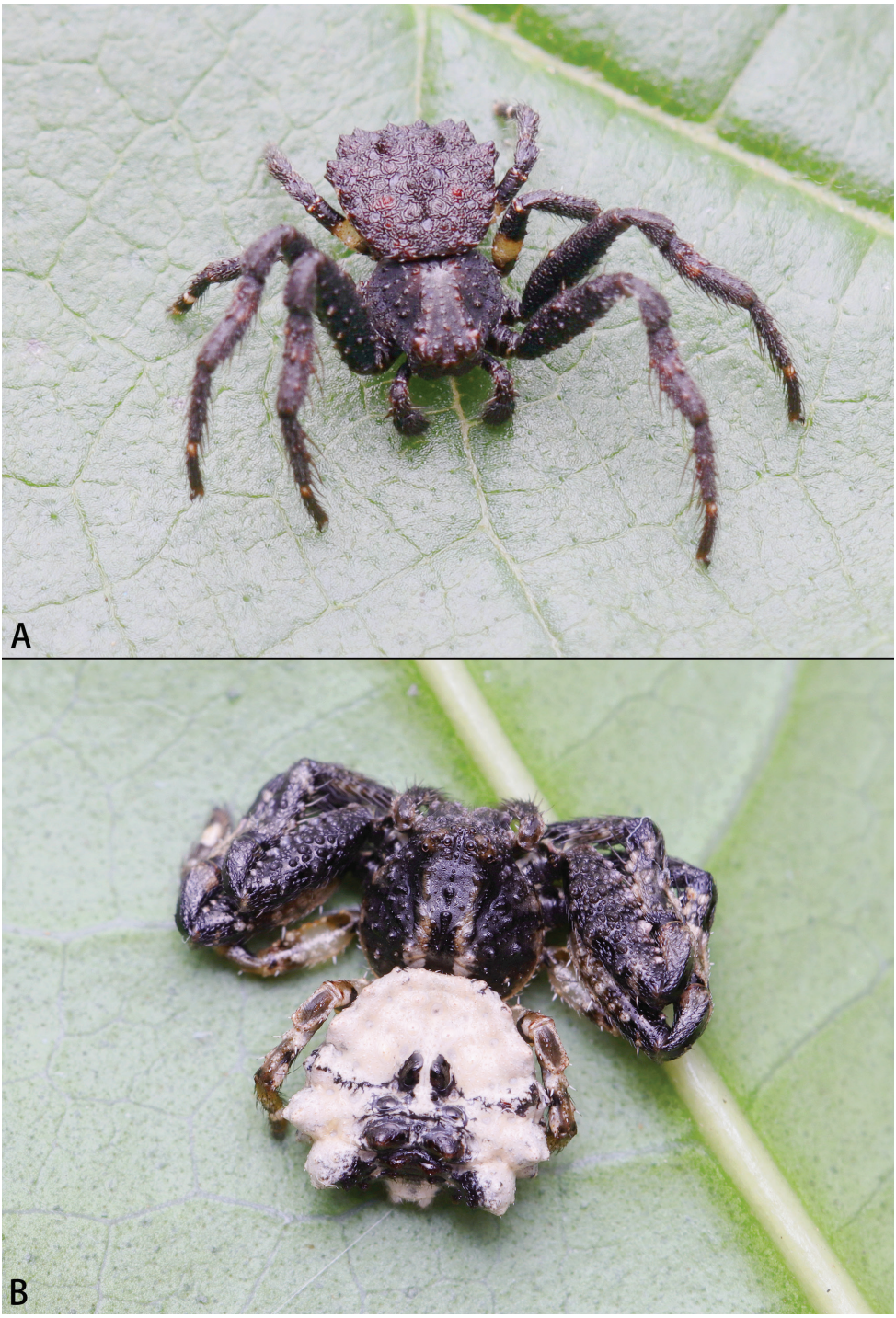

Figure 5. *Phrynarachne huangshanensis*, live **A** male **B** female. Photos by Ruiyang Wang.

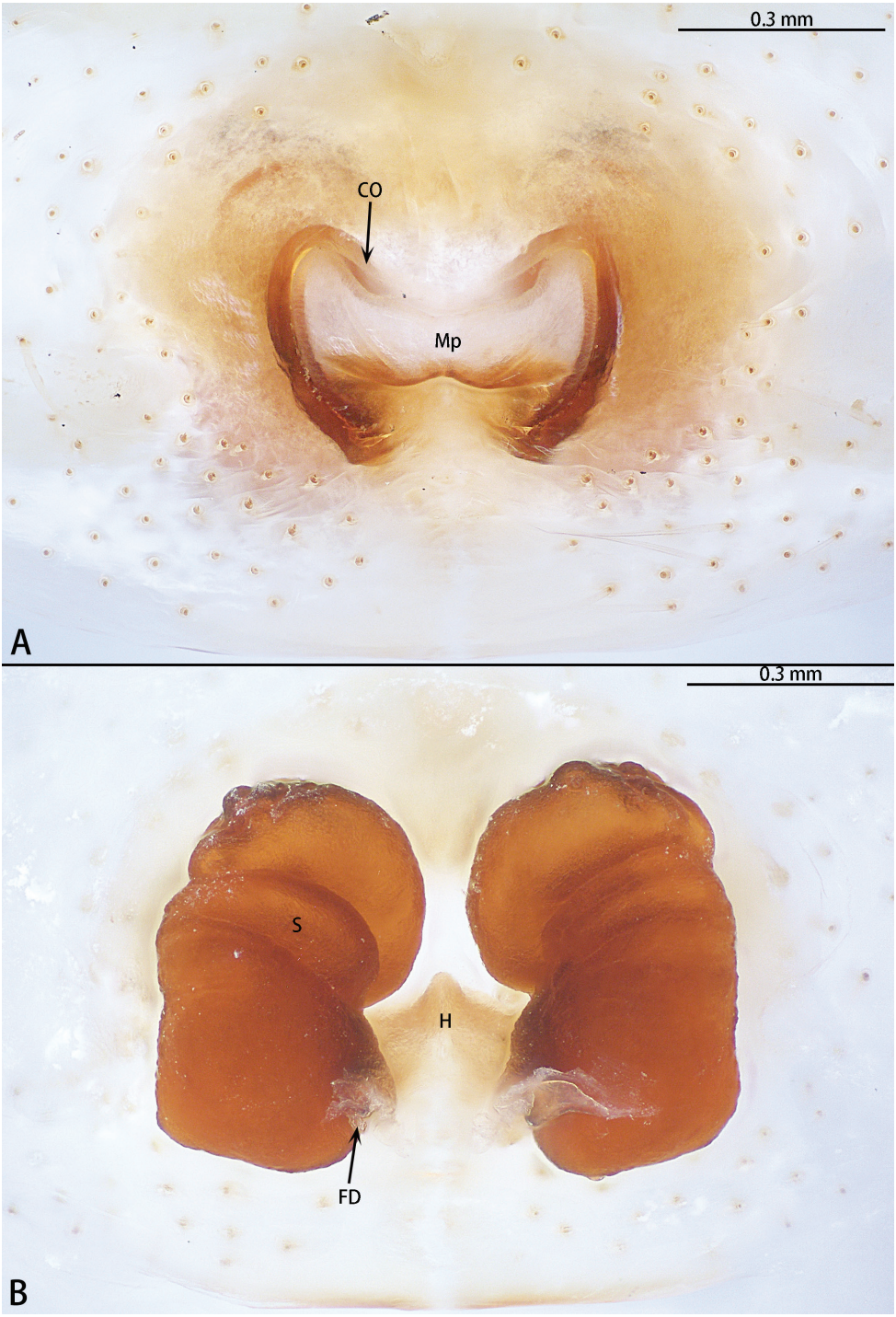

Figure 6. *Phrynarachne brevis*, female **A** epigyne, ventral **B** vulva, dorsal.

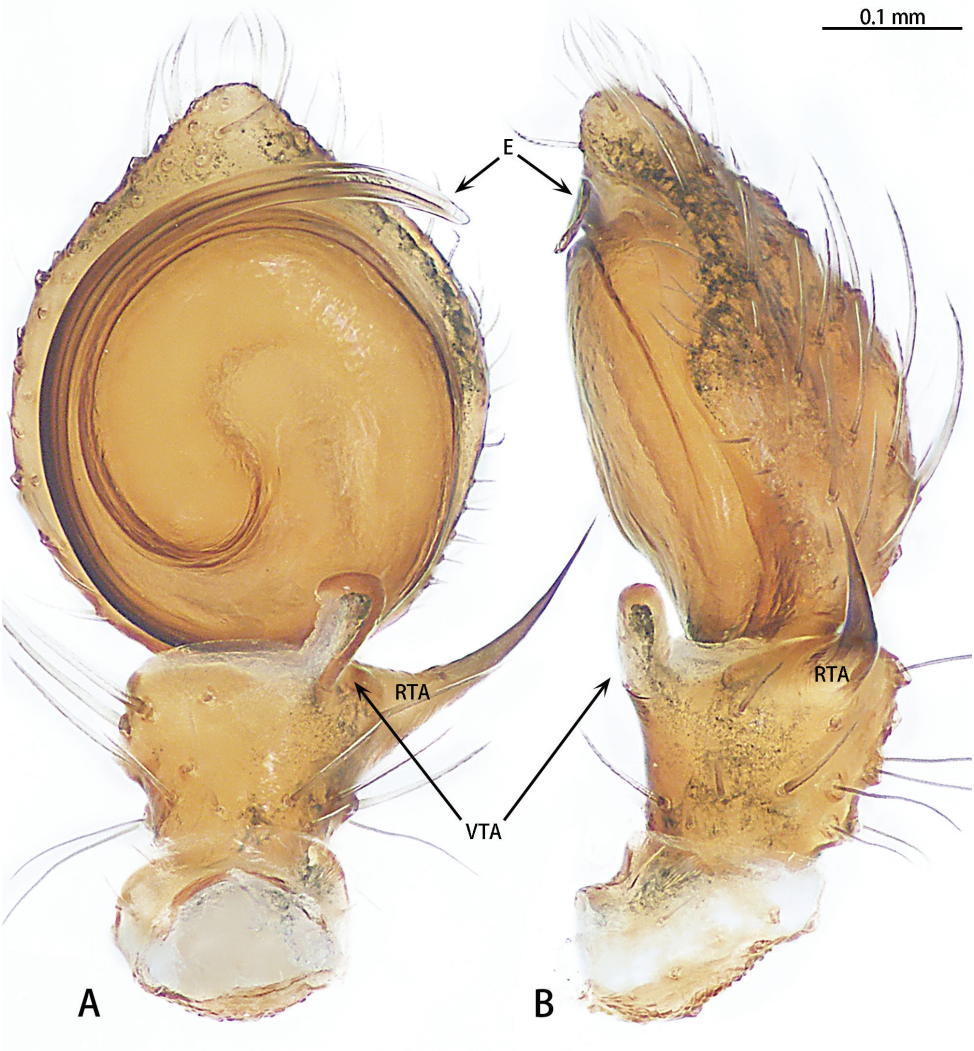

Figure 7. *Phrynarachne dreepy* sp. nov., holotype male, left palp **A** ventral **B** retrolateral.

***Phrynarachne lancea* Tang & S. Li, 2010**
Figs 11, 19A, 21

Phrynarachne lancea Tang & Li, 2010: 53, figs 37A–D, 38A, B.

Type material. ***Holotype*****:** ♂ (IZCAS-Ar18536), **China:** ***Yunnan*****:** Xishuangbanna, Jinghong City, Mengla County, Menglun Town, Menglun Nature Reserve, Tropical seasonal rainforest, 21.9368°N, 101.2701°E, 558 m elev., 1.XII.2009, Guo Tang and Zhiyuan Yao leg., examined. ***Paratype***: 1♂(IZCAS-Ar18537), **China:** ***Yunnan*****:**

Xishuangbanna, Jinghong City, Mengla County, Menglun Town, Menglun Nature Reserve, *Anogeissus acuminata* plantation (about 20 years old), 21.8970°N, 101.2846°E, 609 m elev., 27.XII.2009, Guo Tang and Zhiyuan Yao leg. examined.

Other material examined. 3♀(IZCAS-Ar41661–Ar41663), **China: *Yunnan*:** Xishuangbanna, Jinghong City, Mengla County, Xishuangbanna Tropical Botanic Garden, Rainforest Valley, 21.9277°N, 101.2622°E, 552 m elev., III.2018, Yu Long leg.; 2♀ (IZCAS-Ar41664, Ar41665), same data as above, but II.2019; 3♂(IZCAS-Ar41666–Ar41668), same data as above, but V.2019.

Diagnosis. *Phrynarachne lancea* males can be easily distinguished from other species by the wide, spear-shaped RTA. Females of *P. lancea* are similar to *P. mammillata* in having an M-shaped median plate and kidney-shaped spermathecae. However, *P. lancea* can be distinguished by the length to width ratio of the median plate (7:1 in *P. lancea* vs 4:1 in *P. mammillata*), the straight posterior edge of the median plate (vs procurved in *P. mammillata*), the posterior edge of the spermathecae shorter than the anterior edge (vs of equal length in *P. mammillata*), and the longitudinal fertilization ducts (vs transverse in *P. mammillata*).

Description. Female (Figs 11, 19A): total length 16.49, carapace 6.53 long, 6.82 wide, white, posterior edge black. Eye sizes and interdistances: ALE 0.21, AME 0.20, PLE 0.24, PME 0.21; ALE–AME 0.14, AME–AME 0.25, PLE–PME 0.33, PME–PME 0.28. Chelicerae white, with two promarginal teeth and one retromarginal tooth; gnathocoxae white with black pattern, labium black, 0.88 long, 0.83 wide. Sternum white. Legs white with black markings, femora I and II with dense, varying-sized tubercles; tibiae and metatarsi I, II with dense asymmetrical ventral spines (I, tibia 28, metatarsus 75; II, tibia 26, metatarsus 68). Leg measurements: I 12.45 (4.23, 4.49, 2.41, 1.32), II 12.15 (4.15, 4.41, 2.31, 1.28), III 6.25 (2.12, 2.38, 0.98, 0.87), IV 5.90 (2.18, 2.00, 0.92, 0.80). Leg formula: 1234. Opisthosoma white, posterior grey, with four obvious brown tubercles.

Epigyne (Fig. 11) with sclerotized margins inconspicuous, M-shaped; median plate M-shaped, hood absent, anterior and posterior edges recurved, the ratio of length to width is 7:1; copulatory opening inconspicuous; spermathecae kidney-shaped, the ratio of anterior edge to posterior edge length is 3:1. Fertilization duct longitudinal.

Male. See Tang and Li (2010).

Distribution. China (Yunnan).

Notes. The female is reported here for the first time.

Phrynarachne mammillata Song, 1990

Figs 12, 13, 17B, D, 19B, 21

Phrynarachne mammillata Song in Song & Chai, 1990: 364, fig. 1A–D.For the complete list of references see WSC (2021).

Type material. ***Holotype*:** ♀ (IZCAS-Ar9358), **China: *Guizhou*:** Tongren City, Jiangkou County, Fanjing Mountain, 10.VII.1988, examined.

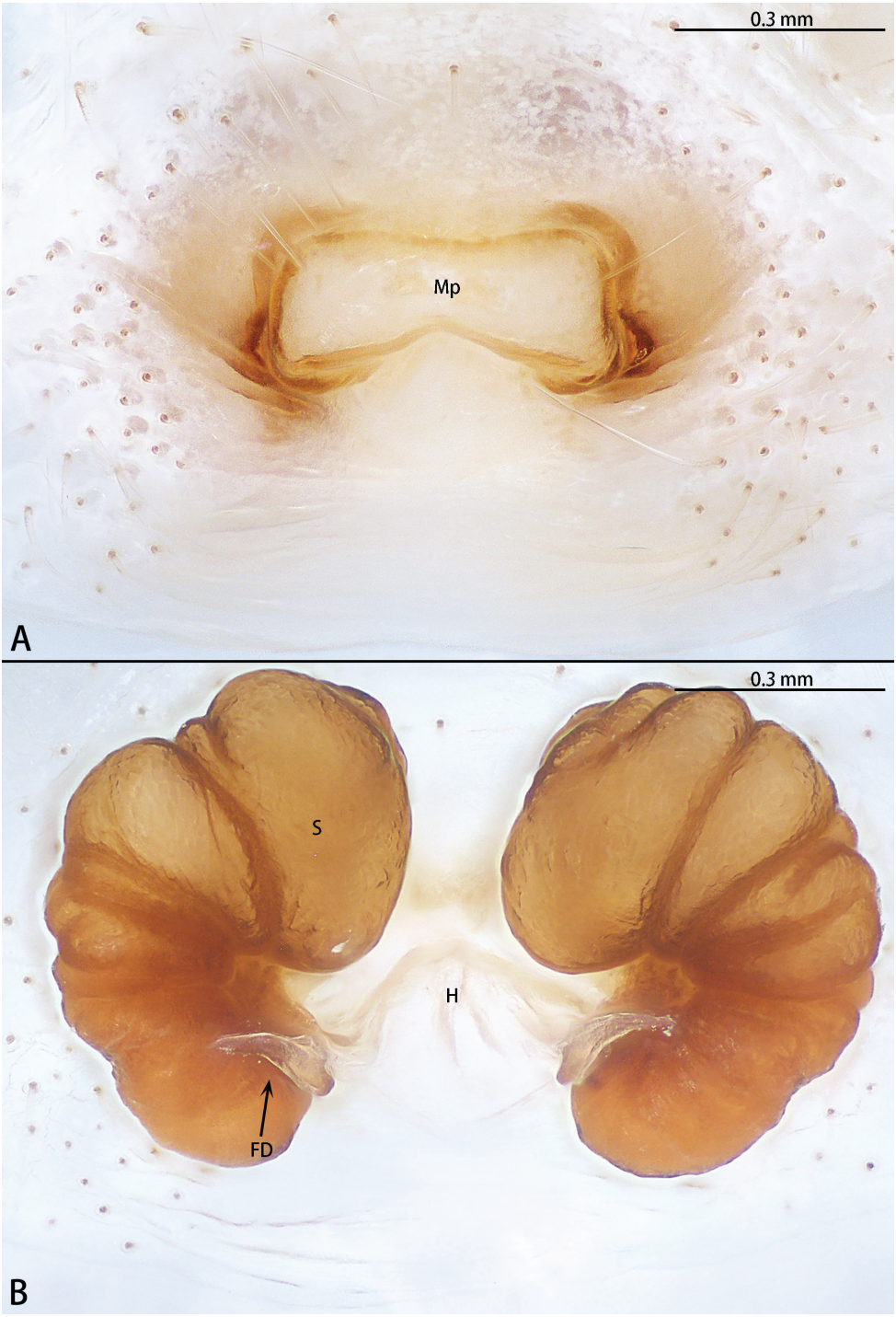

Figure 8. *Phrynarachne dreepy* sp. nov., patatype female **A** epigyne, ventral **B** vulva, dorsal.

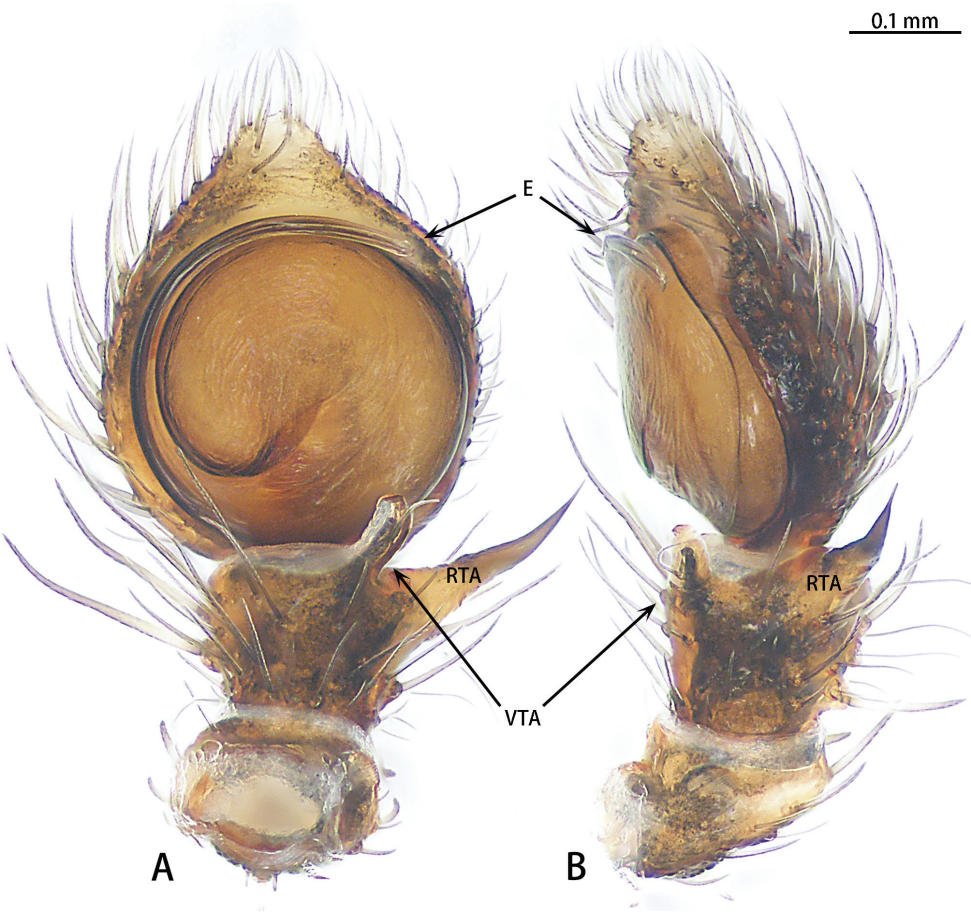

Figure 9. *Phrynarachne huangshanensis*, male left palp **A** ventral **B** retrolateral.

Other material examined. 2♀ (IZCAS-Ar41669, Ar41670), **China, *Yunnan*:** Xishuangbanna, Jinghong City, Mengla County, Xishuangbanna Tropical Botanic Garden, Rainforest Valley, 21.927745°N, 101.262194°E, 552 m elev., 2014/VII, Yu Long leg.; 1♂ (IZCAS-Ar41671), Xishuangbanna, Jinghong City, Guanping Town, Shiwudui, 22.2280°N, 100.8894°E, 888 m elev., 20.VII.2012, Qingyuan Zhao and Zhigang Chen leg.

Diagnosis. See diagnosis of *Phrynarachne huangshanensis*.

Description. Male (Figs 12, 19B): total length 1.82, carapace 0.90 long, 0.97 wide, dark brown, cephalic region yellow-brown. Eye sizes and interdistances: ALE 0.09, AME 0.06, PLE 0.07, PME 0.06; ALE–AME 0.05, AME–AME 0.07, PLE–PME 0.12, PME–PME 0.12. Chelicerae brown, with two promarginal teeth and one retromarginal tooth; gnathocoxae, labium dark brown, labium 0.15 long, 0.19 wide. Sternum brown. Legs black, femora I and II with dense, varying-sized tubercles; tibiae and metatarsi I, II with pairs of ventral spines (I, tibia 6, metatarsus 6; II, tibia 6, metatarsus 6), femora

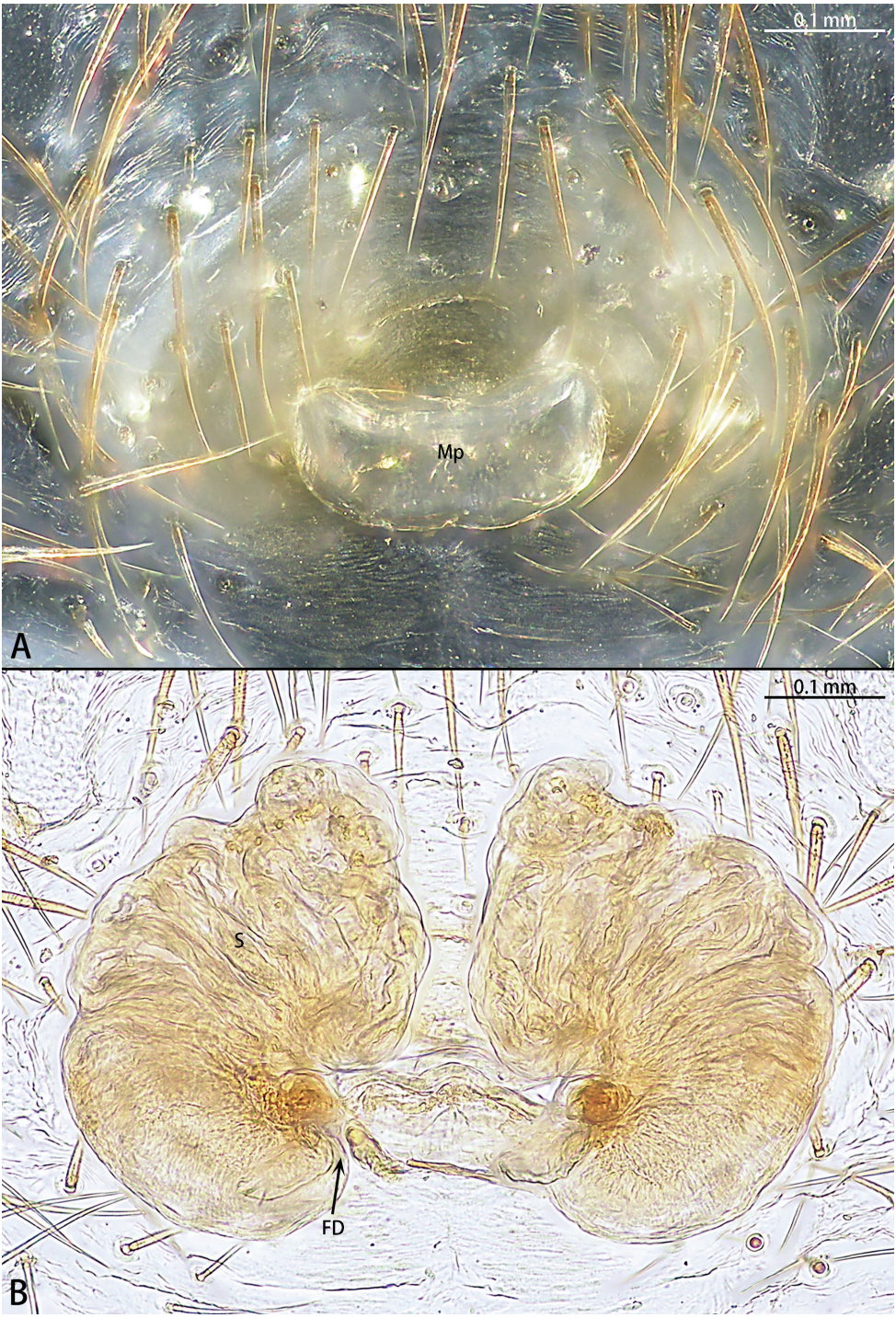

Figure 10. *Phrynarachne huangshanensis*, holotype female **A** epigyne, ventral **B** vulva, dorsal.

III, IV with broad white pattern. Leg measurements: I 2.51 (0.83, 0.83, 0.51, 0.34), II 2.51 (0. 81, 0.86, 0.46, 0.38), III 1.47 (0.47, 0.48, 0.26, 0.26), IV 1.36 (0.48, 0.42, 0.24, 0.22). Leg formula: 1 = 234. Opisthosoma dark brown with yellow-brown spots, each side with 18 tubercles, yellow-brown tubercles, each with a clavate seta.

Male palp (Fig. 12). Tibia brown, VTA club-shaped; RTA long, the length ratio of VTA to RTA is 2:1. Cymbium yellow to brown. Tegulum flat, disk-shaped, with a tegular ridge. Embolus spiraled, thin, the length ratio of embolus to embolus base is 10:1.

Female. See Song and Chai (1990).

Distribution. China (Guizhou, Yunnan).

Notes. The male is reported here for the first time.

Phrynarachne sinensis Peng, Yin & Kim, 2004 *nomen dubium*

Phrynarachne sinensis Peng et al., 2004: 21, figs 1–3; Yin et al. 2012: 1265, fig. 680a–c.

Type material. ***Holotype*****:** ♀ (College of Life Sciences, Hunan Normal University), China (Wang-101), no detailed data, lost, not examined.

Notes. The lost type specimen, lack of clear figures of the holotype, and the vague distributional information make further study of the taxonomy of this species impossible. We treat it as *nomen dubium*.

Phrynarachne xuxiake Lin & S. Li, sp. nov.

http://zoobank.org/BB4750BD-1DC5-4B3C-BF29-2F26118EA68D
Figs 1B, 14, 19C, 21

Type material. ***Holotype*****:** ♀ (IZCAS-Ar41672), **China: *Anhui*:** Huangshan City, Tangkou Town, Fangcunxin Village, ravine, 30.0501°N, 118.1854°E, 450 m elev., IX.2018, Long Yu leg.

Etymology. The species is named after Xu Xiake, a Chinese travel writer and geographer of the Ming dynasty; noun (name) in apposition.

Diagnosis. Females of *Phrynarachne xuxiake* sp. nov. are similar to *P. katoi* but can be distinguished by the length to width ratio of the median plate (3:1 in *P. xuxiake* vs 5:1 in *P. katoi*) and by the rectangular median plate with its posterior edge straight (vs dumbbell-shaped with procurved posterior edge in *P. katoi*).

Description. Female (Figs 14, 19C), ***holotype***: total length 8.78, carapace 3.84 long, 4.45 wide, dark brown with long setae. Eye sizes and interdistances: ALE 0.22, AME 0.17, PLE 0.18, PME 0.15; ALE–AME 0.18, AME–AME 0.24, PLE–PME 0.28, PME–PME 0.28. Chelicerae white, with two promarginal teeth and one retromarginal tooth; gnathocoxae, labium black, labium 0.84 long, 0.74 wide. Sternum black. Legs yellow, femora I and II with dense, varying-sized tubercles; tibiae and metatarsi of I, II with dense ventral spines

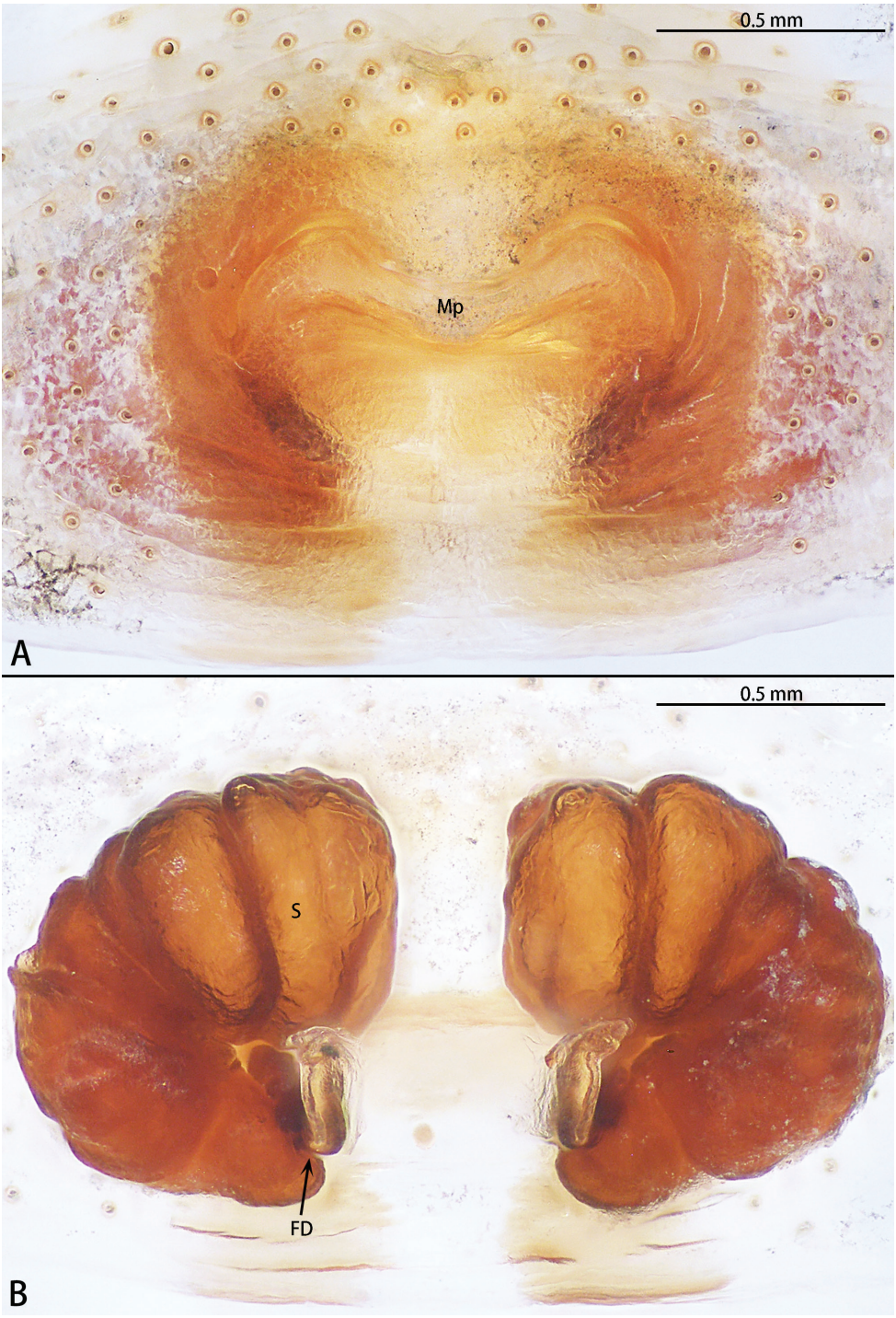

Figure 11. *Phrynarachne lancea*, female **A** epigyne, ventral **B** vulva, dorsal.

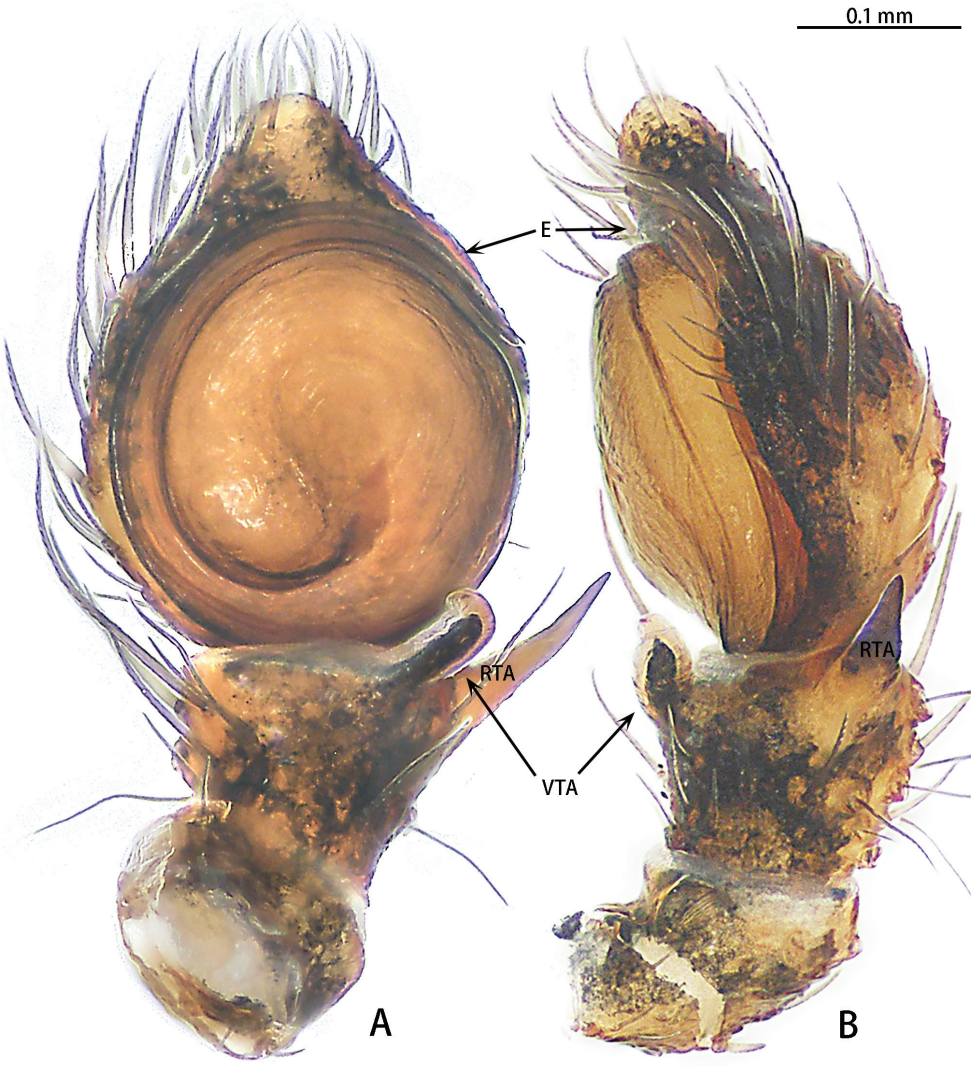

Figure 12. *Phrynarachne mammillata*, male left palp **A** ventral **B** retrolateral.

(I, tibia 26, metatarsus 108; II, tibia 21, metatarsus 89). Leg measurements: I 15.11 (4.17, 4.92, 3.70, 2.32), II 13.93 (4.02, 4.68, 3.13, 2.10), III 6.94 (2.12, 2.71, 1.05, 1.06), IV 6.63 (2.39, 2.54, 0.76, 0.94). Leg formula: 1234. Opisthosoma brown, each side with 19 blunt tubercles, each with a clavate seta, with a pair of black markings medially.

Epigyne (Fig. 14). Sclerotized margins inconspicuous, M-shaped; median plate obvious, with a posterior hood, anterior edge recurved and posterior edge almost straight, the ratio of width to length is 3:1; copulatory opening inconspicuous; Spermathecae kidney-shaped, the ratio of anterior edge to posterior edge length is 3:2. Fertilization duct transverse.

Distribution. Known only from the type locality.

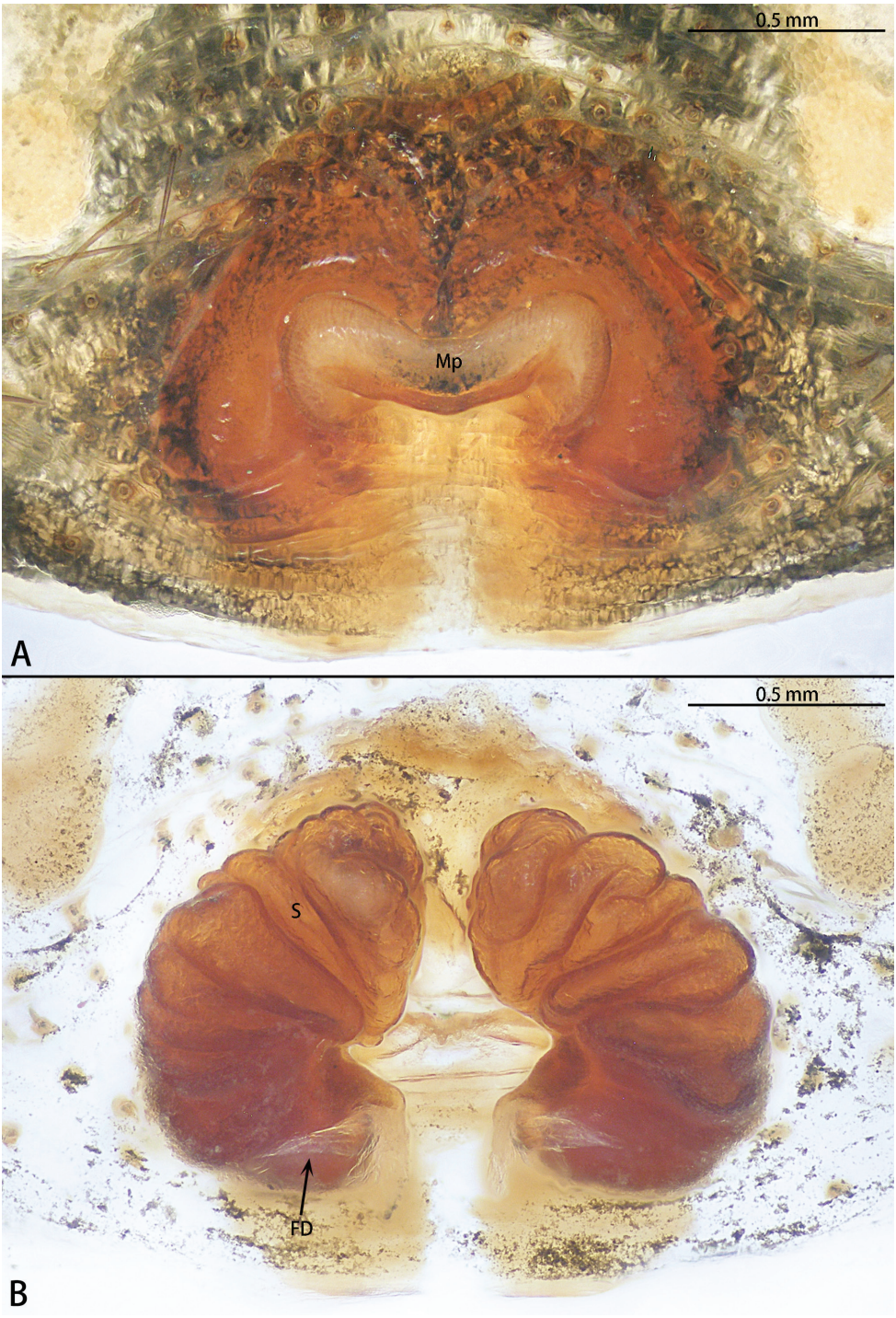

Figure 13. *Phrynarachne mammillata* Song, 1990, female **A** epigyne, ventral **B** vulva, dorsal.

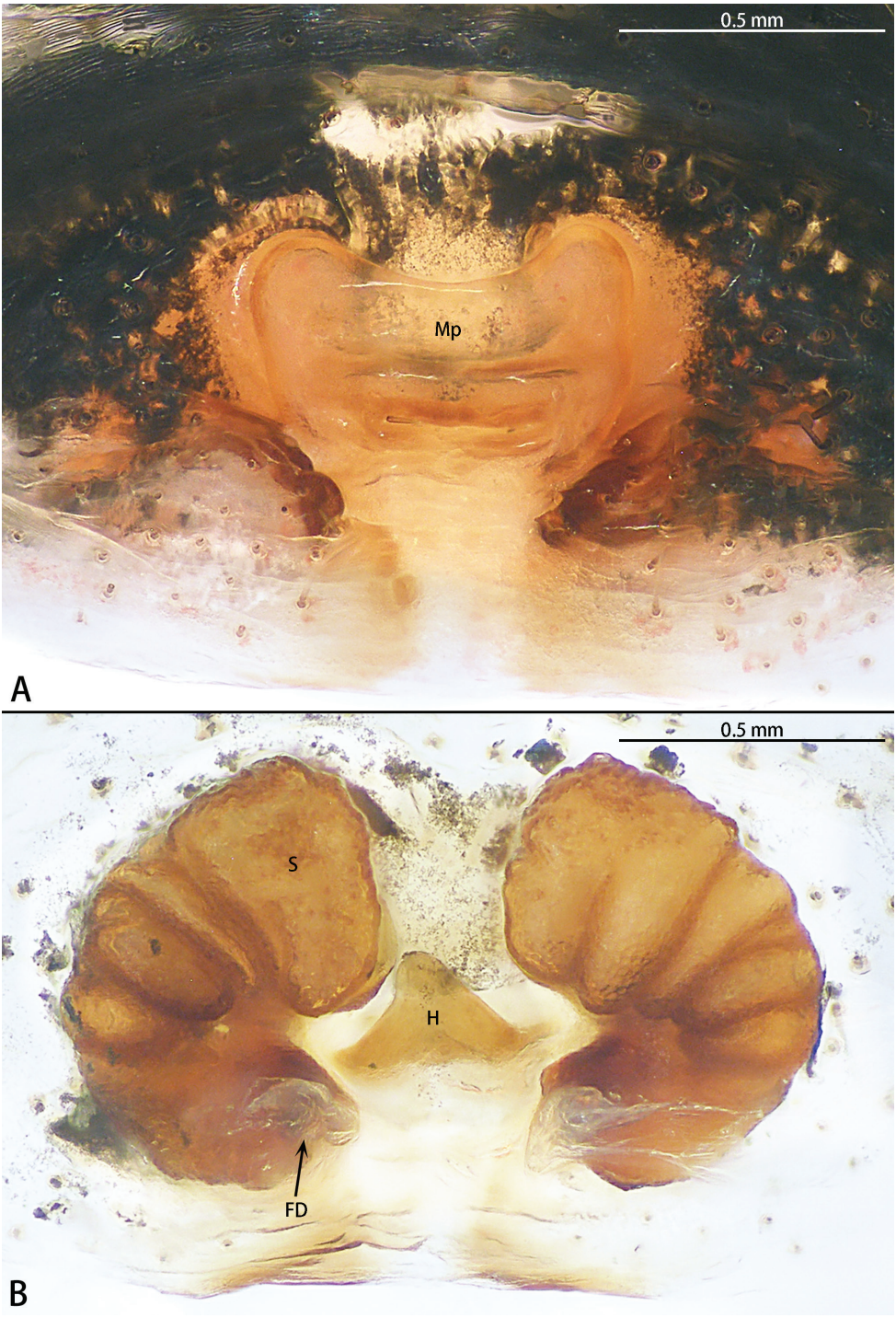

Figure 14. *Phrynarachne xuxiake* sp. nov., holotype female **A** epigyne, ventral **B** vulva, dorsal.

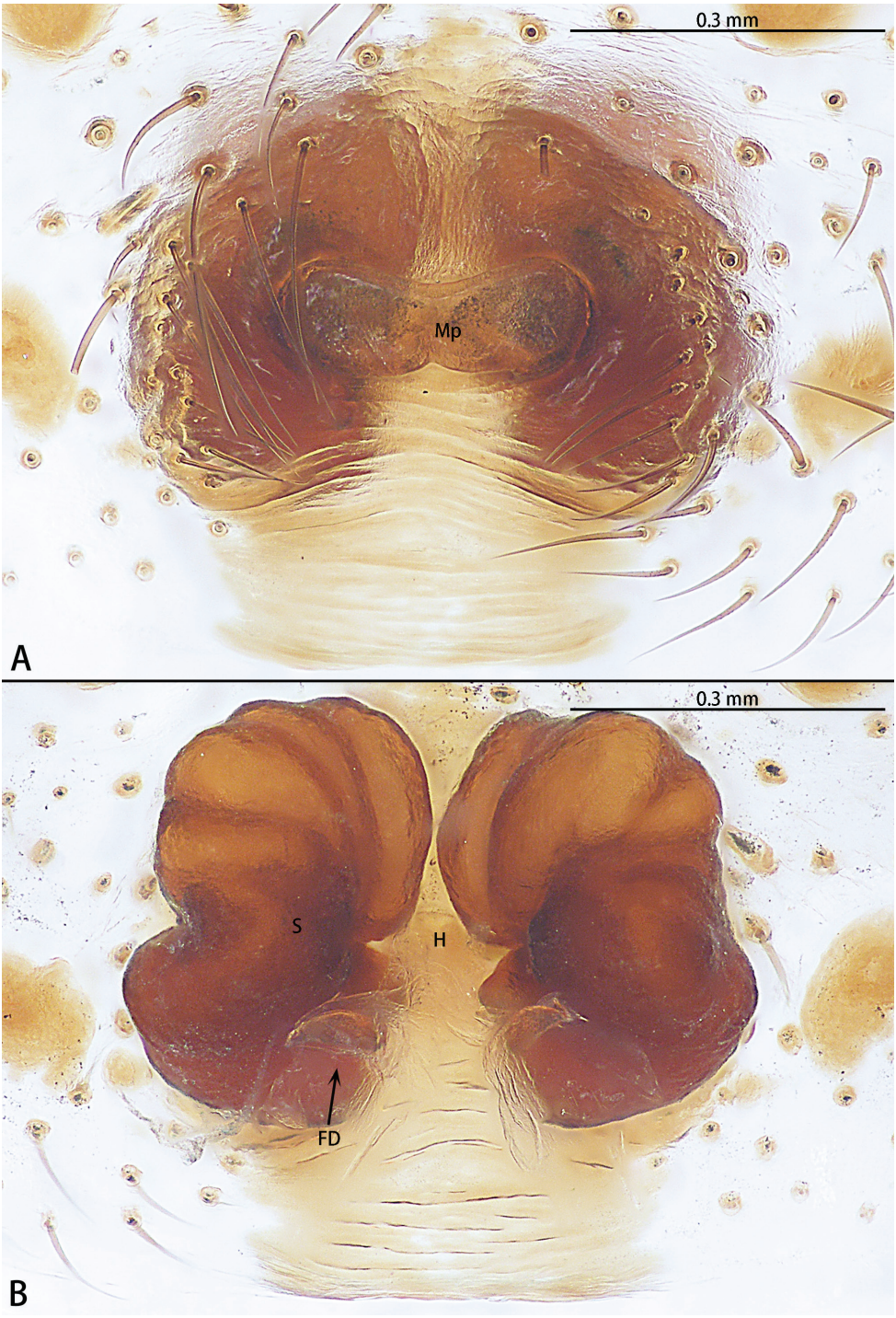

Figure 15. *Phrynarachne yunhui* sp. nov., holotype female **A** epigyne, ventral **B** vulva, dorsal.

Phrynarachne yunhui **Lin & S. Li, sp. nov.**
http://zoobank.org/51542955-2CCB-4A0B-881A-FED561B28CB8
Figs 15, 19D, 21

Type material. ***Holotype*****:** ♀ (IZCAS-Ar41673), **China:** ***Hainan*****:** Ledong County, Jianfengling Nature Reserve, Mingfenggu, 18.7417°N, 108.8417°E, 989 m elev., 1.VII.2020, Yunhu Mo leg.

Etymology. The species is named after Mr Yunhu Mo, who collected the holotype; noun (name) in genitive case.

Diagnosis. Females of *Phrynarachne yunhui* sp. nov. are similar to *P. mammillata* in having the anterior edge and posterior edges of the median plate procurved and the posterior edge with a depression, and in having kidney-shaped spermathecae. However, *Phrynarachne yunhui* sp. nov. can be distinguished by the oval median plate (vs M-shaped in *P. mammillata*) and the broad anterior edge of the spermathecae (vs narrow in *P. mammillata*).

Description. Female (Figs 15, 19D): total length 10.04, carapace 3.67 long, 4.44 wide, black. Eye sizes and interdistances: ALE 0.22, AME 0.19, PLE 0.25, PME 0.20; ALE–AME 0.16, AME–AME 0.27, PLE–PME 0.35, PME–PME 0.29. Chelicerae black, with two promarginal teeth and one retromarginal tooth; Gnathocoxae, labium black, labium 0.83 long, 0.75 wide. Sternum black. Legs black, femora I and II with dense, varying-sized tubercles; tibiae and metatarsi I, II with dense asymmetrical ventral spines (I, tibia 17, metatarsus 41; II, tibia 16, metatarsus 36). Leg measurements: I 13.01 (4.38, 4.63, 2.56, 1.44), II 12.74 (4.33, 4.58, 2.43, 1.40), III 6.78 (2.16, 2.42, 1.18, 1.02), IV 6.44 (2.35, 2.19, 1.07, 0.93). Leg formula: 1234. Opisthosoma grey, with dense, varying-sized, red-brown tubercles, each with a clavate seta.

Epigyne (Fig. 15). Sclerotized margins inconspicuous; median plate obvious, with a small posterior hood, anterior and posterior edges recurved, the ratio of width to length is 15:4; copulatory opening inconspicuous; spermathecae kidney-shaped, the ratio of posterior edge to anterior edge length is 1:1. Fertilization duct transverse.

Distribution. Known only from the type locality.

Phrynarachne zhengzhongi **Lin & S. Li, sp. nov.**
http://zoobank.org/77674036-F817-4088-A525-2DF0AB763CDC
Figs 16, 20, 21

Type material. ***Holotype*****:** ♀ (IZCAS-Ar41674), **China:** ***Yunnan*****:** Xishuangbanna, Jinghong City, Guanping Town, Shiwudui, 22.2310°N, 100.9172°E, 872 m elev., 27.IV.2018, Zhengzhong Huang leg. ***Paratype*** ♀ (IZCAS-Ar41675), same data as holotype.

Etymology. The species is named after Mr Zhengzhong Huang, who collected the holotype and paratype; noun (name) in genitive case.

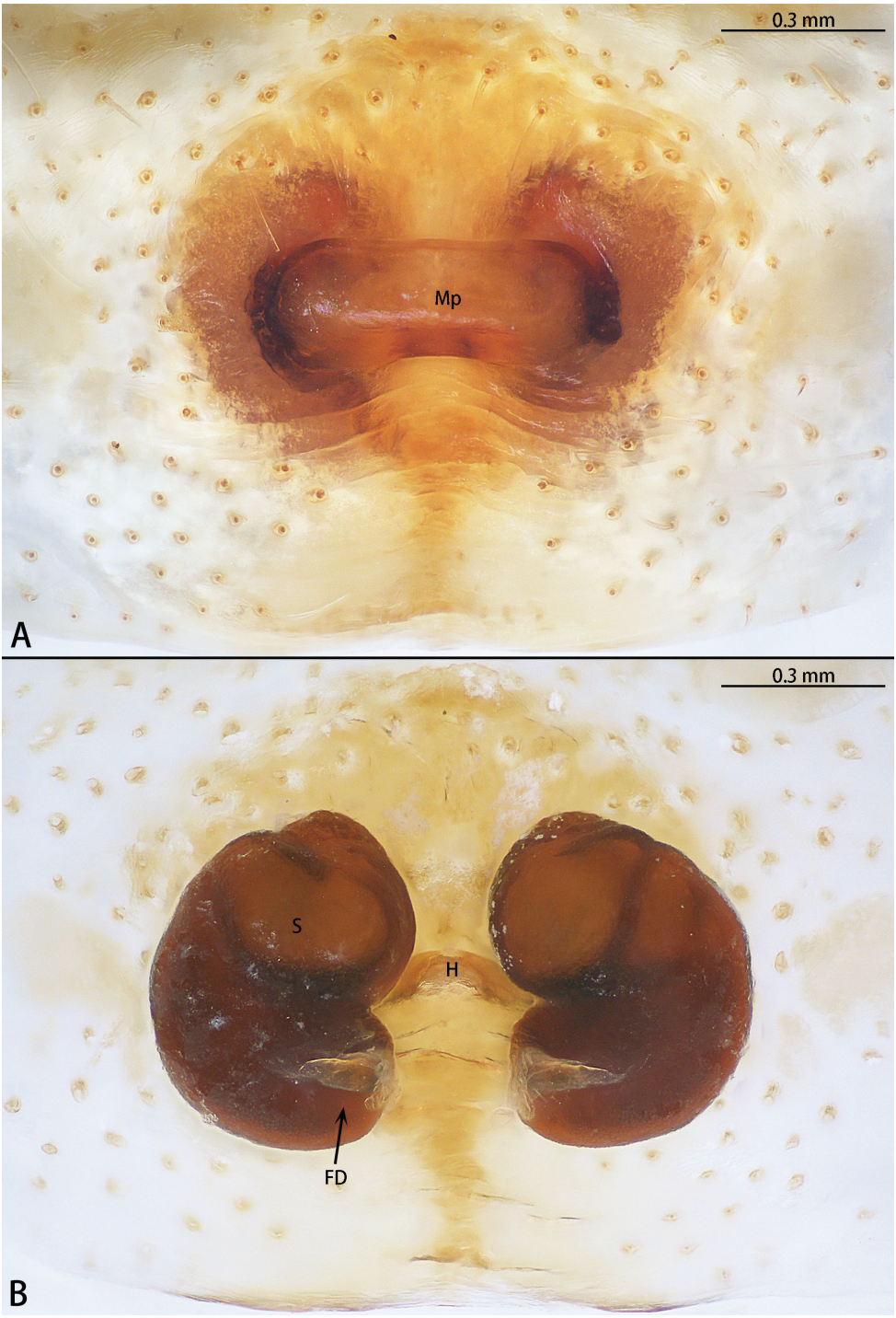

Figure 16. *Phrynarachne zhengzhongi* sp. nov., holotype female **A** epigyne, ventral **B** vulva, dorsal.

Figure 17. *Phrynarachne* spp., holotype females **A, C** habitus (**A**) and original labels (**C** handwriting by Daxiang Song) of *P. huangshanensis* **B, D** habitus (**B**) and original label (**D** handwriting by Daxiang Song) of *P. mammillata*.

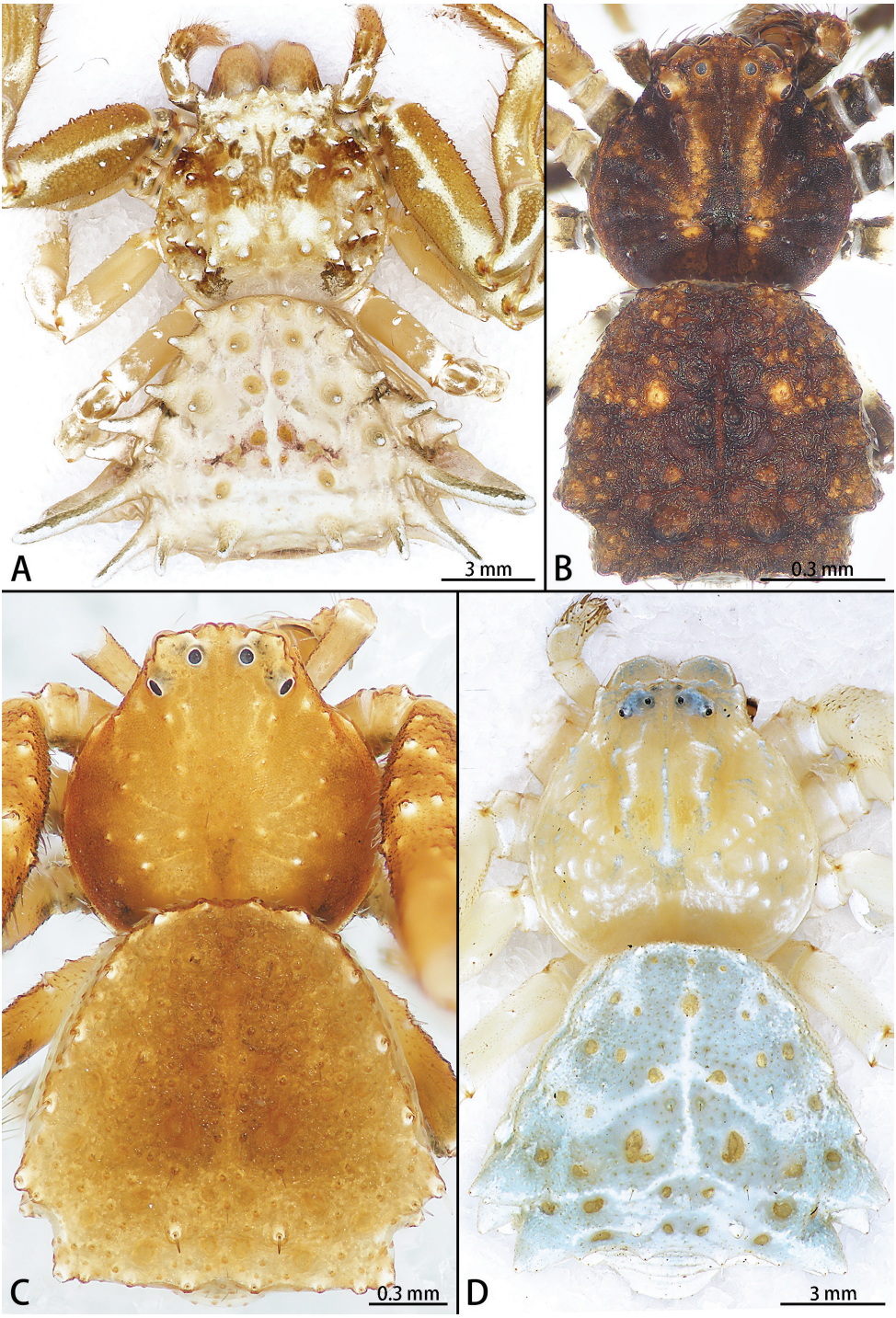

Figure 18. *Phrynarachne* spp., habitus dorsal **A** *P. brevis*, female **B** *P. huangshanensis*, male **C** *P. dreepy* sp. nov., holotype male **D** same, paratype female.

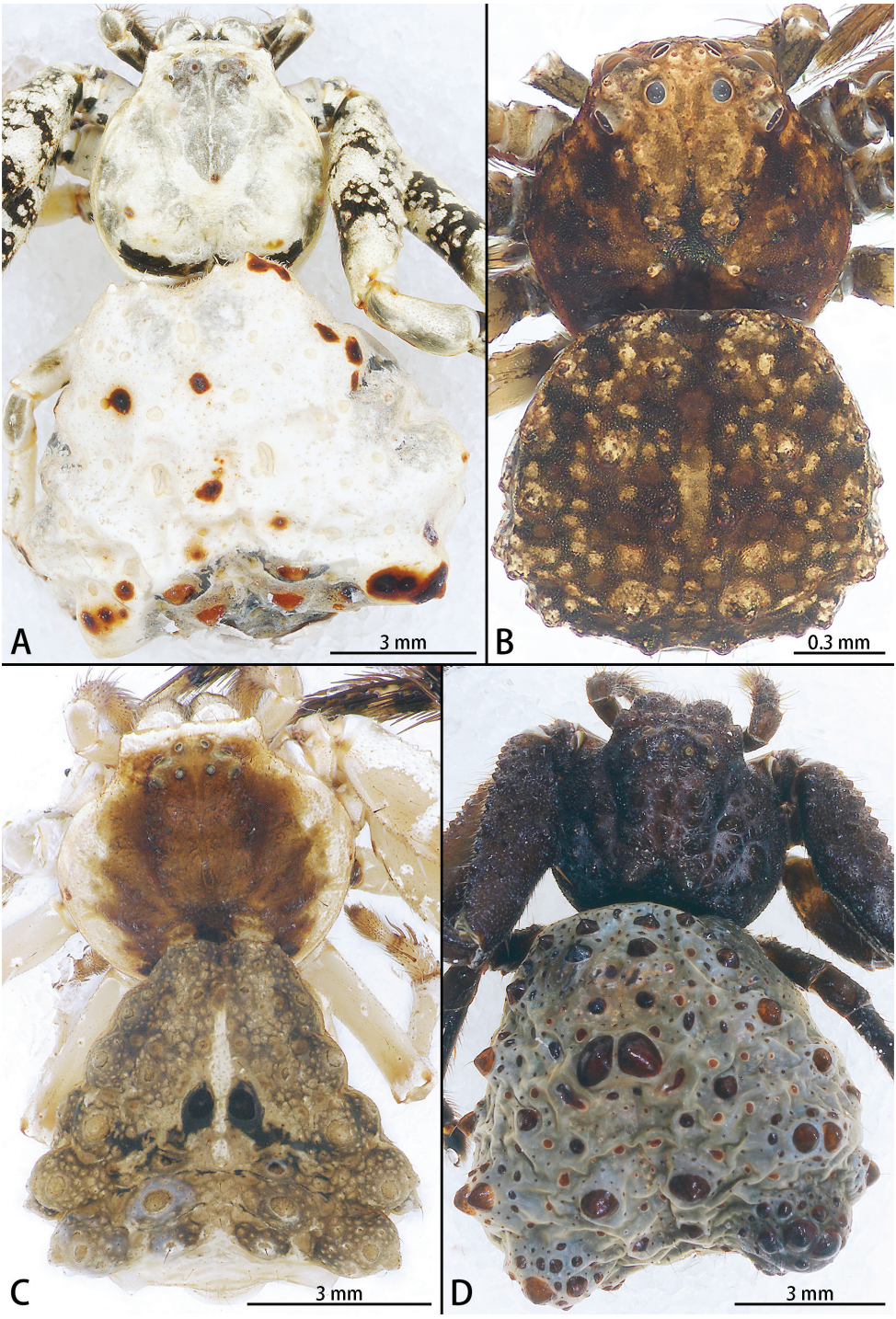

Figure 19. *Phrynarachne* spp., habitus dorsal **A** *P. lancea*, female **B** *P. mammillata*, male **C** *P. xuxiake* sp. nov., holotype female **D** *P. yunhui* sp. nov., holotype female.

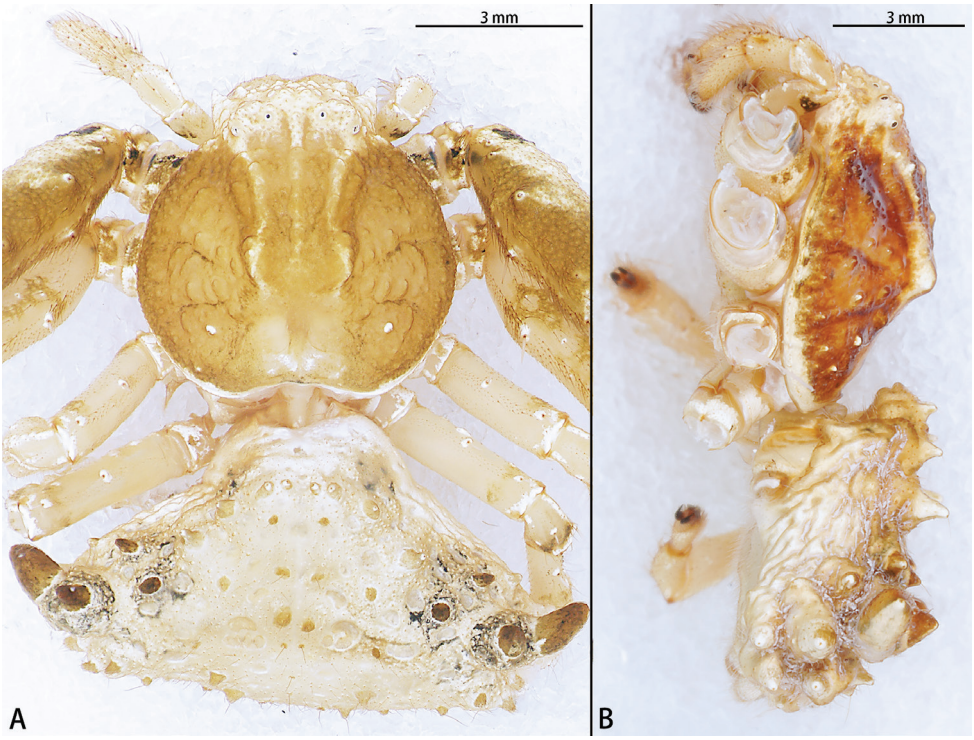

Figure 20. *Phrynarachne zhengzhongi* sp. nov., female holotype (**A**) and paratype (**B**) habitus **A** dorsal **B** lateral.

Diagnosis. Females of *Phrynarachne zhengzhongi* sp. nov. are similiar to *P. brevis* by the shape of the spermathecae; the posterior edge of the spermathecae is as wide as the anterior edge. However, females of *P. zhengzhongi* sp. nov. can be distinguished by the triangular tubercles on the abdomen (vs long, slender apophysis in *P. brevis*), the epigyne with a hood, and the absence of sclerotized margins (vs hood absent, sclerotized margins present in *P. brevis*), and the straight anterior edge of the median plate (vs recurved in *P. brevis*).

Description. Female (Figs 16, 20): total length 10.79, carapace 5.27 long, 5.53 wide, brown, with small projection, ocular tubercle white. Projection present between ALE and PLE. Eye sizes and interdistances: ALE 0.21, AME 0.17, PLE 0.18, PME 0.10; ALE–AME 0.35, AME–AME 0.66, PLE–PME 0.50, PME–PME 0.87. Chelicerae pale yellow, with two promarginal teeth and one retromarginal tooth; gnathocoxae, labium yellow, labium 1.19 long, 0.94 wide. Sternum yellow. Legs brown, femora I and II with dense, varying-sized tubercles; tibiae and metatarsi I, II with dense asymmetrical ventral spines (I, tibia 22, metatarsus 43; II, tibia 17, metatarsus 37). Leg measurements: I 14.43 (4.71, 5.91, 2.35, 1.46), II 14.78 (5.05, 6.31, 2.09, 1.33), III 7.76 (2.24, 3.48, 1.03, 1.01), IV 7.30 (2.44, 3.01, 0.92, 0.93). Leg

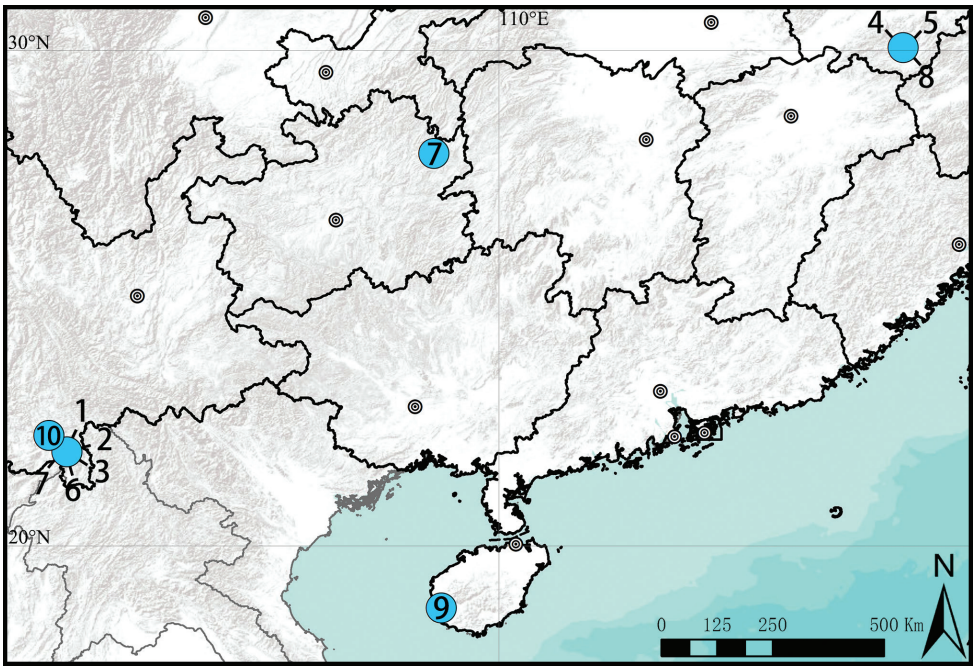

Figure 21. Distribution records of *Phrynarachne* species in China **1** *P. brevis* **2** *P. ceylonica* **3** *P. dreepy* sp. nov. **4** *P. huangshanensis* **5** *P. katoi* **6** *P. lancea* **7** *P. mammillata* **8** *P. xuxiake* sp. nov. **9** *P. yunhui* sp. nov. **10** *P. zhengzhongi* sp. nov.

formula: 2134. Opisthosoma dorsally light yellow, each side with 22 tubercles, each with some tubercles.

Epigyne (Fig. 16). Sclerotized margins inconspicuous; median plate obvious, with a posterior hood, anterior and posterior edges almost straight, the ratio of width to length is 4:1; copulatory opening inconspicuous; spermathecae kidney-shaped, the ratio of posterior edge to anterior edge length is 1:1. Fertilization duct transverse.

Distribution. Known only from the type locality.

Acknowledgements

The manuscript benefited greatly from comments by Hirotsugu Ono,Yuri Marusik, Zhiyuan Yao. Sarah Crews checked the English. Zhengzhong Huang (IZCAS), Fan Gao (Nanjing, China), and Yunhu Mo (Haikou, China) helped with fieldwork. Fan Gao (Nanjing, China), Chao Wu (Beijing, China), and Ruiyang Wang (Nanjing, China) took the photographs.

References

Chikuni Y (1955) Five interesting spiders from Japan highlands. Acta Arachnologica 14: 29–40. https://doi.org/10.2476/asjaa.14.29

Li J, Yan X, Lin Y, Li S, Chen H (2021) Challenging Wallacean and Linnean shortfalls: Ectatosticta spiders (Araneae, Hypochilidae) from China. Zoological Research 42(6): 791–794. https://doi.org/10.24272/j.issn.2095-8137.2021.212

Li Y, Chen F, Song D (1985) A new species of the genus *Phrynarachne* (Araneae: Thomisidae). Journal of Anhui Normal University, Natural Sciences 1985(1): 72–74.

Ono H (1988) A Revisional Study of the Spider Family Thomisidae (Arachnida, Araneae) of Japan. National Science Museum, Tokyo, 252 pp.

Peng X, Yin C, Kim J (2004) One new species of the genus *Phrynarachne* (Araneae, Thomisidae) from China. Korean Arachnology 20: 21–25.

Pickard-Cambridge O (1884) On two new genera of spiders. Proceedings of the Zoological Society of London 52(2): 196–205. [pl. 40] https://doi.org/10.1111/j.1096-3642.1884.tb02819.x

Song D, Chai J (1990) Notes of some species of the family Thomisidae (Arachnida: Araneae) from Wuling Shan area. In: Zhao E (Ed.) From Water onto Land. CSSAR, Beijing, 364–374.

Tang G, Li S (2010) Crab spiders from Xishuangbanna, Yunnan Province, China (Araneae, Thomisidae). Zootaxa 2703: 1–105. https://doi.org/10.11646/zootaxa.2703.1.1

Thorell T (1869) On European spiders. Part I. Review of the European genera of spiders, preceded by some observations on zoological nomenclature. Nova Acta Regiae Societatis Scientiarum Upsaliensis (3)7: 1–108.

Yao Z, Wang X, Li S (2021) Tip of the iceberg: species diversity of *Pholcus* spiders (Araneae, Pholcidae) in Changbai Mountains, Northeast China. Zoological Research 42(3): 267–271. https://doi.org/10.24272/j.issn.2095-8137.2020.214

Yin CM, Peng XJ, Yan HM, Bao YH, Xu X, Tang G, Zhou QS, Liu P (2012) Fauna Hunan: Araneae in Hunan, China. Hunan Science and Technology Press, Changsha, 1590 pp.

WSC (2021) World Spider Catalog. Version 22.5. Natural History Museum Bern. http://wsc.nmbe.ch [Accessed on: 2021–09–11]

ZooKeys 1085: 101–127 (2022)
doi: 10.3897/zookeys.1085.76033
https://zookeys.pensoft.net

RESEARCH ARTICLE

A peer-reviewed open-access journal
ZooKeys
Launched to accelerate biodiversity research

Biodiversity of vertebrates in Argentina: patterns of richness, endemism and conservation status

Valeria Bauni[1], Claudio Bertonatti[1], Adrián Giacchino[1], Facundo Schivo[2,14], Ezequiel Mabragaña[3,14], Ignacio Roesler[4,5,14], Juan José Rosso[3,14], Pablo Teta[6,14], Jorge D. Williams[7,14], Agustín M. Abba[8,14], Guillermo H. Cassini[8,14], María Berta Cousseau[9], David A. Flores[10,14], Damián M. Fortunato[7], María Emilia Giusti[11,14], Jorge Pablo Jayat[12], Jorge Liotta[13], Sergio Lucero[6,14], Tomás Martínez Aguirre[7], Javier A. Pereira[6,14], Jorge Crisci[15]

1 *Fundación de Historia Natural Félix de Azara. Centro de Ciencias Naturales, Ambientales y Antropológicas, Universidad Maimónides. Hidalgo 775 7mo piso, CP 1405, Ciudad Autónoma de Buenos Aires, Argentina* **2** *Instituto de Investigación e Ingeniería Ambiental (IIIA), CONICET-UNSAM, Campus Miguelete, 25 de Mayo y Francia, CP 1650, San Martín, Argentina* **3** *Grupo de Biotaxonomía Morfológica y Molecular de Peces (BIMOPE), Instituto de Investigaciones Marinas y Costeras, Facultad de Ciencias Exactas y Naturales, Universidad Nacional de Mar del Plata- CONICET, Deán Funes 3350, CP 7600, Mar del Plata, Argentina* **4** *Departamento Científico, Aves Argentinas - Asociación Ornitológica del Plata. Matheu 1246/8, CP 1249, Ciudad Autónoma de Buenos Aires, Argentina* **5** *Departamento Análisis de Sistemas Complejos. Fundación Bariloche. EDGE of Existence affiliated. Zoological Society of London, Av. Bustillo 9500, CP 8400, Bariloche, Argentina* **6** *División Mastozoología, Museo Argentino de Ciencias Naturales "Bernardino Rivadavia", Av. Angel Gallardo 470, CP 1405, Ciudad Autónoma de Buenos Aires, Argentina* **7** *Facultad de Ciencias Naturales y Museo, Universidad Nacional de La Plata. Anexo Museo, Laboratorio 105. Calles 122 y 60, CP 1900, La Plata, Argentina* **8** *Centro de Estudios Parasitológicos y de Vectores (CEPAVE, CONICET-UNLP), Boulevard 120 s/n entre Av. 60 y Calle 64, CP 1900, La Plata, Argentina* **9** *Facultad de Ciencias Exactas y Naturales, Universidad Nacional de Mar del Plata, Funes 3550, CP 7602, Mar del Plata, Argentina* **10** *Instituto de Vertebrados, Unidad Ejecutora Lillo (CONICET- Fundación Miguel Lillo), Miguel Lillo 251, CP 4000, San Miguel de Tucumán, Argentina* **11** *Instituto de Ecología, Genética y Evolución de Buenos Aires (IEGEBA-FCEN-UBA), Ciudad Universitaria, Pabellón II, Güiraldes 2160, CP 1428, Ciudad Autónoma de Buenos Aires, Argentina* **12** *Unidad Ejecutora Lillo (CONICET- Fundación Miguel Lillo), Miguel Lillo 251 CP 4000, San Miguel de Tucumán, Argentina* **13** *Museo Regional de Ciencias Naturales "A. Scasso", San Nicolás de los Arroyos, Don Bosco 580, CP 2900, Buenos Aires, Argentina* **14** *Consejo Nacional de Investigaciones Científicas y Técnicas (CONICET), Argentina* **15** *Facultad de Ciencias Naturales y Museo, Universidad Nacional de La Plata. Paseo del Bosque s/n, CP 1900, La Plata, Argentina*

Corresponding author: Valeria Bauni (valeria.bauni@fundacionazara.org.ar)

Academic editor: Aaron Bauer | Received 8 October 2021 | Accepted 7 January 2022 | Published 4 February 2022

http://zoobank.org/79CEBC97-0434-4C7D-BAA7-576137FDC1CC

Citation: Bauni V, Bertonatti C, Giacchino A, Schivo F, Mabragaña E, Roesler I, Rosso JJ, Teta P, Williams JD, Abba AM, Cassini GH, Cousseau MB, Flores DA, Fortunato DM, Giusti ME, Jayat JP, Liotta J, Lucero S, Aguirre TM, Pereira JA, Crisci J (2022) Biodiversity of vertebrates in Argentina: patterns of richness, endemism and conservation status. ZooKeys 1085: 101–127. https://doi.org/10.3897/zookeys.1085.76033

Abstract

Optimising conservation efforts requires an accurate record of the extant species as well as their geographic distributions. Nevertheless, most current conservation strategies start from an incomplete biodiversity inventory. Argentina has an extraordinary diversity of species, however, until now an updated inventory of its fauna has not been carried out. In this context, the main objective of this work is to present the results of the first national inventory of vertebrate species. Experts from each major vertebrate taxonomic group assembled and compiled its respective inventory. The information gathered included taxonomic rank, conservation status, endemism and geographic distribution. Species richness and representativeness were calculated for each taxonomic group, distinguishing between native, endemic and exotic, for each Argentinian province. Our results show Argentina harbours 3,303 species: 574 marine fish, 561 freshwater fish, 177 amphibians, 450 reptiles, 1,113 birds, and 428 mammals. Native species constitute 98.1% of the total taxa. The results achieved were spatially represented showing a pattern of higher richness from north to south and from east to west. Species considered as threatened account for 17.8% and 15.2% are endemic. There are five Extinct species. These results provide key information on developing strategies and public policies at the national and provincial levels and constitute a tool for the management and conservation of biodiversity.

Keywords

Amphibians, biological inventory, birds, freshwater fish, mammals, marine fish, reptiles

Introduction

There are many estimates of the total number of species in the world, which oscillate by tens of millions (Costello et al. 2012). Nevertheless, most of the world´s biodiversity (as much as 80%) is still entirely unknown thus preventing proper estimates of the total number of species on Earth even to the nearest order of magnitude (Wilson 2003, 2017). The most prudent estimates range from 5 to 50 million species, considering that published species are close to 1.9 million (Chapman 2009). Model-based projections have been performed, indicating that 24–31% marine and 21–29% terrestrial species remain to be discovered (Costello et al. 2012). The Catalogue of Life, which contains contributions from 172 taxonomic databases, estimates 2,260,074 species accepted or provisionally accepted in 2020 (Roskov et al. 2020). In 2019, 59,284 species were estimated to have become extinct before and during the Holocene (Roskov et al. 2019). Additionally, it has been estimated that human activities have already led to the extinction of at least 680 species of vertebrates since 1500 (IPBES 2019).

Recently, the IPBES Panel (Intergovernmental Science-Policy Platform on Biodiversity and Ecosystem Services) drew the world's attention by confirming that human actions have raised -and accelerated- the global extinction rate of wild species at an unprecedented rate when compared to the last 10 million years. So much so that 25% of animals and plants species assessed by the International Union for Conservation of Nature (IUCN) are threatened (IPBES 2019).

In this context, optimising conservation efforts requires accurately recording species and assessing where they live (Costello et al. 2013). Regrettably, current conservation efforts usually start from incomplete biodiversity catalogues (Scheffers et al. 2012). An inventory lists, orders, catalogues, and quantifies ecoregions, ecosystems, and/or species (Stork and Samways 1995, PNUD 2007). Inventorying is a fundamental tool for environmental management (McNeely et al. 1995) as what is unknown cannot be protected. Therefore, it constitutes the first and most reasonable conservation action (Evenhuis 2007). Since species are the fundamental units of biology, ecology, and conservation assessments (Mace 2004; Tobias et al. 2010; Costello et al. 2013), most biological inventories are presented at this level of biological hierarchy.

The earliest systematic record of biodiversity in Argentina dates back to the studies of Félix de Azara (Azara 1801, 1802–1805). Since then, lists, catalogues, and reference collections have been added, which require being constantly updated. In Argentina, extraordinary ecosystem diversity results in a great diversity of species. In the case of faunal species, precise estimates of their richness are mostly scattered and outdated. For the case of plant species, there is an updated and complete national catalogue comprising 10,221 species of vascular plants (Zuloaga et al. 2019). According to the IUCN (2021), there are about 320 threatened species at the global scale, including vertebrates, invertebrates, plants, and fungi present in Argentina.

Amidst a global change crisis, knowing the list of existing taxa became essential (Scheffers et al. 2012), especially for different political jurisdictions, including their systematic identification, their geographical distribution and their conservation status. In most countries of the world, this knowledge is fragmentary, incomplete, and outdated. This aspect becomes particularly complex in a context in which global wildlife populations are evidently declining, yet simultaneously, new taxa continue to be described (Costello et al. 2013; Grismado and Ramírez 2018, 2019, 2020).

Despite representing only 3.45% of described species (73,118 species) and a much lower fraction of extant species (IUCN 2021a), vertebrates have been used to make extrapolations in a wide range of biodiversity and conservation analyses (Titley et al. 2017; Fukushima et al. 2020). Particularly in Argentina, there is a lack of a single, complete, and updated inventory of vertebrate fauna at the national or provincial level. Having an inventory of national scale is particularly timely in a context dominated by a widespread land use and land cover change intensification, accompanied by a gradual degradation and destruction of natural communities. Completing an inventory of known species at the country level is therefore a priority for both biodiversity data management and conservation (Costello et al. 2012). In this context, the main objective of our work is to analyse the results of Argentina's first national inventory of vertebrates under the premise that developing objective decision-making and establishing precise public policies demands this type of information (Webb et al. 2010; Costello et al. 2013). As a consequence, the main objective of this collective effort is to be kept up-to-date and free for decision-makers.

Material and methods

Study area

The continental area of Argentina extends for 2,791,810 km² (IGN 2019), which makes it the second largest country in South America after Brazil, and the eighth largest in the world, considering its continental area subject to effective sovereignty (Arana et al. 2021). It covers a large part of the Southern Cone of South America, bordered to the north by Bolivia and Paraguay, to the northeast by Brazil, to the east by Uruguay and the Atlantic Ocean, to the west by Chile, and to the south by Chile and the waters of the Drake Passage (Fig. 1; Arana et al. 2021). Latitudinally, it is an extensive country, ranging from 21°45'S (at its northern limit) to 53°03'S (at its southernmost part). A mountainous range extends along the western edge with peaks exceeding 7,000 metres above sea level. A third of its territory is semi-arid, arid and desert (Morello et al. 2012). A wide diversity of climates is present, from tropical and subtropical in the northwest and northeast, to extreme cold in the mountain zones and the south. The most extensive climate is temperate. As a consequence of its vast territory, it exhibits a great diversity of biomes, from salt flats and deserts, temperate forests to subtropical forests, shrublands, grasslands and wetlands (Arana et al. 2021). The coast covers a distance of 4,645 km (Acha 2014). Morello et al. 2018 identified 16 ecoregions in Argentina, including the Argentinian Sea (Mar Argentino). Argentina's territorial organisation is made up of several levels. It comprises 23 provinces and the autonomous city of Buenos Aires, which is the capital of the nation. Argentina extends its sovereignty over the sea adjacent to its coasts and islands, as well as over the bed and subsoil of marine areas that cover 1,785,000 km² (Fig. 1; Acha 2014; Gaitan 2020). Tierra del Fuego, Antártida e Islas del Atlántico Sur Province includes territories whose sovereignty is in dispute: Islas Malvinas (Malvinas/Falkland Islands), Islas Georgias del Sur (South Georgia Islands), Islas Sandwich del Sur (South Sandwich Islands), Islas Orcadas del Sur (South Orkney Islands), Islas Shetland del Sur (South Shetland Islands), Islas Aurora (Aurora Islands), and Antártida Argentina (Argentina Antarctic Sector).

Database generation

Experts were convened to elaborate and compile an updated inventory of vertebrate species in Argentina: marine and freshwater fishes, amphibians, reptiles, birds, and mammals. In order to expedite the following analyses, a single merged database was compiled for all taxa, which included the following information for each recorded species: Class, Order, Family, scientific name, common name, synonyms, and national conservation status (or international, in the case of groups that did not have national evaluations; e.g., marine fish). If a species was endemic to Argentina, the region of endemism and distribution (presence by province) were also included. Argentinian provinces have authority over their natural resources and conservation actions must be conducted in agreement with the corresponding authorities. Therefore, the presentation

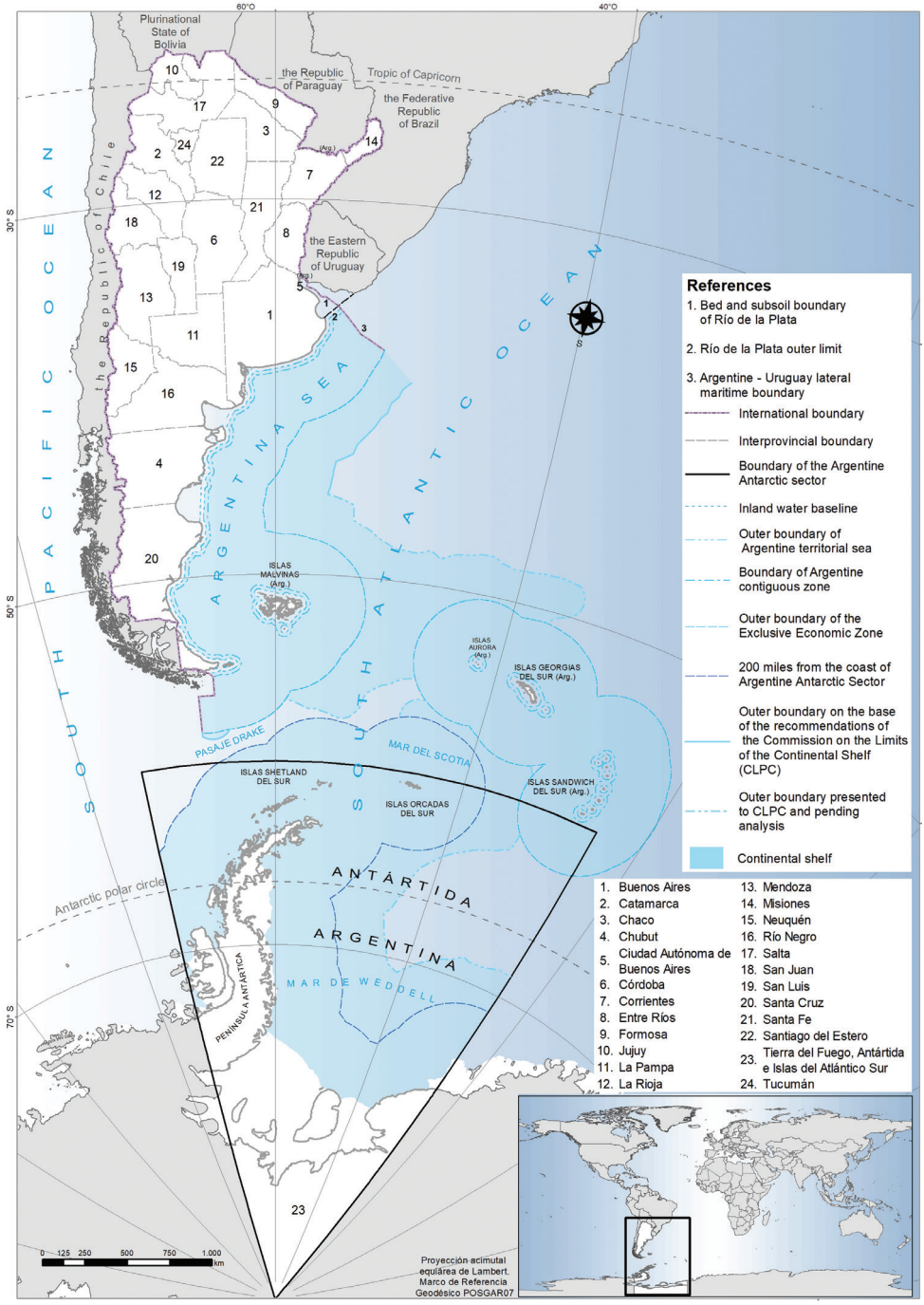

Figure 1. Political map of Argentina. International and national boundaries, including terrestrial and maritime, are indicated. Each of the 23 provinces and the autonomous city of Buenos Aires are depicted. Source of spatial information: National Geographic Institute (IGN 2021).

of results segregated by provinces is not a matter of convenience, but applicability. The inventory also considers introduced, invasive and/or exotic species.

The conservation categories used by the different national lists were homologised to unify criteria differing between them, and fit to the international categories of the IUCN (Table 1). Species classified as Critically Endangered (CR), Endangered (EN) or Vulnerable (VU) were considered threatened (Gärdenfors 2001; IUCN 2019). The "Regionally Extinct" category was incorporated, and was used for those species that are extinct within, for example, a particular country but that are still extant in other parts of the world (Gärdenfors 2001).

Marine fishes. The list of marine fish compiles information that includes the continental shelf and slope between 34°S and 55°S and the Uruguayan shelf based on the existence of the Argentina-Uruguay Common Fishing Zone. It is based on different bibliographic sources (Pozzi and Bordalé 1935; Menni et al. 1984; Cousseau et al. 2010; Cousseau and Rosso 2019; Figueroa 2019) as well as research conducted by the National Institute for Fisheries Research and Development (Instituto Nacional de Investigación y Desarrollo Pesquero, INIDEP) and the Puerto Deseado Oceanographic Vessel. Contributions made by commercial and sport fishermen were also included, since they report their catches to INIDEP (Cousseau et al. 2010). Both valid scientific names and known synonyms of fish species were assigned according to Fricke et al. (2020). For suprageneric categories, Nelson et al. (2016) was followed. Regarding endemics, those reported for the Magellan Province were included (Cousseau et al. 2020). With respect to the geographical distribution of each species, the information available worldwide has been considered, since most species exceed the limits of the Argentinian continental shelf. Conservation status corresponds to that assigned by the IUCN, since no national categorisation exists.

Freshwater fishes. The list was compiled from different information sources regarding the presence and distribution of freshwater fish in Argentina (Ringuelet et al. 1967; López et al. 1987, 2003; Menni 2004; Liotta 2005; Mirande and Koerber 2015, 2020; Cousseau and Rosso 2019, in press) and the database fish from continental water (Base de Datos de peces de Agua Continentales de Argentina). This Inventory includes

Table 1. Conservation categories applied for Argentina´s vertebrate inventory.

Unified Conservation Status Categories	Acronym
Extinct	EX
Extinct in the Wild	EW
Regionally Extinct	EXR
Critically Endangered	CR
Endangered	EN
Vulnerable	VU
Near Threatened	NT
Least Concern	LC
Not Threatened	NA
Data Deficient	DD
Not Evaluated	NE
Not applicable	NAP

some species not considered in previous publications. For systematic information, we followed Nelson et al. (2016) and for the synonymy, Fricke et al. (2020). Conservation aspects have been incorporated considering all currently available works, which have variously conducted evaluations at the national, regional or local level (Chebez 1994; Bello and Ubeda 1998; Orlandini et al. 2001; López et al. 2003; Cordiviola and Zayas 2007; Cappato and Yanosky 2009; Chebez et al. 2009; Cordiviola et al. 2009; Alonso et al. 2018; Cardoso et al. 2019). When a species was placed in different conservation categories according to the various information sources consulted, we kept the highest degree of threat, as a precautionary principle (Bauni et al. 2021). Some exceptions were made for very restricted regional or local evaluations of some species where the highest category did not accurately represent the national scenario for the species.

Amphibians and reptiles. For the compilation of these groups the information was obtained from an exhaustive bibliographic review, comprising lists published by Avila et al. (2013) for lizards and amphisbaenians; Williams and Francini (1991), Giraudo and Scrocchi (2002), and Williams et al. (2021) for snakes; the conservation categorisations published by the Argentina Herpetological Association (AHA, Spanish abbreviation) in 2000 and 2012. Also, different regional field guides were consulted, including digital databases such as "Amphibian Species of the World" (Frost 2021) for amphibians and "The Reptile Database" (Uetz 2021) for reptiles. For the conservation status the last proposal generated by the AHA was followed (Abdala et al. 2012; Giraudo et al. 2012; Prado et al. 2012; Vaira et al. 2012).

Birds. Taxonomic order was based on the combination of different sources frequently used by Neotropical ornithologists, which are mostly used as references in scientific publications from Argentina (e.g., El Hornero and Nuestras Aves). Systematics follows the nomenclature proposed by specialists in the "Argentina Committee of Ornithological Records" (CARO, Spanish abbreviation) (Monteleone et al. 2021) and that proposed by the South American Classification Committee (SACC) (Remsen et al. 2021). However, modifications were made following some extra sources of popular use, such as eBird. In the same way, some updates were made following BirdLife International (2021). To generate Argentina's bird database, the lists of Monteleone and Pagano (in prep.) and Pearman and Areta (2018) were used as the main sources. Field guides were used for provincial distribution (Fjeldså and Krabbe 1990; Rodríguez Mata et al. 2006; Ridgely and Tudor 2009; Narosky and Yzurieta 2010; Pearman and Areta 2018, 2020) as were regional or provincial guides and publications (Nores et al. 1991; Narosky and Giacomo 1993; De La Peña 1997). In order to provide updated information at the provincial level, databases such as eBird were also consulted (eBird 2021), as well as periodic national publications (e.g., Nuestras Aves, Nótulas Faunísticas, Cotinga). Areas of endemism were mainly based on Mazar et al. (2001) and Pearman and Areta (2020) with modifications based on empirical observations and modern literature. Species of hypothetical historical presence were not considered. The species conservation status was based on the last national categorisation (López-Lanús et al. 2017), except for species not yet considered in that list. In those cases, Birdlife was consulted (BirdLife International 2021).

Mammals. The taxonomic list in this work was based on Teta et al. (2018), with modifications according to more recent literature. The aforementioned list includes living species and those considered extinct or potentially extinct in Argentina during historical times (i.e., since 1500 AD). It excludes species of hypothetical or probable presence in the country. In the case of exotic species, only those taxa with one or more recently documented wild populations are considered (Chebez and Rodríguez 2014; Teta et al. 2018). For the conservation status of this group, the last national categorisation was used (SAyDS and SAREM 2019).

Data compilation and analyses

The complete list of all vertebrates was published as a book and is freely accessible at the following web: https://www.fundacionazara.org.ar/img/libros/inventario-biologico-argentino.pdf (Bauni et al. 2021). For each province, species richness and percentage of representativeness were calculated for each taxonomic group, distinguishing between native, exotic, endemic, and threatened taxa. For species representativeness, the total of each category at the national level was considered. The number of exclusive endemic species per province for each group was also evaluated. The results achieved were spatially represented through the elaboration of cartographic products. For each province, we used a colour gradient to depict species richness values. For visualisation, only the continental area of the American continent was mapped (Antarctica was excluded). Marine species were assigned to Argentinian Sea as a whole unit for map representation, but it does not necessarily mean that the species inhabit the entire region. The same criteria were used for Tierra del Fuego, Antártida e Islas del Atlántico Sur, thus the use of the full name does not imply that the species is present throughout that territory.

Results

Argentina's national vertebrate inventory comprises 3,303 species: 574 marine fish, 561 freshwater fish, 177 amphibians, 450 reptiles, 1113 birds and 428 mammals. In total, 98.1% are native (3,240 spp.) and 15.2% (492 spp.) endemic (Table 2). The taxonomic groups with the highest number of introduced, invasive, and/or exotic species are freshwater fish (22 spp.), and mammals (21 spp.). The latter has the highest percentage (4.9%) regarding the total species of its group.

Misiones province exhibits the highest species richness of continental vertebrates in Argentina (1,190 spp.) followed by Salta (1,092 spp.) and Corrientes (1,079 spp., Fig. 2, Appendix 1: Table A1–A3). Misiones also has the highest richness of freshwater fish species (335 spp.) and amphibians (63 spp.), whereas Salta has the largest number of species of native reptiles (116 spp.), birds (603 spp.) and mammals (159 spp.) (Fig. 2, Appendix 1: Table A1–A3). The lowest number of species (304 spp.) is observed in Tierra del Fuego, followed by Santa Cruz (382 spp.) (Fig. 2, Appendix 1: Table A1–A3).

Table 2. Total number (and percentage) of species richness, native species, exotic species, and percentage endemism by taxonomic group. *The percentage of endemic species is calculated over the total of native species of the group.

Taxonomic group	Total	Native	Exotic	Endemic*
Marine fishes	574 (17.4%)	570 (99.3%)	4 (0.7%)	20 (3.5%)
Freshwater fishes	561 (17%)	539 (96.1%)	22 (3.9%)	96 (17.8%)
Amphibians	177 (5.4%)	176 (99.4%)	1 (0.6%)	52 (29.5%)
Reptiles	450 (13.6%)	446 (99.1%)	4 (0.9%)	216 (48.4%)
Birds	1,113 (33.7%)	1,102 (99.0%)	11 (1.0%)	21 (1.9%)
Mammals	428 (13%)	407 (95.1%)	21 (4.9%)	87 (21.4%)
Total	3,303 (100%)	3,240 (98.1%)	63 (1.9%)	492 (15.2%)

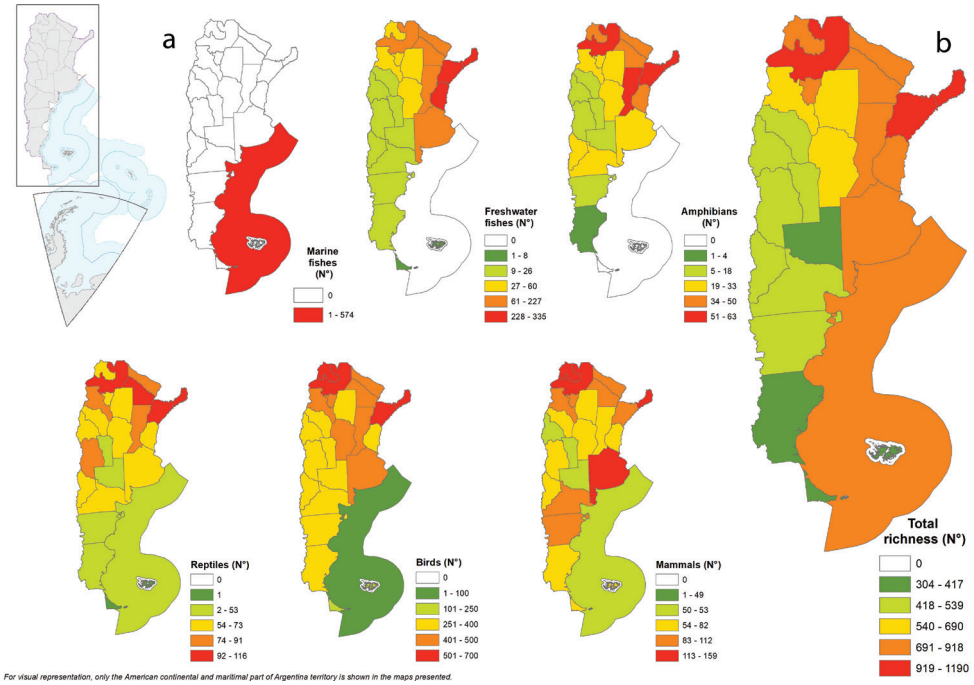

Figure 2. Species richness **a** by taxonomic group by province and **b** total species richness.

Neuquén has the highest number of exotic species, which includes five freshwater fishes and five birds as well as eleven mammals. Santa Cruz has the highest percentage of exotic freshwater fishes (six species, 46.2%; Appendix 1: Table A1–A3).

Catamarca displays the highest number of endemic species (41 reptiles, 23 mammals, nine amphibians, and eight freshwater fishes) (Fig. 3, Appendix 1: Table A1–A3). Misiones has the highest number of endemic freshwater fishes (39 spp.), Jujuy the highest number of endemic amphibians (12 spp.), Neuquén of reptiles (48 spp.), followed by Mendoza and Río Negro (47 spp. each) and Catamarca of birds (11 spp.) and mammals (23 spp.; Fig. 3, Appendix 1: Table A1–A3). Neuquén

is the province with the highest proportion of endemic vertebrate species (17.6%). In particular, reptiles comprise 70% of endemic species in this province. There are 321 endemic species exclusive of some provinces of Argentina (Table A2). Misiones has the largest number of exclusive endemics (38 spp.), with 35 species of freshwater fish, two amphibians, and one mammal. Neuquén has 33 exclusive endemic species, with 26 exclusive species of reptiles, six amphibians and one mammal. Catamarca has 31 exclusive endemic species to the province, including 17 reptiles, five freshwater fish and mammals, and four amphibians (Appendix 2: Table A4).

Species considered as threatened (577 spp.) account for 17.8% of all native species, comprising 198 birds, 133 reptiles, 98 mammals, 74 marine fishes, 27 freshwater fishes, and 47 amphibians (Table 3). Marine fishes under threat represent 13.0%, although none of the 20 endemic species is under threat. Five percent of native species of freshwater fish are under threat and 36% of species are in the Near Threatened category. Endemic freshwater fish under threat represent 11.5% of species. Of amphibians 26.7% of all species under threat and 63.5% of endemic species are threatened. Eighteen percent of reptiles are in threatened categories and 25.9% of endemic species are under threat (Table 3). There are two extinct birds (*Numenius borealis* and *Anodorhynchus glaucus*) and three are categorised as possibly Regionally Extinct (*Taoniscus nanus*, *Primolius maracana* and *chloropterus*). There are 198 birds in threatened categories and 57.1% of endemic species are threatened. There are 98 mammals under threatened categories: three are listed as Extinct (*Dusicyon australis*, *Dusicyon avus* and *Gyldenstolpia fronto*) and two as Regionally Extinct (*Monodelphis unistriata* and *Pteronura brasiliensis*). A total of 32 endemic mammals is threatened (36.8%).

Twenty-one percent of species were Not Evaluated or Data Deficient, with fish contributing the largest number of species (191 freshwaters, 178 marines).

Misiones has the highest number of threatened vertebrate species (CR, EN, VU) with 176, which corresponds to 15% of extant native species in the province. The total

Table 3. Number of species in each conservation status category and total numbers and percentages of threatened and threatened endemic species (EX, Extinct; EXR, Regionally Extinct; CR, Critically Endangered; EN, Endangered; VU, Vulnerable; NT, Near Threatened; LC, Least Concern; NA, Not Threatened; DD, Data Deficient; NE, Not Evaluated; NAP, Not Applicable; "?", possible). *CR, EN, VU, percentages are calculated over the total of native species of the group. ** Percentages are calculated over the total of endemic species of the group.

Taxonomic Group	EX	EXR	EXR?	CR	EN	VU	NT	LC	NA	DD	NE	NAP	Threatened species*	Threatened Endemic species**
Marine fishes	–	–	–	17	17	40	16	300	–	35	143	2	74 (13.0%)	0 (0.0%)
Freshwater fishes	–	–	–	3	2	22	194	115	12	31	160	–	27 (5.0%)	11 (11.5%)
Amphibians	–	–	–	–	18	29	–	–	100	20	9	–	47 (26.7%)	33 (63.5%)
Reptiles	–	–	–	–	38	95	–	–	218	49	46	–	133 (29.8%)	56 (25.9%)
Birds	2	–	3	18	90	90	–	790	–	23	86	–	198 (18.0%)	12 (57.1%)
Mammals	3	2	–	7	26	65	40	175	–	72	6	11	98 (24.1%)	32 (36.8%)
Total	**5**	**2**	**3**	**45**	**191**	**341**	**250**	**1380**	**330**	**230**	**450**	**13**	**577 (17.8%)**	**144 (29.3%)**

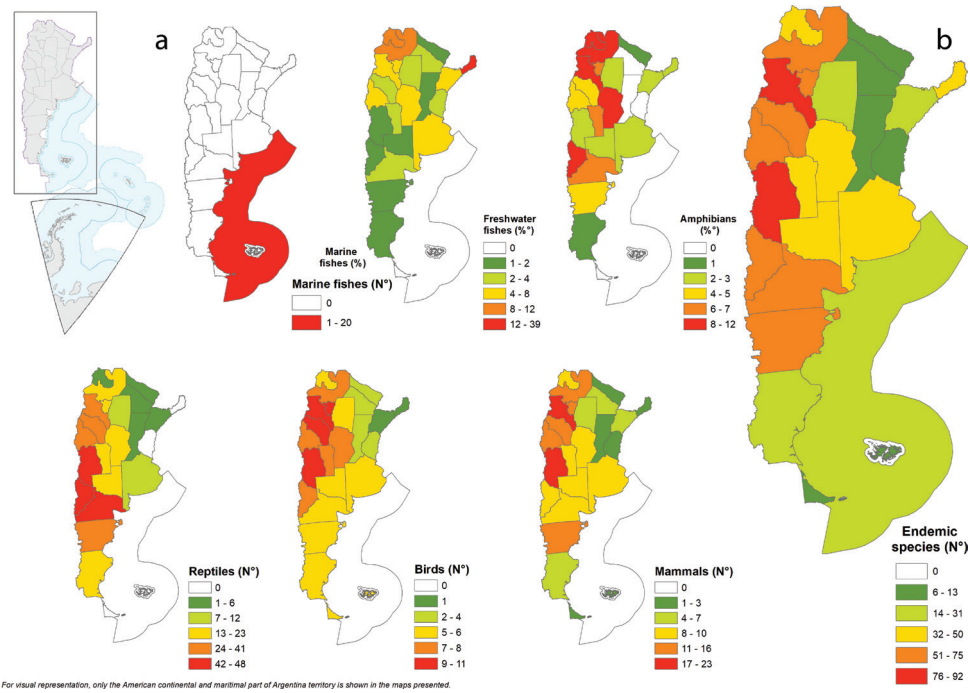

Figure 3. Number of endemics **a** by group by province **b** total species by province.

number of threatened species is higher in northern provinces and in the Argentinian Sea (Fig. 4A), while the percentage of threatened species is higher in southern provinces, except for Misiones (Fig. 4B). In Tierra del Fuego, 80% of freshwater fish are under threat. In Chubut, 41.2% of amphibians present are in danger. Almost 40% of reptiles and 23.7% of extant mammals in Misiones are threatened. In the Argentinian Sea, 100% of present reptiles (e.g., marine turtles) and 26.6% of extant birds are under threat (Fig. 4A, B, Appendix 3: Table A5).

Discussion

The results obtained in this study constitute the first analysis of geographical occurrence and conservation status, which highlights endemism, of all vertebrates that inhabit Argentina. Moreover, results are further disaggregated by both native and exotic species. Altogether, this study represents a precise, updated and spatially explicit source of information of vertebrate species, at both the national and provincial levels, for all assessed taxonomic groups. In this regard, it may serve as a reliable tool for multiple uses and users. The information generated by experts in this study establish the foundations for further research in multiple aspects and disciplines of conservation science, involving the assessed taxa. Our results facilitate prioritising research lines and

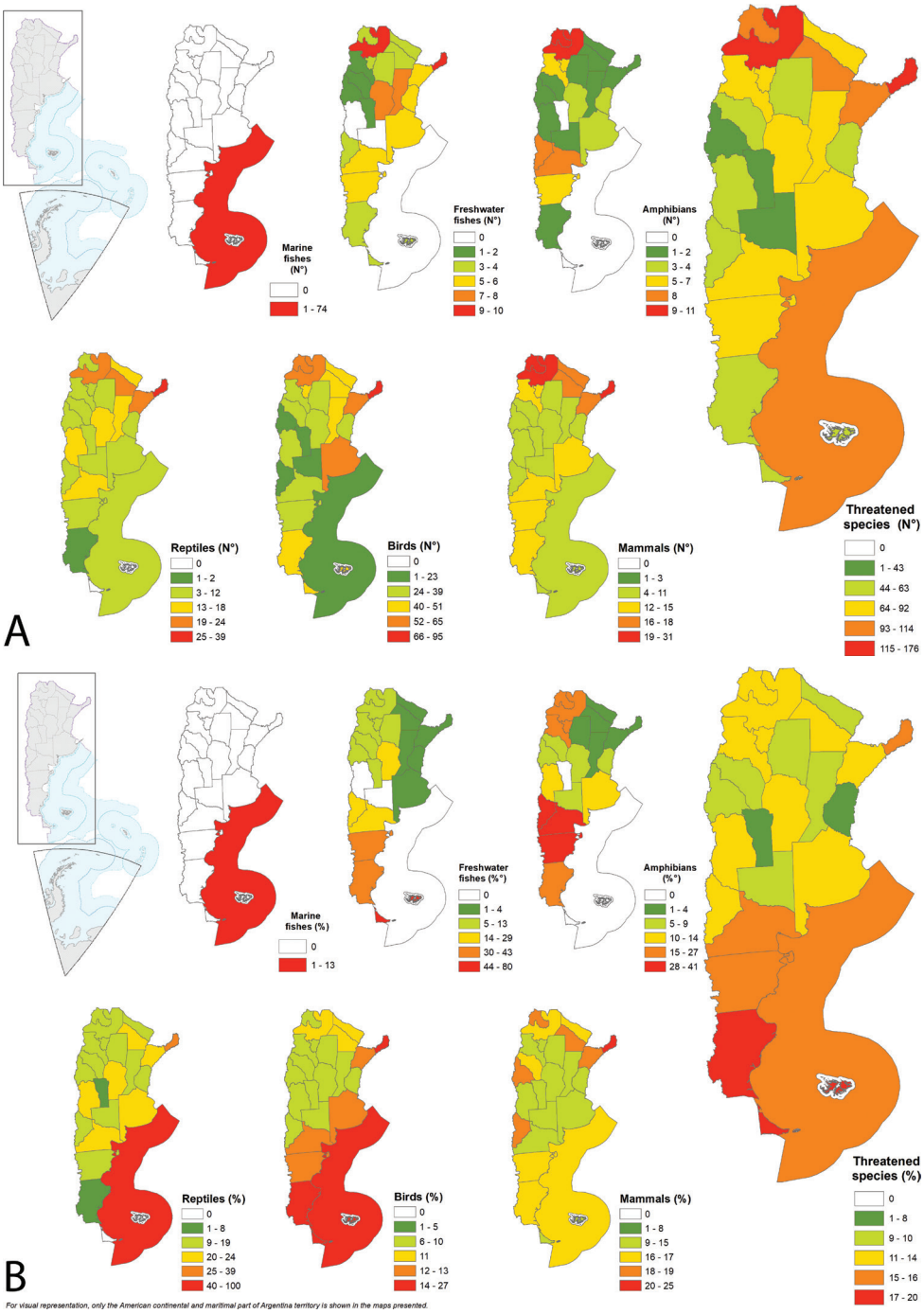

Figure 4. Threatened species by taxonomic group and province **A** number of threatened species by taxonomic group and total number of total threatened vertebrate species in each province **B** percentage of threatened species over the number of total native species of each taxonomic group present in the province and total threatened species in each province as a percentage of total vertebrate species.

conservation programmes in-situ and ex-situ, further assisting researchers and decision-makers focusing on either endemic or threatened species. In addition, we expect our products to become essential for local decision-makers, who usually lack spatially explicit information regarding actual biodiversity in their areas. This inventory might also be used as background information to update legislation in order to strengthen the protection of endemic and endangered species in each province. More importantly, it will provide key assistance in clarifying the potential geographic distribution of species captured, hunted, traded, or illegally introduced into the country.

The National Biodiversity Strategies and Action Plan (NBSAP) is a process by which countries can plan to address the threats to their flora and fauna. They are the principal instruments for the implementation of the Convention on Biological Diversity, both at the national and at the global level (Secretariat of the Convention on Biological Diversity 2011). Since the NBSAP should be a dynamic process by which increasing scientific information and knowledge must be considered as relevant feedback for a permanent review process, the results of this research should be considered in Argentinian strategies. Additionally, neighbouring countries, which share many of the assessed vertebrates species, could find valuable data in this inventory.

Updating inventories of species is a continuous and tedious process, as new descriptions and nomenclatural changes are published. One of the most complex tasks to complete in this study was to collect information, from different sources such as systematic lists or databases, field surveys, bibliographic reviews and analysis of natural history collections. Simultaneously, taxonomic changes may occur while collecting information. Another complex challenge was introduced by non-standardised and differing conservation categories. The differing national catalogues for each taxonomic group, when present, use different criteria in their classifications. To even these differences, this work unifies the aforementioned criteria with the international categories in order to comprehensively analyse data and make worldwide comparisons, when applicable. Marine fishes do not have national categorisation, and the IUCN Red List criteria were applied to assess their extinction risk at the global level. Using these criteria on a national scale poses disadvantages (Gärdenfors 2001) and reveals the importance of being able to categorise all groups based on their current status at the national level.

Latin America and the Caribbean region support rich biological diversity, accounting for around 60% of global terrestrial life, alongside with diverse freshwater and marine flora and fauna (UNEP and WCMC 2016). In Latin America, it is estimated that there are at least 13,600 vertebrate species (Raven et al. 2020). When considering Argentina's neighbouring countries, Brazil, one of the largest countries in the world, exhibits the greatest richness of vertebrate species: 8,930 in 8,516 million km² (ICMBio 2021). Bolivia, which has one of the most diverse vertebrate faunas in the world, has registered 3,329 species (MMAyA 2018) in an area of 1,099 million km². Our results allow us to postulate that the vertebrate richness of Argentina is close to the values reported for Bolivia, with 3,302 reported species. Chile has an incomplete faunal inventory (it is estimated that only 10% has been surveyed) with approximately 2,000 vertebrates verified in a total area of 756,950 km² (Ministerio del Medio Ambiente

2021). In Paraguay, there is an estimated richness of 1,500 vertebrates, although a complete inventory of vertebrate species that inhabit its territory (406,752 km²) is still lacking (Maceo et al. 2015). Finally, Uruguay harbours 912 species of vertebrates (without considering marine fishes) in 176,215 km² (Soutullo et al. 2013; Achaval 2021).

The decline in species richness as latitude increases is one of the most consistent patterns in biogeography, having been identified in groups of organisms such as mammals, fish, insects, and plants (Willig et al. 2003). Argentina shows a pattern of higher richness from north to south and from east to west (Fig. 2b), where Misiones and Salta have the highest number of species and Tierra del Fuego and Santa Cruz, the southernmost provinces, are those with the lowest vertebrate richness. This pattern is consistent with the findings of other researchers who have documented that at the Neotropical/Andean level (Morrone 2015) species richness of terrestrial vertebrates is lower on the west coast and in southern South America (Loyola et al. 2009).

Almost 18% of vertebrate species present in Argentina are threatened. The taxonomic group with the highest number of threatened is reptiles, with almost 30% of their species under some category of threat. On the other hand, amphibians have 63.5% of endemic species under threat. Argentina has five Extinct species, two Regionally Extinct and three possibly Regionally Extinct, belonging to mammals and birds. Among mammals, *Pteronura brasiliensis* has not been recorded in the country since 1980 but a solitary specimen has recently been observed in Chaco and Formosa provinces. Among birds, the extinct *Primolius maracana* was last recorded in the 1990's (Bodrati et al. 2006) and *Paraclaravis geoffroyi*, a Critically Endangered species, is possibly Extinct (Lees et al. 2021). Richness patterns for threatened and endemic species do not show a relationship to latitude and differed in terms of overall richness, which differ substantially among taxa, as observed at the Neotropical/Andean and global scale (Loyola et al. 2009; Jenkins et al. 2013). The highest number of threatened freshwater fishes is concentrated in Corrientes, Entre Ríos, Buenos Aires, Santa Fe and Salta (Fig. 4A). A higher number of threatened amphibians occur in the northwest provinces Jujuy and Salta (Fig. 4A). Threatened mammals and reptiles are concentrated in northern provinces as well (Misiones, Formosa, Chaco, Salta and Jujuy; Fig. 4A). In contrast, threatened birds are scattered throughout the country. Tierra del Fuego, the southernmost province, exhibits the largest proportion of threatened species considering the species that inhabit it (19.2%, Fig. 4B). This might be related to different drivers that cause species declines. For terrestrial and freshwater ecosystems, land-use change has had the largest negative impact on nature, followed by the direct exploitation of organisms. In marine ecosystems, the exploitation of organisms (mainly fishing) has had the largest impact. Climate change is a driver that is increasingly exacerbating the impact of other drivers on nature (Allan et al. 2019; IPBES 2019). Because of its great diversity of environments, Argentina has a wide range of threats and pressures on its ecosystems. Anthropogenic pressures associated with land use, mostly in terrestrial ecoregions, are livestock grazing and agriculture. However, land use intensification is not homogeneous throughout the country. Different human-activities and processes stress biodiversity based on the characteristics of each ecoregion, such as biological

invasions, urbanisation, subsistence livestock, afforestation, the extraction of natural resources, and hunting, among others (Nanni et al. 2020).

Worldwide, 27% of mammals, birds, reptiles, and amphibians are threatened by invasive alien species (Bellard et al. 2016). In this present research, 35% of reported exotic species are freshwater fish and 33% are mammals. Globally, invasive alien species are not the most important contributor to the number of species that are threatened (Bellard et al. 2016), still biological invasions are one of the principal drivers of biodiversity loss (IPBES 2019).

Argentina has 492 endemic vertebrate species, which represent almost 15% of the native vertebrates of the country. Approximately, 50% of reptiles and 30% of amphibians are endemic. This information is valuable for planning conservation strategies. Apart from threatened species, endemic species are indeed an important target of global conservation efforts (Loyola et al. 2009; Murali et al. 2021) since they have a restricted geographical distribution and are more vulnerable to habitat loss or degradation (Prendergast et al. 1993). Our assessment revealed that most endemic species occur in north-western forested areas (Southern Andean Yungas) or in arid to semiarid environments of central, southern, and western Argentina (High and Low Monte and Patagonian Steppe). These results agree with previously performed studies of global phylogenetic endemism patterns for vertebrates (Murali et al. 2021). In this matter, endemism increases southward, peaking at high latitudes in the Southern Hemisphere and coastal areas adjacent to mountain systems (e.g., along the Andes).

If we consider the species in Not Evaluated and Data Deficient categories altogether, they totalise 21% of the total vertebrate diversity of Argentina. Freshwater and marine fish are taxonomic groups with the highest number of Not Evaluated species (35.4% and 31.2%, respectively). This number is higher than threatened species and shows that these species should be regarded as relatively high priorities for research in order to clarify their true status (Butchart and Bird 2010). Birds are the most completely assessed taxonomic group regarding conservation status, with only 10% of the species under the Not Evaluated or Data Deficient categories.

Protected areas (PA) are critical for biodiversity conservation (Saura et al. 2018). The fate of many endangered species depends on PA systems that must be well designed and properly managed (Saura et al. 2017). Nevertheless, the protected area system at the national level in Argentina represents 13.3% (SIFAP 2020), which is still insufficient. Furthermore, the number of protected areas and their included spatial extent are not homogeneously distributed among provinces (SIFAP 2020). Although strongly increased in recent years, Marine Protected Areas represent only ~ 7% of the Argentina Sea (SIFAP 2020), which is still far from the 10% conservation goal set for 2020 in the Convention on Biological Diversity 2010. We believe the information obtained in this research identifies provinces with a particularly high number of threatened or endemic species. Linking this information with the degree of protection at each political district allows the identification of provinces where prioritising the creation of PA is necessary, either by the State, non-governmental organisations or private owners.

Conclusions

The importance of compiling a national inventory of vertebrate species is not only relevant from a taxonomic standpoint. It also constitutes a mandatory input in further assessing current biodiversity, as well as in prioritising efforts in environmental management, decision-making, and development of public policies at the national or provincial level. For instance, identifying priority provinces or taxa for *in situ* or *ex situ* conservation, science and education, and developing monitoring and early warning systems in the presence of exotic species that can potentially become invasive. This inventory provides the basis to analyse, study, objectively quantify, monitor, prioritise and value the vertebrate biodiversity of Argentina. In addition, to update the legislation, document the current diversity and geographic occurrence of species (as a future reference) and provide citizens with a simple tool that allows them to know their natural heritage.

Only results for a single animal subphylum are presented here. In the future, the final objective of our initiative is to include groups of invertebrates, which represent a larger volume of species. When completed, Argentina will have a complete national inventory of animal biodiversity. The effort at this scale should stimulate a continuity that emulates the Catalogue of Life (Roskov et al. 2019) or the Encyclopedia of Life (Parr et al. 2014) at the national and provincial levels.

Acknowledgements

The authors want to thank the work done by Fernando Vázquez Mazzini for materializing the inventory into a book. Thanks are due to Sergio Bogan for his support and advice, to Florencia Chomnalez and Adriana Vescovo for advice on maps, and to the National Geographic Institute (IGN) for the availability of freely accessible layers for the generation of them. Special thanks to Diego S. Aquino for his contribution in language revision and Aaron Bauer for his invaluable contributions to improve the manuscript.

References

Abdala CS, Acosta JL, Acosta JC, Álvarez BB, Avila LJ, Blanco GM, Bonino M, Boretto JM, Brancatelli G, Breitman MF, Cabrera MR, Cairo S, Corbalán V, Hernando A, Ibargüengoytía NR, Kacoliris F, Laspiur A, Montero R, Morando M, Pelegrin N, Hernán C, Pérez F, Quinteros AS, Semhan RV, Tedesco ME, Vega L, Zalba SM (2012) Categorización del estado de conservación de las lagartijas y anfisbenas de la República Argentina. Cuadernos de herpetología 26: 215–247.

Acha HR (2014) Extensión de la plataforma continental argentina. Su relación con el medio ambiente, las aguas marítimas y los recursos subyacentes. Revista Aequitas 9: 1–18.

Achaval F (2021) Lista de los Vertebrados del Uruguay. http://zvert.fcien.edu.uy/listado.html [accessed 17 May 2021]

Alonso F, Terán GE, Calviño P, García I, Cardoso Y, García G (2018) An endangered new species of seasonal killifish of the genus *Aaustrolebias* (Cyprinodontiformes: Aplocheiloidei) from the Bermejo River basin in the western Chacoan region. PLoS ONE 13: 1–20. https://doi.org/10.1371/journal.pone.0196261

Anon (2016) Base de datos de peces de Agua Continentales de Argentina. www.pecesargentina.com.ar

Anon (2021a) BirdLife International. http://datazone.birdlife.org/species/search [accessed 16 April 2021]

Anon (2021b) eBird. https://ebird.org/argentina/home [accessed 16 April 2021]

Arana MD, Natale E, Ferretti N, Romano G, Oggero A, Posadas P, Morrone JJ (2021) Esquema Biogeográfico de la República Argentina, 1st edn. Fundación Miguel Lillo, Tucumán, 240 pp.

Avila LJ, Martinez LE, Morando M (2013) Checklist of lizards and amphisbaenians of Argentina: An update. Zootaxa 3616: 201–238. https://doi.org/10.11646/zootaxa.3616.3.1

Bauni V, Bertonatti C, Giacchino A (2021) Inventario Biológico Argentino: Vertebrados. Fundación de Historia Natural Félix de Azara, Buenos Aires, Argentina, 534 pp.

Bellard C, Genovesi P, Jeschke JM (2016) Global patterns in threats to vertebrates by biological invasions. Proceedings of the Royal Society B: Biological Sciences 283: 1–9. https://doi.org/10.1098/rspb.2015.2454

Bello MT, Ubeda CA (1998) Estado de conservación de los peces de agua dulce de la Patagonia Argentina. Gayana Zoología 62: 45–60.

Bodrati A, Cockle K, Areta JI, Capuzzi G, Fariña R (2006) El Maracaná Lomo Rojo (*Primolius maracana*) en Argentina: ¿de plaga a la extinción en 50 años? El Hornero 21: 037–043.

Butchart SHM, Bird JP (2010) Data Deficient birds on the IUCN Red List: What don't we know and why does it matter? Biological Conservation 143: 239–247. https://doi.org/10.1016/j.biocon.2009.10.008

Cappato J, Yanosky A (2009) Uso sostenible de peces en la Cuenca del Plata. Evaluación subregional del estado de amenaza, Argentina y Paraguay. IUCN, Gland, Switzerland, 74 pp. http://www.sidalc.net/cgi-bin/wxis.exe/?IsisScript=DOCU.xis&method=post&formato=2&cantidad=1&expresion=mfn=005260

Cardoso YP, Brancolini F, Protogino L, Paracampo A, Bogan S, Posadas P, Montoya-Burgos JI (2019) An integrated approach clarifies the cryptic diversity in *Hypostomus* Lacépède 1803 from the Lower La Plata Basin. Anais da Academia Brasileira de Ciencias 91: e20180131. https://doi.org/10.1590/0001-3765201920180131

Chapman AD (2009) Australian Biodiversity Information Services Numbers of Living Species in Australia and the World. 2nd edn. Canberra, Australia, 84 pp. https://doi.org/10.1111/j.1398-9995.1975.tb00205.x

Chebez JC (1994) Los que se van: especies argentinas en peligro. Editorial Albatros (Ed.). Editorial Albatros, Buenos Aires, 604 pp.

Chebez JC, Rodríguez GO (2014) La fauna gringa: especies introducidas en la Argentina. Fundación de Historia Natural Félix de Azara (Ed.). Fundación de Historia Natural Félix de Azara, Buenos Aires, 224 pp.

Chebez JC, López HL, Athor J (2009) Otros que se van. Fauna argentina amenazada. Editorial Albatros, Buenos Aires, 552 pp.

Cordiviola E, Campana M, Demonte D, del Barco D, Trógolo A (2009) Conservation State of Siluriformes Fishes from the Ramsar site Jaaukanigas (Middle Parana River), Argentina. Gayana (Concepción) 73: 222–232. https://doi.org/10.4067/s0717-65382009000200006

Cordiviola MA, Zayas E (2007) Estado de conservación de peces Characidae (Pisces: Characiformes) en un área de la Cuenca del Plata, Argentina. Gayana 71: 178–186. https://doi.org/10.4067/S0717-65382007000200006 [accessed 16 April 2021]

Costello MJ, Wilson S, Houlding B (2012) Predicting total global species richness using rates of species description and estimates of taxonomic effort. Systematic Biology 61: 871–883. https://doi.org/10.1093/sysbio/syr080

Costello MJ, May RM, Stork NE (2013) Can we name earth's species before they go extinct? Science 339: 413–416. https://doi.org/10.1126/science.1230318

Cousseau MB, Rosso JJ (2019) Peces de Argentina. Aguas Marinas. Vázquez Mazzini, Buenos Aires, 151 pp.

Cousseau MB, Rosso JJ (in press) Peces de Argentina. Aguas continentales. Vázquez Mazzini, Buenos Aires.

Cousseau MB, Pequeño G, Mabragaña E, Lucifora LO, Martínez P, Giussi A (2020) The Magellanic Province and its fish fauna (South America): Several provinces or one? Journal of Biogeography 47: 220–234. https://doi.org/10.1111/jbi.13735

Cousseau MB, Denegri MA, Figueroa DE, Boschi EE, Roux A, Bremec CS, Schejter L, Lasta ML, Brunetti NE (2010) Peces, crustáceos y moluscos registrados en el sector del Atlántico Sudoccidental comprendido entre 34°S y 55°S, con indicación de las especies de interés pesquero. 129 pp.

de Azara F (1801) Essais sur l'historie naturelle des Quadrupédes de la Province du Paraguay. Tome Prémier. Charles Pugens, tome sécond, París, 79 pp. https://doi.org/10.5962/bhl.title.112568

de Azara F (1802–1805) Apuntamientos para la Historia Natural de los Páxaros del Paraguay y Río de la Plata. Vda de Ibarra, Madrid, 479 pp.

Evenhuis NL (2007) Helping solve the "Other" taxonomic impediment: Completing the eight steps to total enlightenment and taxonomic nirvana. Zootaxa 1407: 3–12. https://doi.org/10.11646/zootaxa.1407.1.2

Figueroa DE (2019) Clave de peces marinos del Atlántico Sudoccidental, entre los 33° S y 56° S. Mar del Plata, 365 pp.

Fjeldså J, Krabbe N (1990) Birds of the High Andes. University of Copenhagen and Apollo Books Svendborg, Copenhagen, Denmark, 878 pp.

Fricke R, Eschmeyer WN, Van der Laan R (2020) Eschmeyer´s catalog of fishes: Genera, Species, References. https://researcharchive.calacademy.org/research/Ichthyology/catalog/fishcatmain.asp

Frost D (2021) Amphibian species of the world: an online reference. American Museum of Natural History, New York. https://amphibiansoftheworld.amnh.org/ [accessed 16 April 2021]

Fukushima CS, Mammola S, Cardoso P (2020) Global wildlife trade permeates the Tree of Life. Biological Conservation 247: e108503. https://doi.org/10.1016/j.biocon.2020.108503

Gaitan E (2020) Legislación e instrumentos de manejo existentes para la protección de los fondos marinos en la Plataforma Continental Argentina. Marine and Fishery Sciences (MAFIS) 33: 247–263. https://doi.org/10.47193/mafis.3322020301104

Gärdenfors U (2001) Classifying threatened species at national versus global levels. Trends in Ecology & Evolution 16: 511–516. https://doi.org/10.1016/S0169-5347(01)02214-5

Giraudo AR, Arzamendia V, Bellini GP, Bessa CA, Cinthia C, Cardozo G, Chiaraviglio M, Costanzo MB, Eduardo G, Cola V Di, Pietro DO Di, Kretzschmar S, Palomas S, Nenda J, Rivera PC, Rodríguez ME, Scrocchi GJ, Williams JD (2012) Categorización del estado de conservación de las serpientes de la República Argentina. Cuadernos de herpetología 26: 303–326.

Giraudo AR, Scrocchi GJ (2002) Argentinian snakes: an annotated checklist. Smithsonian Herpetological Information Service 132, Washington DC, 53 pp. https://doi.org/10.5479/si.23317515.132.1

Grismado C, Ramírez M (2018) Nuevas especies 2018. Museo Argentino de Ciencias Naturales "Bernardino Rivadavia". Buenos Aires, 24 pp.

Grismado C, Ramírez M (2019) Nuevas especies 2019. Museo Argentino de Ciencias Naturales "Bernardino Rivadavia". Buenos Aires, 21 pp.

Grismado C, Ramírez M (2020) Nuevas especies 2020. Museo Argentino de Ciencias Naturales "Bernardino Rivadavia". Buenos Aires, 36 pp.

ICMBio (2021) Instituto Chico Mendes para la Conservación de la Biodiversidad (ICMBio) – Fauna Brasileña. https://www.icmbio.gov.br/portal/faunabrasileira [accessed 17 May 2021]

IGN (2019) Anuario Estadístico de la República Argentina. https://www.indec.gob.ar/indec/web/Nivel4-Tema-1–15–25

IGN (2021) Capas SIG. https://www.ign.gob.ar/NuestrasActividades/InformacionGeoespacial/CapasSIG

IPBES (2019) Summary for policymakers of the global assessment report on biodiversity and ecosystem services of the intergovernmental Informe de la Evaluación mundial sobre la diversidad biológica y de los servicios de los ecosistemas, Bonn, Germany, 56 pp. https://doi.org/10.5281/zenodo.3553579

IUCN (2019) 14 Directrices de uso de las Categorías y Criterios de la Lista Roja de la UICN. Versión 14. http://www.iucnredlist.org/documents/RedListGuidelines.pdf

IUCN (2021a) Table 1a: Number of species evaluated in relation to the overall number of described species, and number of threatened species by major groups of organisms. Red List Summary Statistics: 1. https://www.iucnredlist.org/resources/summary-statistics#Figure2

IUCN (2021b) The IUCN Red List of Threatened Species. Version 2021–1. The IUCN Red List of Threatened Species. Version 2021–1. https://www.iucnredlist.org/resources/summary-statistics

Jenkins CN, Pimm SL, Joppa LN (2013) Global patterns of terrestrial vertebrate diversity and conservation. Proceedings of the National Academy of Sciences of the United States of America 110: E2603–E2610. https://doi.org/10.1073/pnas.1302251110

De La Peña MR (1997) Lista y distribución de las aves de Santa Fe y Entre Ríos. L.O.L.A., Buenos Aires.

Lees AC, Devenish C, Areta JI, de Araújo CB, Keller C, Phalan B, Silveira LF (2021) Assessing the extinction probability of the Purple-winged Ground Dove, an enigmatic bamboo specialist. Frontiers in Ecology and Evolution 9: e624959. https://doi.org/10.3389/fevo.2021.624959

Liotta J (2005) 31 ProBiota FCNyM, UNLP. Serie Documentos Distribución geográfica de los peces de aguas continentales de la República Argentina, 92 pp. https://doi.org/10.14409/natura.v1i36.3829

López-Lanús B, Grilli P, Coconier E (2017) Ministerio de Ambiente y Desarrollo Sustentable de la Nación y Aves Argentinas. Categorización de las aves de la Argentina según su estado de conservación. Buenos Aires, Argentina, 148 pp.

López H, Menni RC, Miquelarena AM (1987) Lista de los peces de agua dulce de la Argentina. Biología Acuática 12: 1–51.

López HL, Miquelarena AM, Menni RC (2003) Lista comentada de los peces continentales de la Argentina. Probiota. Serie Técnica y Didáctica 5: 1–87.

Loyola RD, Kubota U, da Fonseca GAB, Lewinsohn TM (2009) Key Neotropical ecoregions for conservation of terrestrial vertebrates. Biodiversity and Conservation 18: 2017–2031. https://doi.org/10.1007/s10531-008-9570-6

Mace GM (2004) The role of taxonomy in species conservation. Philosophical Transactions of the Royal Society B: Biological Sciences 359: 711–719. https://doi.org/10.1098/rstb.2003.1454

Maceo B, Vitale C, Soler L, Musalem K, Soria L, Narvaes J (2015) Estrategia nacional y plan de acción para la conservación de la biodiversidad del Paraguay 2015–2020. Secretaría del ambiente de Paraguay. Asunción, 97 pp.

Mazar Barnett J, Pearman M (2001) Lista comentada de las aves argentinas. Lynx Edicions, Barcelona, 164 pp.

McNeely JA, Gadgil M, Leveque C, Padoch C, Redford K (1995) Human influences on biodiversity.pdf. In: Heywood VH, Watson RT (Eds) Global biodiversity assessment. Cambridge University Press, UNEP, Cambridge, 711–821.

Menni RC (2004) Peces y ambientes en la Argentina continental. Monografías del Museo Argentino de Ciencias Naturales 5: 1–316. www.estudiosigma.com.ar

Menni RC, Ringuelet RA, Arámburu RH (1984) Peces marinos de la Argentina y Uruguay. Editorial Hemisferio Sur, Buenos Aires, 361 pp.

Ministerio del Medio Ambiente (2021) Inventario nacional de especies de Chile. http://especies.mma.gob.cl/CNMWeb/Web/WebCiudadana/pagina.aspx?id=88&pagId=85 [accessed 17 May 2021]

Mirande JM, Koerber S (2015) Checklist of the Freshwater Fishes of Argentina (CLOFFAR). Ichtiological Contributios of PecesCriollos 36: 1–68.

Mirande JM, Koerber S (2020) Checklist of the freshwater fishes of Argentina 2nd edn. CLOFFAR-2, 72: 1–81.

MMAyA (2018) Política y estrategia plurinacional para la gestión integral y sustentable de la biodiversidad. Plan de acción 2019–2030. Dirección general de Biodiversidad y Áreas Protegidas, Estado Plurinacional de Bolivia, 120 pp.

Monteleone DL, Pagano LG (in press) Aves Argentina Lista de las Aves Argentinas: con comentarios sobre especies nuevas, raras e hipotéticas.

Monteleone L, Gallegos D, Roesler I, Areta JI, Baigorria J, Vidoz JQ, Mangini G, Imberti S, Jordan E, Pearman M, Gorleri F, La Grotteria J (2021) Comité Argentino de Registros Ornitológicos. Lista de las aves argentinas. https://www.avesargentinas.org.ar/lista-de-las-aves-argentinas

Morello J, Matteucci SD, Rodriguez AF, Silva ME (2012) Ecorregiones y complejos ecosistémicos de Argentina. 1st edn. Orientación Gráfica Editora, Ciudad Autónoma de Buenos Aires, 752 pp.

Morello J, Matteucci SD, Rodriguez AF, Silva M (2018) Ecorregiones y complejos Ecosistémicos de Argentina, 2nd edn. Orientación Gráfica Editora, Ciudad Autónoma de Buenos Aires, 800 pp.

Morrone JJ (2015) Biogeographical regionalisation of the world: A reappraisal. Australian Systematic Botany 28: 81–90. https://doi.org/10.1071/SB14042

Murali G, Gumbs R, Meiri S, Roll U (2021) Global determinants and conservation of evolutionary and geographic rarity in land vertebrates. Science Advances 7: 1–15. https://doi.org/10.1126/sciadv.abe5582

Narosky T, Di Giacomo AG (1993) Las aves de la provincia de Buenos Aires: lista y distribución. Asociación Ornitológica del Plata, Vázquez Mazzini. Asociación Ornitológica Plata, Vázquez Mazzini, L.O.L.A. Ciudad Autónoma de Buenos Aires, 128 pp.

Narosky T, Yzurieta D (2010) Aves de Argentina y Uruguay. Guía de identificación/Birds of Argentina and Uruguay. A field guide. Vázquez Mazzini, Ciudad Autónoma de Buenos Aires, 432 pp.

Nelson JS, Grande TC, Wilson MVH (2016) Fishes of the world. John Wiley & Sons, Hoboken, NJ, 707 pp. https://doi.org/10.1002/9781119174844

Nores M, Yzurieta D, Salvador S (1991) Lista y distribución de las aves de Santiago del Estero. Boletín de la Academia Nacional de Ciencias de Córdoba 59: 157–196.

Orlandini S, Aun L, Martori R (2001) Estado de conservación de la ictiofauna de las Sierras Pampeanas de la provincia de Córdoba. Boletín de la Sociedad de Biología de Concepción, Chile 72: 91–102.

Parr CS, Wilson N, Leary P, Schulz KS, Lans K, Walley L, Hammock JA, Goddard A, Rice J, Studer M, Holmes JTG, Corrigan Jr RJ (2014) The Encyclopedia of Life v2: Providing Global Access to Knowledge About Life on Earth. Biodiversity Data Journal 2: e1079. https://doi.org/10.3897/BDJ.2.e1079

Pearman M, Areta JI (2018) Species lists of birds for South American countries and territories: Argentina. http://www.museum.lsu.edu/~Remsen/SACCCountryLists.htm [accessed 20 December 2018]

Pearman M, Areta J (2020) Field Guide to the birds of Argentina and the Southwest Atlantic. Helm Field Guide, London, 480 pp.

PNUD (2007) Manual de inventarios de la biodiversidad. Ministerio de Medio Ambiente y Recursos Naturales, El Salvador, 120 pp.

Pozzi AJ, Bordalé LF (1935) Cuadro sistemático de los peces marinos de la República Argentina. Anales de la Sociedad Científica Argentina 120: 145–189.

Prado WS, Waller T, Albareda DA, Cabrera MR, Etchepare E, Giraudo AR, Carman VG, Prosdocimi L, Richard E (2012) Categorización del estado de conservación de las tortugas de la República Argentina. Cuadernos de herpetología 26: 375–387.

Prendergast JR, Quinn RM, Lawton JH, Eversham BC, Gibbons DW (1993) Rare species, the coincidence of diversity hotspots and conservation strategies. Nature 365: 335–337. https://doi.org/10.1038/365335a0

Raven PH, Gereau RE, Phillipson PB, Chatelain C, Jenkins CN, Ulloa CU (2020) The distribution of biodiversity richness in the tropics. Science Advances 6: 5–10. https://doi.org/10.1126/sciadv.abc6228

Remsen JVJ, Areta JI, Bonaccorso E, Claramunt S, Jaramillo A, Lane DF, Pacheco JF, Robbins MB, Stiles FG, Zimmer KJ (2021) A classification of the bird species of South America. https://www.museum.lsu.edu/~Remsen/SACCBaseline.htm [accessed 16 April 2021]

Ridgely R, Tudor G (2009) Field Guide to the Songbirds of South America: the Passerines. University of Texas Press, Austin, 760 pp.

Ringuelet RA, Aramburu RH, Alonso A (1967) Los peces argentinos de agua dulce. Comisión de investigación científica provincia de Buenos Aires (Ed.), La Plata, 604 pp.

Rodríguez Mata JR, Erize F, Rumboll M (2006) A Field Guide to the Birds of South America: Non-passerines. Harper Collins, London, 750 pp.

Roskov Y, Ower G, Orrell T, Nicolson D, Bailly N, Kirk PM, Bourgoin T, DeWalt RE, Decock W, Van Nieukerken E, Zarucchi J, Penev L (2019) Species 2000 & ITIS Catalogue of Life, 2019 Annual Checklist. Leiden, the Netherlands. www.catalogueoflife.org/annual-checklist/2019

Roskov Y, Ower G, Orrell T, Nicolson D, Bailly N, Kirk PM, Bourgoin T, DeWalt RE, WD, Van Nieukerken E, Zarucchi J, Penev L (2020) Species 2000 & ITIS Catalogue of Life, 2020–12–01. www.catalogueoflife.org

Saura S, Bastin L, Battistella L, Mandrici A, Dubois G (2017) Protected areas in the world's ecoregions: How well connected are they? Ecological Indicators 76: 144–158. https://doi.org/10.1016/j.ecolind.2016.12.047

Saura S, Bertzky B, Bastin L, Battistella L, Mandrici A, Dubois G (2018) Protected area connectivity: Shortfalls in global targets and country-level priorities. Biological Conservation 219: 53–67. https://doi.org/10.1016/j.biocon.2017.12.020

SAyDS, SAREM (2019) Categorización 2019 de los mamíferos de Argentina según su riesgo de extinción. Lista Roja de los mamíferos de Argentina. http://cma.sarem.org.ar/es [accessed 29 May 2021]

Scheffers BR, Joppa LN, Pimm SL, Laurance WF (2012) What we know and don't know about Earth's missing biodiversity. Trends in Ecology & Evolution 27: 501–510. http://dx.doi.org/10.1016/j.tree.2012.05.008

Secretariat of the Convention on Biological Diversity (2011) NBSAP training modules version 2.1 – Module 1. An Introduction to National Biodiversity Strategies and Action Plans: 1–19. https://www.cbd.int/doc/training/nbsap/b1-train-intro-nbsap-revised-en.pdf

SIFAP (2020) Sistema federal de Áreas Protegidas. https://www.argentina.gob.ar/ambiente/areas-protegidas/sifap

Soutullo A, Clavijo C, Martínez-Lanfranco J (2013) Especies prioritarias para la conservación en Uruguay. Vertebrados, moluscos continentales y plantas vasculares. MEC S y D (Ed.). SNAP/DINAMA/MVOTMA y DICYT/ MEC, Montevideo, 222 pp.

Stork NE, Samways MJ (1995) Inventorying and monitoring. In: Global Biodiversity Assessment. Cambridge University Press, Cambridge, 457–542.

Teta P, Abba AM, Cassini GH, Flores DA, Galliari CA, Lucero SO, Ramírez M (2018) Lista revisada de los mamíferos de Argentina. Mastozoología Neotropical 25: 163–198. https://doi.org/10.31687/saremmn.18.25.1.0.15

Titley MA, Snaddon JL, Turner EC (2017) Scientific research on animal biodiversity is systematically biased towards vertebrates and temperate regions. PLoS ONE 12: 1–14. https://doi.org/10.1371/journal.pone.0189577

Tobias JA, Seddon N, Spottiswoode CN, Pilgrim JD, Fishpool LDC, Collar NJ (2010) Quantitative criteria for species delimitation. Ibis 152: 724–746. https://doi.org/10.1111/j.1474-919X.2010.01051.x

Uetz P [Ed.] (2021) The Reptile Database. http://www.reptile-database.org/db-info/introduction.html#citation [accessed 16 April 2021]

UNEP, WCMC (2016) The State of Biodiversity in Latin America and The Caribbean. UNEP-WCMC (Ed.). UNEP-WCMC, Cambridge, 140 pp.

Vaira M, Akmentins M, Attademo M, Baldo D, Barrasso D, Barrionuevo S, Basso N, Blotto B, Cairo S, Cajade R, Corbalán V, Chilote P, Duré M, Falcione C, Ferraro D, Gutierrez R, Ingaramo R, Junges C, Lajmanovich R, Julián N, Marangoni F, Martinazzo L, Marti R, Moreno L (2012) Categorización del estado de conservación de los anfibios de la República Argentina. Cuadernos de Herpetología 26: 131–159.

Webb CO, Slik JWF, Triono T (2010) Biodiversity inventory and informatics in Southeast Asia. Biodiversity and Conservation 19: 955–972. https://doi.org/10.1007/s10531-010-9817-x

Williams JD, Francini F (1991) A Checklist of the Argentine snakes. Bollettino del Museo Regionale di Scienze Naturali di Torino 9: 55–90.

Williams JD, Vera GD, Di Pietro DO (2021) Lista comentada de las serpientes de la Argentina, con referencias a su sistemática, distribución geográfica, dieta, reproducción, potencial peligrosidad y etimologías. Revista del Museo de La Plata 6: 26–124.

Willig MR, Kaufman DM, Stevens RD (2003) Latitudinal Gradients of Biodiversity: Pattern, Process, Scale, and Synthesis. Annual Review of Ecology, Evolution, and Systematics 34: 273–309. https://doi.org/10.1146/annurev.ecolsys.34.012103.144032

Wilson EO (2003) The encyclopedia of life. Trends in Ecology and Evolution 18: 77–80. https://doi.org/10.1016/S0169-5347(02)00040-X

Wilson EO (2017) Biodiversity research requires more boots on the ground: Comment. Nature Ecology and Evolution 1: 1590–1591. https://doi.org/10.1038/s41559-017-0360-y

Zuloaga FO, Belgrano MJ, Zanotti CA (2019) An update of the catalogue of the vascular plants of the Southern cone. Darwiniana 7: 208–278. https://doi.org/10.14522/darwiniana.2019.72.861

Appendix I

Total number (and percentage, regarding national richness) of native and endemic species by taxonomic group and province. The number of exotic species is the difference between the richness and the number of native species in each case. * Buenos Aires includes Ciudad Autónoma de Buenos Aires. ** Not all species are endemic to the Argentina Sea but may be from a portion of it.

Table A1.

Taxonomic group	Marine fishes				Freshwater fishes				Amphibians			
Province	**Richness**	**Native**	**Exotic**	**Endemic**	**Richness**	**Native**	**Exotic**	**Endemic**	**Richness**	**Native**	**Exotic**	**Endemic**
Buenos Aires*	0 (0.0%)	0 (0.0%)	0 (0.0%)	0 (0.0%)	227 (40.5%)	216 (40.1%)	11 (50.0%)	6 (6.3%)	30 (16.9%)	29 (16.5%)	1 (100.0%)	2 (3.8%)
Catamarca	0 (0.0%)	0 (0.0%)	0 (0.0%)	0 (0.0%)	38 (6.8%)	35 (6.5%)	3 (13.6%)	8 (8.3%)	26 (14.7%)	26 (14.8%)	0 (0.0%)	9 (17.3%)
Chaco	0 (0.0%)	0 (0.0%)	0 (0.0%)	0 (0.0%)	166 (29.6%)	165 (30.6%)	1 (4.5%)	4 (4.2%)	48 (27.1%)	48 (27.3%)	0 (0.0%)	0 (0.0%)
Chubut	0 (0.0%)	0 (0.0%)	0 (0.0%)	0 (0.0%)	17 (3.0%)	12 (2.2%)	5 (22.7%)	2 (2.1%)	17 (9.6%)	17 (9.7%)	0 (0.0%)	4 (7.7%)
Córdoba	0 (0.0%)	0 (0.0%)	0 (0.0%)	0 (0.0%)	56 (10.0%)	50 (9.3%)	6 (27.3%)	7 (7.3%)	33 (18.6%)	32 (18.2%)	1 (100.0%)	10 (19.2%)
Corrientes	0 (0.0%)	0 (0.0%)	0 (0.0%)	0 (0.0%)	297 (52.9%)	296 (54.9%)	1 (4.5%)	8 (8.3%)	59 (33.3%)	59 (33.5%)	0 (0.0%)	2 (3.8%)
Entre Ríos	0 (0.0%)	0 (0.0%)	0 (0.0%)	0 (0.0%)	265 (47.2%)	259 (48.1%)	4 (18.2%)	4 (4.2%)	42 (23.7%)	42 (23.9%)	0 (0.0%)	0 (0.0%)
Formosa	0 (0.0%)	0 (0.0%)	0 (0.0%)	0 (0.0%)	172 (30.7%)	171 (31.7%)	1 (4.5%)	1 (1.0%)	50 (28.2%)	50 (28.4%)	0 (0.0%)	1 (1.9%)
Jujuy	0 (0.0%)	0 (0.0%)	0 (0.0%)	0 (0.0%)	49 (8.7%)	48 (8.9%)	1 (4.5%)	11 (11.5%)	47 (26.6%)	47 (26.7%)	0 (0.0%)	12 (23.1%)
La Pampa	0 (0.0%)	0 (0.0%)	0 (0.0%)	0 (0.0%)	25 (4.5%)	20 (3.7%)	5 (22.7%)	2 (2.1%)	11 (6.2%)	11 (6.3%)	0 (0.0%)	2 (3.8%)
La Rioja	0 (0.0%)	0 (0.0%)	0 (0.0%)	0 (0.0%)	17 (3.0%)	14 (2.6%)	3 (13.6%)	3 (3.1%)	15 (8.5%)	15 (8.5%)	0 (0.0%)	4 (7.7%)
Mendoza	0 (0.0%)	0 (0.0%)	0 (0.0%)	0 (0.0%)	24 (4.3%)	18 (3.3%)	6 (27.3%)	2 (2.1%)	10 (5.6%)	9 (5.1%)	1 (100.0%)	3 (5.8%)
Misiones	0 (0.0%)	0 (0.0%)	0 (0.0%)	0 (0.0%)	335 (59.7%)	331 (61.4%)	4 (18.2%)	39 (40.6%)	63 (35.6%)	62 (35.2%)	1 (100.0%)	2 (3.8%)
Neuquén	0 (0.0%)	0 (0.0%)	0 (0.0%)	0 (0.0%)	19 (3.4%)	14 (2.6%)	5 (22.7%)	1 (1.0%)	23 (13.0%)	23 (13.1%)	0 (0.0%)	9 (17.3%)
Río Negro	0 (0.0%)	0 (0.0%)	0 (0.0%)	0 (0.0%)	24 (4.3%)	19 (3.5%)	5 (22.7%)	4 (4.2%)	24 (13.6%)	24 (13.6%)	0 (0.0%)	7 (13.5%)
Salta	0 (0.0%)	0 (0.0%)	0 (0.0%)	0 (0.0%)	160 (28.5%)	156 (28.9%)	4 (18.2%)	12 (12.5%)	54 (30.5%)	53 (30.1%)	1 (100.0%)	10 (19.2%)
San Juan	0 (0.0%)	0 (0.0%)	0 (0.0%)	0 (0.0%)	26 (4.6%)	20 (3.7%)	6 (27.3%)	6 (6.3%)	15 (8.5%)	14 (8.0%)	1 (100.0%)	5 (9.6%)
San Luis	0 (0.0%)	0 (0.0%)	0 (0.0%)	0 (0.0%)	21 (3.7%)	16 (3.0%)	5 (22.7%)	4 (4.2%)	18 (10.2%)	18 (10.2%)	0 (0.0%)	7 (13.5%)
Santa Cruz	0 (0.0%)	0 (0.0%)	0 (0.0%)	0 (0.0%)	13 (2.3%)	7 (1.3%)	6 (27.3%)	1 (1.0%)	4 (2.3%)	4 (2.3%)	0 (0.0%)	1 (1.9%)
Santa Fe	0 (0.0%)	0 (0.0%)	0 (0.0%)	0 (0.0%)	215 (38.3%)	211 (39.1%)	4 (18.2%)	2 (2.1%)	53 (29.9%)	52 (29.5%)	1 (100.0%)	0 (0.0%)
Santiago del Estero	0 (0.0%)	0 (0.0%)	0 (0.0%)	0 (0.0%)	49 (8.7%)	47 (8.7%)	2 (9.1%)	3 (3.1%)	31 (17.5%)	31 (17.6%)	0 (0.0%)	2 (3.8%)
Tierra del Fuego	0 (0.0%)	0 (0.0%)	0 (0.0%)	0 (0.0%)	8 (1.4%)	5 (0.9%)	3 (13.6%)	0 (0.0%)	0 (0.0%)	0 (0.0%)	0 (0.0%)	0 (0.0%)
Tucumán	0 (0.0%)	0 (0.0%)	0 (0.0%)	0 (0.0%)	60 (10.7%)	56 (10.4%)	4 (18.2%)	6 (6.3%)	27 (15.3%)	27 (15.3%)	0 (0.0%)	7 (13.5%)
Argentina Sea	574 (100%)	570 (99.3%)	4 (0;7%)	20 (3.5%)**	0 (0.0%)	0 (0.0%)	0 (0.0%)	0 (0.0%)	0 (0.0%)	0 (0.0%)	0 (0.0%)	0 (0.0%)

Table A2.

Taxonomic group	Reptiles				Birds				Mammals			
Province	Richness	Native	Exotic	Endemic	Richness	Native	Exotic	Endemic	Richness	Native	Exotic	Endemic
Buenos Aires*	60 (13.3%)	56 (12.6%)	4 (100.0%)	12 (5.6%)	479 (43.0%)	471 (42.7%)	8 (72.7%)	5 (23.8%)	122 (28.5%)	112 (27.5%)	10 (47.6%)	10 (11.5%)
Catamarca	79 (17.6%)	79 (17.7%)	0 (0.0%)	41 (19.0%)	437 (39.3%)	435 (39.5%)	2 (18.2%)	11 (52.4%)	91 (21.3%)	87 (21.4%)	4 (19.0%)	23 (26.4%)
Chaco	100 (22.2%)	99 (22.2%)	1 (25.0%)	1 (0.5%)	422 (37.9%)	419 (38.1%)	2 (18.2%)	3 (14.3%)	102 (23.8%)	96 (23.6%)	6 (28.6%)	5 (5.7%)
Chubut	53 (11.8%)	53 (11.9%)	0 (0.0%)	34 (15.7%)	283 (25.4%)	280 (25.4%)	3 (27.3%)	6 (28.6%)	98 (22.9%)	91 (22.4%)	7 (33.3%)	14 (16.1%)
Córdoba	70 (15.6%)	70 (15.7%)	0 (0.0%)	16 (7.4%)	410 (36.8%)	406 (36.8%)	4 (36.4%)	7 (33.3%)	74 (17.3%)	64 (15.7%)	10 (47.6%)	10 (11.5%)
Corrientes	104 (23.1%)	103 (23.1%)	1 (25.0%)	4 (1.9%)	511 (45.9%)	509 (46.2%)	2 (18.2%)	1 (4.8%)	108 (25.2%)	98 (24.1%)	10 (47.6%)	5 (5.7%)
Entre Ríos	63 (14.0%)	63 (14.1%)	0 (0.0%)	0 (0.0%)	385 (34.6%)	381 (34.6%)	4 (36.4%)	3 (14.3%)	64 (15.0%)	56 (13.8%)	8 (38.1%)	3 (3.4%)
Formosa	91 (20.2%)	90 (20.2%)	1 (25.0%)	2 (0.9%)	429 (38.5%)	427 (38.7%)	2 (18.2%)	2 (9.5%)	108 (25.2%)	102 (25.1%)	6 (28.6%)	3 (3.4%)
Jujuy	65 (14.4%)	65 (14.6%)	0 (0.0%)	6 (2.8%)	584 (52.5%)	582 (52.8%)	2 (18.2%)	6 (28.6%)	139 (32.5%)	135 (33.2%)	4 (19.0%)	8 (9.2%)
La Pampa	48 (10.7%)	48 (10.8%)	0 (0.0%)	20 (9.3%)	280 (25.2%)	277 (25.1%)	3 (27.3%)	6 (28.6%)	53 (12.4%)	45 (11.1%)	8 (38.1%)	10 (11.5%)
La Rioja	60 (13.3%)	60 (13.5%)	0 (0.0%)	33 (15.3%)	370 (33.2%)	368 (33.4%)	2 (18.2%)	10 (47.6%)	67 (15.7%)	63 (15.5%)	4 (19.0%)	16 (18.4%)
Mendoza	80 (17.8%)	80 (17.9%)	0 (0.0%)	47 (21.8%)	325 (29.2%)	321 (29.1%)	4 (36.4%)	9 (42.9%)	74 (17.3%)	65 (16.0%)	9 (42.9%)	21 (24.1%)
Misiones	100 (22.2%)	99 (22.2%)	1 (25.0%)	0 (0.0%)	561 (50.4%)	559 (50.7%)	2 (18.2%)	1 (4.8%)	131 (30.6%)	126 (31.0%)	5 (23.8%)	3 (3.4%)
Neuquén	69 (15.3%)	69 (15.5%)	0 (0.0%)	48 (22.2%)	268 (24.1%)	263 (23.9%)	5 (45.5%)	7 (33.3%)	69 (16.1%)	58 (14.3%)	11 (52.4%)	10 (11.5%)
Río Negro	73 (16.2%)	72 (16.1%)	1 (25.0%)	47 (21.8%)	323 (29.0%)	320 (29.0%)	3 (27.3%)	6 (28.6%)	95 (22.2%)	87 (21.4%)	8 (38.1%)	9 (10.3%)
Salta	116 (25.8%)	116 (26.0%)	0 (0.0%)	23 (10.6%)	603 (54.2%)	600 (54.4%)	3 (27.3%)	8 (38.1%)	159 (37.1%)	155 (38.1%)	4 (19.0%)	15 (17.2%)
San Juan	63 (14.0%)	63 (14.1%)	0 (0.0%)	38 (17.6%)	316 (28.4%)	314 (28.5%)	2 (18.2%)	8 (38.1%)	50 (11.7%)	46 (11.3%)	4 (19.0%)	14 (16.1%)
San Luis	50 (11.1%)	50 (11.2%)	0 (0.0%)	19 (8.8%)	319 (28.7%)	316 (28.7%)	3 (27.3%)	8 (38.1%)	51 (11.9%)	42 (10.3%)	9 (42.9%)	9 (10.3%)
Santa Cruz	31 (6.9%)	31 (7.0%)	0 (0.0%)	17 (7.9%)	252 (22.6%)	249 (22.6%)	3 (27.3%)	5 (23.8%)	82 (19.2%)	76 (18.7%)	6 (28.6%)	7 (8.0%)
Santa Fe	82 (18.2%)	81 (18.2%)	1 (25.0%)	3 (1.4%)	437 (39.3%)	434 (39.4%)	3 (27.3%)	4 (19.0%)	72 (16.8%)	62 (15.2%)	10 (47.6%)	2 (2.3%)
Santiago del Estero	68 (15.1%)	68 (15.2%)	0 (0.0%)	9 (4.2%)	376 (33.8%)	374 (33.9%)	2 (18.2%)	5 (23.8%)	74 (17.3%)	72 (17.7%)	2 (9.5%)	6 (6.9%)
Tierra del Fuego	1 (0.2%)	1 (0.2%)	0 (0.0%)	0 (0.0%)	228 (20.5%)	226 (20.5%)	2 (18.2%)	5 (23.8%)	64 (15.0%)	57 (14.0%)	7 (33.3%)	1 (1.1%)
Tucumán	68 (15.1%)	66 (14.8%)	2 (50.0%)	19 (8.8%)	500 (44.9%)	498 (45.2%)	2 (18.2%)	10 (47.6%)	112 (26.2%)	107 (26.3%)	5 (23.8%)	15 (17.2%)
Argentina Sea	3 (0.7%)	3 (0.7%)	0 (0.0%)	0 (0.0%)	64 (5.8%)	64 (5.8%)	0 (0.0%)	0 (0.0%)	52 (12.1%)	52 (12.8%)	0 (0.0%)	0 (0.0%)

Table A3.

Province	Total			
	Richness	Native	Exotic	Endemic
Buenos Aires*	918 (27.8%)	884 (27.3%)	34 (54.0%)	35 (7.1%)
Catamarca	671 (20.3%)	662 (20.4%)	9 (14.3%)	92 (18.7%)
Chaco	838 (25.4%)	828 (25.6%)	10 (15.9%)	13 (2.6%)
Chubut	468 (14.2%)	453 (14.0%)	15 (23.8%)	60 (12.2%)
Córdoba	643 (19.5%)	622 (19.2%)	21 (33.3%)	50 (10.2%)
Corrientes	1,079 (32.7%)	1,065 (32.9%)	14 (22.2%)	20 (4.1%)
Entre Ríos	819 (24.8%)	801 (24.7%)	16 (25.4%)	10 (2.0%)
Formosa	850 (25.7%)	840 (25.9%)	10 (15.9%)	9 (1.8%)
Jujuy	884 (26.8%)	877 (27.1%)	7 (11.1%)	43 (8.7%)
La Pampa	417 (12.6%)	401 (12.4%)	16 (25.4%)	40 (8.1%)
La Rioja	529 (16.0%)	520 (16.0%)	9 (14.3%)	66 (13.4%)
Mendoza	513 (15.5%)	493 (15.2%)	20 (31.7%)	82 (16.7%)
Misiones	1,190 (36.0%)	1177 (36.3%)	13 (20.6%)	45 (9.1%)
Neuquén	448 (13.6%)	427 (13.2%)	21 (33.3%)	75 (15.2%)
Río Negro	540 (16.3%)	523 (16.1%)	17 (27.0%)	73 (14.8%)
Salta	1,092 (33.1%)	1,080 (33.3%)	12 (19.0%)	68 (13.8%)
San Juan	470 (14.2%)	457 (14.1%)	13 (20.6%)	71 (14.4%)
San Luis	459 (13.9%)	442 (13.6%)	17 (27.0%)	47 (9.6%)
Santa Cruz	382 (11.6%)	367 (11.3%)	15 (23.8%)	31 (6.3%)
Santa Fe	859 (26.0%)	840 (25.9%)	19 (30.2%)	11 (2.2%)
Santiago del Estero	598 (18.1%)	592 (18.3%)	6 (9.5%)	25 (5.1%)
Tierra del Fuego	304 (9.2%)	292 (9.0%)	12 (19.0%)	6 (1.2%)
Tucumán	767 (23.2%)	754 (23.3%)	13 (20.6%)	57 (11.6%)
Argentina Sea	119 (3.6%)	119 (3.7%)	0 (0.0%)	20 (4.1%)

Appendix 2

Number of exclusive endemic species. * Buenos Aires includes Ciudad Autónoma de Buenos Aires.

Table A4.

Province	Marine fishes	Freshwater fishes	Amphibians	Reptiles	Birds	Mammals	Total
Buenos Aires*	–	3	1	6	–	4	**14**
Catamarca	–	5	4	17	–	5	**31**
Chaco	–	2	–	–	–	1	**3**
Chubut	–	1	1	13	–	4	**19**
Córdoba	–	3	2	–	–	4	**9**
Corrientes	–	1	2	3	–	2	**8**
Entre Ríos	–	2	–	–	–	–	**2**
Formosa	–	–	–	1	–	–	**1**
Jujuy	–	3	6	2	–	2	**13**
La Pampa	–	–	–	–	–	1	**1**
La Rioja	–	2	1	7	–	3	**13**
Mendoza	–	1	1	12	–	5	**19**
Misiones	–	35	2	–	–	1	**38**

Province	Marine fishes	Freshwater fishes	Amphibians	Reptiles	Birds	Mammals	Total
Neuquén	–	–	6	26	–	1	**33**
Río Negro	–	1	2	21	–	–	**24**
Salta	–	5	2	8	–	2	**17**
San Juan	–	5	2	9	–	3	**19**
San Luis	–	–	–	–	–	–	–
Santa Cruz	–	1	–	10	1	–	**12**
Santa Fe	–	1	–	–	–	1	**2**
Santiago del Estero	–	–	–	–	–	–	–
Tierra del Fuego	–	–	–	–	5	1	**6**
Tucumán	–	3	1	5	–	8	**17**
Argentina Sea	20	–	–	–	–	0	**20**
	20	**74**	**33**	**140**	**6**	**48**	**321**

Appendix 3

Number and percentage of threatened (CR, EN, VU) species per taxonomic group and province. Percentages are calculated in relation to the total native species of the group present in the province. * Total over the number of threatened native species present in the province. ** Buenos Aires includes Ciudad Autónoma de Buenos Aires.

Table A5.

Province	Marine fishes	Freshwater fishes	Amphibians	Reptiles	Birds	Mammals	Total*
Buenos Aires**	0 (0.0%)	6 (2.8%)	4 (13.3%)	12 (20.0%)	56 (11.7%)	14 (11.5%)	92 (10.4%)
Catamarca	0 (0.0%)	2 (5.7%)	7 (26.9%)	12 (15.2%)	38 (8.7%)	13 (14.3%)	72 (10.9%)
Chaco	0 (0.0%)	4 (2.4%)	1 (2.1%)	24 (24.0%)	46 (10.9%)	18 (17.6%)	93 (11.2%)
Chubut	0 (0.0%)	5 (41.7%)	7 (41.2%)	9 (17.0%)	35 (12.4%)	14 (14.3%)	70 (15.5%)
Córdoba	0 (0.0%)	8 (16.0%)	3 (9.1%)	15 (21.4%)	34 (8.3%)	9 (12.2%)	69 (11.1%)
Corrientes	0 (0.0%)	5 (1.7%)	2 (3.4%)	24 (23.1%)	65 (12.7%)	17 (15.7%)	113 (10.6%)
Entre Ríos	0 (0.0%)	5 (1.9%)	3 (7.1%)	9 (14.3%)	34 (8.8%)	6 (9.4%)	57 (7.1%)
Formosa	0 (0.0%)	3 (1.8%)	1 (2.0%)	17 (18.7%)	46 (10.7%)	17 (15.7%)	84 (10.0%)
Jujuy	0 (0.0%)	4 (8.3%)	11 (23.4%)	9 (13.8%)	59 (10.1%)	24 (17.3%)	107 (12.2%)
La Pampa	0 (0.0%)	0 (0.0%)	1 (9.1%)	6 (12.5%)	23 (8.2%)	4 (7.5%)	34 (8.5%)
La Rioja	0 (0.0%)	1 (7.1%)	1 (6.7%)	10 (16.7%)	28 (7.6%)	10 (14.9%)	50 (9.6%)
Mendoza	0 (0.0%)	0 (0.0%)	1 (10.0%)	18 (22.5%)	29 (8.9%)	9 (12.2%)	57 (11.6%)
Misiones	0 (0.0%)	10 (3.0%)	1 (1.6%)	39 (39.0%)	95 (16.9%)	31 (23.7%)	176 (15.0%)
Neuquén	0 (0.0%)	4 (28.6%)	8 (34.8%)	12 (17.4%)	23 (8.6%)	11 (15.9%)	58 (13.6%)
Río Negro	0 (0.0%)	5 (26.3%)	8 (33.3%)	15 (20.5%)	39 (12.1%)	13 (13.7%)	80 (15.3%)
Salta	0 (0.0%)	9 (5.8%)	11 (20.4%)	21 (18.1%)	65 (10.8%)	25 (15.7%)	131 (12.1%)
San Juan	0 (0.0%)	1 (5.0%)	1 (6.7%)	10 (15.9%)	22 (7.0%)	8 (16.0%)	42 (9.2%)
San Luis	0 (0.0%)	2 (12.5%)	0 (0.0%)	4 (8.0%)	21 (6.6%)	6 (11.8%)	33 (7.5%)
Santa Cruz	0 (0.0%)	3 (42.9%)	1 (25.0%)	2 (6.5%)	42 (16.7%)	12 (14.6%)	60 (16.3%)
Santa Fe	0 (0.0%)	8 (3.8%)	2 (3.8%)	14 (17.1%)	43 (9.8%)	8 (11.1%)	75 (8.9%)
Santiago del Estero	0 (0.0%)	3 (6.4%)	1 (3.2%)	10 (14.7%)	31 (8.2%)	10 (13.5%)	55 (9.3%)
Tierra del Fuego	0 (0.0%)	4 (80.0%)	0 (0.0%)	0 (0.0%)	45 (19.7%)	7 (10.9%)	56 (19.2%)
Tucumán	0 (0.0%)	3 (5.4%)	6 (22.2%)	9 (13.2%)	51 (10.2%)	15 (13.4%)	84 (11.1%)
Argentina Sea	74 (13.0%)	0 (0.0%)	0 (0.0%)	3 (100%)	17 (26.6%)	8 (15.4%)	102 (14.9%)

ZooKeys 1085: 129–143 (2022)
doi: 10.3897/zookeys.1085.76868
https://zookeys.pensoft.net

RESEARCH ARTICLE

A peer-reviewed open-access journal
ZooKeys
Launched to accelerate biodiversity research

The South American moth *Rheumaptera mochica* (Dognin, 1904) (Lepidoptera, Geometridae, Larentiinae) rediscovered after more than a century of anonymity

Héctor A. Vargas[1], M. Alma Solis[2], Marcelo Vargas-Ortiz[3]

1 *Departamento de Recursos Ambientales, Facultad de Ciencias Agronómicas, Universidad de Tarapacá, Arica, Chile* **2** *Systematic Entomology Laboratory, PSI, Agricultural Research Service, U.S. Department of Agriculture, c/o National Museum of Natural History, Smithsonian Institution, P.O. Box 37012, MRC 168, DC Washington, USA* **3** *Programa de Doctorado en Sistemática y Biodiversidad, Departamento de Zoología, Facultad de Ciencias Naturales y Oceanográficas, Universidad de Concepción, Concepción 4030000, Chile*

Corresponding author: Héctor A. Vargas (lepvargas@gmail.com)

Academic editor: Gunnar Brehm | Received 21 October 2021 | Accepted 14 January 2022 | Published 7 February 2022

http://zoobank.org/A38FC518-796A-4087-BFB1-4F731B8D3191

Citation: Vargas HA, Solis MA, Vargas-Ortiz M (2022) The South American moth *Rheumaptera mochica* (Dognin, 1904) (Lepidoptera, Geometridae, Larentiinae) rediscovered after more than a century of anonymity. ZooKeys 1085: 129–143. https://doi.org/10.3897/zookeys.1085.76868

Abstract

Rheumaptera mochica (Dognin, 1904) (Lepidoptera, Geometridae, Larentiinae) is reported from Chile for the first time. It was described from the western slopes of the Andes of southern Peru more than 100 years ago, and was recently rediscovered in Chile after larvae were collected and reared on the shrub *Senna birostris* var. *arequipensis* (Meyen ex Vogel) H.S. Irwin & Barneby (Fabaceae). This discovery expands the known distribution of this moth and provides its first host plant record. The genitalia of *R. mochica* are described and illustrated for the first time and compared to those of *R. affirmata* (Guenée, [1858]). A maximum likelihood analysis based on mitochondrial DNA sequences clustered *R. mochica* as sister to *R. affirmata* with 3.6–3.8% divergence (K2P). A lectotype is designated for *Calocalpe mochica* Dognin, 1904.

Keywords

DNA barcodes, Fabaceae, genitalia, Rheumapterini, *Senna birostris*

Introduction

Rheumaptera Hübner, 1822 (Lepidoptera, Geometridae, Larentiinae) is a widespread moth genus with 66 species, mostly from the Palearctic and Oriental regions; 14 species are recorded in the Western Hemisphere (Parsons et al. 1999). A recent molecular phylogenetic analysis strongly supports its monophyly and resulted in the transfer of three New World species from *Coryphista* Hulst, 1896 and *Triphosa* Stephens, 1829 to *Rheumaptera* (Brehm et al. 2019).

The Neotropical *Rheumaptera mochica* (Dognin, 1904) was originally described in *Calocalpe* Hübner, [1825], a junior synonym of *Rheumaptera* (Parsons et al. 1999). The species was based on two syntypes, a male and a female, from Arequipa on the western slopes of the Andes in southern Peru (Dognin 1904). No additional specimens have been reported in the literature since its original description. However, recently, adults of *R. mochica* were reared from larvae collected on a native shrub in northern Chile, a discovery that sheds light on this obscure geometrid moth.

The goals of this study were to confirm the identity of the reared adults, describe and illustrate their genitalia, and analyze their DNA from the COI barcode region (sensu Hebert et al. 2003) for the first time. Also, we report the host plant of *R. mochica* for the first time and expand its known distribution range. We designate a lectotype for *Calocalpe mochica* Dognin, 1904, to stabilize its nomenclature.

Material and methods

Specimens

Adults of *R. mochica* were reared from folivorous larvae collected on the native shrub *Senna birostris* var. *arequipensis* (Meyen ex Vogel) H.S. Irwin & Barneby (Fabaceae), near the villages of Belén (18°28'01"S, 69°30'37"W), Chapiquiña (18°23'34"S, 69°31'55"W), and Socoroma (18°16'03"S, 69°36'01"W) in the Parinacota Province of northern Chile, at about 3200–3400 m elevation on the western slopes of the Andes. Genitalia dissections were performed using standard procedures. Images of the genitalia were captured with a Sony CyberShot DSC-HX200V digital camera attached to a Leica M125 stereomicroscope and a Micropublisher 3.3 RTV-QImaging digital camera attached to an Olympus BX51 optical microscope. The distribution map was generated using SimpleMappr (Shorthouse 2010).

Abbreviations of institutional collections

DZUP Pe. Jesus de Santiago Moure Collection, Universidade Federal do Paraná, Paraná, Brazil;

IDEA Colección Entomológica de la Universidad de Tarapacá, Arica, Chile;
USNM United States National Museum of Natural History, Smithsonian Institution, Washington, D.C., USA.

DNA extraction, sequencing, and analysis

Genomic DNA was extracted from legs of five adults from Socoroma following the procedures described in Huanca-Mamani et al. (2015). DNA purification, PCR amplification, and sequencing of the barcode fragment with the primers LCO-1490 and HCO-2198 (Folmer et al. 1994) were performed by Macrogen Inc. (Seoul, South Korea) following the PCR program described in Escobar-Suárez et al. (2017). Additional sequences (Table 1) with species-level identification and 658 base pair (bp) length were downloaded from BOLD (Ratnasingham and Hebert 2007) for analysis, including congenerics and representatives of the phylogenetically close genera *Philereme* Hübner, [1825] and *Triphosa* Stephens, 1829 as outgroups, following a recent phylogeny of Geometridae (Brehm et al. 2019). The software MEGAX (Kumar et al. 2018) was used to perform sequence alignment with the ClustalW method, to estimate sequence divergence with the Kimura 2-Parameter (K2P) method, and choose the nucleotide substitution model using the lowest Bayesian information criterion value. A substitution saturation test, Xia test (Xia et al. 2003), was performed with the software DAMBE7 (Xia 2018), to evaluate the utility of the alignment for phylogenetic inference (ISS was lower than ISS.C). The phylogenetic tree was inferred through a maximum likelihood (ML) analysis with 1000 bootstrap replications and GTR+G as an evolutionary model in the software MEGAX (Kumar et al. 2018).

Table 1. DNA barcode sequences used in the molecular analysis.

Species	BOLD accession	GenBank accession	Country
Rheumaptera affirmata (Guenée, [1858])	GWOTG471-12		Bolivia
Rheumaptera cervinalis (Scopoli, 1763)	GBMIN33816-13	JF784768	Finland
Rheumaptera exacta (Butler, 1882)	GWOR2488-08		Chile
Rheumaptera fuegata (Staudinger, 1899)	GWOR2273-08		Chile
Rheumaptera hastata (Linnaeus, 1758)	ALLEP184-13		Canada
Rheumaptera incertata (Staudinger, 1882)	GBGL30834-19	KX343620	Kyrgyzstan
Rheumaptera meadii (Packard, 1874)	GWNR428-07	HQ647618	Canada
Rheumaptera mochica (Dognin, 1904)	RHEMO001-22	OK484459	Chile
Rheumaptera mochica (Dognin, 1904)	RHEMO002-22	OK484460	Chile
Rheumaptera undulata (Linnaeus, 1758)	BBLPB099-10	JF842111	Canada
Philereme transversata (Hufnagel, 176)	CGUKB362-09		United Kingdom
Philereme vetulata (Denis & Schiffermüller, 1775)	CGUKB463-09		United Kingdom
Triphosa dubitata (Linnaeus, 1758)	FGMLD158-13		Germany
Triphosa sabaudiata (Duponchel, 1830)	GWOR4460-09	KX071922	Greece

Results

Rheumaptera mochica (Dognin, 1904)

Calocalpe mochica Dognin, 1904: 361.
Rheumaptera mochica: Parsons et al. 1999.

Type material examined. Peru. The male ***lectotype*** and one female ***paralectotype*** are here designated (Figs 1, 2). The lectotype and its genitalia slide are deposited in the USNM and bear the following labels: Aréquipa/Pérou; *Calocalpe*/*mochica*/Dgn/type ♂ [Dognin handwriting]; *Calocalpe*/(*pallidata*)/Warren 04 [Dognin handwriting]; Dognin/Collection; Type No./32520/USNM [red label]; Genitalia Slide ♂/by B. Proshek/USNM 116,127 [green label]; USNMENT/01769001. The paralectotype and its genitalia slide are deposited in the USNM and bear the following labels: Aréquipa/Pérou; *Calocalpe*/*mochica*/Dgn/type ♀ [Dognin handwriting]; Dognin/Collection; Type No./32521/USNM [red label]; USNMENT/01769017.

Additional material examined. Chile – Parinacota Province • 2 ♂♂; Socoroma, 18°16'03"S, 69°36'01"W, December 2017, H.A. Vargas leg., ex larva *Senna birostris* var. *arequipensis*, October 2017; [genitalia slide numbers] HAV1423, 1454; IDEA • 5 ♀♀; same data as previous; [genitalia slide numbers] HAV1424, 1440, 1455, 1456, 1457; IDEA • 2 ♂♂; same locality, August 2009, H.A. Vargas leg., ex larva *Senna birostris* var. *arequipensis*, June 2009; [genitalia slide numbers] HAV1335, 1439; IDEA • 1 ♂; same locality, December 2008, H.A. Vargas leg., ex larva *Senna birostris* var. *arequipensis*, October 2008; [genitalia slide number] HAV1438; IDEA • 1 ♂; Chapiquiña, 18°23'34"S, 69°31'55"W, October 2015, H.A. Vargas leg., ex larva *Senna birostris* var. *arequipensis*, August 2015; [genitalia slide number] HAV1333; IDEA • 1 ♀; same data as for preceding; [genitalia slide number] HAV1339; IDEA • 1 ♂; Belén, 18°28'01"S, 69°30'37"W, October 2015, H.A. Vargas leg., ex larva *Senna birostris* var. *arequipensis*, August 2015; [genitalia slide number] HAV1337; IDEA • 1 ♀; same data as previous; [genitalia slide number] HAV1334; IDEA.

Identification. The identification of the Chilean specimens as *R. mochica* was based on comparisons of their male genitalia with those of the lectotype.

Wing pattern (Figs 3, 4) The forewing pattern of the Chilean specimens of *R. mochica* is slightly variable; the area between the postmedial line and the termen can be mostly light whitish-brown or mostly dark greyish-brown. This variation is not associated to sex.

Male segment *VIII* (Fig. 5) Tergum a narrow, longitudinal plate; anterior third triangular; distal two-thirds a narrow stripe; anterior margin widely rounded, laterally projected; posterior margin rounded. Sternum a narrow triangular longitudinal plate; anterior margin widely excavated, laterally projected; posterior margin narrowly excavated.

Male genitalia (Figs 6–9) Uncus well-sclerotized, triangular. Tegumen with two lateral, sclerotized stripes separated by a wide membranous area. Saccus triangular. Juxta trapezoidal with a narrow, drop-like ventral projection and a wide, U-shaped dorsal projection. Labides long, narrow, setose, finger-like, distal half slightly dilated.

Figure 1. *Rheumaptera mochica* (Dognin, 1904), male lectotype, dorsal view. Scale bar: 10 mm.

Valva mostly membranous; costal sclerotized band not reaching apex; sacculus well-sclerotized, with a narrow, dorsal, sclerotized stripe arising from near the apex, sacculus projection narrow, strongly distally curved, with a small basal process. Phallus cylindrical, slightly longer than the costal margin of the valva; vesica with group of spine-like cornuti shorter than half of the phallus length.

Female genitalia (Figs 10, 11) Papillae anales membranous, with setae. Apophyses posteriores rod-shaped, about 2.2 times length of papillae anales. Apophyses an-

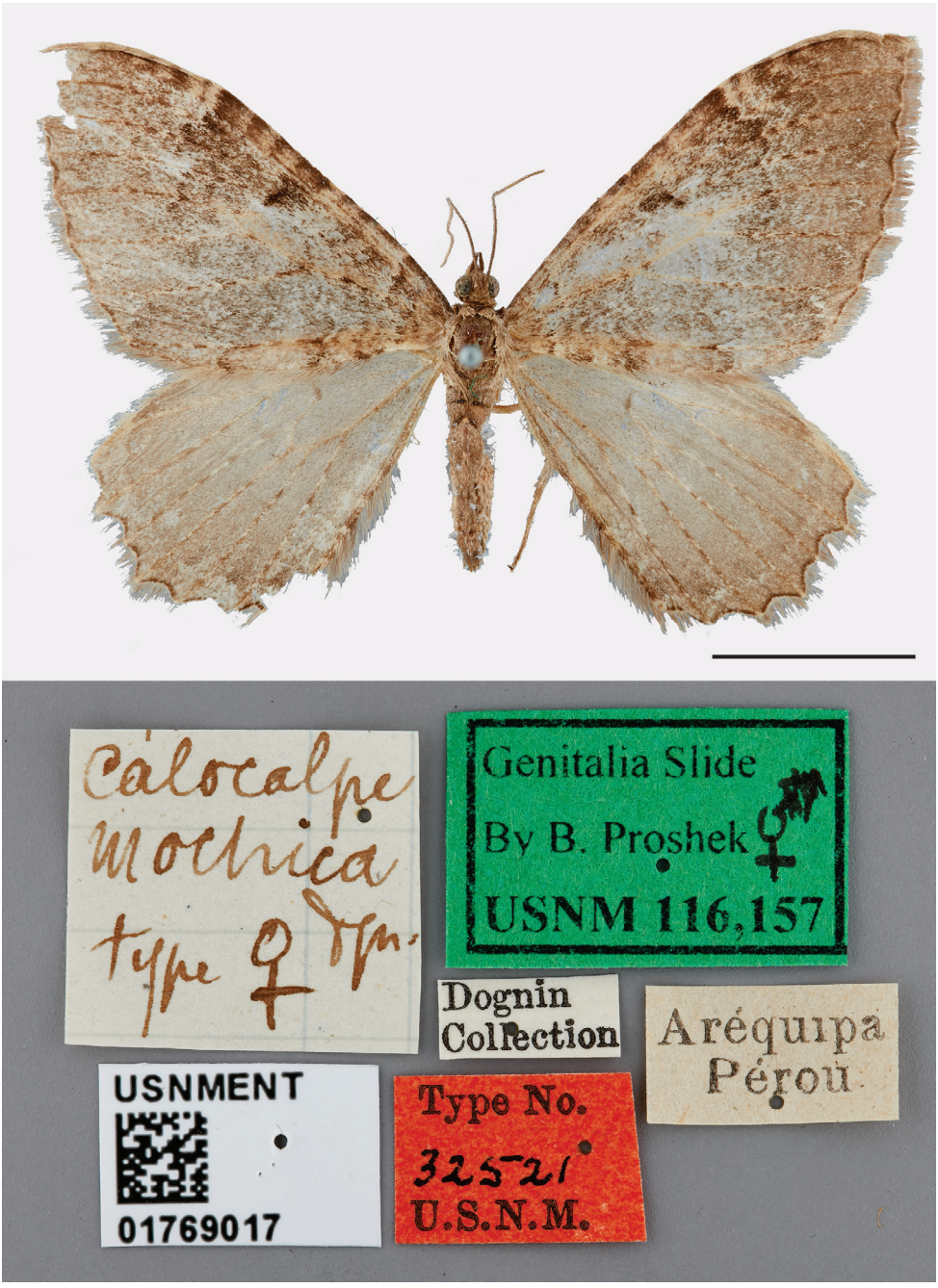

Figure 2. *Rheumaptera mochica* (Dognin, 1904), female paralectotype, dorsal view. Scale bar: 10 mm.

teriores about 0.8 times the length of apophyses posteriores, with a short ventral arm near base. Lamella antevaginalis as two transverse, sclerotized stripes, not connected medially, laterally continuous with ventral arm of apophyses posteriores. Antrum

Figures 3–4. *Rheumaptera mochica* (Dognin, 1904), male adults from northern Chile. Scale bar: 10 mm.

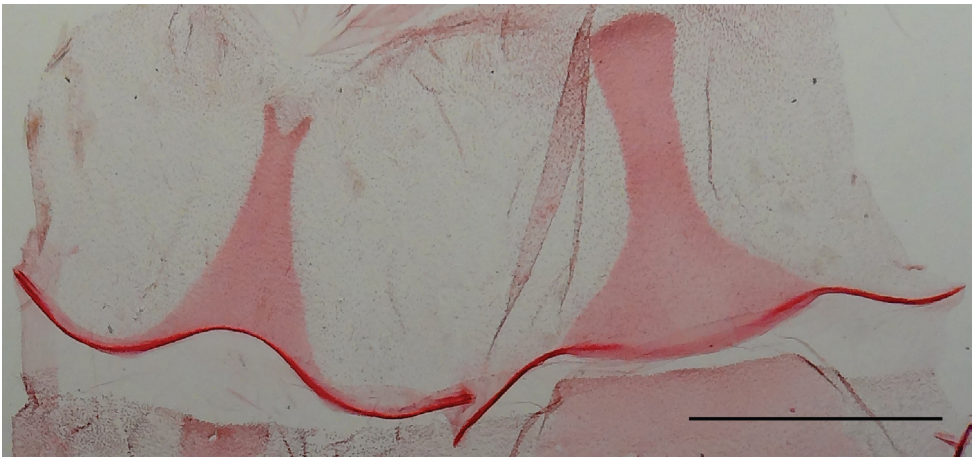

Figure 5. *Rheumaptera mochica* (Dognin, 1904), tergum (right) and sternum (left) of male abdominal segment VIII. Scale bar: 1 mm.

membranous. Ductus bursae almost as long as antrum, sclerotized. Corpus bursae in two sections; posterior section narrow, sinuous, mainly membranous, with longitudinal folds ventrally and numerous spine-like signa arising from a dorsal sclerotized plate; anterior section membranous, spherical. Ductus seminalis a membranous projection at base of corpus bursae.

DNA barcodes (Fig. 12). Five DNA barcodes (658 bp length) were obtained (GenBank accessions: OK484459, OK484460) from the specimens collected at Socoroma. Two haplotypes, with 0.2% (K2P) divergence between them, were detected. The sequences of *R. mochica* clustered as sister to the Neotropical congener *Rheumaptera affirmata* (Guenée, [1858]) in the ML analysis, with 3.6–3.8% (K2P) divergence.

Host plant (Fig. 13). *Senna birostris* var. *arequipensis* (Fabaceae) is the first host plant recorded for *R. mochica*.

Geographic distribution. (Fig. 14) The three localities in northern Chile represent new, expanded distribution records for *R. mochica*.

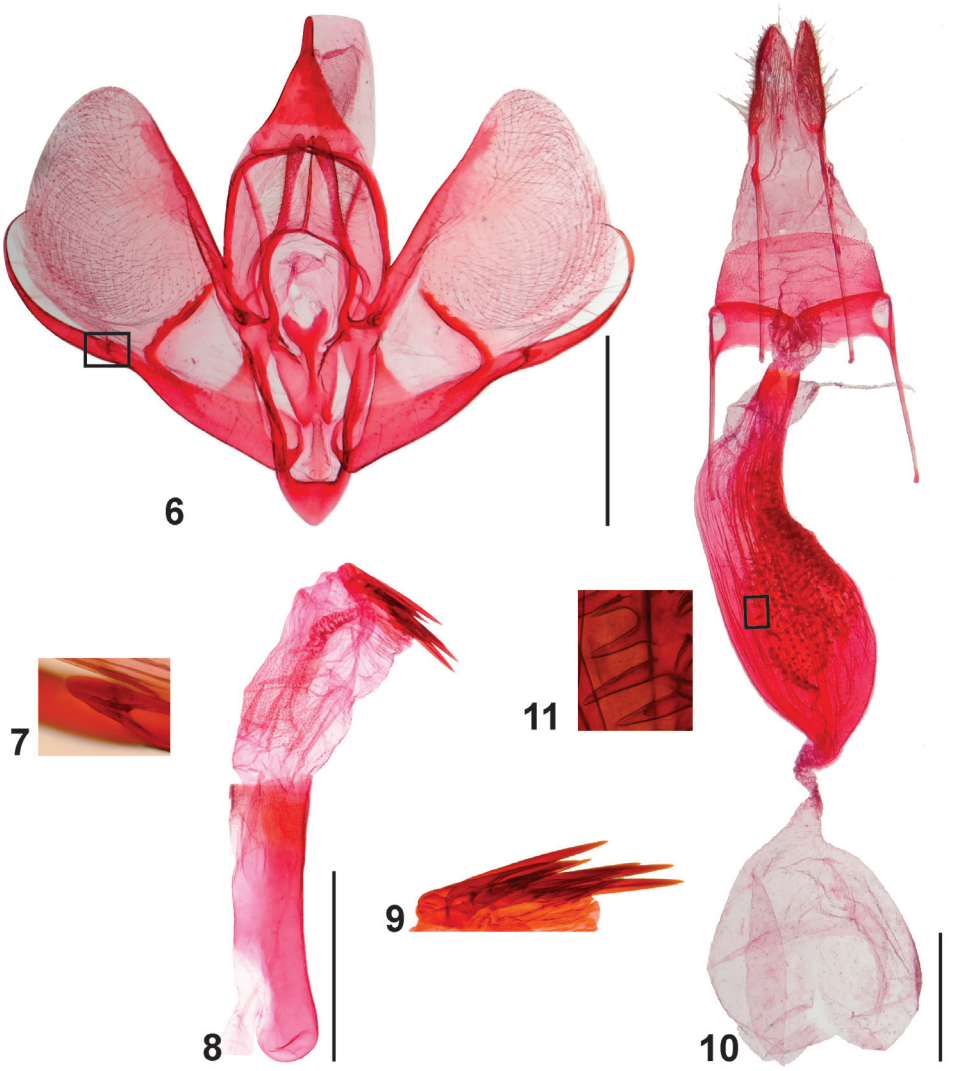

Figures 6–11. *Rheumaptera mochica* (Dognin, 1904), genitalia **6** male genitalia, ventral view, phallus removed **7** basal process of sacculus projection (rectangle in Fig. 6) **8** phallus **9** cornuti **10** female genitalia in ventral view **11** signa (rectangle in Fig. 10). Scale bar: 1 mm.

Discussion

The moth family Geometridae is more species-rich in the Neotropical Region than in any other (Brehm et al. 2016; 2019). More than 6400 species have been described from the Neotropics (Scoble et al. 1995), many of which are known only from their type material. The specimens of *R. mochica* from northern Chile are the first to be reported in the literature after more than one hundred years since this species was described by Dognin (1904).

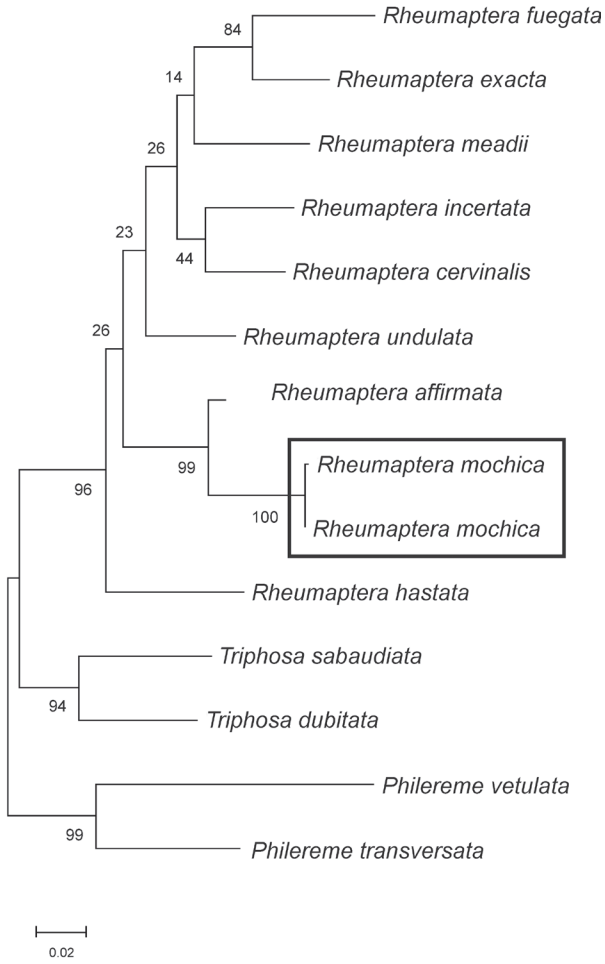

Figure 12. *Rheumaptera mochica* (Dognin, 1904) and congeners, maximum likelihood tree of DNA barcodes. Numbers indicate bootstrap values (1000 replicates).

The wing pattern of *R. mochica* is similar to that of the syntype of *R. affirmata* (Fig. 15). The subterminal line could be a diagnostic character to separate the two species, as this is absent or slightly differentiated in *R. mochica* (Figs 1–4), whereas this line is well-differentiated and creamy white on the fore- and hindwing of *R. affirmata*. However, additional specimens of these two Neotropical species must be examined to more accurately characterize their wing pattern, because high intraspecific variation occurs in Holarctic representatives of *Rheumaptera* (McGuffin 1973).

Genitalia morphology provides important characters for the identification of species of *Rheumaptera* and related genera (McGuffin 1973; Wanke et al. 2019). But the genitalia of *R. mochica* had remained a mystery since the species was described. The genitalia of both sexes are here described and illustrated for the first time; they are very similar to those of *R. affirmata* (Figs 16–18) based on Brazilian specimens from the DZUP collection. However, the two species can be accurately identified and separated

Figure 13. *Senna birostris* var *arequipensis* (Fabaceae), host plant of *R. mochica.*

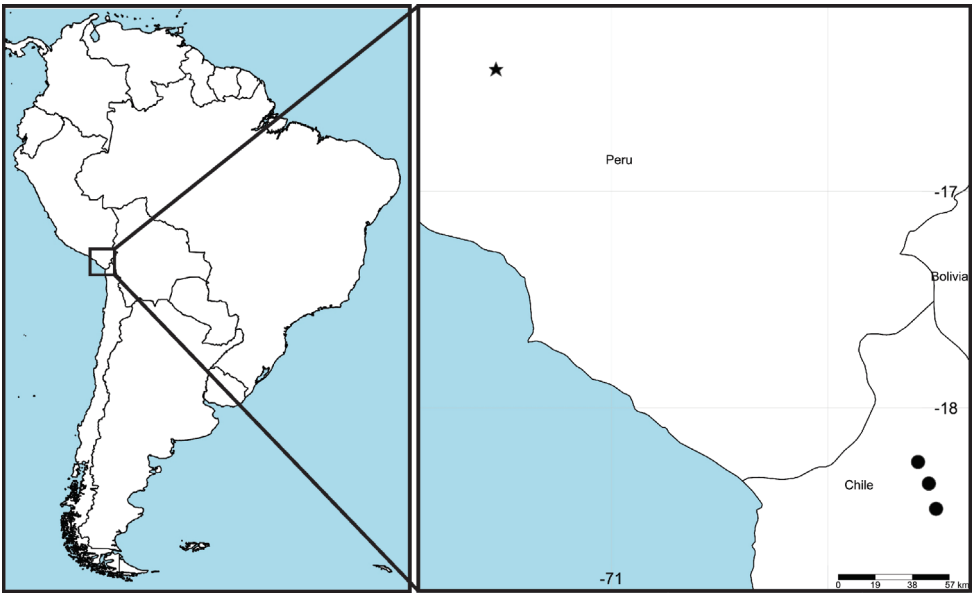

Figure 14. *Rheumaptera mochica* (Dognin, 1904), geographic distribution. Star indicates type locality (Arequipa, Peru), circles indicate new distribution records in northern Chile.

Figure 15. *Rheumaptera affirmata* (Guenée, [1858]), Brazil, syntype (dorsal, ventral) and labels. Photos kindly provided by Gunnar Brehm. Scale bar: 10 mm.

based on morphology of the genitalia. In the male of *R. mochica*, the sacculus projection is strongly curved distally and has a small basal process, and the vesica has spine-like cornuti the longest of which is slightly shorter than half the phallus length. In contrast, the male of *R. affirmata* has the sacculus projection only slightly curved and lacks a basal process, and the vesica has serrated cornuti the longest of which is slightly shorter than a quarter of the phallus length. In the female of *R. mochica*, signa are mainly concentrated near the middle of the posterior part of the corpus bursae, whereas in *R. affirmata* signa are mainly concentrated on the anterior half of the posterior part of the corpus bursae.

This preliminary assessment of *R. mochica* provides a few interesting results, although the molecular analysis presented here was based on a single mitochondrial marker. First, *R. mochica* is confidently recovered as a member of *Rheumaptera* as proposed by Parsons et al. (1999). Second, *R. affirmata* was found to be the nearest congener to *R. mochica*, in agreement with genitalia morphology. Third, the transfer of three New World species to *Rheumaptera*, *R. affirmata*, *R. pallidividata* (Snellen, 1874), and *R. meadii* (Packard, 1874), based on a multilocus molecular analysis (Brehm et al. 2019), was supported in our analysis. Clearly, analysis of additional molecular markers and a more complete taxon sampling would provide a more robust reconstruction of the phylogenetic relationships of *R. mochica* and its congeners.

Host plants remain unknown for most species of *Rheumaptera*. Available records indicate that their host ranges can be remarkably wide, such as in the Holarctic *R. hastata* (Linnaeus, 1758) and *R. subhastata* (Nolcken, 1879), whose larvae feed on

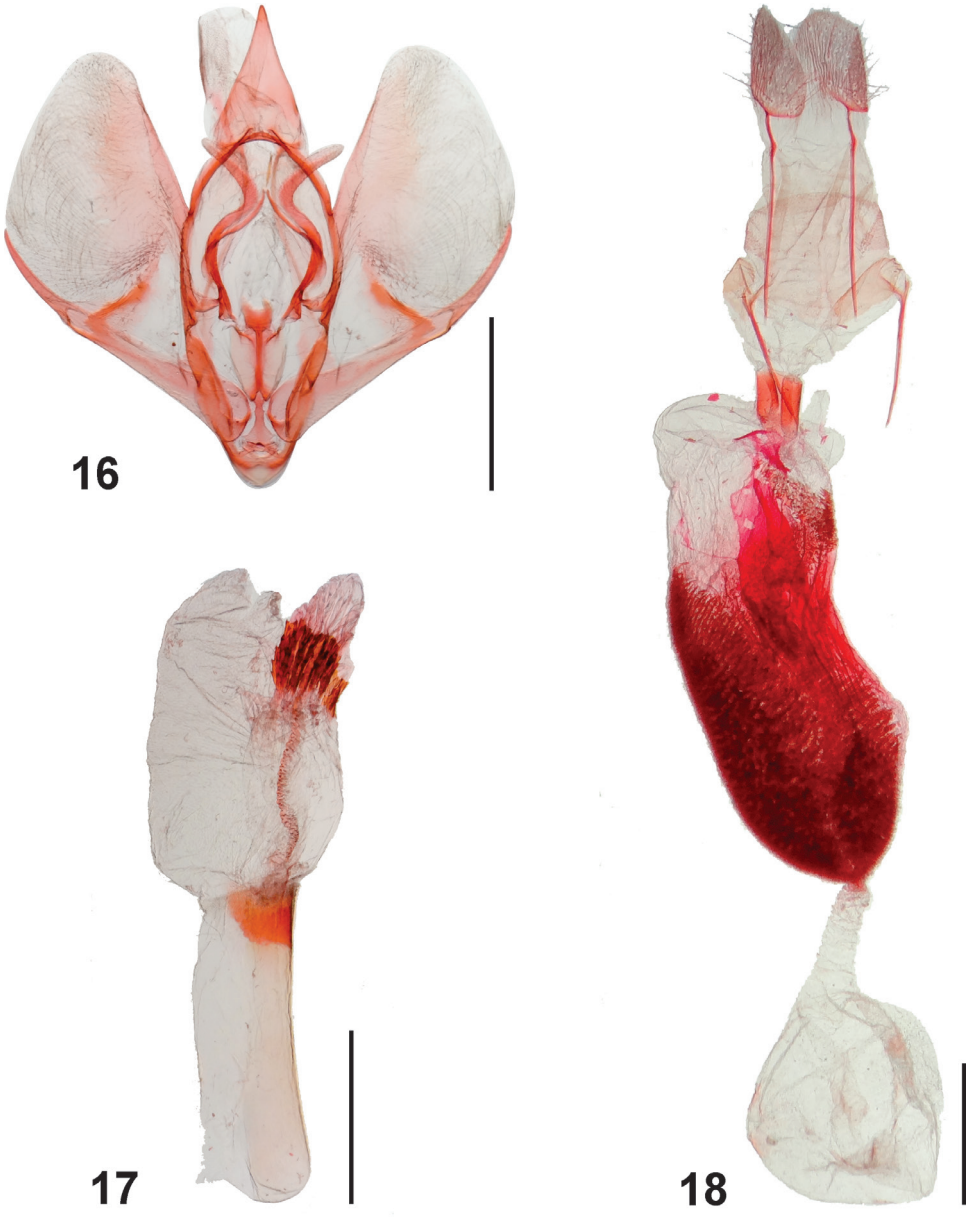

Figures 16–18. *Rheumaptera affirmata* (Guenée, [1858]), Brazil, genitalia **16** male genitalia in ventral view, phallus removed **17** phallus **18** female genitalia, ventral view. Scale bar: 1 mm.

plants of at least three families (McGuffin 1973; Hausmann and Viidalepp 2012) or are restricted to a single plant genus, such as in *R. affirmata*, whose larvae feed on at least two species of *Vicia* (Fabaceae) in the Neotropics (Brehm 2002). *Senna birostris* var. *arequipensis* is the first, and only, host plant ever recorded for *R. mochica*. The first author searched for geometrid larvae on other native plants in the vicinity of *Senna* sp.

at the study site, including other representatives of Fabaceae (Vargas et al. 2020; Vargas 2021), but larvae of *R. mochica* were not found.

The discovery of *R. mochica* in northern Chile expands the previously documented distribution range of this geometrid moth by about 300 km to the southeast. The geographic distribution of its host plant is from southern Peru to northern Chile at elevations between 2200 and 3900 m (Irwin and Barneby 1982), encompassing the localities of the type specimens of *R. mochica* and those newly reported here.

Previous Chilean records of *Rheumaptera* were restricted to the southern zone of Chile (Parsons et al. 1999). Five species have been recorded from the rainforests of northern Patagonia at about 42°S in southern Chile (Hausmann and Parra 2009). In contrast, *R. mochica* is the first species of the genus recorded in the extremely arid environments of the northernmost part of the country. This discovery suggests that, despite their remarkable aridity, these harsh environments may harbour more undiscovered or obscure, native geometrid moths whose biology deserves further attention.

Acknowledgements

We thank Olaf H. H. Mielke (Universidade Federal do Paraná, Brazil) for the loan of the *R. affirmata* specimens for dissection, Wilson Huanca-Mamani for the use of the molecular biology equipment, and Ben Proshek, Systematic Entomology Laboratory, ARS, USDA, for dissection and photography of the type specimens. We thank the reviewers Daniel Bolt and Axel Hausmann, who provided kind, helpful comments on the manuscript, and Subject Editor Gunnar Brehm for kindly sharing photos of the syntype of *R. affirmata* (Fig. 15) deposited in the Natural History Museum (NHMUK), London, UK. Mention of trade names or commercial products in this publication is solely for the purpose of providing specific information and does not imply recommendation or endorsement by USDA. USDA is an equal opportunity provider and employer. This study was supported by project UTA-MAYOR 9729–21.

References

Brehm G (2002) Diversity of geometrid moths in a montane rainforest in Ecuador. PhD Thesis, University of Bayreuth, Bayreuth.

Brehm G, Hebert PDN, Colwell RK, Adams MO, Bodner F, Friedemann K, Möckel L, Fiedler K (2016) Turning up the heat on a hotspot: DNA barcodes reveal 80% more species of geometrid moths along an Andean elevational gradient. PLoS ONE 11(3): e0150327. https://doi.org/10.1371/journal.pone.0150327

Brehm G, Murillo-Ramos L, Sihvonen P, Hausmann A, Schmidt BC, Õunap E, Moser A, Mörtter R, Bolt D, Bodner F, Lindt A, Parra LE, Wahlberg N (2019) New World geom-

etrid moths (Lepidoptera: Geometridae): Molecular phylogeny, biogeography, taxonomic updates and description of 11 new tribes. Arthropod Systematics & Phylogeny 77: 457–486. https://doi.org/10.26049/ASP77-3-2019-5

Dognin P (1904) Hétérocères noveaoux de l'Amérique du Sud. Annales de la Société Entomologique de Belgique 48: 358–369.

Hausmann A, Parra LE (2009) An unexpected hotspot of moth biodiversity in Chilean northern Patagonia (Lepidoptera, Geometridae). Zootaxa 1989: 23–38. https://doi.org/10.11646/zootaxa.1989.1

Hausmann A, Viidalepp J (2012) Larentiinae I. In: Hausmann A (Ed.) The Geometrid Moths of Europe, volume 3, 743 pp. Apollo Books, Stenstrup.

Hebert PDN, Cywinska A, Ball SL, deWaard JR (2003) Biological identification through DNA barcode. Proceedings of the Royal Society B Biological Science 270: 313–321. https://doi.org/10.1098/rspb.2002.2218

Huanca-Mamani W, Rivera-Cabello D, Maita-Maita J (2015) A simple, fast, and inexpensive CTAB-PVP-Silica based method for genomic DNA isolation from single, small insect larvae and pupae. Genetics and Molecular Research 14: 7990–8001. https://doi.org/10.4238/2015.July.17.8

Irwin HS, Barneby RC (1982) The American Cassiinae: A synoptical revision of Leguminosae tribe Cassieae subtribe Cassiinae in the New World. Memoirs of the New York Botanical Garden 35: 1–454.

Kumar S, Stecher G, Li M, Knyaz C, Tamura K (2018) MEGA X: Molecular Evolutionary Genetics analysis across computing platforms. Molecular Biology and Evolution 35: 1547–1549. https://doi.org/10.1093/molbev/msy096

McGuffin WC (1973) The *Rheumaptera* of North America (Lepidoptera: Geometridae). Canadian Entomologist 105: 383–398. https://doi.org/10.4039/Ent105383-3

Parsons MS, Scoble MJ, Honey MR, Pitkin LM, Pitkin BR (1999) The Catalogue. In: Scoble MJ (Ed.) Geometrid Moths of the World: a Catalogue (Lepidoptera: Geometridae) xxv, 1016 pp. (2 volumes). CSIRO Publishing, Collingwood. https://doi.org/10.1071/9780643101050

Ratnasingham S, Hebert PDN (2007) BOLD: the barcode of life data system (www.barcodinglife.org). Molecular Ecology Notes 7: 355–367. https://doi.org/10.1111/j.1471-8286.2007.01678.x

Scoble MJ, Gaston KJ, Crook A (1995) Using taxonomic data to estimate species richness in Geometridae. Journal of the Lepidopterists' Society 49: 136–147.

Shorthouse DP (2010) SimpleMappr, an online tool to produce publication-quality point maps. https://www.simplemappr.net [Accessed September 30, 2021]

Vargas HA (2021) *Iridopsis socoromaensis* sp. n., a geometrid moth (Lepidoptera, Geometridae) from the Andes of northern Chile. Biodiversity Data Journal 9: e61592. https://doi.org/10.3897/BDJ.9.e61592

Vargas HA, Hausmann A, Parra LE (2020) A new species of *Macaria* Curtis (Lepidoptera: Geometridae: Ennominae) from the Andes of northern Chile. Revista Brasileira de Entomologia 64(2): e20200016. https://doi.org/10.1590/1806-9665-RBENT-2020-0016

Wanke D, Hausmann A, Rajaei H (2019) An integrative taxonomic revision of the genus *Triphosa* Stephens, 1829 (Geometridae: Larentiinae) in the Middle East and Central Asia, with description of two new species. Zootaxa 4603: 039–065. https://doi.org/10.11646/zootaxa.4603.1.2

Xia X (2018) DAMBE7: New and improved tools for data analysis in molecular biology and evolution. Molecular Biology and Evolution 35: 1550–1552. https://doi.org/10.1093/molbev/msy073

Xia X, Xie Z, Salemi M, Chen L, Wang Y (2003) An index of substitution saturation and its application. Molecular Phylogenetics and Evolution 26: 1–7. https://doi.org/10.1016/S1055-7903(02)00326-3

ZooKeys 1085: 145–163 (2022)
doi: 10.3897/zookeys.1085.72927
https://zookeys.pensoft.net

RESEARCH ARTICLE

A peer-reviewed open-access journal
ZooKeys
Launched to accelerate biodiversity research

A new species of *Bundoksia* Lucañas, 2021 with comments on its subfamilial placement, based on morphological and molecular data

Yong Li[1], Xinxing Luo[1], Jiawei Zhang[1], Zongqing Wang[1], Yanli Che[1]

1 *College of Plant Protection, Southwest University, Beibei, Chongqing 400715, China*

Corresponding author: Yanli Che (shirleyche2000@126.com)

Academic editor: Fred Legendre | Received 12 August 2021 | Accepted 19 January 2022 | Published 8 February 2022

http://zoobank.org/1A95B02B-8770-4E56-AC6C-B017FF3618E6

Citation: Li Y, Luo X, Zhang J, Wang Z, Che Y (2022) A new species of *Bundoksia* Lucañas, 2021 with comments on its subfamilial placement, based on morphological and molecular data. ZooKeys 1085: 145–163. https://doi.org/10.3897/zookeys.1085.72927

Abstract

One new species of *Bundoksia* Lucañas, 2021 from China is described. We construct a haplotype network from 21 *COI* sequences to display the relationships amongst populations of *Bundoksia longissima* **sp. nov.**, mainly from Hainan Island, Yunnan Province and Guangxi Province, China. For the first time, we provide the details of female genitalia in addition to the known external morphology and male genitalia of the genus. Six molecular markers (*12S*, *16S*, *18S*, *28S*, *COI* and *COII*) from a total of 38 samples, including three samples of *Bundoksia longissima* **sp. nov.**, are used to reconstruct phylogenetic trees using Maximum Likelihood (ML) and Bayesian Inference (BI) to assess the phylogenetic affinities of *Bundoksia*. Photographs of the morphology and a key to the three *Bundoksia* species are also provided.

Keywords

Bayesian Inference, cockroaches, DNA barcodes, haplotype network, Maximum Likelihood

Introduction

The genus *Bundoksia* Lucañas, 2021 was established with *Bundoksia rufocercata* (Shelford, 1911) as type species, based on its smooth pronotum, flattened tibiae, the meso- and metafemur sparsely armed with dissimilarly-sized spines. Up to now, the genus *Bundoksia* contained two species, *Bundoksia rufocercata* and *Bundoksia sibuyania*, both distributed in the Philippines. Lucañas (2021) mentioned that the genus *Bundoksia*

can be distinguished from *Cartoblatta* Shelford, *Shelfordella* Adelung and *Deropeltis* Burmeister by the specialised first abdominal tergite. Moreover, the genus *Bundoksia* possesses some of the characteristics of the subfamilies Archiblattinae and Blattinae.

COI has been recommended as a useful DNA barcode to solve the sexual dimorphism existed in cockroach (Yang et al. 2019) and judge intraspecific variation or interspecific difference for cockroaches (Li et al. 2020) combined with other data. In addition, use of multi-gene combinations to infer phylogenetic trees has gradually become an available tool to confirm the taxonomic status of cockroach genus (Djernæs et al. 2015). With the discovery of the new species *Bundoksia longissima* sp. nov., based on morphological and molecular data (*COI*), four mitochondrial markers (*12S*, *16S*, *COI* and *COII*) and two nuclear markers (*18S, 28S*) were sequenced to explore the phylogenetic affinities of the genus *Bundoksia*.

Materials and methods:

Taxon sampling

Specimens were collected mainly from Yunnan, Hainan and Guangxi Province, China during 2014 to 2019 (Suppl. material 1: Table S1, Fig. 1). The samples were stored in absolute ethanol at –20 °C. All voucher specimens (Suppl. material 1: Table S1) were deposited in the Institute of Entomology, College of Plant Protection, Southwest University Chongqing, China (SWU). Voucher numbers and GenBank accession numbers are provided in Suppl. material 1: Table S1 and Suppl. material 2: Table S2.

Figure 1. Geographic distribution of *Bundoksia longissima* sp. nov. Numbers for sampling localities match those in Suppl. material 1: Table S1. Different colours represent different populations. Purple circles indicate no molecular data.

Morphological study

Morphological terminology used in this article mainly follows McKittrick (1964) and Li et al. (2013) for male and female genitalia, Roth (2003) and Li et al. (2018) for other characters. Terminology abbreviations in this study are as follow:

ScP	subcostal posterior	**v.II.**	second valve
R	radius	**v.III.**	third valve
Cu	cubitus	**vlf.I**	first valvifer
CuA	cubitus anterior	**p.l.**	posterior lobes of valvifer II
CuP	cubitus posterior		
Pcu	postcubitus	**ltst.IX**	laterosternite IX
M	media	**pt.**	paratergites
V[1], **V[s]**	vannal veins	**a.a.**	anterior arch
L1, **L2d/L2v**, **L3**	sclerites of the left phallomere	**sp.pl.**	spermathecal plate
		sp.o.	spermathecal opening
R1, **R2**, **R3**	sclerites of the right phallomere	**sp.**	spermatheca
		bsv.	basivalvula
v.ph	ventral phallomere	**ltst.sh**	laterosternal shelf
TX	tergum X	**vst.s**	vestibular sclerite
pp.	paraprocts	**inst.f.**	intersternal fold
v.I.	first valve		

Measurement data of the specimens were obtained by vernier caliper and Leica M205A microscopic system, such as body length including tegmen, body length, pronotum length × width, interantennal distance, interocular distance, head length × width, tegmina length, approximate length ratio of 3rd-5th segments of maxillary palps. Genital segments of examined specimens were soaked with 10% sodium hydroxide (NaOH) for 10 minutes, observed in glycerol with a Motic K400 stereomicroscope and preserved with the remainder of the specimen in ethyl alcohol at –20 °C. The photographs of samples and genitalia were obtained by using a Leica M205A microscopic system. All of the images and photographs were processed in Adobe Photoshop CS6. Type materials are deposited in the Institute of Entomology, College of Plant Protection, Southwest University Chongqing, China (SWU).

DNA extraction, amplification and sequencing

A total of 21 *COI* sequences of *Bundoksia longissima* sp. nov. were sequenced to determine the intraspecific variation, accession numbers: OM370873-OM370893 (Suppl. material 1: Table S1). The *COI* fragment was amplified by PCR, and PCR primers were as follows: *COI*-F3 (5'-CAACYAATCATAAAGANATTGGAAC-3') and *COI*-R3 (5'-TAAACTTCTGGRTGACCAAARAATCA-3'). The conditions of amplification were: 98 °C initial denaturation for 2 min, followed by 35 cycles at 98 °C

for 10 s, 51 °C for 10 s, and 72 °Cfor 10 s, with a final extension at 72 °C for 5 min. DNA was then sent to TsingKe Co. Ltd., Chongqing, China for sequencing.

We sequenced five additional markers of *Bundoksia longissima* sp. nov.: mitochondrial *12S*, *16S*, *COII* and nuclear *18S*, *28S* (Suppl. material 2: Table S2). We used an insect DNA extraction kit (D3121-02, Magen, Guangzhou, China) to extract the total DNA of examined specimens from hind-leg tissue. Total DNA was first stored at –20 °C then sent to TsingKe Co. Ltd., Chongqing, China for sequencing. The library generation and paired-end sequencing were completed on the Illumina HiSeq 2000 platform. Mitochondrial gene fragments *12S*, *16S*, *COII* and nuclear *18S* rRNA and *28S* rRNA were obtained by mapping sequence reads to the reference gene sequence of relative species, with the aid of Geneious Prime v.2021.1 (Biomatters Ltd., Auckland, New Zealand).

Sequence alignment and phylogenetic analyses

A total of 27 *COI* sequences (excluding the primer, 658 bp), including 21 sequences of *Bundoksia longissimi* sp. nov. from Hainan, Yunnan and Guangxi in this study, along with others from GenBank corresponding to six outgroup species, were aligned using MEGA 7.0 (Kumar et al. 2007) and adjusted visually after translation into amino acid sequences. The genetic divergence values were calculated in MEGA 7 (Kumar et al. 2007) on the basis of the Kimura 2 - parameter (K2P) model (Kimura, 1980). For Neighbour-Joining (NJ), implemented in MEGA 7 (Kumar et al. 2007), the outgroups contained six taxa (*Mantis religiosa*, *Protagonista lugubris*, *Homalosilpha arcifera*, *Mimosilpha disticha*, *Homalosilpha nigricans* and *Homalosilpha* sp.). In the meantime, *COI* data of *Bundoksia longissimi* sp. nov. were used to construct the haplotype network for inferring relationships amongst different populations, which were constructed in the software PopART v.1.7 (Leigh and Bryant 2015).

The rest of the five markers (*12S*, *16S*, *COII*, *18S* and *28S*) acquired were 412 bp (*12S*), 450 bp (*16S*), 582 bp (*COII*), 594 bp (*28S*) and 1831 bp (*18S*). In order to infer the phylogenetic relationships between *Bundoksia longissimi* sp. nov. and other blattid species, we assembled a dataset with 38 samples from 33 cockroach species and two mantid species (*Bantia werneri* and *Mantis religiosa*) as the outgroup species downloaded from GenBank. Sequence alignment was performed through online MAFFT v.7 (Katoh et al. 2013). The Q-INS-i algorithm was used for non-coding protein genes (*12S*, *16S*, *18S*, *28S*) which were checked visually in MEGA 7 (Kumar et al. 2007); poorly aligned characters within the intergenic region were removed. The G-INS-i algorithm was selected for protein-coding genes (*COI*, *COII*) with other parameters default values, then they were manually adjusted after translation into amino acids in MEGA 7. The total length of the concatenated alignment is 4112 bp.

Using Xia's method, implemented in DAMBE 7 (Xia 2018), the third codon position (PCG3) (I_{SS} = 0.723) was much more saturated than the first (I_{SS} = 0.294) and second codon position (I_{SS} = 0.206), indicating the third codon position is less suitable for further analyses. Due to the higher mutation saturation, the third codon was excluded in our study. Based on the combined dataset, the Maximum Likelihood (ML) and

Bayesian Inference (BI) methods were used to construct the phylogenetic trees. ML inference was performed in RAxML v.7.7.1 (Stamatakis et al. 2008), using a GTR-GAMMA model with 1,000 bootstrap replicates. Bayesian phylogenetic analyses was conducted in MrBayes3.2 (Ronquist et al. 2012) with the substitution models selected by PartitionFinder v.1.1.1 (Lanfear et al. 2012) as follows, GTR+I+G for *12S* and *16S*, TrNef+I+G for *18S*, TrN+I+G for *28S* and *COII*_pos12 and TIM+I+G for *COI*_pos12. Posterior distribution was estimated by Markov Chain Monte Carlo (MCMC) sampling with three hot and one cold chains and a total of 10,000,000 generations. When the average standard differentiation frequency deviation was less than 0.01, the convergence was inferred; then the first 25% of samples were discarded as the burn-in.

Taxonomy

Bundoksia Lucañas, 2021

Bundoksia Lucañas, 2021: 1012 (Type species: *Bundoksia rufocercata* (Shelford, 1911), by original designation)

Diagnosis. Sexual dimorphism and ocelli spots distinct. **Male.** Pronotum nearly trapezoidal or subelliptical, uneven with depressions in medium surface, posterior margin rounded. Tegmina and wings fully developed. Front femur usually type A. Tibia flattened with sparse spines. Tarsus with smooth pulvillus. Claws symmetrical and unspecialised, arolium present. The first abdominal tergum of males specialised or not. Supra-anal plate symmetrical; subgenital plate symmetrical, styli stick-like, similar size. **Male genitalia.** L2d base with several rows of serration, L2v distal part armed with spines; L3 unciform. R1 of right phallomere armed with spines. **Female.** Body thicker than the male. Pronotum parabolic, posterior margin straight. Tegmina reduced, only reaching hind margin of first abdominal tergite or metathorax; triangular or quadrate; wings reduced to small lobe. Supra-anal plate truncate, symmetrical. Subgenital plate valvular.

Remarks. Lucañas (2021) mentioned that the first abdominal tergite specialised with setose gland was diagnostic for *Bundoksia* and distinguished *Bundoksia* from the other Archiblattinae by its smooth pronotum and flattened tibiae and Blattinae in terms of distinct femoral armament (meso- and metafemur sparsely armed with dissimilarly-sized spines). In previous studies, it is common that species of the same genus have or lack the abdominal tergite tergal glands, i.e. *Episymploce* (Li et al., 2020), *Scalida* (Wang et Che, 2010) in Ectobiidae and *Periplaneta* (Roth, 1994) in Blattidae. We consider that the first abdominal tergum of males, specialised or not, is not a diagnostic character of the genus *Bundoksia*, which can be distinguished from the genus, *Cartoblatta* Shelford by other characters (tegmina short and quadrate, not covering the first abdominal tergite; female supra-anal plate with hind margin cleft). Therefore, we revised the generic diagnostic 'the first abdominal tergum of males specialised' to 'specialised or not'.

Key to known species of *Bundoksia* Lucañas, 2021

1 Pronotum black with one pair of yellow-orange antero-lateral markings, female tegmina quadrate..... ***B. rufocercata*** **(Shelford, 1911)**
– Pronotum black without marking, female tegmina triangular **2**
2 Cercus black; male: first abdominal tergite with setose gland ....***B. sibuyania*** **Lucañas, 2021**
– Cercus pale yellow with apex black; male: first abdominal tergite unspecialised .....***B. longissima*** **Li & Che, sp. nov.**

Bundoksia longissima **Li & Che, sp. nov.**
http://zoobank.org/FC409991-0647-4793-B53E-A7A39277A536
Figs 2–5

Type materials (all deposited in SWU). ***Holotype*****. China• Hainan:** male, Mingfenggu, Mt Jianfengling, Ledong County, 26.IV.2015, Lu Qiu & Qikun Bai leg.; SWU-B-BL0201001. ***Paratypes*****. China• Hainan:** 9 males and 1 female, Mingfenggu, Mt Jianfengling, Ledong County, 26.IV.2015, Lu Qiu & Qikun Bai leg; SWU-B-BL0201001 to 0201010 • 1 male and 1 female, Mt Wuzhi, Wuzhishan City, 795 m alt., 18.V.2014, Shunhua Gui leg; SWU-B-BL0201101 to 0201102. **China•Guangxi:** 1 male, Mt Dayao, Jinxiu County, 15.VI.1974, Ping Lin & Yuliang Jia & Yaoquan Li leg; SWU-B-BL0201301 • 1 female, Mt Dayao, Jinxiu County, 7.VII.2015, Lu Qiu & Qikun Bai leg; SWU-B-BL0201201 • 1 female, Jinxiu County, 16-17.VII.2015, Lu Qiu & Qikun Bai leg; SWU-B-BL0201202. **China•Yunnan:** 1 male and 1 female, Mt Dawei, Pingbian County, 15-17.V.2016, Lu Oiu & Zhiwei Oiu leg; SWU-B-BL0201401, SWU-B-BL0201403 • 1 male, Jinping County, 14-16.V.2015, Jianyue Qiu leg; SWU-B-BL0201501 • 1 male, Meizi Lake, Pu'er City, 30.IV.2014, collector unknown; SWU-B-BL0201602 • 1 male, Meizi Lake, Pu'er City, 20. V. 2018, Lu Oiu & Zhiwei Oiu leg; SWU-B-BL0201601 • 1 male, Xishuangbanna Tropical Botanical Garden, Chinese Academy of Sciences, Menglun Town, Mengla County, Xishuangbanna Prefecture, 27.V.2016, Lu Oiu & Zhiwei Oiu leg; SWU-B-BL0201701 • 1 male, Wangtianshu, Mengla County, Xishuangbanna Prefecture, 24.V.2016, Lu Oiu & Zhiwei Oiu leg; SWU-B-BL0201801.

Other material examined (all deposited in SWU). **China• Guangdong:** 1 female, Nanling National Nature Reserve, 18.VIII.2010, Haoyu Liu leg. **China•Guangxi:** 1 female, Mt Mao'er, Xingan County, Guilin City, 20.VIII.2020, Lu Oiu leg; 1 nymph, Mt Daming, Nanning City, 2.VII.2015, Lu Qiu & Qikun Bai leg; **China•Yunnan:** 3 nymphs, Mt Dawei, Pingbian County, 17.V.2016, Lu Oiu & Zhiwei Oiu leg.

Diagnosis. *Bundoksia longissima* sp. nov., differs from the two known species, *B. rufocercata* (Shelford, 1911) and *B. sibuyania* Lucañas, 2021 by the following characteristics: 1) pronotum: with slightly thickened lateral margin; 2) mid- and hind- femur with only distal spines on ventral margin; 3) the first abdominal tergite

unspecialised. In addition, *Bundoksia longissima* sp. nov. can be distinguished from *B. rufocercata* as follows: pronotum black and female tegmina triangular in the former, whereas pronotum with yellow orange marking and female tegmina quadrate in *B. rufocercata*.

Measurements (mm). Male. Body length including tegmen: 22.6–26.4; body length: 17.0–19.4; pronotum length × width: 3.8–5.0 × 5.0–5.9; interantennal distance: 1.25–1.39; interocular distance: 0.81–1.08; head length × width: 2.95–3.35 × 2.91–3.22; tegmina length: 18.9–23.4; approximate length ratio of 3rd–5th segments of maxillary palps about 1:0.75:1. **Female.** Body length: 18.8–21.6; pronotum length × width: 4.5–5.0 × 6.6–7.4; interantennal distance: 1.62–1.83; interocular distance: 1.55–1.84; head length × width: 3.84–4.49 × 0.80-1.05; tegmina length: 4.42–5.74; approximate length ratio of 3rd–5th segments of maxillary palps about 1:0.75:1.

Description. Male. Colouration. Body unicoloured dark reddish-brown to blackish-brown, except the following portions: ocelli white; clypeus light brown or yellowish-brown; antennae yellowish-brown, basal and distal portion darker, apex distinctly light coloured; wings with anal area transparent, the remaining part yellowish-brown; tibiae and tarsi slightly light coloured (reddish-brown), except the joints; cerci yellowish, apex segment black, with white tip (Fig. 2A–B).

Body slender, flattened. ***Head.*** Vertex unconcealed by pronotum, smooth, slightly punctured. Interocular space wide, as wide as the distance between ocelli, narrower than the distance between antennal sockets. Ocelli oval (Fig. 2D). **Thorax.** Pronotum nearly subelliptical, wider than long. Surface smooth, disc with unequal-sized punctures. The border of pronotum thickening, anterior margin slightly elevated, lateral margins rounded, hind margin slightly arched (Fig. 2C). **Tegmina and wings.** Tegmina fully developed, extending well beyond the end of abdomen. Outer margins of tegmina straight, apex of tegmen rounded. Tegmen with ScP slightly curved; R ended at the margin about 1/3 from the apex; M and Cu with numerous branches (Fig. 2E). Wings with ScP slightly vague; M with a dichotomy in base, pseudostem distinct; CuA simple and linear or lattice-like; CuP simple and obvious (Fig. 2F, G). **Legs.** Front femur type A2 (ending with a large, curved spine and a smaller spine, hind margin of front femur with a row of rough, distant spaced spins) (Fig. 2H); tibia flattened with sparse spines; tarsus with large tarsal pulvillus. Mid- and hind femur with only distal spines on ventral margin. Hind metatarsus obviously longer than the remaining tarsomeres combined (Fig. 2I). Claws symmetrical and unspecialised, arolium large. **Abdomen.** Supra-anal plate symmetrical, quadrate, with hind angles rounded, hind margin straight, median less sclerotised. Paraprocts similar, hind margin straight, central areas sclerotised. Cerci distinct pubescent ventrally, smooth dorsally, apex truncated, with membrane (Fig. 2J). Subgenital plate nearly symmetrical, styli similar, distant (Fig. 2K).

Male genitalia. Left phallomere complex, distal part of L1 enlarged, edge with dense minute sawtooth; L2d base part with two or three rows of serrations, L2v distal part with spines; L3 unciform and apex blunt or slightly acuminate, curved part has an inward spinous protuberance. R1 of right phallomere with one or two spines with the sizes of the two spines varied; R2 expanded, irregular; R3 broad and slightly curved, likely spoon-shaped (Fig. 2L).

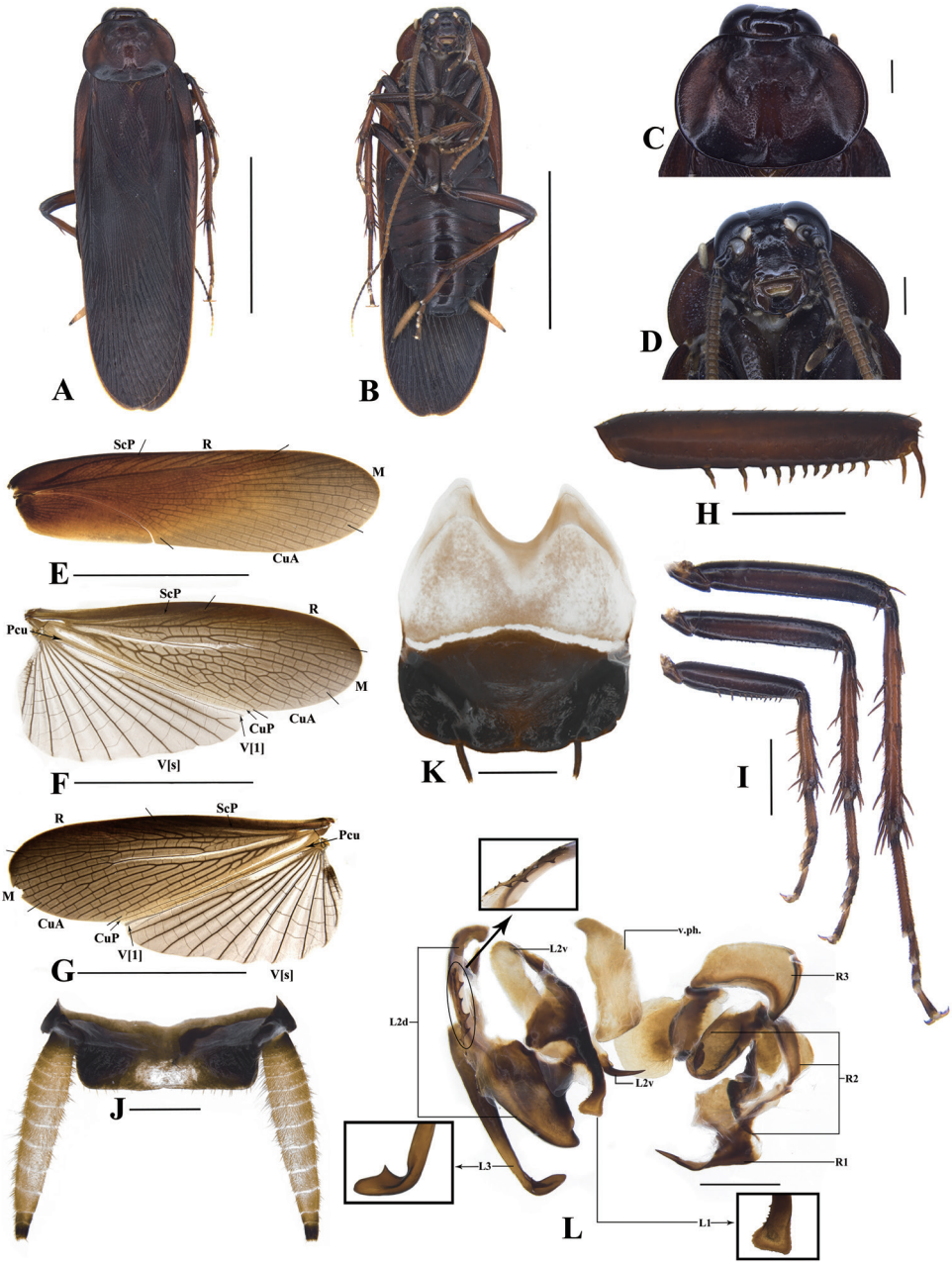

Figure 2. *Bundoksia longissima* Li & Che, sp. nov. (male) **A** dorsal view **B** ventral view **C** pronotum **D** head **E** tegmen **F** right hind wing **G** left hind wing **H** front femur **I** leg (front, mid, hind) **J** supra-anal plate **K** subgenital plate **L** phallomere; Scale bars: 10.0 mm (**A, B, E–G**); 2.0 mm (**I**); 1.0 mm (**H, J–L**).

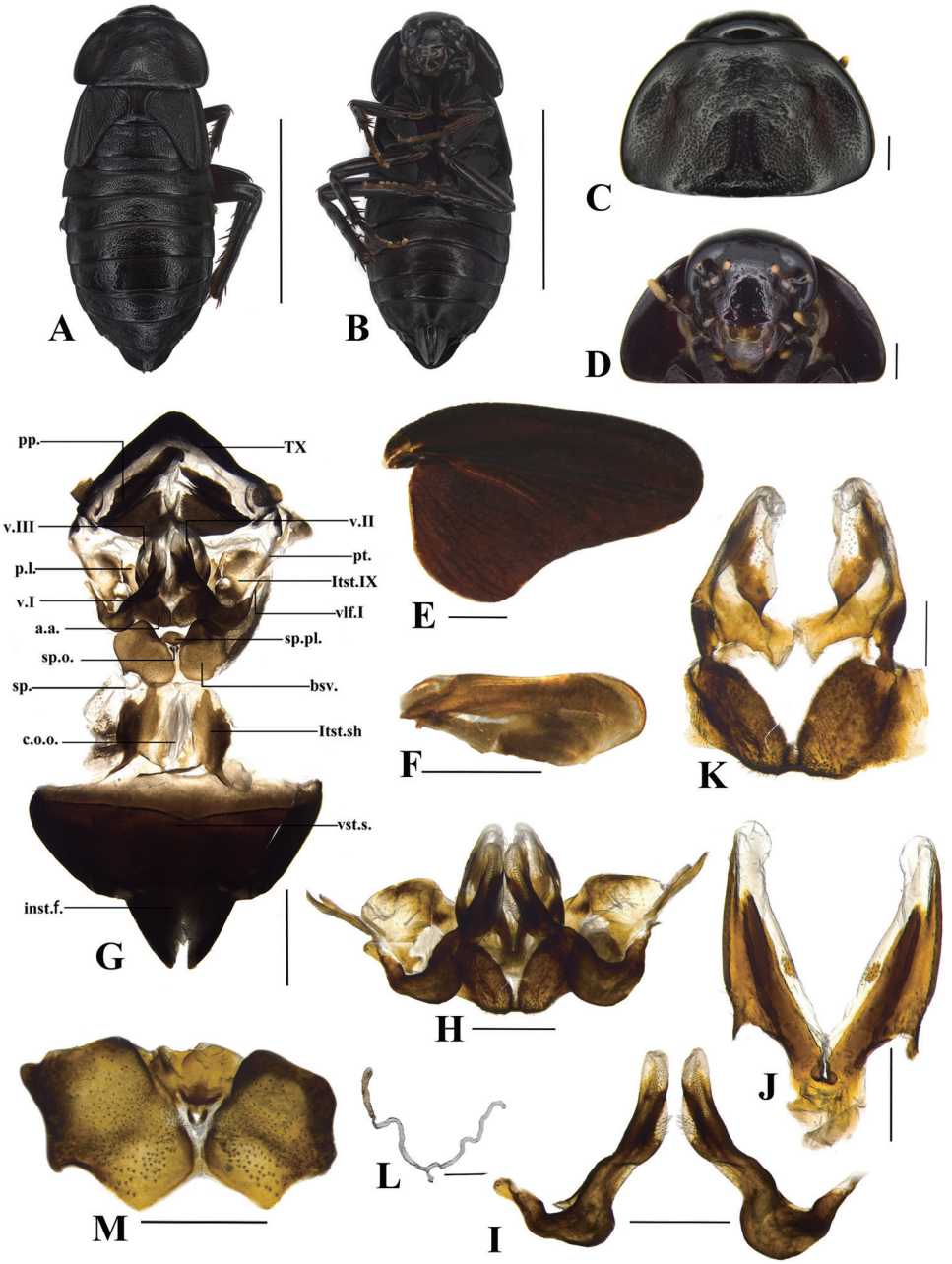

Figure 3. *Bundoksia longissima* Li & Che, sp. nov. (female) **A** dorsal view **B** ventral view **C** pronotum **D** head **E** tegmen **F** hind wing **G** genitalia, posterior view **H** valves and accessory sclerites **I** first valvule (v.I.) **J** second valvule (v.II.) **K** third valvule (v.III) and anterior arch **L** spermatheca (sp.) **M** basivalvula (bsv.); Scale bars: 10.0 mm (**A, B**); 1.0 mm (**C–I, M**); 0.5mm (**K, J, L**).

Figure 4. Habitats of *Bundoksia longissima* Li & Che, sp. nov. **A** female on tree trunk **B** male on tree leaf **C** mating on tree trunk (**A–C** from Jianfengling, Ledong, Hainan) **D** male on tree trunk (Xishuangbanna Tropical Botanical Garden, Yunnan) **E** nymph on the moss-covered ground (Daweishan, Pingbian, Yunnan). Photographed by Lu Qiu.

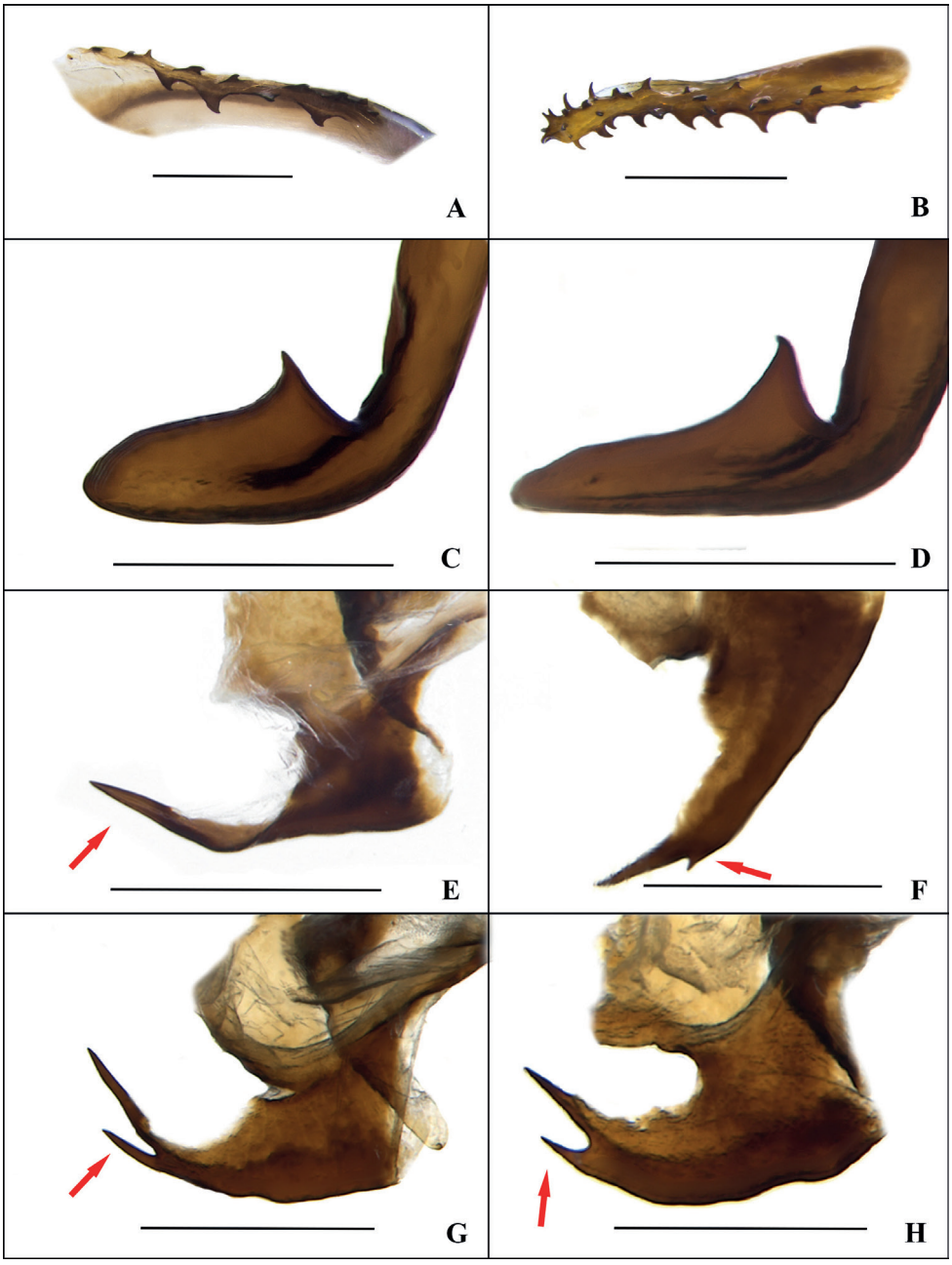

Figure 5. Variations on the male genitalia of *Bundoksia longissima* Li & Che, sp. nov. **A–B** L2d of left phallomere (**A** Hainan **B** Yunnan) **C–D** L3 of left phallomere (**C** Hainan **D** Yunnan) **E–H** R1 of right phallomere (**E** Hainan **F–H** Yunnan). Scale bars: 0.5 mm (**A–D**); 1.0 mm (**E–H**).

Female (Fig. 3A–M)**. Description. Colouration.** Body darker than male. (Fig. 3A, B).

Body thicker than the male. ***Head*.** Interocular space wider than the distance between ocelli, narrower than the distance between antennal sockets (Fig. 3D). **Thorax.** Pronotum nearly trapezoidal, punctuated, hind angles rounded, posterior margin almost straight (Fig. 3C). **Tegmina and wings.** Tegmina reduced, only reaching hind margin of first abdominal tergite; triangular, thickened, angles rounded (Fig. 3E); wings small lobed (Fig. 3F). **Legs.** Femur and tibia stronger than male. **Abdomen.** Hind margin of tergum X (TX) blunt. Paraprocts (pp.) wide and symmetrical, with the gap between pp. narrow. Subgenital plate divided at the end, the middle with distinct intersternal fold (inst.f.) (Fig. 3G). **Genitalia.** The base of first valve (v.I.) (Fig. 3I) more sclerotised and fused with first valvifer (vlf.I), vlf.I short. Laterosternite IX (ltst.IX) large and sheet-like, with outer margin hyaline, fused with paratergites (pt.). Second valve (v.II) small, slender, the base fused, connecting to third valve (v.III) by membrane (Fig. 3J). Posterior lobes of valvifer II (p.l.) sclerotised, cricoid, distal uneven and fused with ltst.IX. Third valve (v.III) large, the base sclerite convex, highly sclerotised (Fig. 3K). Anterior arch (a.a.) hip-shaped, the base deeply concave, with dense spines. Spermathecal plate (sp.pl.) slightly sclerotised, fused with basivalvula (bsv.). Spermathecal opening (sp.o.) located at the base of sp.pl., with small sclerites on two sides and highly sclerotised. Spermatheca (sp.) with two branches near the base and one branch with a rod-shaped enlargement distally (Fig. 3L). Basivalvulae (bsv.) developed and divided into two parts, with bristle-shaped spins (Fig. 3M). Laterosternal shelf (ltst.sh.) developed and symmetrical, extending backwards. Vestibular sclerite (vst.s.) unclear in outline; the base with a transverse sclerotised plate.

Nymph. Wingless, with light body colour and thin body size, compared to females. Other characteristics are similar to females (Fig. 4E).

Etymology. The scientific epithet is derived from the Latin word *longissimus*, referring to the long and narrow body.

Ecology. According to our collecting information, *Bundoksia longissima* is active at night to forage and mate. It is distributed mainly on tree trunks, a few on leaves (Fig. 4). Once frightened, the female will emit an acidic liquid (lemon smell), whose specific components have not been analysed.

Remarks. Samples from Yunnan show a range of slight morphological differences (mainly male genitalia) compared with Hainan and Guangxi: 1) the samples from Hainan and Guangxi with L2d base part with two-rows of serration (Fig. 5A), but the one from Yunnan with L2d base part with three-rows of serration (Fig. 5B); 2) the samples from Hainan and Guangxi with L3 unciform and apex blunt (Fig. 5C), but the Yunnan specimens with L3 unciform and apex slightly acuminate (Fig. 5D); 3) the samples from Hainan and Guangxi with R1 apically unforked (Fig. 5E), but three samples from Yunnan with R1 apically forked (Fig. 5 F–H). On the other hand, only the right hind-wing of the holotype was found as CuA with lattice-like, angular cross-veins, while the left hind-wing of the holotype and hind-wings of the remaining samples were simple and linear. In addition, all female individuals of *Bundoksia*

longissima sp. nov. appear to be highly conserved in terms of external morphology and genital structure (Fig. 3). Given this, it is difficult to distinguish them, based only on these slight variations in the shape of the male genitalia, so we temporarily consider them to be intraspecific variations in morphology.

Due to the similarities in the femoral armature, *Catara hainanica* described by Liu et al. (2017) might belong to *Bundoksia* or perhaps a closely-related genus. However, Liu et al. (2017) only described a single female nymph, so male adults of *C. hainanica* should be carefully examined to confirm the above hypothesis in the future.

Known distribution. China (Hainan, Guangxi, Yunnan, Guangdong Province)

Results

Relationships amongst different populations of *Bundoksia longissima* sp. nov., based on COI data

Pairwise genetic distances in *Bundoksia longissima* sp. nov. range from 0.0 to 7.2%, with an average of 3.35% (Suppl. material 3: Table S3). The largest distance 7.2% exists between Xishuangbanna Botanical Garden, Yunnan (YNBG1) and Jianfengling of Hainan (HIJFL1, HIJFL2, HIJFL7), Mt. Daming of Guangxi (GXDMM1). Combined with male and female morphological characteristics, including and genital structures (Fig. 2, 3), despite the large genetic distance and other existing slight variations, all samples studied here are still treated as one species, *Bundoksia longissima* sp. nov.

In the NJ tree, all individuals of *Bundoksia longissima* sp. nov. are clustered together to form a monophyletic group (Fig. 6A), solving the sexual dimorphism of *Bundoksia longissima* sp. nov. Samples from Guangxi are more related to those from Hainan than the others. Yunnan samples are split into several distinct groups in the NJ tree, which corresponds with the types of variations on R1. These groups represent different geographical locations from Yunnan Province.

Thirteen haplotypes were recorded from 21 *COI* sequences of *Bundoksia longissima* sp. nov. (Fig. 6B), of which, four haplotypes (A1, A2, B1, B2) were from Hainan, two (C1, D1) from Guangxi and seven (E1, E2, E3, F1, G1, H1, I1) from Yunnan. The haplotype network showed that there were no shared haplotypes amongst different geographic populations. Haplotypes from Yunnan except E1, E2, E3 and G1, were connected via at least 18 mutational steps. Haplotypes from Hainan were well connected via a maximum of five mutations.

Taxonomic affinities of *Bundoksia* inferred from two phylogenetic analyses

Our Maximum Likelihood and Bayesian Inference analyses yielded almost identical topologies, based on the concatenated dataset (Fig. 7, Suppl. material 4: Fig. S1). In our study, Blattidae was recovered to be monophyletic with high support values (MLB = 100, BPP = 1) (Fig. 7). Two major lineages of Blattidae, Polyzosteriinae and

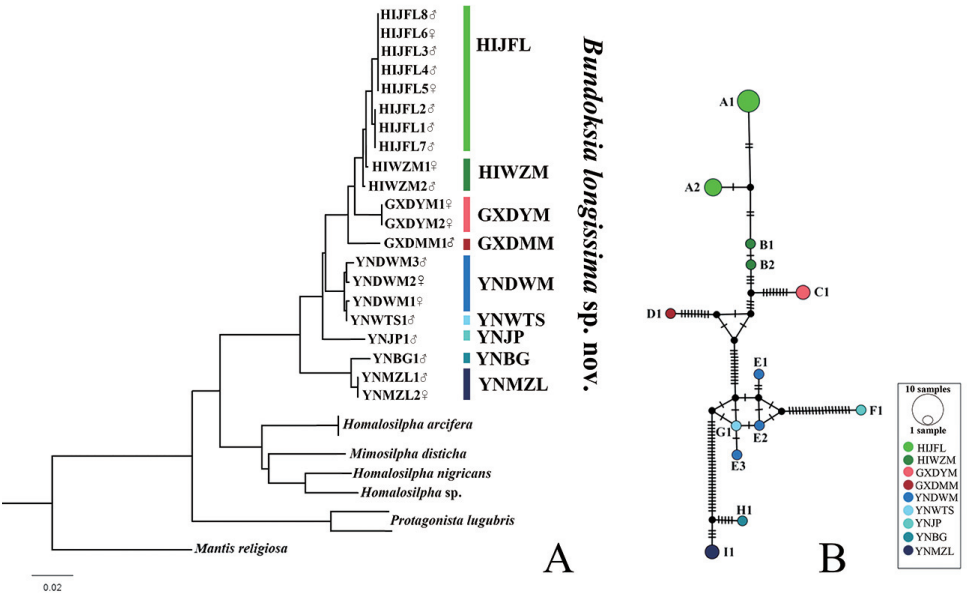

Figure 6. Neighbour-Joining (NJ) tree and haplotype network structure, based on COI data of *Bundoksia longissima* sp. nov. **A** NJ tree **B** haplotype network **A–B** different colours represent different populations and the black circles represent missing haplotypes in the mutation process. The colour of all circles of the NJ tree and haplotype network is consistent. More details of abbreviation of locations are included in Suppl. material 1: Table S1.

Archiblattinae + Blattinae, were revealed in both analyses. According to our inferred trees, both Archiblattinae and Blattinae were paraphyletic. *Bundoksia longissima* sp. nov. was found to be the sister group of *Homalosilpha* + *Mimosilpha* with high support (MLB = 100, BPP = 1). In addition, *Bundoksia longissima* sp. nov., together with other Blattinae and Archiblattinae members, form a monophyletic group with strong support, as the sister group of Polyzosteriinae.

Discussion

The haplotype network diagram (Fig. 6B) showed that there was no shared haplotype amongst geographical populations and suggested that the Hainan haplotypes are relatively less diverse, while the haplotypes from Yunnan showed more genetic diversification. In addition, the pairwise genetic distances amongst samples in Yunnan varied greatly from 0 to 7.2%. The NJ tree showed the same result, especially samples from Yunnan forming several distinct groups. We suggest that the larger genetic distance and morphological differences might be related to the natural barriers (mountains or rivers in Yunnan), which reduce gene communication amongst populations, which might lead to a high genetic diversity.

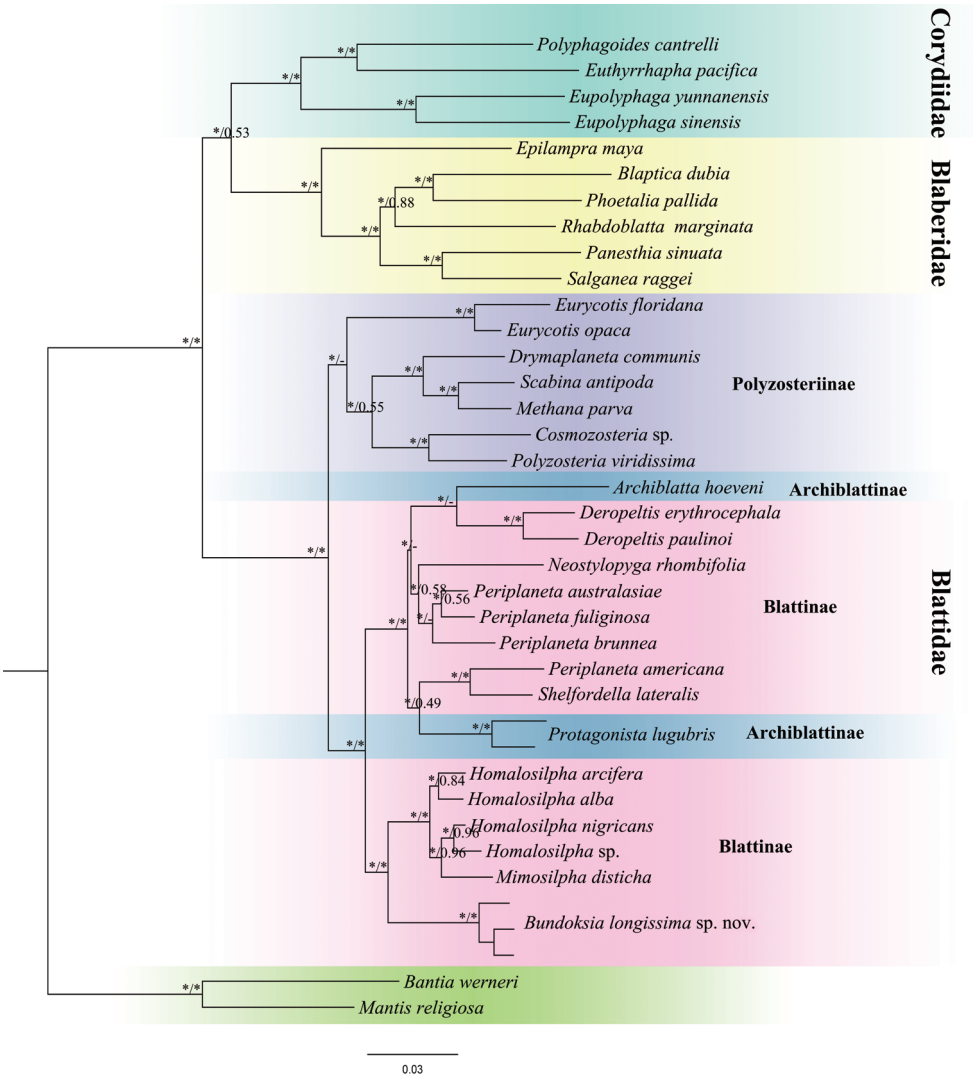

Figure 7. Maximum Likelihood (ML) tree of cockroaches inferred from four mitochondrial markers *12S* rRNA, *16S* rRNA, *COI, COII* and two nuclear markers *28S* rRNA, *18S* rRNA. Branch support labels are as follows: bootstrap supports of the Maximum-Likelihood tree/Bayesian posterior probabilities of the Bayesian tree; (*) indicate the branch label of given analysis is maximal (i.e. MLB = 100 or BPP = 1.0), (-) means the node is absent for the given analysis.

Mimosilpha and *Homalosilpha* are closely related to *Bundoksia longissima* sp. nov. according to our phylogenetic reconstruction, which could be distinguished from *B. longissima* sp. nov. by the flattened tibiae, the distinct femoral armament and the maculae bearing in the pronotum. In previous works, the subfamilies Archiblattinae and Blattinae were recovered as monophyletic (Inward et al. 2007; Djernaes et al. 2015; Legendre et al. 2015) or paraphyletic (Liao et al. 2021). According to our inferred trees,

Archiblattinae and Blattinae are paraphyletic. Archiblattinae is embedded in Blattinae, indicating Archiblattinae might be a synonym of Blattinae. Lucañas (2021) also believed that the genus *Bundoksia* not only possesses the characteristics of the subfamily Archiblattinae (the distinct femoral armament, meso- and metafemur sparsely armed with dissimilarly-sized spines), but also those of Blattinae (the smooth pronotum and flattened tibiae). Wang et al. (2016) discovered that the male genitalia of Archiblattinae was similar to that of Blattinae. Therefore, in follow-up works, we need more molecular data and morphological evidence to solve the relationship between Archiblattinae and Blattinae and then settle the subfamilial status of the genus *Bundoksia*.

Acknowledgements

We thank all collectors in this paper for their efforts in collecting specimens. We especially thank Wenbo Deng for professional suggestions and we also thank Dr. John Richard Schrock (Department of Biological Sciences, Emporia State University) for revising the English and Dr. Lu Qiu for providing the photos. This study is supported by the National Natural Science Foundation of China (Nos. 31772506, 32070468, 32170458).

References

Djernæs M, Klass KD, Eggleton P (2015) Identifying possible sister groups of Cryptocercidae + Isoptera: a combined molecular and morphological phylogeny of Dictyoptera. Molecular Phylogenetics and Evolution 84: 284–303. https://doi.org/10.1016/j.ympev.2014.08.019

Inward D, Beccaloni G, Eggleton P (2007) Death of an order: a comprehensive molecular phylogenetic study confirms that termites are eusocial cockroaches. Biology Letters 3: 331–335. https://doi.org/10.1098/rsbl.2007.0102

Katoh K, Standley DM (2013) MAFFT multiple sequence alignment software version 7: improvements in performance and usability. Molecular Biology and Evolution 30(4): 772–780. https://doi.org/10.1093/molbev/mst010

Kimura MA (1980) A simple method for estimating evolutionary rates of base substitutions through comparative studies of nucleotide sequences. Journal of Molecular Evolution 16: 111–120. https://doi.org/10.1007/BF01731581

Kumar NP, Rajavel AR, Natarajan R, Jambulingam P (2007) DNA barcodes can distinguish species of Indian mosquitoes (Diptera: Culicidae). Journal of Medical Entomology 44: 1–7. https://doi.org/10.1093/jmedent/41.5.01

Lanfear R, Calcott B, Ho SY, Guindon S (2012) PartitionFinder: combined selection of partitioning schemes and substitution models for phylogenetic analyses. Molecular Biology and Evolution 29(6): 1695–1701. https://doi.org/10.1093/molbev/mss020

Legendre F, Nel A, Svenson GJ, Robillard T, Pellens R, Grandcolas P (2015) Phylogeny of Dictyoptera: dating the origin of cockroaches, praying mantises and termites with molecular

data and controlled fossil evidence. PLoS ONE 10: e0130127. https://doi.org/10.1371/journal.pone.0130127

Leigh JW, Bryant D (2015) POPART: full-feature software for haplotype network construction. Methods in Ecology and Evolution 6(9): 1110–1116. https://doi.org/10.1111/2041-210X.12410

Liao SR, Wang YS, Jin DT, Chen R, Wang ZQ, Che YL (2021) Exploring the relationship of *Homalosilpha* and *Mimosilpha* (Blattodea, Blattidae, Blattinae) from a morphological and molecular perspective, including a description of four new species. PeerJ 9: e10618. https://doi.org/10.7717/peerj.10618

Liu XW, Zhu WB, Dai L, Wang HQ (2017) Cockroaches of Southeastern China. Henan Science and Technology Press, Zhengzhou, 228 pp.

Li M, Zhao QY, Chen R, He JJ, Peng T, Deng WB, Che YL, Wang ZQ (2020) Species diversity revealed in *Sigmella* Hebard, 1929 (Blattodea, Ectobiidae) based on morphology and four molecular species delimitation methods. PLoS ONE 15: e0232821. https://doi.org/10.1371/journal.pone.0232821

Li TT, Liu DX, Qiu DY, Yue QY (2020) Two new species of *Episymploce* Bey-Bienko, 1950 (Blattodea, Ectobiidae, Blattellinae) from China. ZooKeys 954: 31–46. https://doi.org/10.3897/zookeys.954.49738

Li XR, Zheng YH, Wang CC, Wang ZQ (2018) Old method not old-fashioned: parallelism between wing venation and wing-pad tracheation of cockroaches and a revision of terminology. Zoomorphology 137: 519–533. https://doi.org/10.1007/s00435-018-0419-6

Li Y, Wang ZQ, Che YL (2013) A comparative study on the oothecae and female genitalia of seven species of Blattodea. Zoological Systematics 38: 16–26.

Lucañas CC (2021) *Bundoksia* gen. nov. (Dictyoptera: Blattodea: Blattidae), a new sexually dimorphic cockroach from the Philippines. Journal of Natural History 55: 1009–1020. https://doi.org/10.1080/00222933.2021.1928317

McKittrick FA (1964) Evolutionary studies of cockroaches. Cornell University Agricultural Experiment Station Memoir 389: 1–197.

Ronquist F, Teslenko M, van der Mark P, Ayres DL, Darling A, Höhna S, Larget B, Liu L, Suchard MA, Huelsenbeck, JP (2012) MrBayes 3.2: efficient Bayesian phylogenetic inference and model choice across a large model space. Systematic Biology 61: 539–542. https://doi.org/10.1093/sysbio/sys029

Roth LM (1994) New Queensland cockroaches of *Macrocerca* Hanitsch and *Periplaneta* Burmeister (Blattidae). Memoirs of the Queensland Museum 35: 225–233.

Roth LM (2003) Systematics and phylogeny of cockroaches (Dictyoptera: Blattaria). Oriental Insects 37: 1–186. https://doi.org/10.1080/00305316.2003.10417344

Shelford R (1910) Orthoptera Fam. Blattidae Subfam. Blattinae (= Periplanetinae). In: Wytsman P (Ed.) Genera Insectorum. Belgique: 1–27.

Shelford R (1911) Descriptions of some new species of Blattidae. The Annals and Magazine of Natural History 8(8): 1–13. https://doi.org/10.1080/00222931108692992

Stamatakis A, Hoover P, Rougemont J (2008) A rapid bootstrap algorithm for the RAxML web servers. Systematic Biology 57: 758–771. https://doi.org/10.1080/10635150802429642

Wang CC, Wang ZQ, Che YL (2016) *Protagonista lugubris*, a cockroach species new to China and its contribution to the revision of genus *Protagonista*, with notes on the taxonomy of Archiblattinae (Blattodea, Blattidae). ZooKeys 574: 57–73. https://doi.org/10.3897/zookeys.574.7111

Wang ZQ, Che YL (2010) The genus *Scalida* Hebard (Blattaria: Blattellidae, Blattellinae) in China. Zootaxa 2502(1): 37–46. https://doi.org/10.11646/zootaxa.2502.1.3

Xia XH (2018) DAMBE7: New and improved tools for data analysis in molecular biology and evolution. Molecular Biology and Evolution 35: 1550–1552. https://doi.org/10.1093/molbev/msy073

Yang R, Wang Z, Zhou Y, Wang Z, Che Y (2019) Establishment of six new *Rhabdoblatta* species (Blattodea, Blaberidae, Epilamprinae) from China. ZooKeys 851: 27–69. https://doi.org/10.3897/zookeys.851.31403

Supplementary material 1

Table S1

Authors: Yong Li, Xinxing Luo, Jiawei Zhang, Zongqing Wang, Yanli Che

Data type: xlsx file

Explanation note: Samples used in Neighbor joining (NJ) tree and haplotype network: GenBank accession numbers, number of location, sample ID, sample localities and data and voucher numbers.

Link: https://doi.org/10.3897/zookeys.1085.72927.suppl1

Supplementary material 2

Table S2

Authors: Yong Li, Xinxing Luo, Jiawei Zhang, Zongqing Wang, Yanli Che

Data type: xlsx file

Explanation note: Specimen used in molecular phylogenetic analysis (ML and BI), with details of family, sample id, collecting localities, references and GenBank accession numbers.

Link: https://doi.org/10.3897/zookeys.1085.72927.suppl2

Supplementary material 3

Table S3

Authors: Yong Li, Xinxing Luo, Jiawei Zhang, Zongqing Wang, Yanli Che

Data type: xlsx file

Explanation note: Pairwise genetic distances with standard errors of Bundoksia longissima sp. nov. calculated by using K2P model using cytochrome oxidase subunit I (COI) gene sequences in MEGA. Bold text denotes the standard errors of distances and black denotes pairwise genetic distances.

Link: https://doi.org/10.3897/zookeys.1085.72927.suppl3

Supplementary material 4

Figure S1

Authors: Yong Li, Xinxing Luo, Jiawei Zhang, Zongqing Wang, Yanli Che

Data type: jpg file

Link: https://doi.org/10.3897/zookeys.1085.72927.suppl4

ZooKeys 1085: 165–182 (2022)
doi: 10.3897/zookeys.1085.76853
https://zookeys.pensoft.net

RESEARCH ARTICLE

A peer-reviewed open-access journal
ZooKeys
Launched to accelerate biodiversity research

Integrative taxonomy reveals overlooked cryptic diversity in the conifer feeding *Batrachedra pinicolella* (Zeller, 1839) (Lepidoptera, Batrachedridae)

Kai Berggren[1], Leif Aarvik[2], Peter Huemer[3], Kyung Min Lee[4,5], Marko Mutanen[5]

1 *Bråvann terrasse 21, NO-4624 Kristiansand, Norway* **2** *Natural History Museum, University of Oslo, P.O. Box 1172 Blindern, NO-0318 Oslo, Norway* **3** *Tiroler Landesmuseen Betriebgsges.m.b.H., Sammlungs- und Forschungszentrum, Naturwissenschaftliche Sammlungen, Krajnc-Str. 1, A-6060 Hall in Tirol, Austria* **4** *Zoology Unit, Finnish Museum of Natural History, University of Helsinki, Finland* **5** *Ecology and Genetics Research Unit, University of Oulu, Finland*

Corresponding author: Peter Huemer (p.huemer@tiroler-landesmuseen.at)

Academic editor: Mark Metz | Received 21 October 2021 | Accepted 20 January 2022 | Published 8 February 2022

http://zoobank.org/0ED94C60-8235-413B-99F5-F3D52F2E66D5

Citation: Berggren K, Aarvik L, Huemer P, Lee KM, Mutanen M (2022) Integrative taxonomy reveals overlooked cryptic diversity in the conifer feeding *Batrachedra pinicolella* (Zeller, 1839) (Lepidoptera, Batrachedridae). ZooKeys 1085: 165–182. https://doi.org/10.3897/zookeys.1085.76853

Abstract

During efforts to generate DNA barcodes for all European Lepidoptera, *Batrachedra pinicolella* (Zeller, 1839) was found to comprise two genetically distinct clusters. Morphological investigation and results from two nuclear markers and ddRAD sequencing furthermore support the existence of two distinct taxa which we treat as two separate species, *B. pinicolella* and *B. confusella* **sp. nov.** A lectotype for *B. pinicolella* is designated. Available data indicate that the biology of both species also differs, with *Picea abies* (L.) Karsten as a proved host-plant for *B. pinicolella* and *Pinus sylvestris* L. for *B. confusella* **sp. nov.** Both species are mainly distributed on the European continent with *B. pinicolella* occurring in boreal parts of North and Central Europe and introduced to Canada, reflecting a boreo-montane distribution pattern. *Batrachedra confusella* **sp. nov.** is more widely distributed in temperate Northern and Central Europe.

Keywords

Boreo-montane, ddRAD sequencing, DNA barcoding, Europe, Gelechioidea, new species, nuclear genes, Pinaceae

Introduction

During the last two decades, aided by DNA barcoding, several cryptic species have been discovered among European Lepidoptera (Huemer and Hebert 2011; Mutanen et al. 2012a, 2012b, 2020; Hernández-Roldán et al. 2016; Zlatkov and Huemer 2017, 2019; Huemer and Karsholt 2018; Huemer 2020; Wikström et al. 2020). The first suspicion that the widespread European pine feeding moth *Batrachedra pinicolella* (Zeller, 1839) consists of more than one species arose after the publication of the monograph of the European Momphidae s.l. (Koster and Sinev 2003). When the first author compared the genitalia figures on page 53 and 54 with the figures on page 253 and 319, discrepancies between these illustrations were observed. Independently within the framework of national barcoding initiatives in Norway and Finland as well as a supranational barcoding campaign in the Alps, we found striking genetic diversity in *B. pinicolella* indicating potential cryptic diversity (Huemer and Hebert 2016). Following this discovery, examination of morphological characters of representatives of the two clusters was made and additional molecular markers studied. Results confirm the presence in Europe of two separate species confused under the name *Batrachedra pinicolella*, one feeding on *Pinus* and the other on *Picea*.

Material and methods

DNA barcodes refer to a 658 base-pair long fragment of the mitochondrial cytochrome c oxidase subunit 1 (CO1). Legs from 49 specimens of the involved species pair were prepared according to the prescribed standards and successfully processed at the Canadian Centre for DNA Barcoding (CCDB, Biodiversity Institute of Ontario, University of Guelph) to obtain DNA barcodes and using the standard high-throughput protocol described in deWaard et al. (2008). These sequences are supplemented by 16 DNA barcodes belonging to the two further known congeneric species of the European fauna. All sequences were submitted to GenBank, and further details including complete voucher data and images can be accessed in the public dataset "*Batrachedra pinicolella* species group [DS-BATRAPIN]" in the Barcode of Life Data Systems (BOLD; Ratnasingham and Hebert 2007). Degrees of intra- and interspecific variation of DNA barcode fragments were calculated under the Kimura 2 parameter model of nucleotide substitution using analytical tools of BOLD systems v. 4.0. (http://www.boldsystems.org). A neighbor-joining tree of DNA barcode data was constructed using MEGA 6 (Tamura et al. 2013) under the Kimura 2 parameter model for nucleotide substitutions.

We attempted to obtain data of six nuclear genes, wingless, *CAD* (carbamoyl-phosphate synthetase), *EF-1a* (elongation factor 1 alpha), *MDH* (malate dehydrogenase), *RpS5* (ribosomal protein S5), and *IDH* (isocitrate dehydrogenase), for specimens rep-

resenting the two clusters of *B. pinicolella*. Five of these specimens represented BIN AAF0077 and three BIN AAF0078. Nuclear sequences were obtained for both clusters only for two of these genes, *EF-1a* and *MDH*. A few sequences of *CAD* and wingless were also recovered, but representing of only one of the BINs, and were therefore not considered in this study. We also studied the presence of *Wolbachia* bacteria in all eight specimens using *ftsZ* ja *wsp* markers (Zhou et al. 1998; Baldo et al. 2006). DNA extraction, PCR, and sequencing were conducted at the university of Oulu using standard Sanger sequencing protocols as outlined in Wahlberg and Wheat (2008), with slight modifications for example for purification of sequencing reactions. Sequencing was performed with an ABI 3730 capillary sequencer. Nuclear sequences were deposited in the Voseq database (Peña and Malm 2012). Genetic distances were calculated under Kimura 2 parameter model in MEGA 6 (Tamura et al. 2013). Nuclear sequences are available in GenBank under the accession numbers OM296685–OM296699. Genetic divergences between all four European species of *Batrachedra* were visualized with a neighbor-joining tree as conducted under Kimura 2 parameter model in MEGA 6 (Tamura et al. 2013).

We used DNA aliquots that were extracted at CCDB for ddRAD-seq library preparation. The quantity of DNA extracts was checked using PicoGreen kit (Molecular Probes). The ddRAD library was implemented following protocols in Lee et al. (2018) with few modifications: digestion with *Pst*I and *Msp*I, and the size distribution measurement with Bioanalyzer (Agilent Technologies). The de-multiplexed fastq data are archived in the NCBI SRA: PRJNA725165. Initial filtering steps, SNP calling, and alignment were carried out using *ipyrad* v.0.9.11 (Eaton and Overcast 2020). The following parameters were changed from the default settings: restriction overhang to *TGCAG*, *CGG*, minimum depth for majority-rule base calling to 3, clustering threshold to 0.88, and minimum number of samples with a given locus to 3.

To infer maximum likelihood (ML) tree, we used IQ-TREE (Nguyen et al. 2015), and branch support bootstrap values were calculated with ultrafast bootstrap (UFBoot, 1000 bootstraps). Prior to analyses, the best fitting mutational model was obtained through ModelFinder (Kalyaanamoorthy et al. 2017) based on Bayesian information criterion, which selected "TVM+F+I" for ddRAD data. The ML tree generated using FigTree v.1.4.2 (Rambaut 2015) and modified using Adobe Illustrator CS6. To investigate genetic variation between individuals, we inferred population clustering with admixture from SNP frequency data using STRUCTURE (Pritchard et al. 2000). Ten replicates were run at each value of K between 1 and 3. Each run had a burn-in of 50K generations followed by 500K generations of sampling. We used StrAuto to automate Structure processing of samples (Chhatre and Emerson 2017). Replicates were permuted in CLUMPP (Jakobsson and Rosenberg 2007) according to the ad hoc ΔK statistics (Evanno et al. 2005), and the results were visualised using DISTRUCT (Rosenberg 2004).

Dissections of genitalia followed Robinson (1976). Photos of genitalia were taken through a Leica DM 6000B microscope using a Leica DFC 420 digital camera.

Depository of examined material

KBE	Collection of Kai Berggren, Kristiansand, Norway
NHMO	Natural History Museum, University of Oslo, Norway
NHMUK	The Natural History Museum, London, U.K.
TLMF	Tiroler Landesmuseum Ferdinandeum, Innsbruck, Austria
ZMUC	Zoological Museum, Natural History Museum of Denmark, Copenhagen, Denmark
ZMUO	Zoological Museum, University of Oulu, Finland

Type material and nomenclature

Zeller (1839) described *Cosmopteryx pinicolella* from a series collected from *Pinus* near Glogau, "häufig bei Gl. im Juni und Juli an Kiefern" [common near Gl. = Glogau in June and July on pine], and another series collected near Salzbrunn, "noch häufiger bei Salzbrunn an Tannen" [more common near [Bad] Salzbrunn on fir]. Glogau (now Glógow) is situated in the south-western present-day Poland, and Bad Salzbrunn (now Szczawno-Zdrój) in Silesia (Poland) near the Czech border. Two potential syntypes of *pinicolella* are present in NHMUK where the collection of Zeller is preserved (David Lees, email 29 August 2019). One is without abdomen and has no locality label attached to it, and thus syntype status is uncertain. The other specimen is a male in good condition, labelled "Salzbrunn 19.7.[18]38". We select the male from Salzbrunn as lectotype (Fig. 1) in order to fix the identity of the species and conserve stability of nomenclature. Though we have not been able to dissect this specimen, it can be identified without any doubt. The reasons for this are that it has a definite (type) locality and an indication to the alleged host tree. Zeller (1839) stated to have collected syntypes from Salzbrunn on "Tannen". In Zeller's work from 1839 "Tanne" (*Abies alba* in current sense) is mentioned several times, whereas "Fichte" (*Picea abies*) is completely missing. Even species considered monophagous on "Fichte", such as *Chionodes electella* (Zeller, 1839), are attributed to "Tanne". Our hypothesis is that "Tanne" sensu Zeller (1839) is identical with *Picea abies*. This is also supported by, for example, the later description of *Pammene ochsenheimeriana* (Lienig & Zeller, 1846) (known from *Picea* and *Pinus* but not from *Abies*). Also, in this description it is stated "im Mai auf Tannen" (Lienig and Zeller 1846). In the German language *Picea* is also called "Rottanne" and *Abies* "Weißtanne". Our conclusion is that the name *B. pinicolella* (Zeller, 1839) must be attributed to the *Picea*-feeder and not to the *Pinus*-feeder, whereas *Abies alba* seems an exceptional hostplant of this group with only one proven record of four larva collected in Slovakia (Patočka 1960). We are aware that attribution of the name *B. pinicolella* to the *Picea*-feeding taxon may cause confusion, but one should bear in mind that at the time of the description of *B. pinicolella* conifer trees currently in *Pinus*, *Picea*, *Abies*, and even *Larix* were all listed in one genus, *Pinus* (Hausmann 1852). Thus, the name *pinicolella* refers to the family Pinaceae rather than to the present genus *Pinus*. Furthermore, even in current European literature the name *B. pinicolella* is sometimes already expressively combined with the species from *Picea abies* whereas *Pinus sylvestris*

Figures 1–4. Adults and labels of *Batrachedra* **1** lectotype *Cosmopteryx pinicolella* Zeller, 1839 (NHMUK; copyright Trustees of the Natural History Museum, London) **2** labels of lectotype **3** holotype of *Batrachedra confusella* sp. nov. **4** adult of *Batrachedra pinicolella*. Scale: 10 mm.

is considered as doubtful hostplant which requires confirmation (Emmet and Langmaid 2002). Following the selection of a lectotype from *Picea abies* there is no synonym of *B. pinicolella* that could potentially be used for the species feeding on *Pinus sylvestris* (Koster and Sinev 2003) and, hence, this species is without name.

Results

***Batrachedra confusella* sp. nov.**
http://zoobank.org/AE37C32C-7D9A-4436-AAB2-339F486FF239
Figs 3, 5, 6, 9

Material. ***Holotype*** 1♂ Ø, Moss: Rygge, Sildebauen, 59.3268°N; 10.7101°E; 9.vii.1980; L. Aarvik leg.; NHMO prep. 3943 (NHMO). ***Paratypes*** Finland 1♂ A, Sund; 14.vii.2007; M. Mutanen leg.; L. Aarvik prep. 2015.022; BOLD sample ID: MM22065; ZMUO. 1♂ PPe, Oulu; 7.vii.2011; M. Mutanen leg.; L. Aarvik prep. 2015.023; BOLD sample ID: MM21051; ZMUO. 1♀ U, Kirkkonummi; 11.vii.2007; M. Mutanen leg.; L. Aarvik prep. 2015.025; BOLD sample ID: MM06674; ZMUO.

Norway 1♂ AAY, Arendal: Havsøy; 10.vii.2015; K. Berggren leg.; BOLD sample ID: NHMO-DAR-12592; KBE. 1♀ AAY, Arendal: Tromøy, Skottjern; 22.vii.1983; K. Berggren leg.; KBE prep. 13534; KBE; 1♂, same locality and date; S. Svendsen leg.; NHMO prep. 2833; NHMO. 1♂ AAY, Arendal: Siring; 25–30.vi.2002; S.A. Bakke leg., NHMO prep. 3936; NHMO. 1♀ AAY, Grimstad: Søm; 8.vii.2017; K. Berggren leg., BOLD sample ID: NHMO-DAR-13683; KBE. 1♀ AAY, Grimstad: Søm; 24.vii.2017; K. Berggren leg.; BOLD sample ID: NHMO-DAR-14041; KB. 1♂ AAY, Lillesand: Lillesand; 7.vii.1984; K. Berggren leg.; KBE prep. 13515; KBE. 1♂ AAY, Lillesand: Svinøya; 29.vii.2005, K. Berggren leg.; KBE prep. 13520; KBE. 1♂ AAY Tvedestrand: Lyngør, Sønnerstrand; 30.vi–4.vii.2013; K. Berggren & B. Johansen leg.; KBE prep. 13524; KBE. 1♂ AK, Asker: Brønnøya; 11.vii.1981; K. Berggren leg.; KBE prep. 13528; KBE. 1♀ AK, Bærum: Ostøya; 10.vii.1984; L. Aarvik leg.; NHMO prep. 2887; NHMO. 1♂ AK, Oslo: Bleikøya; 14.vii.2009; K. Berggren & A. Endrestøl leg.; BOLD sample ID: NHMO-DAR-5192; KBE. 1♀ AK, Oslo: Bygdøy, Rodeløkka; 4–19.vii.2016; A. Endrestøl & K. Berggren leg.; KBE prep. 13536; KBE. 1♂ AK, Oslo: Bygdøy, Rodeløkka; 4–19.vii.2016; A. Endrestøl & K. Berggren leg.; KBE prep. 13532; KBE. 1♂ AK, Oslo: Ekebergskråninga; 25.vi.2008; L. Aarvik leg.; NHMO prep. 2835; BOLD sample ID: NHMO-08107; NHMO. 1♀ AK, Ås: Ås; 30.vii.1982; L. Aarvik leg.; L. Aarvik prep. 2725; NHMO. 1♀ HES, Åsnes: Sønsterud; 16–25.vii.1998; L. Aarvik & A. Bakke leg.; NHMO prep. 2832; NHMO. 1♀ TEY, Kragerø: Jomfruland, Øytangen; 16.vii.2003; L. Aarvik leg.; NHMO prep. 3937; NHMO. 1♂ TEY, Porsgrunn: Sandøya; 10.vii.2003; R. Voith leg.; KBE prep. 13521; KBE. 1♂ VAY, Kristiansand: Augland; 8.vii.1985; K. Berggren leg.; KBE prep. 13529; KBE. 1♂ VAY, Kristiansand: Bråvann; 14.vii.2015; K. Berggren leg., BOLD sample ID: NHMO-DAR-12591; KBE. 1♂ VAY, Kristiansand: Bråvann; 17.vii.2017; K. Berggren leg., BOLD sample ID: NHMO-DAR-14027; KBE. 1♀ VAY, Kristiansand: Bråvann; 10.viii.2012; K. Berggren leg.; KBE prep. 13537; KBE. 1♀ VAY, Kristiansand: Bråvann; 26.viii.2016; K. Berggren leg.; KBE prep. 13538; KBE. 1♂ VAY, Kristiansand: Bråvann; 26.viii.2016; K. Berggren leg.; BOLD sample ID: NHMO-DAR-12591; KBE prep. 13538; KBE. 1♂ VAY, Kristiansand: Flekkerøy, Belteviga; 28.vii.1999, K. Berggren leg.; KBE prep. 6141; KBE. 1♀ VAY, Kristiansand: Flek-

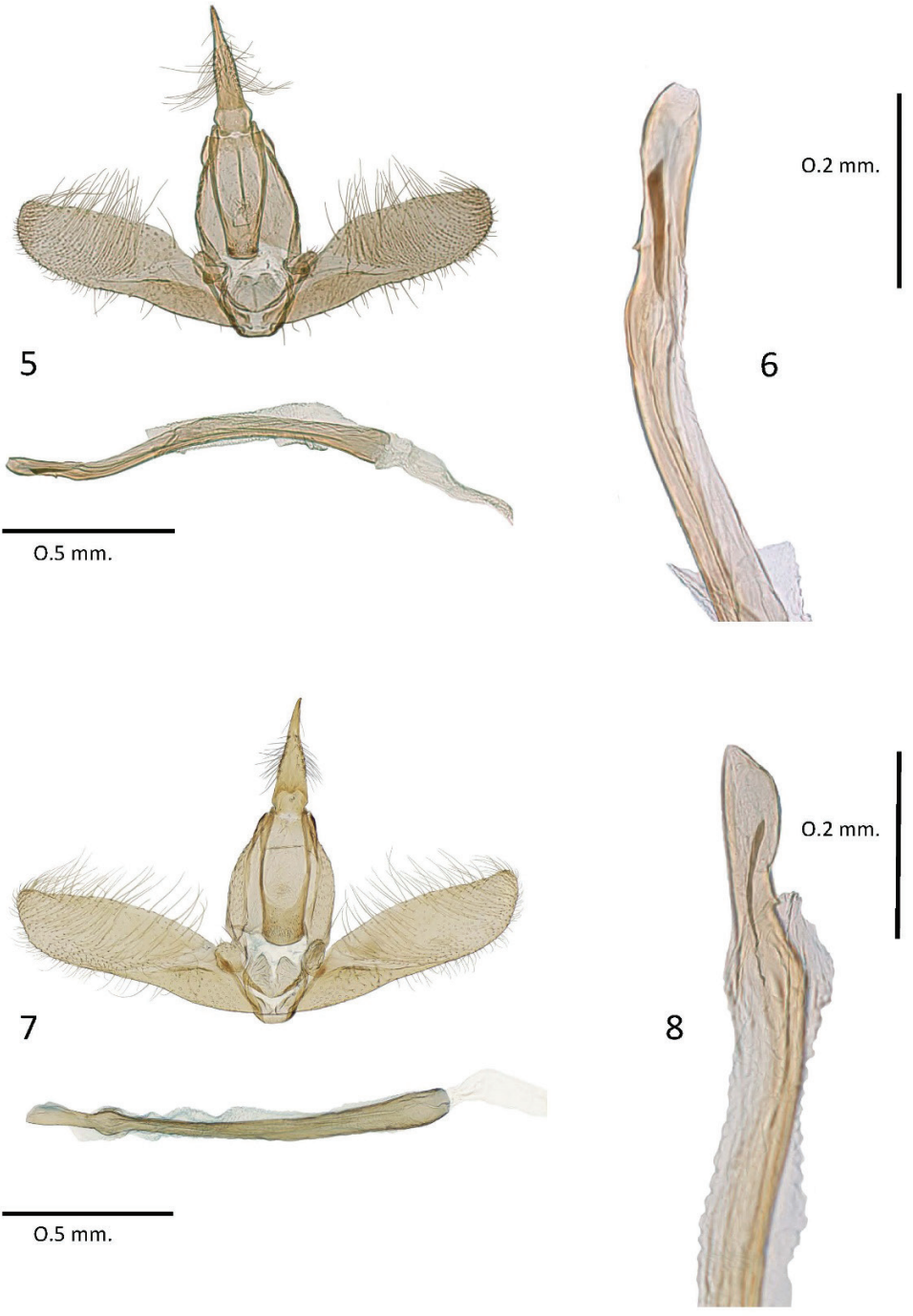

Figures 5–8. Male genitalia of *Batrachedra* **5** *B. confusella* sp. nov., genitalia slide NHMO 3899 **6** *B. confusella* sp. nov., distal end of phallus, genitalia slide NHMO 3899 **7** *B. pinicolella*, genitalia slide NHMO 3891 **8** *B. pinicolella*, distal end of phallus, genitalia slide NHMO 3892.

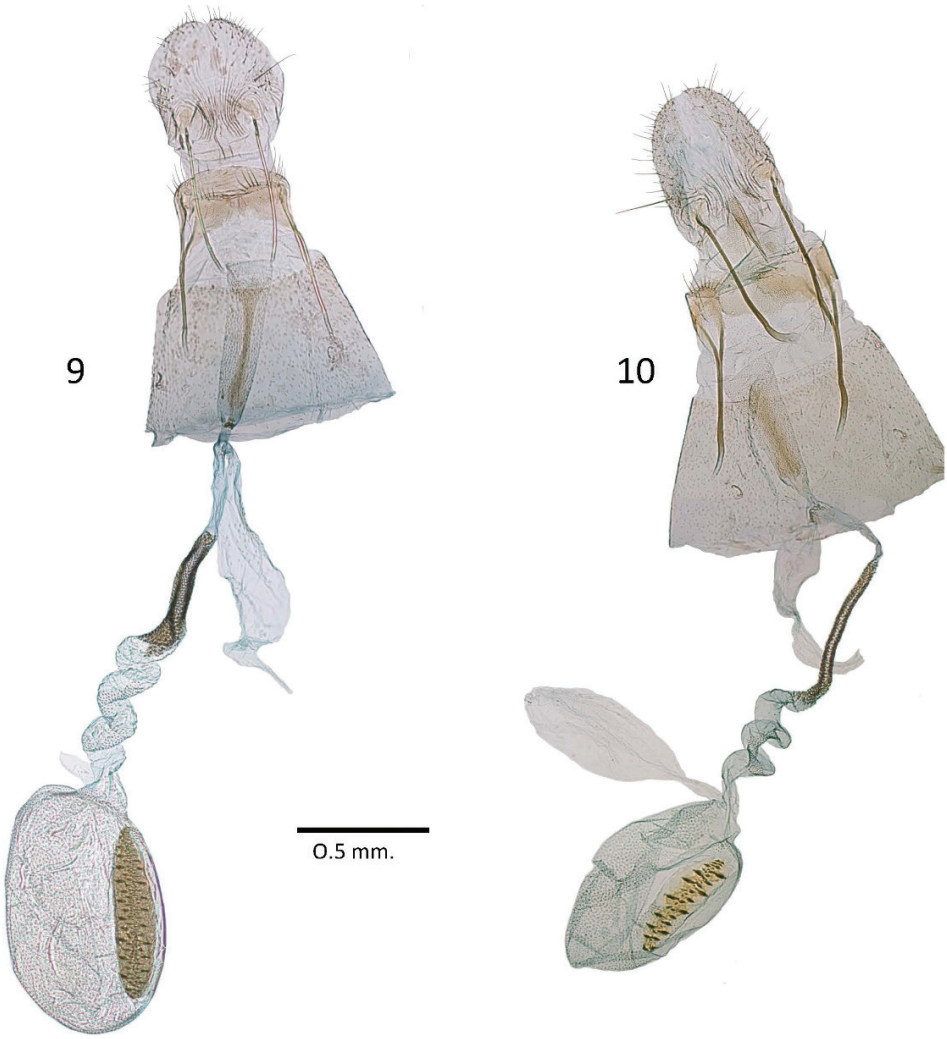

Figures 9–10. Female genitalia of *Batrachedra* **9** *B. confusella* sp. nov., genitalia slide NHMO 3937 **10** *B. pinicolella*, genitalia slide NHMO 3961.

kerøy, Belteviga; 16–23.vii.2000, K. Berggren leg.; KBE prep. 6196; KBE. 1♀ VAY, Kristiansand: Nedre Timenes; 7–14.vii.2001, K. Berggren leg.; KBE prep. 101696; KBE. 1♂ VAY, Kristiansand: Nedre Timenes; 28.vii.2015, K. Berggren leg.; KBE prep. 13533; KBE. 1♀ VAY, Kristiansand: Nedre Timenes; 31.vii.2017, K. Berggren leg.; KBE prep. 13535; KBE. 1♂ VAY, Kristiansand: Østre Randøy; 9.vi.2006, K. Berggren leg.; KBE prep. 13530; KBE. 1♂ VAY, Kristiansand: Skålevik; 12.vii.2019; K. Berggren leg., BOLD sample ID: KBE-2019077; KBE. 1♂ VAY, Kristiansand: Stangenes; 4.vii.1981; S. Svendsen leg.; NHMO prep. 3899; NHMO. 1♀ VAY, Kristiansand: Ådnevik, Unndalen; 6.vii.2012; K. Berggren leg.; KBE prep. 13512; KBE. 1♀ VAY,

Mandal: Hoven; 24–27.vii.2017; K. Berggren & K. Hoven leg.; KBE prep. 13513; KBE. 1♂ VAY, Mandal: Hoven; 22–24.vii.2017; K. Berggren & K. Hoven leg.; KBE prep. 13516; KBE. 1♂ VE, Horten: Knutsrød; 20–21.vi.2008; L. Aarvik leg.; NHMO prep. 3898; NHMO. 1♀ VE, Nøtterøy: Østre Bolærne; 27.vii.2006; R. Voith & K. Berggren leg.; KBE prep. 6104; KBE. 1♂ VE, Nøtterøy: Østre Bolærne; 9.vii.2006; R. Voith & K. Berggren leg.; KBE prep. 10171; KBE. 1♀ VE, Tønsberg: Karlsvikodden; vii.2005; R. Voith leg.; KBE prep. 10170; KBE. 1♂ Ø, Fredrikstad: Blåsopp; 4–19.vii.2013; O.J. Lønnve leg.; KBE prep. 13531; KBE. 1♂ Ø, Halden: Orød Grustak; 5.vi–1.vii.2009, F. Ødegaard leg.; BOLD sample ID: NHMO-DAR-4107 (failed); KBE prep. 9438; KBE. 1♂ Ø, Hvaler: Asmaløy, Huser; 3.vii.1994; L. Aarvik leg.; NHMO prep. 3965; NHMO. 1♂ Ø, Hvaler: Vesterøy, Slettevika; 25.vi.2018; J.R. Gustad leg.; NHMO prep. 3980; NHMO. 1♂ Ø, Moss: Rygge, Sildebauen; 13.vii.1980; L. Aarvik leg.; NHMO prep. 3890; NHMO. 1♂ Ø, Sarpsborg: Tune, Råkil; 4.vii.2002; T.J. Olsen leg., NHMO prep. 3935; NHMO.

Sweden 1♂ Öland, Borgholm: Byrums Sandvik; 23.vii.1985; K. Berggren leg.; KBE prep. 13527; KBE. 1♂ Öland, Borgholm: Byrums Sandvik; 23.vii.1985; K. Berggren leg.; KBE prep. 6142; KBE.

Denmark 1♂ EJ, Anholt; 1.viii.1975; E. S. Nielsen leg., Lundquist prep. 2050; ZMUC. 1♀ F, Æbelø; 25.vi.-9.vii.1943; Worm-Hansen leg.; Rasmussen prep. 3936; ZMUC. 1♂ NWZ, Kåruphøj; 18.vii.2003; H. Hendriksen leg.; Hendriksen prep. 4194; ZMUC. 1♂ LFM, Bøtø; 29.vi.1968; E. Traugott-Olsen leg.; Traugott-Olsen prep. 1242; ZMUC. 1♂, 1♀ LFM, Vålse Skov; 10.vii.1982; J. Lundqvist leg.; Lundqvist prep. 1343, 1344; ZMUC. 1♀ LFM, Ulfshale; 19.vii.1987; O. Karsholt leg.; Karsholt prep. 5381; ZMUC. 1♀ B, Slotslyngen; 31.vii.1967; H.K. Jensen leg.; Jensen prep. 692; ZMUC. 1♀ B, Boderne; 8.viii.1968; H.K. Jensen leg., Jensen prep. 810; ZMUC.

Austria 1♀, Oberösterreich, NP Kalkalpen, Spering-Lackerbodenstraße, ca 700 m; 16.vii.2004; J. Wimmer leg; genitalia in glycerine; TLMF. 1♀, ditto, but 653 m, 14.vi.2009; J. Wimmer leg; gen. slide GEL 1287 P. Huemer; TLMF. 1♂ Nordtirol, Umhausen N, unterh. Farst, 1370 m, 27.vi.2017, P. Huemer leg; GEL 1276 P. Huemer; TLMF. 1♂ Nordtirol, Umhausen N, unterh. Farst, 1370 m, 11.vi.2017, P. Huemer leg; DNA Barcode ID TLMF Lep 26819; TLMF. 1♂ Nordtirol, Zirl, Eigenhofen, linke Innau, 600 m, 7.vi.2012, P. Huemer leg.; DNA Barcode ID TLMF Lep 09322; TLMF. 1♂ Nordtirol, Brandenberg, Tiefenbachklamm, 645 m, 16.vi.2013, P. Huemer leg.; DNA Barcode ID TLMF Lep 10349; TLMF. 1♂ Osttirol, Lengberg, Drau-Auen, Schattseite, 630 m, 25.vi.2008, H. Deutsch leg.; DNA Barcode ID TLMF Lep 24185; TLMF. 1♂ Vorarlberg, Frödischtal, Schönebuchweg, Klausen, 755 m, 14.vi.2017, A. Mayr leg; DNA Barcode ID TLMF Lep 25068; coll. A. Mayr.

Germany 1♀, Bavaria, Inning/A, 550 m, mid vii.1970 Zürnbauer F. leg.; genitalia in glycerin PH; TLMF.

Italy 1♂ Südtirol, Oberrasen, Biotop Rasner Möser S, 1100 m, 5.vii.2015, P. Huemer leg.; DNA Barcode ID TLMF Lep 17982; TLMF. 1♂ Südtirol, Laas, Tschenglser Au, Biotop Rasner Möser S, 900 m, 20.vi.2015, P. Huemer leg.; DNA Barcode ID TLMF Lep 18779; TLMF.

Armenia 1♂, Tavush Province, Diljan, 1395 m; 13.vii.2011; O. Karsholt leg.; BOLD sample ID: ZMUC00029754; ZMUC.

Morphological diagnosis. *Batrachedra confusella* sp. nov. (Fig. 3) and *B. pinicolella* (Fig. 4) cannot be separated externally with certainty though it is remarkable that none of the 56 specimens of *B. confusella* with images in BOLD has a spot at about the one-third the length of the forewing fold, a character commonly present in *B. pinicolella*. All 47 specimens of Norwegian dissected or barcoded specimens of *B. confusella* sp. nov. are without the spot on the fold. In eight of 20 dissected or barcoded Norwegian specimens of *B. pinicolella* the spot is present. Thus, the presence of the spot in the fold strongly indicates that the actual specimen belongs to *B. pinicolella*. With a wingspan of 11.0–12.0 mm, *B. pinicolella* is slightly larger than *B. confusella* sp. nov. on average. In the male genitalia we found a diagnostic character in the shape of the valva and the uncus. On average *B. pinicolella* (Fig. 7) has a longer and more slender valva than *B. confusella* sp. nov. (Fig. 5). The uncus is slightly different in the two species in shape and width. In *B. confusella* sp. nov. the lateral sides are smoother and with finer and longer setae than in *B. pinicolella*. In *B. pinicolella* the uncus is laterally distinctly rugose with coarse setae. The tip of the phallus in *B. confusella* sp. nov. (Fig. 6) is armed with a distinct cornutus. In *B. pinicolella* (Fig. 8) the cornutus is narrower and often will appear merely as a fold inside the phallus. The gnathos tends to be broader distally in *B. pinicolella* than in *B. confusella* sp. nov. In the female genitalia, the two species differ in the length of the signum. In *B. pinicolella* (Fig. 10) the signum is in the range 290–380 μm. In *B. confusella* sp. nov. (Fig. 9) the length of the signum ranges from 490 to 600 μm. In *B. pinicolella* the sclerotized portion of the ductus bursae is narrower and straighter than in *B. confusella* sp. nov. Fig. 22 of the female genitalia given by Koster and Sinev (2003) represents *B. pinicolella* in the present interpretation of the name.

Molecular diagnosis. Sequences of *B. pinicolella* and *B. confusella* sp. nov. form two well-defined clusters which received separate Barcode Index Numbers (BIN-codes): AAF0078 and AAF0077 respectively. The DNA barcode region of *B. confusella* sp. nov. shows 0.95% intraspecific divergence and a minimum divergence of 6.82% to its closest relative *B. pinicolella* (Fig. 11). The latter species shows no intraspecific variability in our material (the slight apparent variation in the neighbor-joining tree results only from variation in sequence lengths). Therefore, DNA barcodes allow safe identification of the two species. The 407-bp long fragment of the nuclear MDH gene differs by 5.8% from that of *B. pinicolella*. The 506-bp long fragment of EF-1a differs by 3.1% from that of *B. pinicolella*. Therefore, both examined nuclear genes support the status of the two species and permit their identification by these markers as well. All examined five specimens were infected by *Wolbachia*, while none of the specimens of *B. pinicolella* were infected, suggesting a difference between the two species also in this regard.

We generated a genomic dataset from nine individuals of *B. pinicolella* using ddRAD sequencing. We obtained 1.24 million reads per individual on average after quality filtering steps. After clustering 88% sequence similarity, we recovered 19,292 clusters per sample were retained with an average of 82.26 per sample for cluster depth (Table 1). A total length of ddRAD data is 926,224 bp, of which 9,242 are single nucleotide polymorphisms (SNP). Phylogenetic analysis using SNP data produced ro-

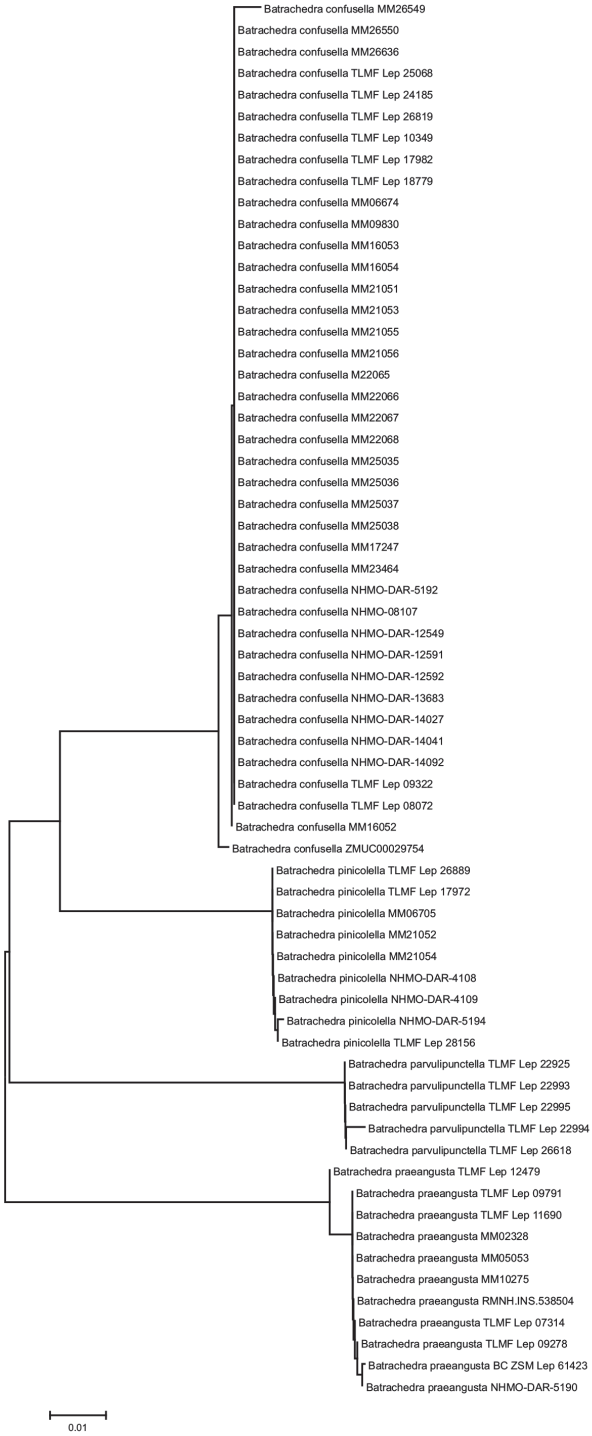

Figure 11. Neighbor-joining visualization of genetic divergences of DNA barcode fragment of COI gene within and between European species of *Batrachedra*. The scale indicates 1% genetic divergence as calculated under Kimura 2 parameter model for nucleotide substitution.

Table 1. A summary of the ddRAD data.

Species	SampleID	Reads passed filter	Clusters at 88%	Coverage	Retained loci	Consensus loci
B. confusella	MM22066	1520904	29400	40.06	11608	4488
B. confusella	MM22068	1624893	31776	45.71	12030	4346
B. confusella	MM23464	2976135	62919	43.18	19568	4557
B. confusella	TLMF Lep 10349	1353160	16809	60.85	5292	2563
B. confusella	TLMF Lep 18779	624001	11396	47.99	3177	917
B. pinicolella	MM06705	808698	4251	163.44	572	149
B. pinicolella	MM21052	971904	6440	131.25	1305	200
B. pinicolella	MM21054	931540	7060	118.22	1344	370
B. pinicolella	TLMF Lep 17972	370227	3579	89.61	611	155
	Total	**1242385**	**19292**	**82.26**	**6167**	**1972**

bust support for the relationship between the individuals (Fig. 12). The two revealed lineages corresponding to *B. confusella* sp. nov. and *B. pinicolella*, which have 100% bootstrap support. STRUCTURE also identified two genetic clusters (Fig. 11).

Description. Male (Fig. 3). Wingspan 10–11 mm. Labial palp 2.3 times diameter of eye, cream, porrect, slightly curved, second segment longer than third, outer side with brownish suffusion, third segment on outer side with two bands. Head cream, with appressed scaling. Antenna glabrous, with appressed scales, pale ochreous brown, weakly ringed, rings becoming more distinct distally. Thorax ochreous yellow. Forewing ochreous yellow, with scattered dark brown scales, denser distally and on costa, discal spot small; cilia brownish grey; hindwing grey, cilia grey. Legs cream, inner sides with brownish suffusion, which on tarsi forms bands. Abdomen cream, with lateral grey suffusion.

Female. Externally similar to male.

Male genitalia (Figs 5, 6) Uncus gradually narrowed towards tip, slightly concave at two-thirds length, medially with lateral setae, lateral margins smooth, with fine hairs; gnathos gradually narrowed, becoming parallel-sided before distal end, distal end spinose; valva nearly parallel-sided, dorsal margin curved distally, costa angled or slightly hooked at distal end; anellus lobes rounded; phallus long and slender, subdistally with bulge, cornutus near distal end distinct, tapered proximally.

Female genitalia (Fig. 9) Papillae anales broad with short setae; apophyses posteriores and anteriores of similar length, apophyses anteriores with basal fork; antrum funnel-shaped with medial ridge; ductus bursae with medial portion sclerotized and curved, anterior portion with two or three coils; corpus bursa with long (490–600 μm) and oval signum; signum with numerous short, transverse ridges.

Etymology. The species' name, *confusella*, indicates the confusion with its sister species, *B. pinicolella*.

Biology. Due to the confusion of the two species, the biology is insufficiently known. *Batrachedra confusella* sp. nov. is the well-known species affecting *Pinus*, and it has been found in several localities of pure pine forests. However, a female beaten from an artificial afforestation of *Larix* at a lowland locality in Switzerland without *Pinus* in the nearby surroundings (Bryner in litt.) also belongs to *B. confusella* sp. nov., indicating that *Larix* may be an additional host-plant. *Batrachedra pinicolella*, in contrast,

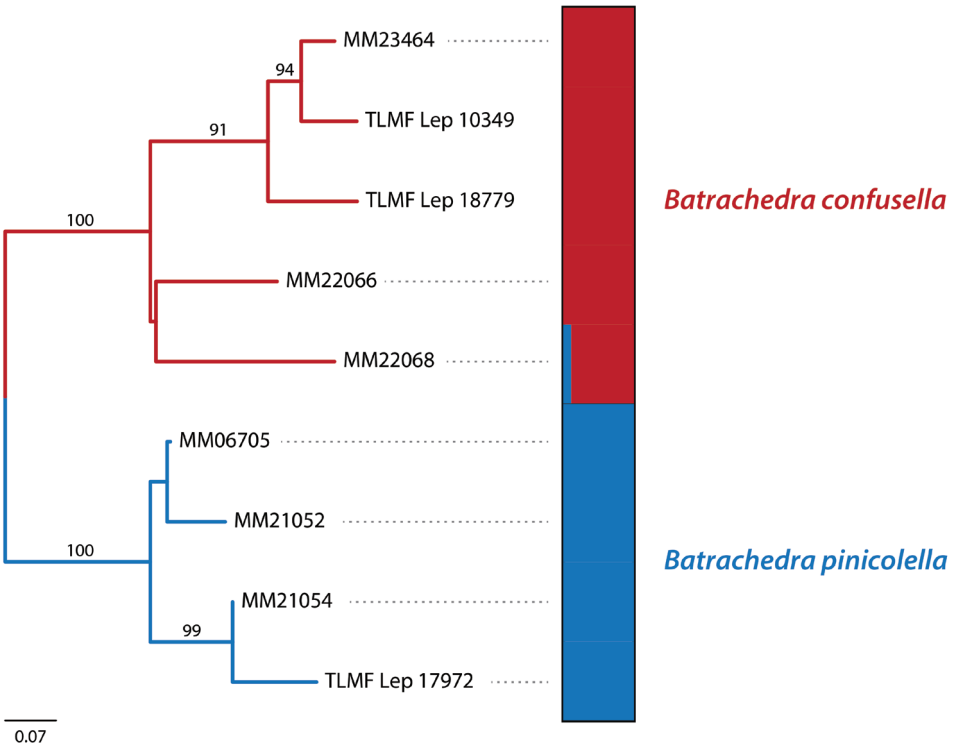

Figure 12. Maximum-likelihood tree inferred from the ddRAD SNP data. Bootstrap support values are indicated above the branches and only the values > 50% are shown. The barplot shows the assignments of individuals into two genetic clusters, the red clusters referring to *Batrachedra confusella*, the blue clusters to *B. pinicolella*. Each bar represents one individual and colours represent the proportion of the individuals that belong to each of the genetic cluster.

seems to be restricted to forests of Norway spruce (*Picea abies*), which is considered to be the host-plant. This hypothesis is proved by a dissected Finnish female specimen bred from *Picea*.

Bolov and Sinev (1990) recorded outbreaks of *B. pinicolella* on *Picea orientalis*, *P. abies*, *P. pungens*, *Abies* sp. ("European"), *A. nordmanniana*, and less frequently on *Pinus* sp. ("eastern"), *P. silvestris*, and *P. pityusa* from the Kabardino-Balkaria republic in northern Caucasus. Possibly both species were involved.

Verified specimens of *Batrachedra pinicolella*. Finland 1♂ PPe, Oulu; 7.vii.2011; M. Mutanen leg.; L. Aarvik prep. 2015.024; BOLD sample ID: MM21054; ZMUO. 1♀ PPe, Oulu; 7.vii.2011; M. Mutanen leg.; L. Aarvik prep. 2016.001; BOLD sample ID: MM21052; ZMUO. 1♀ A, Eckerö; 12.vii.2007; M. Mutanen leg.; L. Aarvik prep. 2016.002; BOLD sample ID: MM06705; ZMUO. 1♀ St, Rauma; la. *Picea abies*; 5.iv.2019; J. Itämies leg.; L. Aarvik prep. 2021.01; ZMUO.

Norway 1♀ AAI, Bygland: Heddevika; 29.vii.2008; K. Berggren leg.; BOLD sample ID: NHMO-DAR-5194; KBE. 1♂ AAY, Birkenes: Nordåsen; vii–viii.2016; S.

Svendsen leg.; KBE prep. 13526; KBE. 1♂ AAY, Birkenes: Bjorvand; 30.vii.2002; K. Berggren & S. Svendsen leg.; KBE prep. 13510; KBE. 1♀ AAY, Lillesand: Kjøstvedt; 9.vii.2007; K. Berggren leg.; KBE prep. 13514; KBE. 1♂ AK, Bærum: Isi; 11.vii.2003; P. Seglen leg; KBE prep. 13525; KBE. 1♂ AK, Bærum: Sandvika; 20.vii.1928; E. Barca leg.; NHMO prep. 2834; NHMO. 1♂ AK, Ås: Ås; 1.viii.1982; L. Aarvik leg.; NHMO prep. 3900; NHMO. 1♂ AK, Ås: Ås; 11.vii.1983; L. Aarvik leg.; NHMO prep. 3892; NHMO. 1♂ OS, Nordre Land: Tranligrenda; 5.vii.2010; K. Berggren leg.; KBE prep. 13519; KBE. 1♂ VAY, Flekkefjord: Helle; 18.vii.2013; K. Berggren leg.; BOLD sample ID: NHMO-DAR-4109; KBE prep. 13504; KBE. 1♂ VAY, Kristiansand: Gimle Gård; 11.vii.2003; K. Berggren leg.; BOLD sample ID: NHMO-DAR-5193 (failed); KBE prep. 13523; KBE, 1♀ VAY, Kristiansand: Kuholmen; 17.vii.1970; K. Berggren leg.; KBE prep. 13511; KBE. 1♂ VAY, Kristiansand: Nedre Timenes; 31.vii.2011; K. Berggren leg.; BOLD sample ID: NHMO-DAR-4108; KBE prep. 13503; KBE. 1♂ VAY, Kristiansand: Stokken; 8.vii.1978; K. Berggren leg.; KBE prep. 13522; KBE. 1♂ VAY, Kristiansand: Søgne, Torvesanden; 27.vi.2014; K. Berggren leg.; KBE prep. 13517; KBE. 1♂ VE, Larvik: Frydenlund; 12.vii.2013; K. Berggren leg.; KBE prep. 13518; KBE. 1♀ Ø, Fredrikstad: Onsøy, Rauer; 21.vii.1920; E. Barca leg.; NHMO prep. 3961; NHMO. 1♂ Ø, Moss: Rygge, Sildebauen; 10.vii.1981; L. Aarvik leg.; NHMO prep. 3891; NHMO.

Switzerland 1♀, BE, La Neuveville, Ligeresse, 810 m, 4.vii.2002, Larix decidua; leg. R. Bryner; coll. R. Bryner.

Austria 1♂ Vorarlberg, Gaschurn-Partenen, Schuttfluren Lifinar, 1150 m, 31.vii.2018; P. Huemer leg.; BOLD sample ID: TLMF Lep 26889; TLMF. 1♂ Vorarlberg, Gaschurn-Partenen, Schuttfluren Lifinar, 1150 m, 2.vii.2018; P. Huemer leg.; GEL 1275 P. Huemer; TLMF. 1♀ Vorarlberg, Gaschurn-Partenen, u. Ganifer-Schrofen, 1460–1500 m, 19.vii.2019; P. Huemer leg.; GEL 1282 P. Huemer; TLMF. 1♀ Oberösterreich, Nationalpark Kalkalpen, Lackerbodenstraße, 653 m, 14.vi.2009; J. Wimmer leg.; GEL 1287 P. Huemer; TLMF.

Germany 1♀ Baden-Württemberg, Schwarzwald, Buchenberg, 21.vii.1954; H.G. Amsel leg; genitalia in gylcerine; TLMF.

Italy 1♂ Südtirol, Oberrasen, Biotop Rasner Möser S, 1100 m, 5.vii.2015, P. Huemer leg.; DNA Barcode ID TLMF Lep 17972; TLMF.

Distribution. The species pair *B. confusella* sp. nov. and *B. pinicolella* is widely distributed in Europe but seems to be absent from the Mediterranean (http://www.faunaeur.org; accessed on 25.iv.2021). However, as former records have been summarized among the latter taxon, a detailed study of distribution of both species is required for future studies. From our sequenced and/or genitalized material, *B. confusella* sp. nov. together with its major hostplant, *Pinus sylvestris*, is distributed in the temperate zones between the Alps in the South and Fennoscandia in the north. *Batrachedra pinicolella* in concordance with its major host-plant, *Picea abies*, shows a boreo-montane distribution pattern with isolated records from the Alps and mountainous areas of Central Europe as well as northern and north-western Europe. A barcoded specimen of *B.*

confusella sp. nov. from Armenia (coll. ZMUC) confirms the presence of this species in Caucasus. According to images of genitalia on the mothdissection.co.uk website, both species are present in the United Kingdom (https://mothdissection.co.uk/species.php?Tx=Batrachedra_pinicolella; accessed on 30.iv.2021)

Discussion

Because of their external similarity, the two species have until present been confused. This is in spite of the fact that they have different host plants. Specimens collected in localities with *Pinus* (and no *Picea* present) belong to *B. confusella* sp. n., i.e. from Byrum Sandvik, Öland in Sweden, where only *Pinus* is present and from Belteviga and Bråvann, Kristiansand, Norway. In Finland and Austria, *B. pinicolella* has been collected in places where only *Picea* grows but rarely both species have been found in syntopy. Further breeding experiments are needed to confirm additional hostplants, e.g., in the genera *Abies* and *Larix*. The issue dealt with in the present paper is not unique. DNA barcoding has revealed that there still exist numerous taxonomic problems in the European lepidopteran fauna; see for instance Huemer et al. (2020) concerning Gelechiidae and Lopez-Vaamonde et al. (2021) concerning Gracillariidae. To deal with this situation, systematic and targeted collecting should be encouraged to make material available for taxonomic revisions.

Acknowledgements

Paul D.N. Hebert and the entire team at the Canadian Centre for DNA Barcoding (Guelph, Canada) are gratefully acknowledged for continuous support with sequencing work. The study was partially funded by the Promotion of Educational Policies, University and Research Department of the Autonomous Province of Bolzano - South Tyrol with grants to the projects “Genetische Artabgrenzung ausgewählter arktoalpiner und boreomontaner Tiere Südtirols” and “Erstellung einer DNA-Barcode-Bibliothek der Schmetterlinge des zentralen Alpenraumes (Süd-, Nord- und Osttirol)”. DNA barcoding in Finland was supported by the Kone Foundation, Finnish Cultural Foundation, and the Academy of Finland through their grants to the Finnish Barcode of Life (FinBOL) and Finnish Biodiversity Information Facility (FinBIF). We cordially thank David Lees (NHMUK) for important help with type material. We are very grateful to Jonna Autto who conducted sequencing of the nuclear markers and *Wolbachia* as a part of her MSc thesis in the University of Oulu. Similarly, we are indebted to Laura Törmälä for her meticulous work on ddRAD library preparation. We are indebted to Ole Karsholt, Copenhagen, who checked and identified material of *Batrachedra* in the collection of ZMUC, and to Sergey Sinev (St. Petersburg) for help with literature. We thank Per Kristian Slagsvold, Larvik, Norway, for taking photos of adults.

References

Baldo L, Hotopp JCD, Jolley KA, Bordenstein SR, Biber SA, Choudhury RR, Hayashi C, Maiden MCJ, Tettelin H, Werren JH (2006) Multilocus sequence typing system for the endosymbiont *Wolbachia pipientis*. Applied and Environmental Microbiology 72(11): 7098–7110. https://doi.org/10.1128/AEM.00731-06

Bolov AP, Sinev SYu (1990) *Batrachedra pinicolella* Dup. (Lepidoptera, Batrachedridae) – a pest of conifers in Kabardino-Balkaria. Entomological Review 69(3): 16–20.

Chhatre VE, Emerson KJ (2017) StrAuto: automation and parallelization of STRUCTURE analysis. BMC Bioinformatics 18: e192. https://doi.org/10.1186/s12859-017-1593-0

deWaard JR, Ivanova NV, Hajibabaei M, Hebert PDN (2008) Assembling DNA barcodes: analytical protocols. In: Martin CC (Ed.) Methods in Molecular Biology: Environmental Genomics. Humana Press, Totowa, 275–293. https://doi.org/10.1007/978-1-59745-548-0_15

Eaton DAR, Overcast I (2020) ipyrad: Interactive assembly and analysis of RADseq datasets. Bioinformatics 36: 2592–2594. https://doi.org/10.1093/bioinformatics/btz966

Emmet AM, Langmaid JR (eds) (2002) The Moths and Butterflies of Great Britain and Ireland. Vol. 4, Part I. Harley Books, Colchester, 326 pp.

Evanno G, Regnaut S, Goudet J (2005) Detecting the number of clusters of individuals using the software structure: a simulation study. Molecular Ecology 14: 2611–2620. https://doi.org/10.1111/j.1365-294x.2005.02553.x

Hernández-Roldán JL, Dapporto L, Dincă V, Vicente JC, Hornett EA, Šíchová J, Lukhtanov V, Talavera G (2016) Integrative analyses unveil speciation linked to host plant shift in *Spialia* butterflies. Molecular Ecology 25: 4267–4284. https://doi.org/10.1111/mec.13756

Hausmann F (1852) Flora von Tirol. Ein Verzeichnis der in Tirol und Vorarlberg wild wachsenden und häufiger gebauten Gefässpflanzen. Zweites Heft. Wagner´sche Buchhandlung, Innsbruck, 509 pp. https://doi.org/10.5962/bhl.title.9855

Huemer P (2020) Integrative revision of the *Caryocolum schleichi* species group – a striking example of a temporally changing species concept (Lepidoptera, Gelechiidae). Alpine Entomology 4: 39–63. https://doi.org/10.3897/alpento.4.50703

Huemer P, Hebert PDN (2011) Cryptic diversity and phylogeography of high alpine *Sattleria* – a case study combining DNA barcodes and morphology (Lepidoptera: Gelechiidae). Zootaxa 2981: 1–22. https://doi.org/10.11646/zootaxa.2981.1

Huemer P, Hebert PDN (2016) DNA Barcode Bibliothek der Schmetterlinge Südtirols und Tirols (Italien, Österreich) – Impetus für integrative Artdifferenzierung im 21. Jahrhundert. Gredleriana 16: 141–164.

Huemer P, Karsholt O (2018) Revision of the genus *Megacraspedus* Zeller, 1839, a challenging taxonomic tightrope of species delimitation (Lepidoptera, Gelechiidae). ZooKeys 800: 1–278. https://doi.org/10.3897/zookeys.800.26292

Huemer P, Karsholt O, Aarvik L, Berggren K, Bidzilya O, Junnilainen J, Landry J-F, Mutanen M, Nupponen K, Segerer A, Šumpich J, Wieser C, Wiesmair B, Hebert PDN (2020) DNA barcode library for European Gelechiidae (Lepidoptera) suggests greatly underestimated species diversity. ZooKeys 921: 141–157. https://doi.org/10.3897/zookeys.921.49199

Jakobsson M, Rosenberg NA (2007) CLUMPP: a cluster matching and permutation program for dealing with label switching and multimodality in analysis of population structure. Bioinformatics 23: 1801–1806. https://doi.org/10.1093/bioinformatics/btm233

Kalyaanamoorthy S, Minh BQ, Wong TKF, Von Haeseler A, Jermiin LS (2017) ModelFinder: Fast model selection for accurate phylogenetic estimates. Nature Methods 14: 587–589. https://doi.org/10.1038/nmeth.4285

Koster S, Sinev SYu (2003) Momphidae, Batrachedridae, Stathmopodidae, Agonoxenidae, Cosmopterigidae, Chrysopeleiidae. In: Huemer P, Karsholt O, Lyneborg L (Eds) Microlepidoptera of Europe 5: 1–387.

Lee KM, Kivelä SM, Ivanov V, Hausmann A, Kaila L, Wahlberg N, Mutanen M (2018) Information dropout patterns in restriction site associated DNA phylogenomics and a comparison with multilocus Sanger data in a species-rich moth genus. Systematic Biology 67: 925–939. https://doi.org/10.1093/sysbio/syy029

Lienig F, Zeller PC (1846) Lepidopterologische Fauna von Livland und Curland. Bearbeitet von Friederike Lienig, geb. Berg, mit Anmerkungen von P.C. Zeller. Isis oder Encyclopaedische Zeitung von Oken, Leipzig 39(3/4): 175–302.

Lopez-Vaamonde C, Kirichenko N, Cama A, Doorenweerd C, Godfray HCJ, Guiguet A, Gomboc S, Huemer P, Landry J-F, Laštůvka A, Laštůvka Z, Min Lee K, Lees DC, Mutanen M, Nieukerken EJ von, Segerer AH, Triberti P, Wieser C, Rougerie R (2021) Evaluating DNA barcoding for species identification and discovery in European gracillariid moths. Frontiers in Ecology and Evolution 9: 1–16. https://doi.org/10.3389/fevo.2021.626752

Mutanen M, Aarvik L, Huemer P, Kaila L, Karsholt O, Tuck K (2012a) DNA barcodes reveal that the widespread European tortricid moth *Phalonidia manniana* (Lepidoptera: Tortricidae) is a mixture of two species. Zootaxa 3262: 1–21. https://doi.org/10.11646/zootaxa.3262.1

Mutanen M, Aarvik L, Landry J-F, Segerer AH, Karsholt O (2012b) *Epinotia cinereana* (Haworth, 1811) bona sp., a Holarctic tortricid distinct from *E. nisella* (Clerck, 1759) (Lepidoptera: Tortricidae: Eucosmini) as evidenced by DNA barcodes, morphology and life history. Zootaxa 3318: 1–25. https://doi.org/10.11646/zootaxa.3318.1

Mutanen M, Huemer P, Autto J, Karsholt O, Kaila L (2020) *Monopis jussii*, a new species (Lepidoptera, Tineidae) inhabiting nests of the boreal owl (*Aegolius funereus*). ZooKeys 992: 157–181. https://doi.org/10.3897/zookeys.992.53975

Nguyen LT, Schmidt HA, von Haeseler A, Minh BQ (2015) IQ-TREE: a fast and effective stochastic algorithm for estimating maximum-likelihood phylogenies. Molecular Biology and Evolution 32: 268–274. https://doi.org/10.1093/molbev/msu300

Patočka, J (1960) Die Tannenschmetterlinge der Slowakei. Verlag der Slowakischen Akademie der Wissenschaften, Bratislava, 216 pp.

Peña C, Malm T (2012) VoSeq: a voucher and DNA sequence web application. PLoS ONE 7(6): e39071. https://doi.org/10.1371/journal.pone.0039071

Pritchard JK, Stephens M, Donnelly P (2000) Inference of population structure using multilocus genotype data. Genetics 155: 945–959. https://doi.org/10.1093/genetics/155.2.945

Rambaut A (2015) FigTree, v1. 4.2: tree figure drawing tool. Molecular evolution, phylogenetics and epidemiology. http://tree.bio.ed.ac.uk/software/figtree/

Ratnasingham S, Hebert PDN (2007) BOLD: The Barcode of Life Data System (www.barcodinglife.org). Molecular Ecology Notes 7: 355–364. https://doi.org/10.1111/j.1471-8286.2007.01678.x

Robinson GS (1976) The preparation of slides of Lepidoptera genitalia with special reference to the Microlepidoptera. Entomologist's Gazette 27: 127–132.

Rosenberg N (2004) DISTRUCT: a program for the graphical display of population structure. Molecular Ecology Notes 4: 137–138.

Tamura K, Stecher G, Peterson D, Filipski A, Kumar S (2013) MEGA6: Molecular Evolutionary Genetics Analysis version 6.0. Molecular Biology and Evolution 30: 2725–2729. https://doi.org/10.1093/molbev/mst197

Wahlberg N, Wheat CH (2008) Genomic outposts serve the phylogenetic pioneers: designing novel nuclear markers for genomic DNA extractions of Lepidoptera. Systematic Biology 57: 231–242. https://doi.org/10.1080/10635150802033006

Wikström B, Huemer P, Mutanen M, Tyllinen J, Kaila L (2020) *Pyralis cardinalis*, a charismatic new species related to *P. regalis* [Denis & Schiffermüller], 1775, first recognized in Finland (Lepidoptera, Pyralidae). Nota Lepidopterologica 43: 337–364. https://doi.org/10.3897/nl.43.54916

Zeller PC (1839) Versuch einer naturgemässen Eintheilung der Schaben. Isis Oken, Leipzig 1839(3): 169–220.

Zlatkov B, Huemer P (2017) Allopatric cryptic diversity in the alpine species complex *Phtheochroa frigidana* s. lat. (Lepidoptera: Tortricidae). European Journal of Taxonomy 368: 1–25. https://doi.org/10.5852/ejt.2017.368

Zhou W, Rousset F, O'Neil S (1998) Phylogeny and PCR-based classification of Wolbachia strains using wsp gene sequences. Proceedings of the Royal Society B: Biological Sciences 265: 509–515. https://doi.org/10.1098/rspb.1998.0324

Zlatkov B, Huemer P (2019) Remarkable confusion in some Western Palearctic *Clepsis* leads to a revised taxonomic concept (Lepidoptera, Tortricidae). ZooKeys 885: 51–87. https://doi.org/10.3897/zookeys.885.38655

ZooKeys @@: #–## (2021)
doi: 10.3897/zookeys.@@.72978
https://zookeys.pensoft.net

RESEARCH ARTICLE

A peer-reviewed open-access journal
ZooKeys
Launched to accelerate biodiversity research

On two new species of deep-sea carrier crabs (Crustacea, Brachyura, Homolodromiidae, *Dicranodromia*) from Taiwan and the Philippines, with notes on other Indo-West Pacific species

Peter K. L. Ng[1], Chien-Hui Yang[2]

1 *Lee Kong Chian Natural History Museum, National University of Singapore, 2 Conservatory Drive, Singapore 117377, Republic of Singapore* **2** *Institute of Marine Biology, National Taiwan Ocean University, 2 Pei-Ning Road, Keelung 20224, Taiwan*

Corresponding author: Chien-Hui Yang (chyang@ntou.edu.tw)

Academic editor: I. S. Wehrtmann | Received 13 August 2021 | Accepted 1 November 2021 | Published ## Month 2021

http://zoobank.org/3C4A5D71-A951-4B72-8055-EBDFF0785DED

Citation: Ng PKL, Yang C-H (2021) On two new species of deep-sea carrier crabs (Crustacea, Brachyura, Homolodromiidae, *Dicranodromia*) from Taiwan and the Philippines, with notes on other Indo-West Pacific species. ZooKeys @@: #–##. https://doi.org/10.3897/zookeys.@@.72978

Abstract

The systematics of four species of the homolodromiid genus *Dicranodromia* A. Milne-Edwards, 1880, from East Asia and the Philippines is reappraised: *D. danielae* Ng & McLay, 2005, *D. doederleini* Ortmann, 1892, *D. karubar* Guinot, 1993, and *D. martini* Guinot, 1995; and key characters such as the epistome, gonopods, and spermatheca are figured in detail. Two new species, *D. erinaceus* **sp. nov.** and *D. robusta* **sp. nov.,** are described from Taiwan and the Philippines, respectively. *Dicranodromia erinaceus* **sp. nov.** resembles *D. spinulata* Guinot, 1995, and *D. delli* Ahyong, 2008 (from New Caledonia and New Zealand) but can be separated by its distinctly spinulated carapace surfaces and proportionately shorter fifth ambulatory legs. *Dicranodromia robusta* **sp. nov.** is superficially similar to *D. baffini* (Alcock & Anderson, 1899) and *D. karubar* Guinot, 1993, but can easily be separated by possessing a broad dorsoventrally flattened infraorbital tooth. A genetic study of the species using the mitochondrial cytochrome c oxidase I gene confirms that the taxa are distinct, with *D. erinaceus* **sp. nov.** coming out in a well-supported clade from congeners. The megalopa of *D. doederleini* is also reported for the first time.

Keywords

Comparative taxonomy, deep-sea crab, East Asia, Homolodromioidea, systematics.

Introduction

The deep-water carrier crabs of the homolodromiid genus *Dicranodromia* A. Milne-Edwards, 1880, are represented by 20 species from the Atlantic, Indian, and Pacific Oceans (Guinot 1995; Ng and McLay 2005; Ng and Naruse 2007; Ahyong 2008; Ng et al. 2008; Tavares and Lemaitre 2014). Of these, 11 species are known from the Indo-West Pacific: *D. baffini* (Alcock & Anderson, 1899), *D. chenae* Ng & Naruse, 2007, *D. crosnieri* Guinot, 1995, *D. danielae* Ng & McLay, 2005, *D. delli* Ahyong, 2008, *D. doederleini* Ortmann, 1892, *D. foersteri* Guinot, 1993, *D. karubar* Guinot, 1993, *D. martini* Guinot, 1995, *D. nagaii* Guinot, 1995, and *D. spinulata* Guinot, 1995.

We describe two additional species from Taiwan and the Philippines. The Taiwanese material had been misidentified as "*D. doederleini*" by earlier workers, while the Philippine specimens had been incorrectly identified by field collectors as "*D. delli*". We also take this opportunity to update the character states of some poorly known species and refigure them so that they are better defined. In particular, we add male first and second gonopod characters for the species as they are useful to discriminate some of the taxa. Their taxonomy is also discussed. In addition, we also report on the larvae of an ovigerous female of *D. doederleini* which had been kept in the aquarium.

Materials and methods

Material examined is deposited in the National Taiwan Ocean University (**NTOU**), Keelung, Taiwan; and the Zoological Reference Collection (**ZRC**) of the Lee Kong Chian Natural History Museum, National University of Singapore. Measurements are provided in millimetres of the maximum carapace width and length. The ambulatory leg articles are measured along their maximum length while the width is determined at midlength where it is widest.

The terminology used follows Guinot (1995) and Davie et al. (1995). In *Dicranodromia*, the groove of G1 in which the G2 is inserted is on the dorsal surface of the structure (relative to the carapace), and in situ, the lobes present on the subdistal part are on the outer margin, i.e., directed laterally outwards. The following abbreviations are used: coll. = collected by; G1 = male first gonopod; G2 = male second gonopod; P2–P5 = pereiopods 2–5 (ambulatory legs 1–4).

For the molecular analysis, a total of seven individuals were used (as indicated on the material examined of each species below). Two species, *D. danielae* and *D. robusta* sp. nov., could not be tested as they had originally been preserved in formalin. Crude genomic DNA was extracted from the muscles of the pleon using QIAamp DNA Micro Kit (Qiagen, Cat. No. 56304, Valencia, CA, USA) following the protocol of the manufacturer. The DNA barcoding gene (mitochondrial cytochrome c oxidase I, COI; cf. Hebert et al. 2005) was amplified using the universal primer set (LCO1490/HCO2198, 657 bp; Folmer et al. 1994). PCR reaction components, temperature cycling conditions and sequencing reaction followed those used in Ng

et al. (2018). For comparisons, the COI sequence of *Homolodromia kai* Guinot, 1993 (voucher number ZRC 2018.0109) was obtained and used as the outgroup for the analysis.

The resulting sequences were firstly translated into the corresponding amino acids by EditSeq (LASERGENE; DNASTAR) to check for pseudogenes (Song et al. 2008). BioEdit v.7.1.3.0 (Hall 1999) was then used to align and edit the COI dataset, with MEGA v. 7 (Kumar et al. 2016) used to calculate the uncorrected pairwise distances (*p*-distance). Maximum likelihood (ML) method was used to construct the phylogenetic tree by RAxML v.7.2.6 (Stamatakis 2006). ML analysis settings followed the model of general time reversible with a gamma distribution GTRGAMMA) for the COI dataset. Branch confidence of the tree topology was assessed using 1,000 bootstrap replicates (Felsenstein 1985).

Systematic account

Family Homolodromiidae Alcock, 1899

Genus *Dicranodromia* A. Milne-Edwards, 1880

Type species. *Dicranodromia ovata* A. Milne-Edwards, 1880, by monotypy; gender feminine).

Remarks. As the number of species has increased and more material has been examined since the revision by Guinot (1995), a revised key to *Dicranodromia* is provided below for the Indo-West Pacific species. To date, there are no shared species between the Atlantic and Indo-West Pacific.

Key to Indo-West Pacific species of *Dicranodromia*

1 Basal antennal article relatively short, stout; anteroexternal tooth long, subequal to or longer than rest of article **2**

– Basal antennal article more elongate; anteroexternal tooth short, distinctly shorter than rest of article **7**

2 Carapace and pereiopods covered with short and very dense plumose setae, forming velvet-like tomentum, obscuring surfaces and margins of pereiopods **3**

– Setae of various types and lengths on carapace and pereiopods, can be relatively dense but never obscuring surfaces and margins of pereiopods **4**

3 Carapace proportionately wider, anterolateral and posterolateral margins unarmed or only with small granules [southern Java and Moluccas] ..... ***D. karubar* Guinot, 1993**

– Carapace proportionately narrower, anterolateral and posterolateral margins lined with sharp spinules or granules [Indian Ocean] ..... ***D. baffini* (Alcock & Anderson, 1899)**

4 Infraorbital tooth broad, dentiform to linguiform, subequal or larger than exorbital tooth [Philippines] ..... ***D. robusta* sp. nov.**
– Infraorbital tooth triangular, smaller than exorbital tooth..... **5**
5 Anterior surface of epistome prominently spinose; P2 and P3 merus with distinct spines on flexor margin [Philippines] ..... ***D. danielae* Ng & McLay, 2005**
– Anterior surface of epistome at most granulate or with scattered spinules; flexor margin of P2 and P3 merus unarmed..... **6**
6 P2 and P3 dactyli short, propodus more than twice length of dactylus [Philippines] ..... ***D. chenae* Ng & Naruse, 2007**
– P2 and P3 dactyli long, propodus 1.5–1.6× length of dactylus carapace [Philippines] ..... ***D. martini* Guinot, 1995**
7 Dorsal surface of carapace covered with distinct spinules, especially along lateral parts, those on median parts may be present as granules; flexor margin of P2–P5 merus distinctly lined with spines **8**
– Dorsal surface of the carapace almost smooth, with granules or spinules present only on lateral parts; P2 and P3 merus unarmed except for flexor margin sometimes with spinules, P4 and P5 merus unarmed **11**
8 Exorbital tooth exorbital tooth triangular, dentiform; posterior margin of epistome prominently spinose [Madagascar] ..... ***D. crosnieri* Guinot, 1995**
– Exorbital tooth slender, spiniform; posterior margin of epistome entire, adjacent area smooth or with scattered spinules **9**
9 Median part of dorsal surface of carapace covered with distinct spinules; submarginal area of posterior margin of epistome with several spinules; P2 and P3 relatively short (e.g., P3 propodus less than 7× longer than wide; propodus 1.7× length of dactylus) [New Caledonia; New Zealand] ..... ***D. spinulata* Guinot, 1995**
– Median part of dorsal surface of carapace covered with granules, not spinules; submarginal area of posterior margin of epistome unarmed; P2 and P3 relatively longer (e.g., P3 propodus more than 8× longer than wide; propodus 1.7× length of dactylus)... **10**
10 P2–P5 proportionately shorter (e.g., P3 merus 4.5× longer than wide; P5 merus just reaching branchiocardiac groove when folded dorsally) [Taiwan]..... ..... ***D. erinaceus* sp. nov.**
– P2–P5 proportionately longer (e.g., P3 merus 6.6× longer than wide; P5 merus longer and more slender, extending beyond branchiocardiac groove when folded dorsally) [New Zealand]..... ***D. delli* Ahyong, 2008**
11 Posterior margin of epistome entire; outer surface of palm in both sexes evenly covered with granules [Chesterfield Islands] ..... ***D. foersteri* Guinot, 1993**
– Posterior margin of epistome crenulate; median outer surface of palm in both sexes smooth, granules only present on subdorsal and subventral margins..... **12**
12 Carapace and pereiopods covered with numerous long stiff setae but not obscuring surfaces and margins [known for certain only from Japan] .... ***D. doederleini* Ortmann, 1892**
– Carapace and pereiopods densely covered with numerous setae of different types; partially obscuring carapace surface and margins, but almost completely obscuring surfaces and margins of pereiopods [Japan] ..... ***D. nagaii* Guinot, 1995**

***Dicranodromia doederleini* Ortmann, 1892**
Figures 1–3

Dicranodromia doederleini Ortmann, 1892: 549, pl. 26, fig. 4; Guinot 1995: 202, figs 2C, 11a, c, d, 12A–C; Ikeda 1998: 54–55, pl. 1 figs 1–6; Ng et al. 2008: 39 (for complete synonymy, see Guinot 1995: 202).

Material examined. Japan: 1 ♀ with 1 megalops (15.9 × 20.2 mm), Sagami Bay, from aquarium trade, 8 Apr. 2015 (ZRC 2017.1214, COI sequence: OK351331); 1 ovigerous ♀ (14.5 × 19.2 mm), 35°32.51'N, 139°54.74'E, Futttsu, Kanaya, Chiba Prefecture, 200–250 m, 19 Sep. 2007 (ZRC 2021.0469, COI sequence: OK351333); 1♂ (10.3 × 8.5 mm), station 29, 34°40.21'N, 139°18.62'E, SW of Izu-Ohshima Island, Izu Islands, 289-307 m, TRV Shin'yo-maru, 2002 research cruise, coll. T. Komai, 24 Oct. 2002 (CBM-ZC 16572, COI sequence: OK351332).

Remarks. This species is well known (for synonymy and records, see Guinot 1995; Ikeda 1998) but may be a species complex, and specimens from outside the type locality in Japan all need to be rechecked (see Guinot 1995; Ng and McLay 2005).

One female specimen (ZRC 2017.1214) was imported to Singapore via the aquarium trade in early April 2015. On 8 April, the specimen was obtained by Paul YC Ng and observed to have between 10–20 large eggs under the pleon with the eyes just visible. It was kept in a cold-water aquarium (ca. 15–20°C) with other crustacean and fish species. On 18 April, he noted that several eggs had been released into the aquarium (Fig. 1D) which appeared ready to hatch, and that some of the egg membranes had ruptured revealing what appeared to be a dead first zoeal stage (Fig. 1E). One specimen, however, was apparently a freshly hatched and dead megalopa (Fig. 1F). He observed the first free-crawling megalopa on the female specimen on 24 April (Fig. 1B, G). Unfortunately, no larvae except one megalopa was preserved (PYC Ng, personal communication).

The observations above on the eggs and megalopa of *D. doederleini* provide some clarity on the larval development in the genus. While it is known the eggs are large and the development is abbreviated, it is not sure of the eggs hatch into an advanced zoeal stage or directly into megalopa. Caustier (1895) was the first to report on the first zoea of *Dicranodromia ovata* A. Milne-Edwards, 1880, from the Atlantic but he based this on unhatched embryos and unfortunately, the description was brief, and no figures were provided. Martin (1991) found a specimen of *D. felderi* Martin, 1990 from the western Atlantic, which had well-developed eggs and removed some embryos. On the basis of these, he described what he regarded was the first zoea. Guinot (1995: 105) reported that a specimen of *D. nagaii* from Japan had about 20 megalopae under the pleon and suggested the eggs hatched directly into this stage. The eggs of *D. doederleini* are full of yolk, and even the "first zoea" observed are of the lecitotrophic type, with yolk sacs and appendages, which are poorly or not setose (Fig. 1E). They are very similar to the condition observed or the dromiid *Cryptodromia pileifera* Alcock, 1900 which has only one lecitrophic first zoeal stage before the megalopa (Tan et al. 1986). In *Cryptodromia pileifera*, however, the zoea is still able to swim and move around in

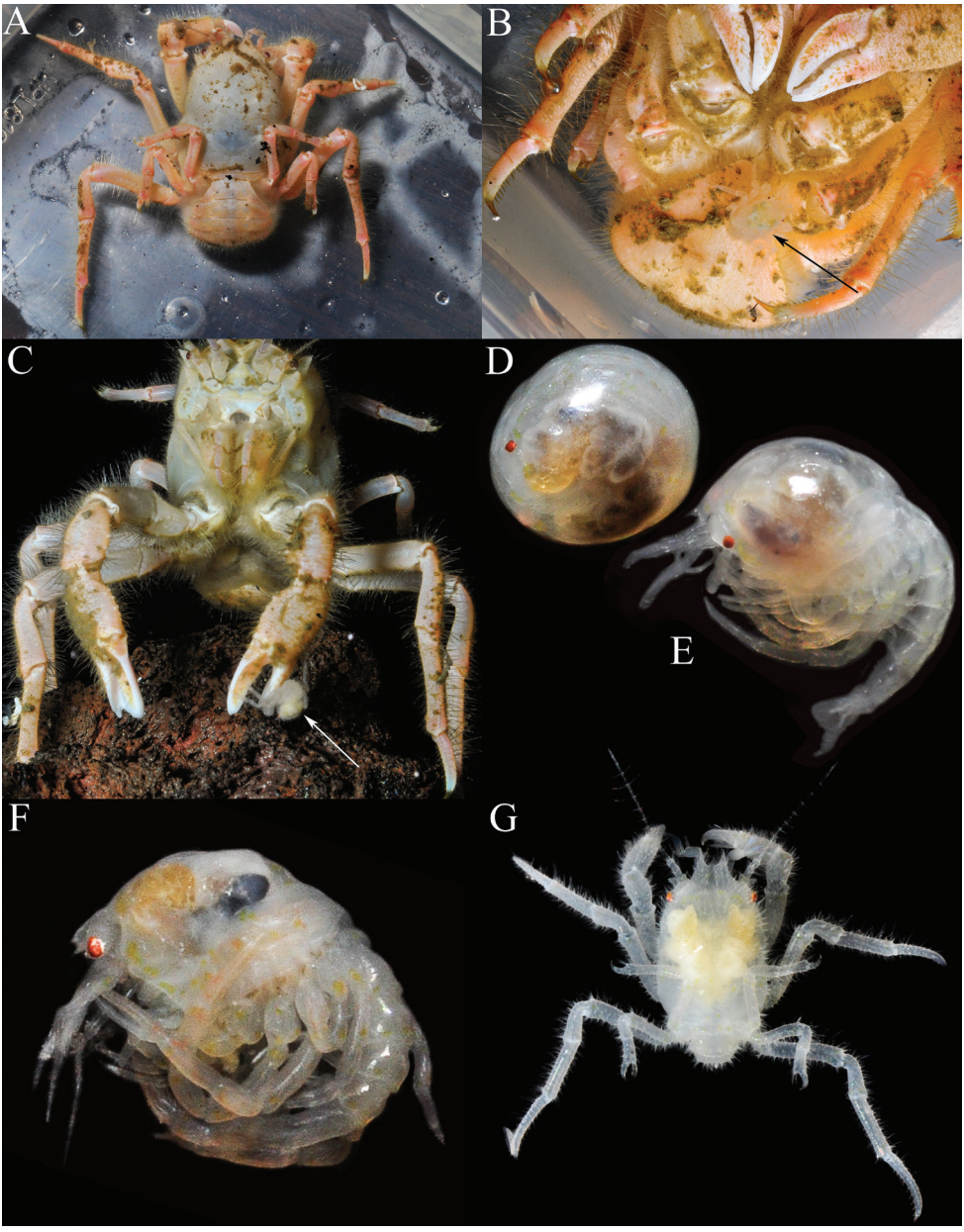

Figure 1. *Dicranodromia doederleini* Ortmann, 1892, ♀ (15.9 × 20.2 mm) (ZRC 2017.1214), Japan **A** colour in life (26 April 2015) **B** ventral surface showing megalopa (arrow) (26 April 2015) **C** frontal view showing megalopa crawling on chela (arrow) and larvae under pleon (24 April 2015) **D** fresh eyed egg (not preserved, 18 April 2015) **E** first zoea (not preserved, 18 April 2015) **F** freshly hatched megalopa (not preserved, 18 April 2015) **G** dorsal view of free moving megalops (26 April 2015). Photographs: PYC Ng.

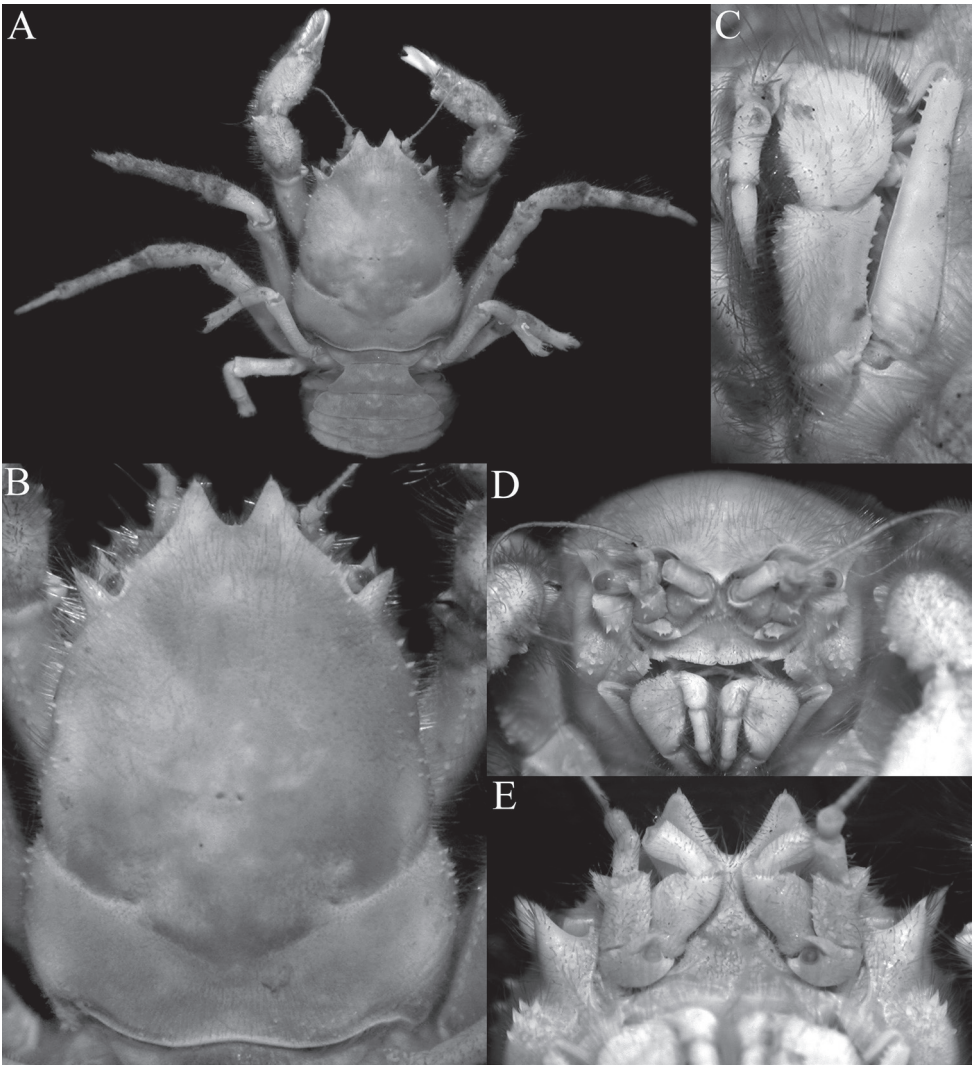

Figure 2. *Dicranodromia doederleini* Ortmann, 1892, ovigerous ♀ (14.5 × 19.2 mm) (ZRC 2021.0469), Japan **A** overall view **B** dorsal view of carapace **C** left third maxilliped **D** frontal view of cephalothorax **E** epistome, antennules, antennae and orbits.

the water column although it only lasts two days before metamorphosing. For the specimen of *D. doederleini* that was kept in the aquarium, it would appear that if it was natural, the young would develop into an advanced zoeal stage while still inside the egg membrane, and break free only after it metamorphoses into the megalopa. The transition between the "first zoea" and megalopa, however, is clearly very short, perhaps a day or less. The condition for *Dicranodromia* is thus probably similar to that

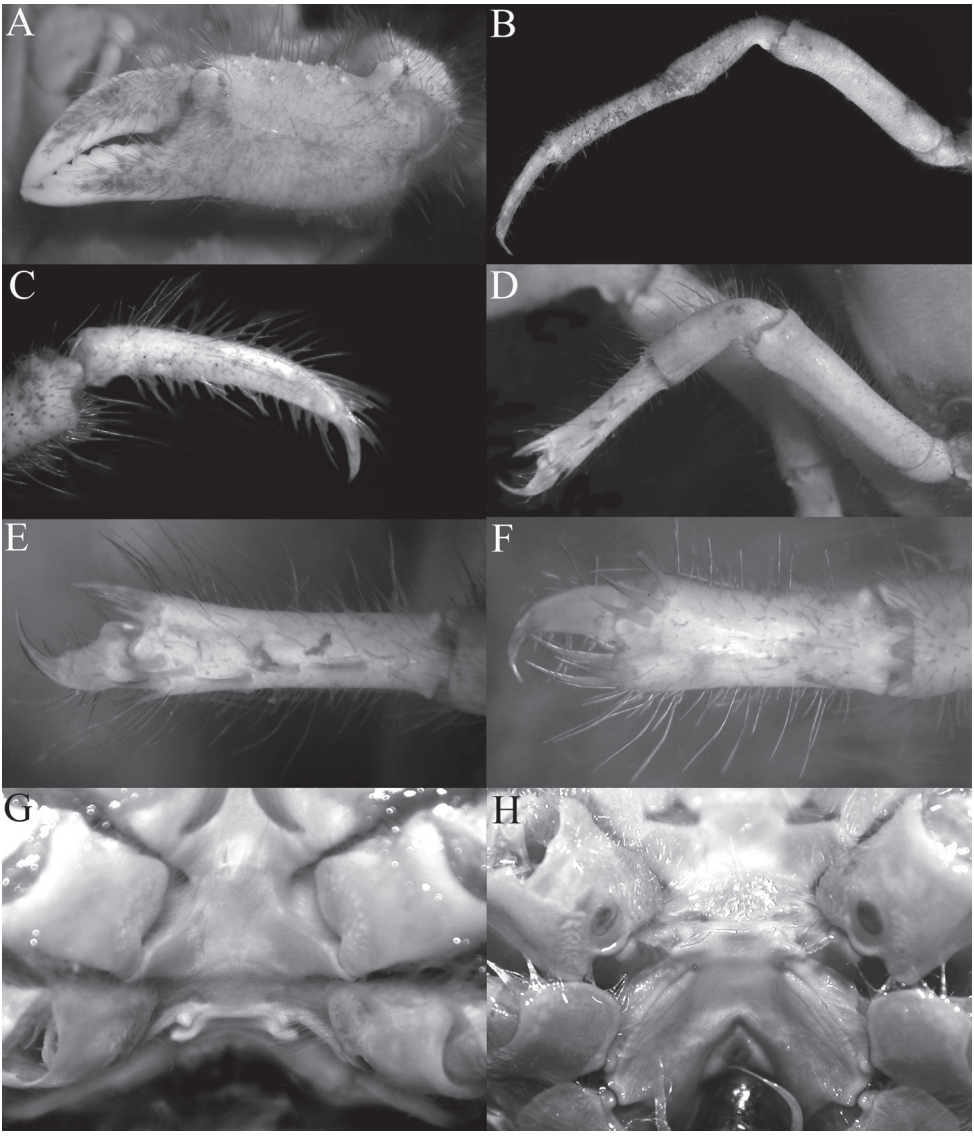

Figure 3. *Dicranodromia doederleini* Ortmann, 1892, ovigerous ♀ (14.5 × 19.2 mm) (ZRC 2021.0469), Japan **A** left chela **B** left P3 **C** right P3 dactylus **D** left P5 **E** left P5 propodus and dactylus **F** left P4 propodus and dactylus **G** anterior thoracic sternum and spermatheca **H** posterior thoracic sternum showing spermatheca and female gonopores.

of eubrachyuran marine crabs, some other podotreme crabs and various enbrachyurans like the epialtids *Paranaxia serpulifera* (Guérin, 1832) and *P. keesingi* Hosie & Hara, 2016 (Rathbun 1914, 1924; Morgan 1987; Hosie and Hara 2016), and the pilumnids *Pilumnus novaezealandiae* Filhol, 1885 and *P. lumpinus* Bennett, 1964 (cf. Wear 1967); taxa which undergo direct development.

***Dicranodromia martini* Guinot, 1995**
Figures 4–6, 11A–C

Dicranodromia martini Guinot, 1995: 221, figs 19a–e, 20A–C; Ng and Naruse 2007: 48, figs 1, 3a, b, 4; Ng et al. 2008: 39, fig. 11.

Material examined. Philippines: 1 ♂ (12.3 × 16.6 mm), station CP2396, 9°36.3'N, 123°42.0'E, Maribohoc Bay, Panglao, Bohol, Visayas, 609–673 m, PANGLAO 2005

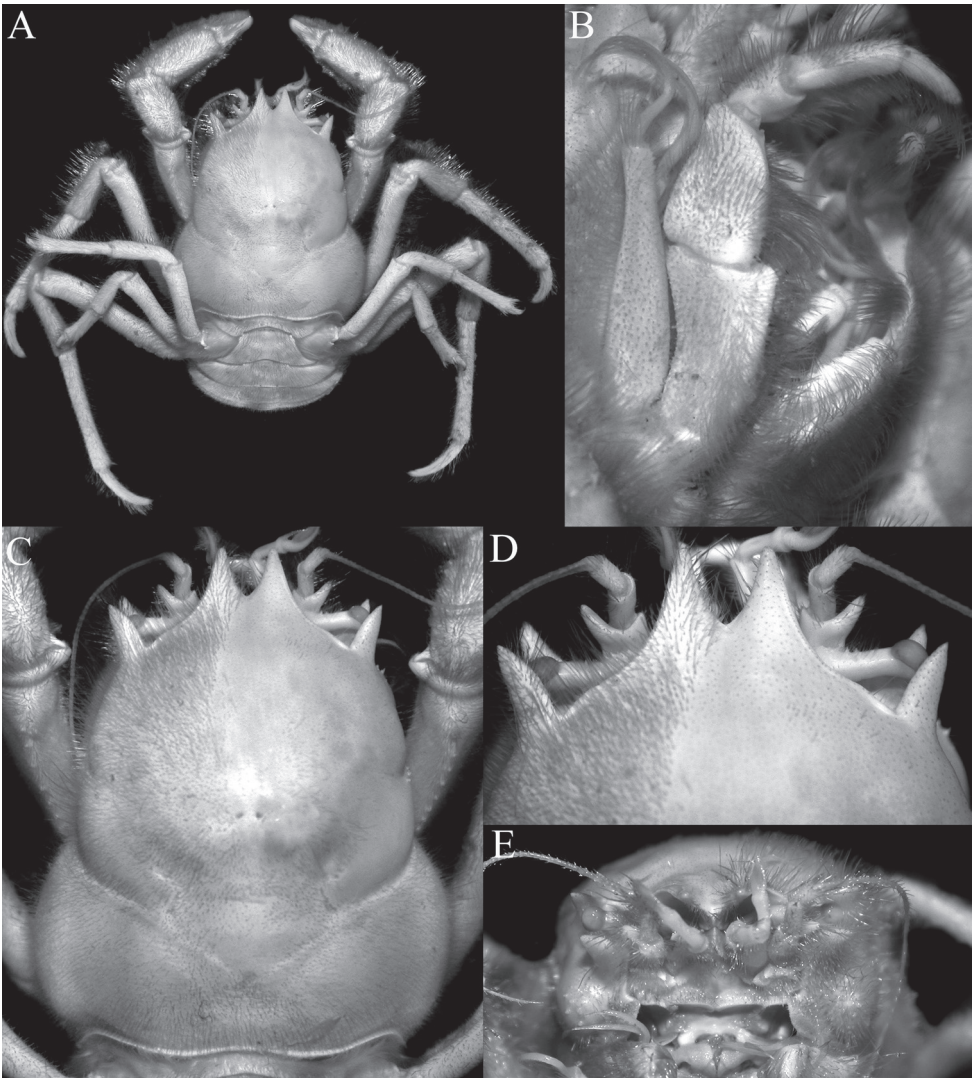

Figure 4. *Dicranodromia martini* Guinot, 1995, ♀ (28.1 v 34.2 mm) (ZRC 2007.0106), Philippines **A** overall view **B** right third maxilliped **C** dorsal view of carapace **D** anterior part of carapace (right side denuded) **E** frontal view of cephalothorax.

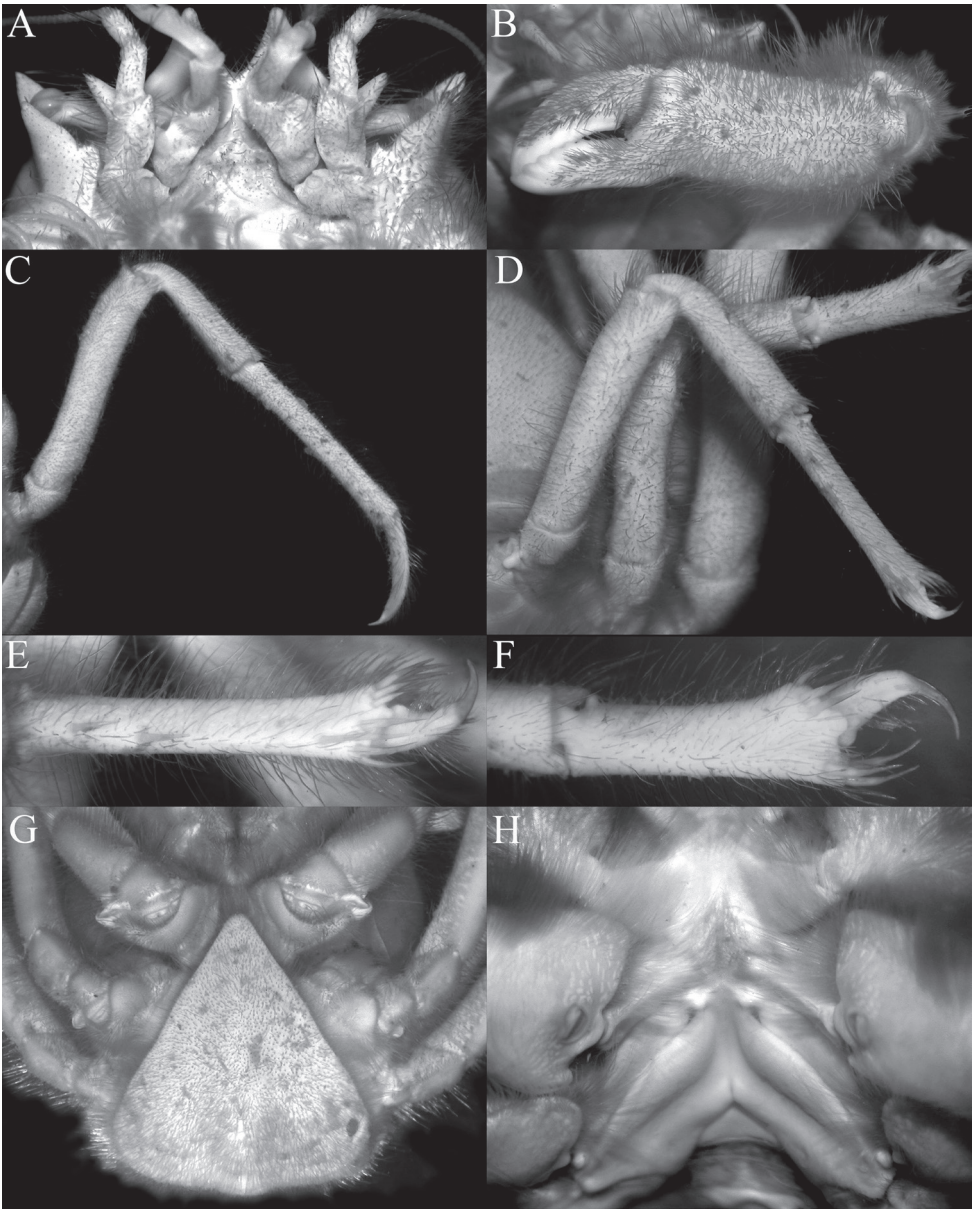

Figure 5. *Dicranodromia martini* Guinot, 1995, ♀ (28.1 × 34.2 mm) (ZRC 2007.0106), Philippines **A** epistome, antennules, antennae and orbits **B** left chela **C** right P3 **D** right P5 **E** right P5 dactylus **F** right P4 **G** telson **H** posterior thoracic sternum showing spermatheca and female gonopores.

Expedition, coll. MV DA-BFAR, 31 May 2005 (ZRC 2007.0105); 1 ♀ (28.1 × 34.2 mm), station CP2363, 9°06.0'N, 123°25.0'E, Bohol and Sulu Seas, 437–439 m, PANGLAO 2005 Expedition, coll. MV DA-BFAR, 26 May 2005 (ZRC 2007.0106, COI sequence: OK331337).

Figure 6. *Dicranodromia martini* Guinot, 1995, ♂ (12.3 × 16.6 mm) (ZRC 2007.0105), Philippines **A** overall view **B** dorsal view of carapace **C** anterior part of carapace (partially denuded) **D** male telson.

Remarks. Ng and Naruse (2007: 49) commented that the largest female they examined (28.1 × 34.2 mm, ZRC 2007.0106) has the carapace relatively more inflated with the posterolateral margin distinctly convex and the external orbital tooth more anteriorly directed when compared to smaller males. In addition, this female specimen is also relatively more hirsute (Fig. 4A, C, D versus Fig. 6A–C). We see a similar pattern of variation in *D. erinaceus* sp. nov., where the smaller males are less swollen and with less setae overall when compared to larger females (Fig. 16A, B versus Fig. 13A, B). In *D. karubar*, the exorbital tooth varies in the angle its directed outwards (Figs 8B, C, 10B). As such, the differences observed for the specimens of *D. martini* examined here are regarded as intraspecific and/or size related.

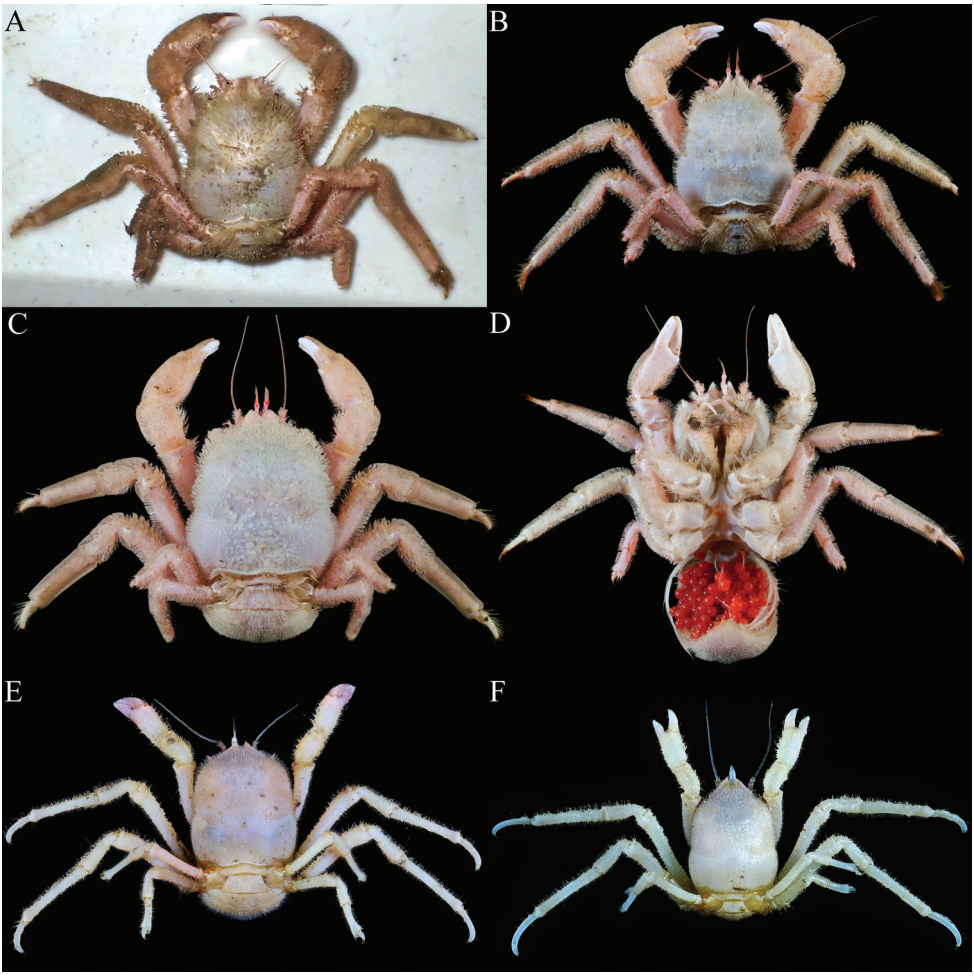

Figure 7. Colour in life. **A,B** *Dicranodromia karubar* Guinot, 1993, ♂ (28.7 × 34.7 mm) (ZRC 2020.0348), Java **C** *D. karubar* Guinot, 1993, ovigerous ♀ (30.1 × 35.5 mm) (ZRC 2020.0349), Java **D** *D. karubar* Guinot, 1993, ovigerous ♀ (24.8 × 31.5 mm) (ZRC 2020.0348), Java **E** *D. erinaceus* sp. nov., holotype ♀ (14.0 × 18.0 mm) (NTOU B00126), Taiwan **F** *D. erinaceus* sp. nov., paratype ♂ (6.9 × 9.5 mm) (ZRC 2021.0084), Taiwan. Photographs: T.-Y. Chan.

Dicranodromia karubar Guinot, 1993

Figures 8–10, 11D–F

Dicranodromia karubar Guinot, 1993: 213, figs 15A–C, 16A–D, 25A, B; Ng et al. 2008: 39; Mendoza et al. 2021: 284, fig. 1A, B.

Material examined. Indonesia: 1 ♂ (28.7 × 34.7 mm), 3 ovigerous ♀♀ (24.8 × 31.5 mm, 27.1 × 33.4 mm, 27.6 × 33.8 mm), station CP39, 8°15.885'S, 109°10.163'E – 8°16.060'S, 109°10.944'E, 528–637 m, substrate partially muddy, plenty of glass sponges,

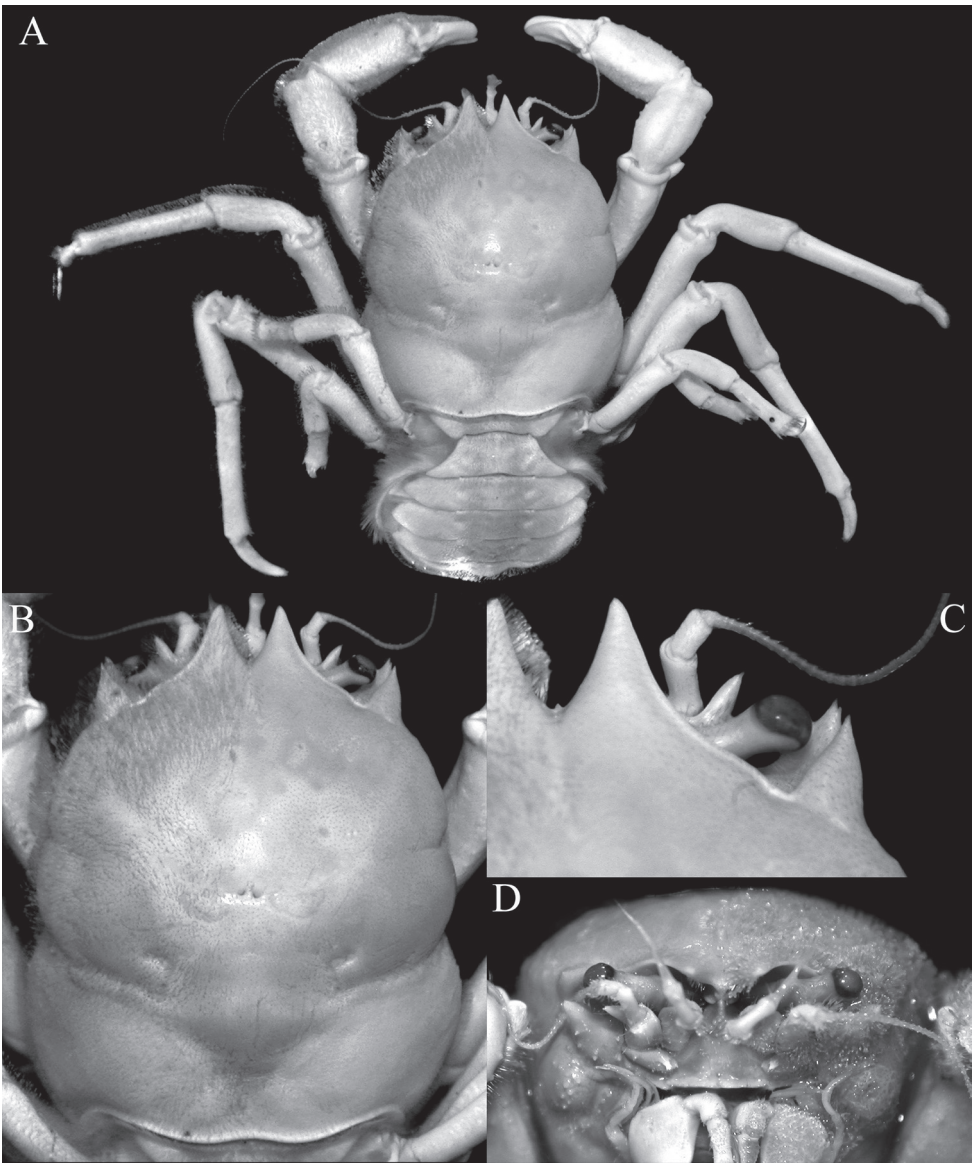

Figure 8. *Dicranodromia karubar* Guinot, 1993, ♀ (27.1 × 33.4 mm) (ZRC 2020.0348), Java **A** overall view **B** dorsal view of carapace **C** anterior right part of carapace (denuded) **D** frontal view of cephalothorax.

echinoderms, polychaeta, galatheids, fishes, sea anemone, gastropods and bivalves, south of Cilacap, south Java, Indian Ocean, South Java Deep Sea cruise, coll. beam trawl, 30 Mar. 2020 (ZRC 2020.0348); 1 ovigerous ♀ (30.1 × 35.5 mm), station CP51, 7°04.874'S, 106°25.396'E – 7°05.348'S, 106°25.044'E, 569–657 m, substrate coarse sand, mud and some plastic trash, small crabs, ophiuroids, stalk crinoids, chitons, limpets and sea daisies on fallen bamboo, Pelabuhanratu Bay, south Java, Indian Ocean, South Java Deep Sea cruise, coll. beam trawl, 2 Apr. 2020 (ZRC 2020.0349, COI sequence: OK331336).

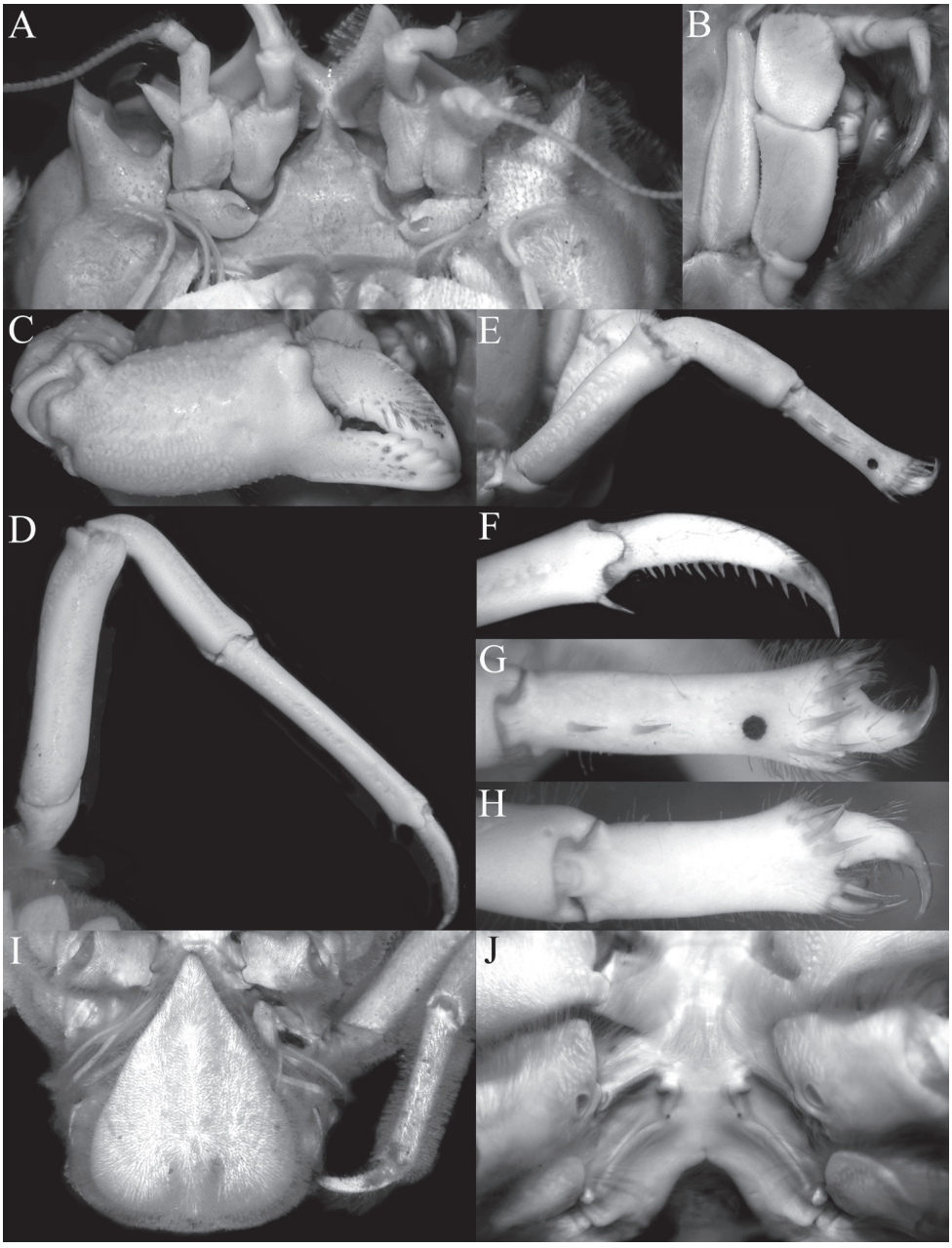

Figure 9. *Dicranodromia karubar* Guinot, 1993. **A–H, J** ♀ (27.1 × 33.4 mm) (ZRC 2020.0348), Java **I** ♀ (27.6 × 33.8 mm) (ZRC 2020.0348), Java **A** epistome, antennules, antennae and orbits **B** left third maxilliped **C** right chela (denuded) **D** right P3 (denuded) **E** right P3 dactylus (denuded) **F** right P5 (denuded) **G** right P5 propodus and dactylus (partially denuded) **H** right P4 propodus and dactylus (partially denuded) **I** telson **J** posterior thoracic sternum showing spermatheca and female gonopores.

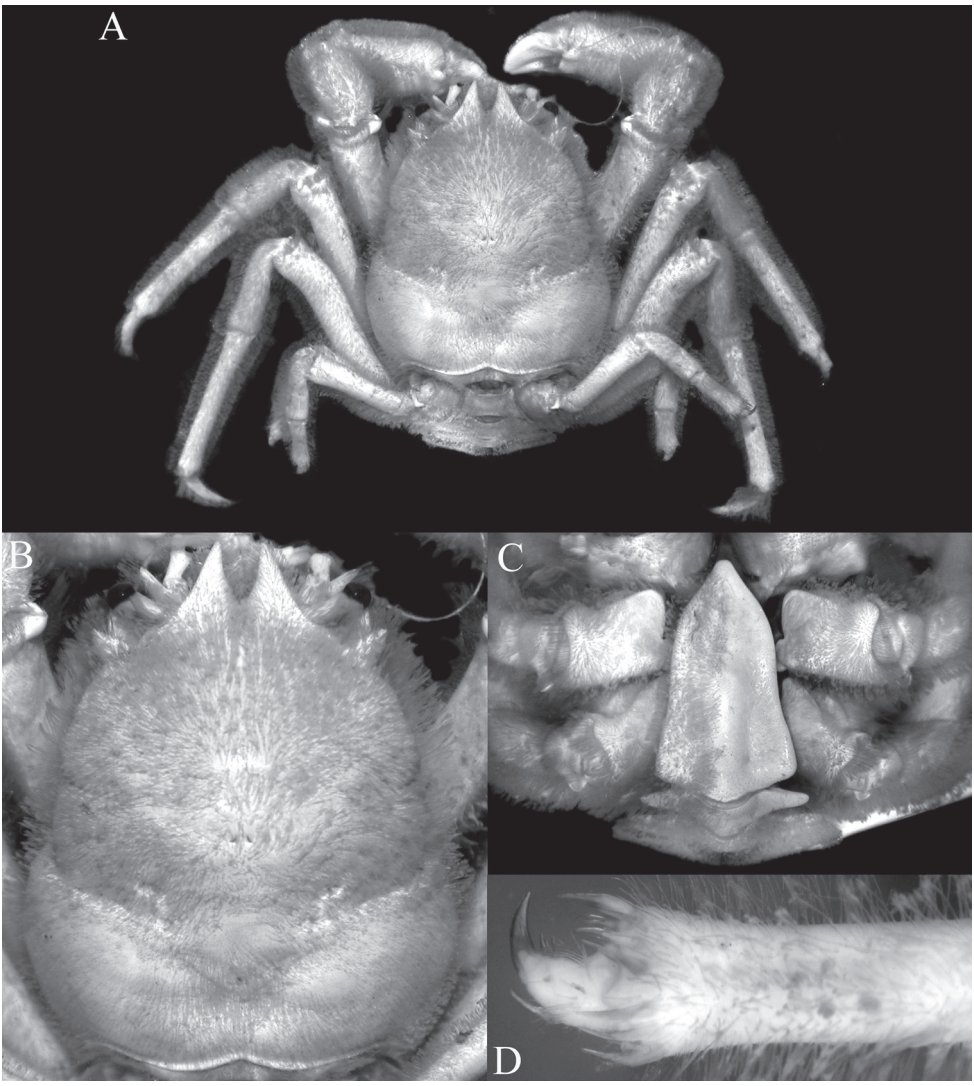

Figure 10. *Dicranodromia karubar* Guinot, 1993. **A–C** ♂ (28.7 × 34.7 mm) (ZRC 2020.0348), Java **D** ♀ (27.6 × 33.8 mm) (ZRC 2020.0348), Java **A** overall view **B** dorsal view of carapace **C** telson **D** left P5 propodus and dactylus.

Remarks. Mendoza et al. (2021) recently recorded *D. karubar* from southern Java, over 1000 km from its type locality in the Moluccas. The specimens, however, agree very well with the descriptions and figures of Guinot (1995) and they are clearly conspecific.

Guinot (1995: 215) noted that the rostrum of this species is at most a tubercle, which is in conformity with the present material. The merus, carpus and dactylus were

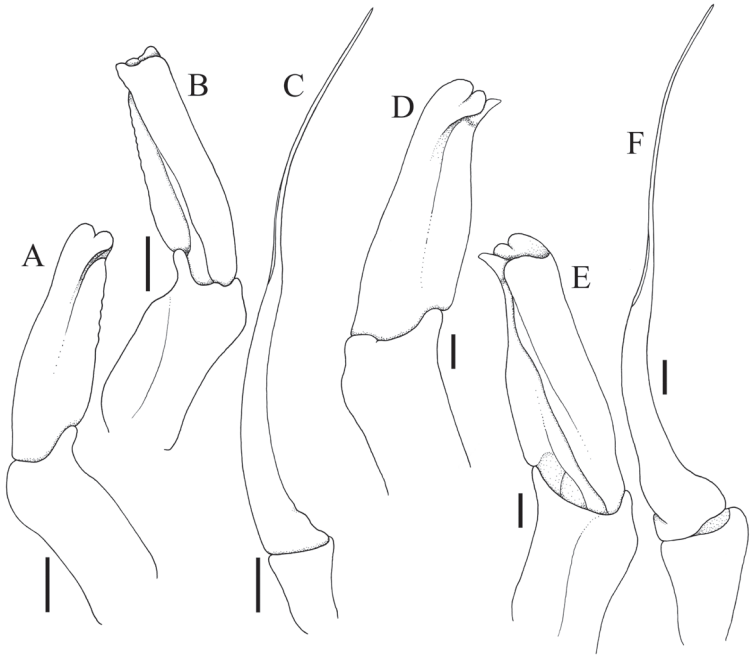

Figure 11.A–C *Dicranodromia martini* Guinot, 1995, ♂ (12.3 × 16.6 mm) (ZRC 2007.0105), Philippines **D–F** *D. karubar* Guinot, 1993, ♂ (28.7 × 34.7 mm) (ZRC 2020.0348), Java **A,D** left G1 (ventral view) **B,E** left G1 (dorsal view) **C,F** left G2. Setae for all structures not figured. Scale bars: 1.0 mm.

described as unarmed by Guinot (1995), but the P5 propodus actually has one or two spines on the outer surface, which are hard to see as the dense plumose setae obscure them. In some specimens, the P5 dactylus has a prominent spine on the extensor margin (Fig. 10D), but as reported by Ng and Naruse (2007), it is absent in others (Fig. 9G, H). The form of the exorbital tooth varies to some degree. In the female specimens, the tooth is clearly directed anteriorly (Fig. 8B, C) but in the male, it is pointed obliquely laterally (Fig. 10B).

The setae on *D. karubar* are unusual in that they are plumose at the distal part (Guinot 1995: fig. 16D). When the animals are freshly collected, the setae lock together to form a dense coat, which traps fine mud and completely obscure the carapace and pereiopod surfaces and margins (Fig. 7A). After the specimen is cleaned gently with a brush and the sediment removed, the surfaces and margins become more visible with the distal plumose parts no longer meshed together. The margins of the pereiopods, however, are still partially obscured as the setae there are denser (Fig. 7B, C). In the form of the setae, *D. karubar* is most similar to *D. baffini* from the Indian Ocean, although the tomentum of the latter species is relatively less dense (cf. Padate et al. 2020: fig. 2a).

Dicranodromia karubar can easily be separated from *D. baffini* by its proportionately broader carapace (Figs 8B, 10B) (versus relatively narrower and longer in *D. baffini*; cf. Guinot 1995: fig. 13, Padate et al. 2020: fig. 2a); the antero- and posterolateral

margins almost smooth, except sometimes for a few scattered granules (Figs 8B, 10B) (versus lined with granules and spinules in *D. baffini*; cf. Guinot 1995: fig. 13, Padate et al. 2020: fig. 2a); and the subdistal lobe on the outer margin of the endopod curved and beak-like (Fig. 11D, E) (versus lobe rounded in *D. baffini*; cf. Padate et al. 2020: fig. 2g, i). Based on the figures of Gordon (1950), Guinot (1995: fig. 16C) commented that the structure of the spermatheca was different in the two species, but we do not discern any major differences since both species possess an unusual and prominent comma-shaped tubercle on each side of sternite 7, with the spermatheca at the base of this tubercle (Fig. 9J). The spermathecal structure in the *D. baffini* from the Andamans (cf. Padate et al. 2020: fig. 2j) is almost identical to the condition observed in *D. karubar* (Fig. 9J). Alcock and Anderson (1899: 8) described the structure as "sternal grooves of the female end, without tubercles, at the level of the openings of the oviducts", which does not match the description and figures of Gordon (1950: 205, text-fig. 1) and Padate et al. (2020: fig. 2j). As noted by Padate et al. (2020: 3), the condition observed by Alcock and Anderson (1899) may be because their specimen was a juvenile.

Dicranodromia karubar is known thus far only from the Moluccas and eastern part of the Indian Ocean while *D. baffini* has been recorded from western India, Maldives and Andamans (Alcock 1899, 1901; Gordon 1950; Padate et al. 2020).

All the females of *D. karubar* collected from the south Javan cruise were ovigerous, the eggs being bright red in life, in a prominent brood pouch (Fig. 7D). One female specimen (27.6 × 33.8 mm, ZRC 2020.0348) had 362 eggs, each about 2.5 mm in diameter.

Dicranodromia danielae Ng & McLay, 2005

Figure 12

Dicranodromia danielae Ng & McLay, 2005: 40, figs 1–4; Ng and Naruse 2007: 47, fig. 3c; Ng et al. 2008: 39.

Material examined. Philippines: holotype ovigerous ♀ (broken, 10.8 × 14.2 mm), Balicasag Island, Panglao, Bohol, Visayas, in tangle nets, ca. 200–300 m, coll. local shell fishermen, 2 Mar. 2004 (ZRC 2005.0094).

Remarks. The broken holotype female was re-examined and some characters need to be added or amended from Ng and McLay (2005). Ng and Naruse (2007: fig. 3c) had already noted that the P5 dactylus has a distinct spine on the extensor margin (Fig. 12F, G); but in addition, the P5 propodus has three spines on the outer surface (Fig. 12G). The P2 and P3 meri were described being unarmed but this is not correct. The extensor margin has low spines while the flexor margin has a row of slender spines partially covered by the dense stiff setae (Fig. 12D). In addition, the basal antennal article is relatively short with the anteroexternal tooth long and subequal in length to the article (Fig. 12C). In addition, the epistome of this species is unusual in that the distal part is strongly spinose, with the median lateral part possessing a sharp anteriorly directed tooth; and the rostrum consists of two lateral

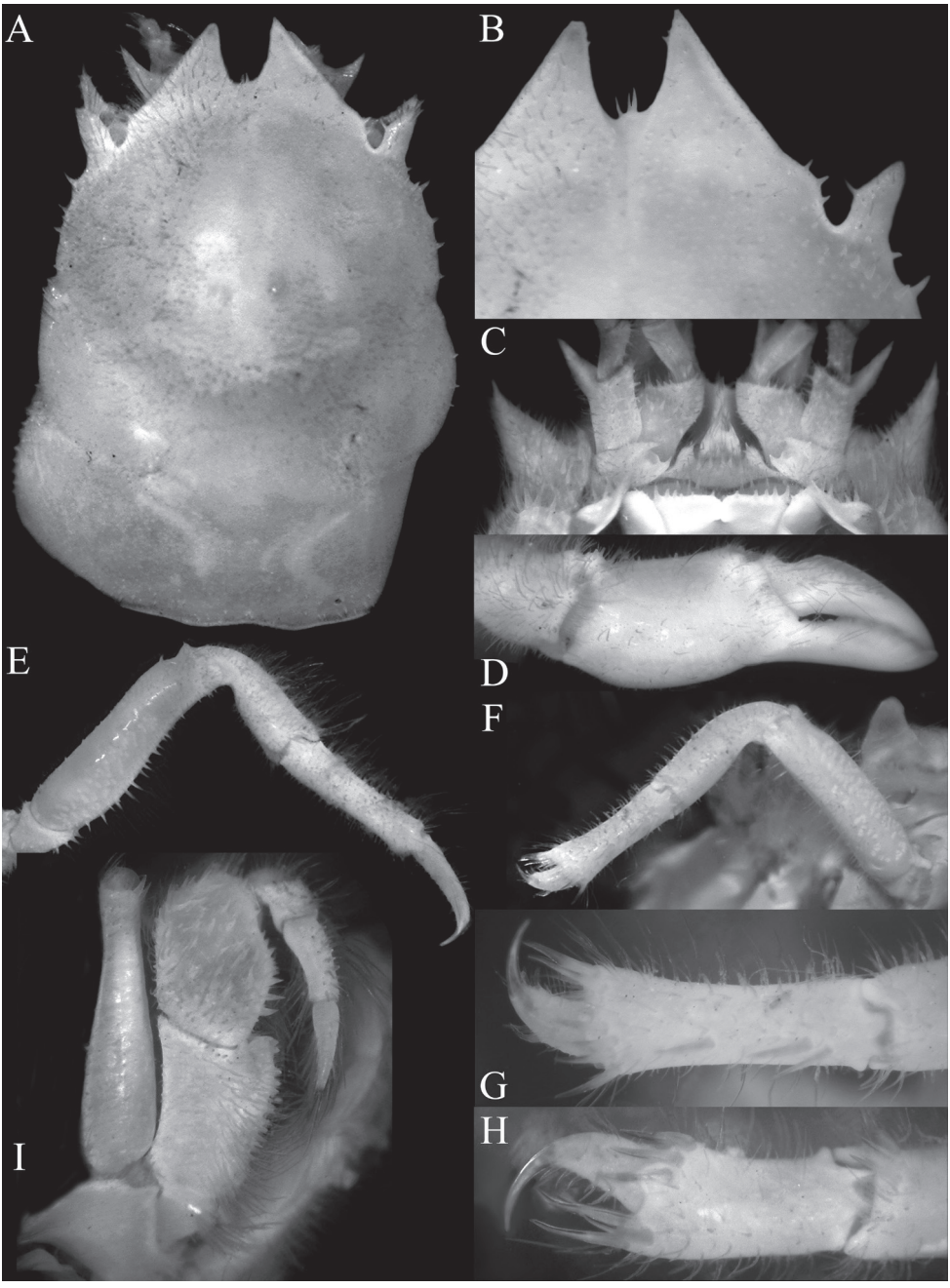

Figure 12. *Dicranodromia danielae* Ng & McLay, 2005, holotype ovigerous ♀ (broken, 10.8 × 14.2 mm) (ZRC 2005.0094), Philippines **A** dorsal view of carapace **B** frontal region showing rostrum **C** epistome, antennules, antennae and orbits **D** right chela **E** right P3 **F** left P5 **G** left P5 propodus and dactylus **H** left P4 propodus and dactylus **I** right third maxilliped.

and one median slender spinules (Fig. 12B, C). The merus of the third maxilliped is distinctive, being strongly spinose, with the inner margin lined with strong spines; the exopod is essentially unarmed (Fig. 12I).

Some of the characters of *D. danielae* resemble the male specimen 9.7 × 14.0 mm from Uraga Strait in Japan (35°4.833'N, 139°38.3'E) which Guinot (1995: 207, fig. 11b) referred to "*Dicranodromia* aff. *doederleini*". She described the carapace, proepistome, antennae, antennules, buccal frame, ventral surfaces and merus of the third maxilliped are being more spiny than typical *D. doederleini* even though the outer surface of the chela was smooth. The more spinous features of the specimen (notably the ventral surfaces, antennae, epistome and third maxillipeds), resemble the condition in *D. danielae*, but whether the flexor margin of the pereiopods of the specimen was also spinous was not stated. In addition, the carapace of *D. danielae* is less spinous compared to that figured by Guinot (1995: fig. 11b) for her "*Dicranodromia* aff. *doederleini*". It would appear that this Japanese specimen is a species close to, but probably different from, *D. danielae*.

***Dicranodromia erinaceus* sp. nov.**

http://zoobank.org/C1BEA5CC-F350-47D1-8A66-ECBFC3606197

Figures 7E, F, 13–16, 21A, B, D–F, K–M

Dicranodromia doederleini – Ho et al. 2004: 643, fig. 1B; Ahyong et al. 2009: 129, fig. 93 (not fig. 94); Ng et al. 2017: 27 (list). (non *Dicranodromia doederleini* Ortmann, 1892)

Material examined. TAIWAN: holotype ♀ (14.0 × 18.0 mm), station CP4091, 22°14'N, 119°59'E, among numerous mud tubes, off small Liu-Qiu Island, southeast Taiwan, 974–994 m, coll. N.O. Ocean Researcher 1, 27 May 2013 (NTOU B00126); paratypes 2 ♀♀ (13.2 × 17.6 mm, 13.8 × 18.5 mm), same data as holotype (ZRC 2020.0467, COI sequence: OK351335); 1 ♂ (6.9 × 9.5 mm), station CP4212, 22°18.34'N, 119°59.51'E, southwestern Taiwan, 961–1008 m, coll. T.-Y. Chan, 15 Nov. 2020 (ZRC 2021.0084, COI sequence: OK331334); 1 ♂ (8.2 × 12.5 mm), station CP4212, 22°18.34'N, 119°59.51'E, southwestern Taiwan, 961–1008 m, coll. T.-Y. Chan, 15 Nov. 2020 (ZRC 2021.0085). Others: 1 ♀ (7.5 × 11.1 mm, carapace badly damaged), 24°26.9'N, 122°18.1'E, Taiwan, 638–824 m, coll. R/V "Fishery Researcher 1", 4 August 2000 (NTOU B00127).

Diagnosis. Carapace longitudinally subovate, widest across intestinal-mesobranchial regions; dorsal surface prominently convex, lateral surfaces covered with numerous spinules, those on median part relatively lower, sometimes granular, with short stiff setae, denser on lateral parts but not obscuring margins; short stiff setae present on pereiopods, thoracic sternum and pleon but not obscuring surface or margins.

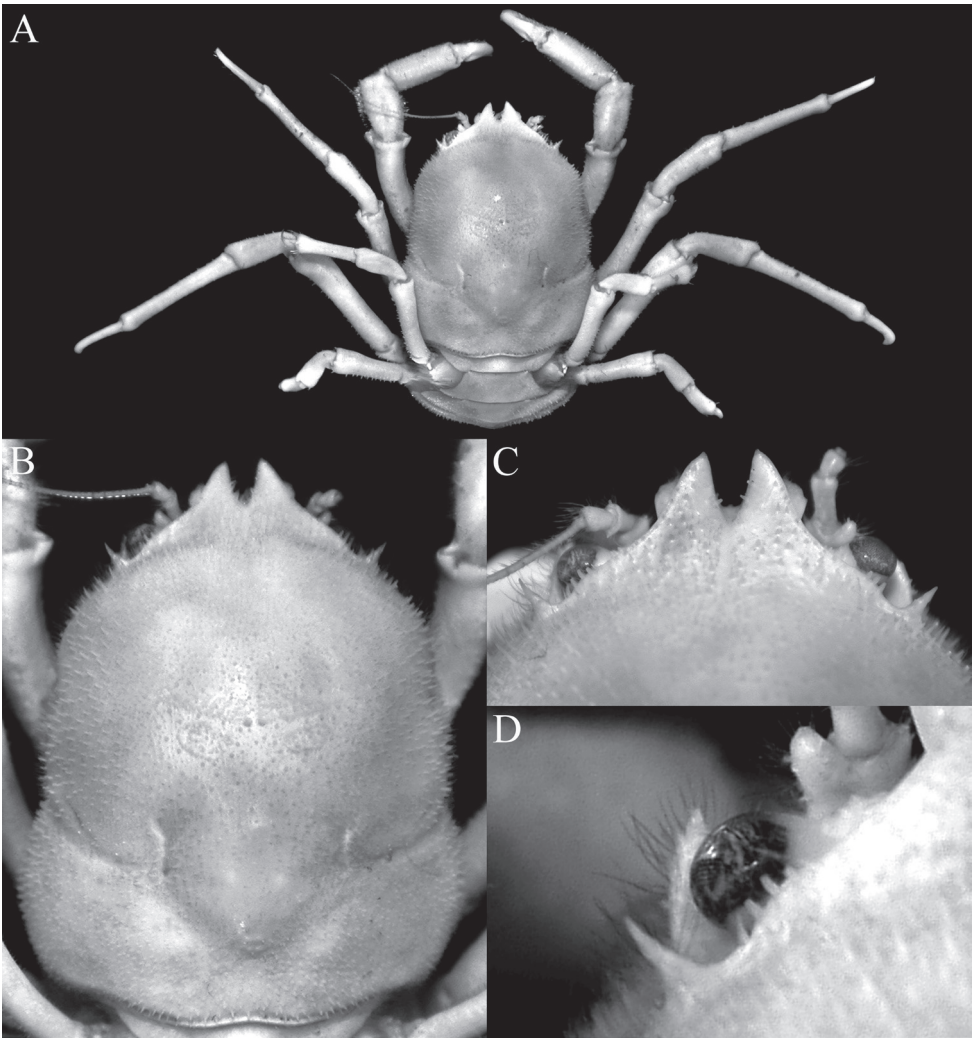

Figure 13. *Dicranodromia erinaceus* sp. nov., holotype ♀ (14.0 × 18.0 mm) (NTOU B00126), Taiwan **A** overall view **B** dorsal view of carapace **C** front and anterior part of carapace **D** left orbit and first anterolateral spine.

Branchiocardiac groove distinct, curving medially anteriorly. Each pseudorostral lobe triangular, inner margin straight, outer margin gently convex, directed anteriorly, inner margin with two or three spinules; exorbital tooth spiniform, directed obliquely laterally, anterior margin with two or three spinules; supraorbital margin separated from external orbital tooth by shallow concave cleft, posterior part with three spines; infraorbital margin with prominent triangular lobe, posterior margin with spinules, just visible in dorsal view. Rostrum present as one or two longer spinules in small specimens, barely discernible or just visible as a sharp granule in larger specimens. Epistome covered with spinules on anterior half; posterior half gently upturned, with

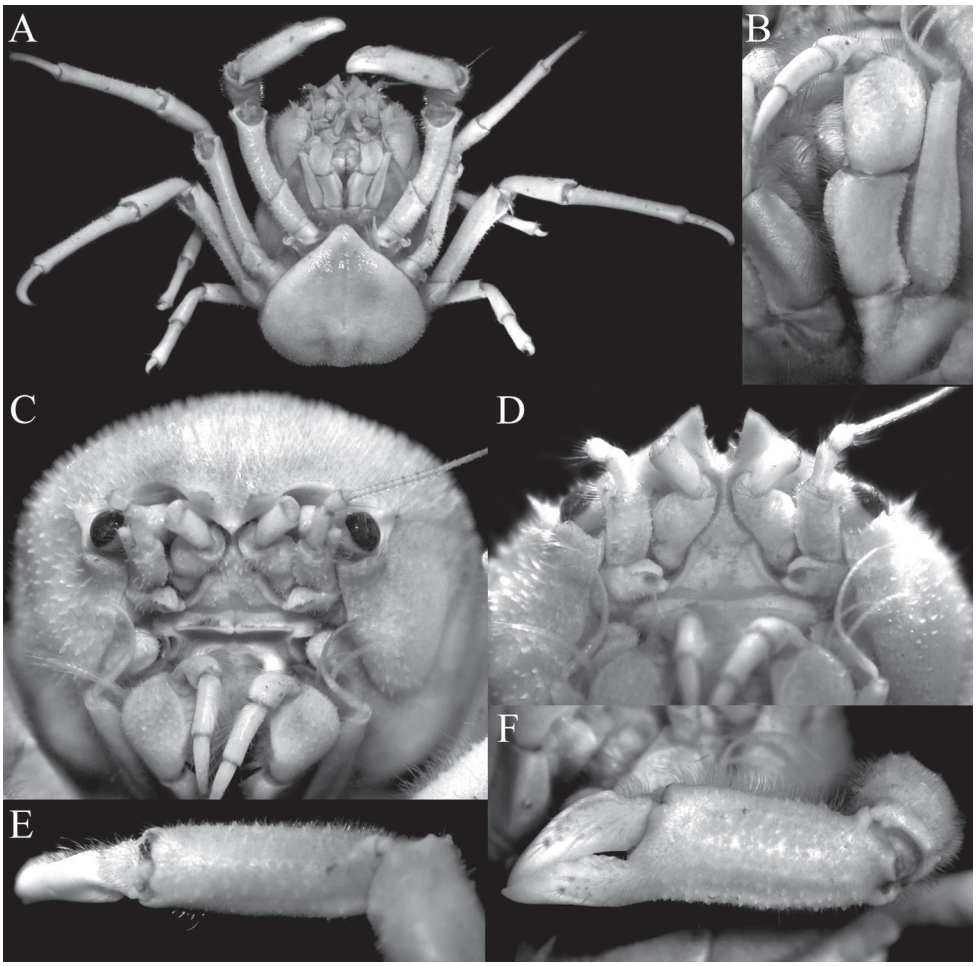

Figure 14. *Dicranodromia erinaceus* sp. nov., holotype ♀ (14.0 × 18.0 mm) (NTOU B00126), Taiwan **A** ventral view of cephalothorax **B** left third maxilliped **C** frontal view of cephalothorax **D** epistome, antennules, antennae and orbits **E** dorsal view of right chela **F** left chela.

median fissure, surface not covered with spinules, posterior margin entire. Basal antennal article subquadrate; surfaces covered by spinules and granules; anteroexternal tooth short. Eyes with short peduncle. Third maxilliped relatively narrow; merus subovate with low anterointernal lobe, slightly shorter than ischium; ischium subtrapezoidal, distal half wider than proximal part with inner margin convex; palp (carpus, propodus, dactylus) long, reaching to median part of ischium when folded; exopod with proximal third widest, outer margin with low sharp granules on proximal third. Chelipeds densely covered with stiff setae on most parts; merus and carpus with outer surface and margins lined with spinules and granules; palm relatively short, outer surface and margins covered with numerous sharp granules; fingers thick, wide, occluding surface hollowed; pollex with deep U-shaped depression distally. P2 and P3

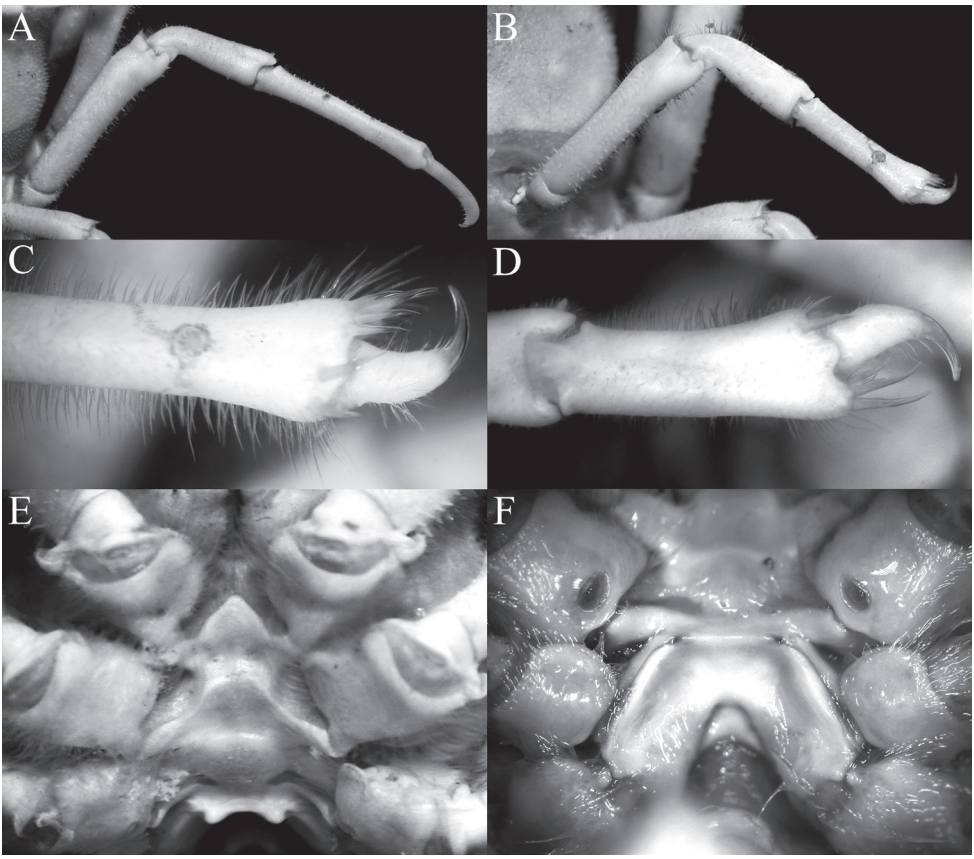

Figure 15. *Dicranodromia erinaceus* sp. nov. **A–E** holotype ♀ (14.0 × 18.0 mm) (NTOU B00126), Taiwan **F** paratype ♀ (13.8 × 18.5 mm) (ZRC 2020.0467), Taiwan **A** right P3 **B** right P5 **C** right P5 propodus and dactylus **D** right P4 propodus and dactylus **E** anterior thoracic sternum and spermatheca **F** posterior thoracic sternum showing spermatheca and female gonopores.

relatively long, P3 longer than P2; merus with low tooth on distal extensor margin, length to width ratio of P2 and P3 merus 5.2 and 4.5, respectively; proximal part of extensor margin with low spinules, flexor margin with numerous spinules; propodus almost straight, unarmed, length to width ratio of P2 and P3 propodus 6.7 and 8.0, respectively; dactylus sickle-shaped, flexor margin lined with 15 or 16 spines, terminating in strongly incurved claw, propodus about twice length of dactylus. P4 stouter, shorter than P5; length to width ratio of P4 and P5 merus 3.5 and 5.0, respectively; proximal part of extensor margin of merus with low spinules, flexor margin with numerous spinules; P4 and P5 propodus without median spinules on outer surface, length to width ratio of P4 and P5 propodus 3.5 and 4.7, respectively, distal margin fringed by sharp spines bracketing dactylus; dactylus claw-like, strongly incurved, extensor margin unarmed, flexor margin unarmed or with two weak spines. Thoracic sternite 7 with strong transverse ridge from posterior inner part of female gonopore,

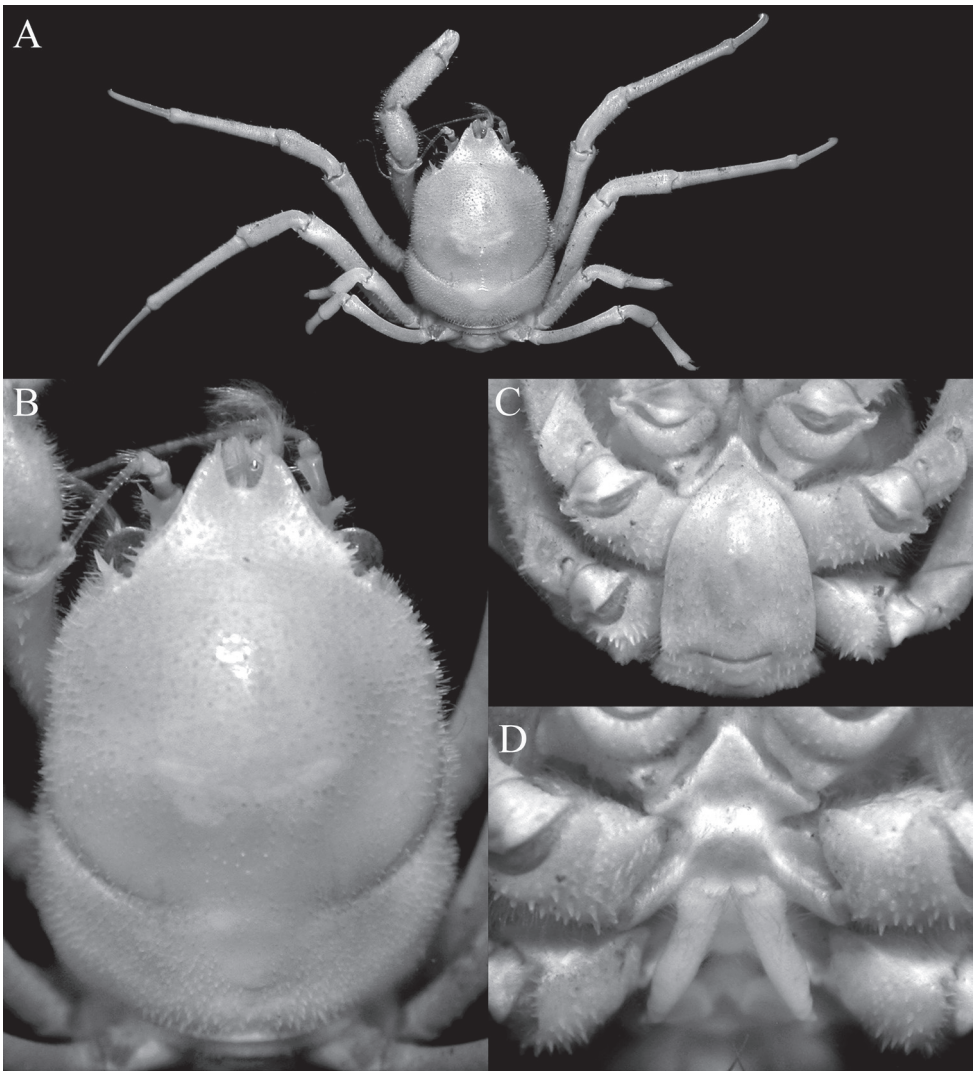

Figure 16. *Dicranodromia erinaceus* sp. nov., paratype ♂ (8.2 × 12.5 mm) (ZRC 2021.0085), Taiwan **A** overall view **B** dorsal view of carapace **C** pleon **D** anterior thoracic sternum and G1s in situ.

lateral part raised, forming triangular tubercle, curving posteriorly to join oblique ridge formed by sternites 7 and 8 with distinct groove between them that leads to spermathecal aperture at centre of triangular tubercle. Male and female pleons with six free somites and telson; male telson distinctly subovate; female telson wide, triangular, with gently sinuous margins. G1 stout, endopod distally covered by dense long setae, subdistal part of outer margin with two lobes, proximal lobe larger, prominent; G2 endopod gradually tapering to sharp tip.

Variation. None of the specimens examined had a spine or spinule on the extensor margin of the P5 dactylus; and outer surface of the P5 propodus was also unarmed

(Fig. 21E). Most of the flexor margins of the dactylus were not armed with obvious spines or spinules, although two or three stout setae may be present.

Etymology. The species is named after the hedgehog, *Erinaceus*, alluding to the spiny appearance of the carapace and legs. The name is used as a noun in apposition.

Remarks. *Dicranodromia erinaceus* sp. nov. belongs to the same group of species as *D. spinulosa* and *D. delli* in its spinose carapace surface and pereiopods, slender and spiniform exorbital tooth, and an acutely triangular suborbital tooth. *Dicranodromia erinaceus* is most similar to *D. delli* from New Zealand but can be distinguished by the ischium of the third maxilliped being relatively shorter and wider especially at the distal half (Fig. 14B) (versus more slender and rectangular in *D. delli*, cf. Ahyong 2008: fig. 4C); proportionately shorter P2 and P3 (e.g., P3 merus 4.5× longer than wide, propodus 8.0× longer than wide, Figs 13A, 15A) (versus P3 merus 6.6× longer than wide, propodus 11.1× longer than wide in *D. delli*, cf. Ahyong 2008: fig. 2A, 3D); the proportionately shorter and stouter P4 and P5 (e.g., P5 merus just reaches the branchiocardiac groove in dorsal position, Figs 13A, 15B) (versus longer and more slender, extending beyond branchiocardiac groove in dorsal position in *D. delli*, cf. Ahyong 2008: fig. 2A, B); the relatively stouter palm (Fig. 14F) (versus more slender in *D. delli*, cf. Ahyong 2008: fig. 3B); and the proportionately wider female telson (Fig. 14A) (versus less wide in *D. delli*, cf. Ahyong 2008: fig. 3C). The holotype and only known specimen of *D. delli*, an ovigerous female 15.5 × 19.0 mm from Nukuliau Seamount in New Zealand, is comparable in size to the ovigerous female holotype of *D. erinaceus* (14.0 × 18.0 mm) so the differences are not size-related. The characters of P2–P5 and third maxilliped are also obvious in the smaller female paratype of *D. erinaceus* as well as in the smaller male paratypes.

Compared to *D. spinulosa*, *D. erinaceus* can be separated by the carapace being proportionately wider (Figs 13B, 16B) (versus carapace transversely narrower in *D. spinulosa*, cf. Guinot 1995: fig. 21a; Ahyong 2008: fig. 1C); the median dorsal surface of the carapace covered with low sharp granules (Figs 13B, 16B) (versus covered with spinules in *D. spinulosa*, cf. Guinot 1995: fig. 21a; Ahyong 2008: fig. 1C); the submarginal surface of the posterior margin of the epistome is unarmed (Fig. 14C, D) (versus area armed with short spines in *D. spinulosa*, cf. Guinot 1995: fig. 22B); the ischium of the third maxilliped relatively shorter and wider especially at the distal half (Fig. 14B) (versus more slender and rectangular in *D. spinulata*, cf. Guinot 1995: fig. 21c); the relatively longer P2 and P3 (e.g., P3 propodus 8.0× longer than wide, Figs 13A, 15A) (versus P3 propodus less than 7× longer than wide), the P2 and P3 propodus twice the length of the dactylus (Fig. 15A) (versus 1.7× in *D. spinulosa*; Guinot 1995: fig. 21a; Ahyong 2008: fig. 1C); and the male telson subovate in shape (Fig. 16C) (versus triangular in *D. spinulosa*, cf. Guinot 1995: figs 21c, 25D). *Dicranodromia spinulosa* was described from three males and one female from New Caledonia, the holotype female being 7.5 × 11.0 mm; a size comparable to that of the male specimens of *D. erinaceus* we examined.

Ho et al. (2004) recorded *D. doederleini* from Taiwan from one badly damaged female specimen from northeastern Taiwan (see also Ahyong et al. 2009). The specimen is now referred to *D. erinaceus*.

***Dicranodromia robusta* sp. nov.**
http://zoobank.org/ADCE5085-D836-4A3E-8CF9-5BEB79ED3FE1
Figures 17–20, 21C, G–J, N–P

Material examined. Philippines: ***Holotype*** ♀ (19.6 × 26.4 mm), ca. 5°24'N, 125°22.5'E, Balut Island, Sarangani Islands, Davao Occidental Province, south of Mindanao Island, coll. tangle nets, local fishermen, 26 Nov. 2017 (ZRC 2018.0161); ***Paratype*** ♂ (15.2 × 21.0 mm), same location as holotype, coll. tangle nets, local fishermen, 2017 (ZRC 2018.0095).

Diagnosis. Carapace longitudinally subquadrate, widest across intestinal-mesobranchial regions; dorsal surface gently convex, lateral surfaces covered with low spinules, median part smooth, margins with scattered short stiff setae, not obscuring margins; short stiff setae present on pereiopods, thoracic sternum and pleon but not obscuring surface or margins. Branchiocardiac groove distinct, curving medially anteriorly. Each pseudorostral lobe triangular, inner margin straight, outer margin gently convex, directed anteriorly, inner margin entire; exorbital tooth dentiform, directed obliquely laterally, anterior margin with two or three spinules; supraorbital margin separated from external orbital tooth by shallow concave cleft, posterior part with five or six spinules; infraorbital margin with large dorsoventrally flattened lobe which is dentiform to linguiform, larger than exorbital tooth, distal part with spine, anterior margin with two spinules, prominently visible in dorsal view. Rostrum present as one sharp granule. Epistome covered with scattered granules on anterior half; posterior half gently upturned, with median fissure, surface not covered with spinules, posterior margin gently convex, median part entire, lateral part gently serrate. Basal antennal article subquadrate; surfaces covered by spinules and granules; anteroexternal tooth short. Eyes with long peduncle. Third maxilliped relatively narrow; merus subovate with low anterointernal lobe, shorter than ischium; ischium subtrapezoidal, distal half slightly wider than proximal part; palp (carpus, propodus, dactylus) long, reaching to median part of ischium when folded; exopod with proximal third widest. Chelipeds covered with stiff setae on most parts; merus and carpus with margins uneven or lined with granules; palm relatively short, subdorsal and subventral margins with low sharp granules, median part smooth; fingers thick, wide, occluding surface hollowed; pollex with deep U-shaped depression distally. P2 and P3 relatively short, P3 longer than P2; merus with low tooth on distal extensor margin, length to width ratio of P2 and P3 merus 4.2 and 3.9, respectively; margins unarmed; propodus almost straight, unarmed, length to width ratio of P2 and P3 propodus 5.2 and 6.4, respectively; dactylus curved, flexor margin lined with 8 or 9 spines, terminating in strongly gently curved claw, propodus about 2.4× length of dactylus. P4 stouter, shorter than P5; length to width ratio of P4 and P5 merus 2.4 and 3.4, respectively; margins of merus unarmed; P4 and P5 propodus with submedian spinule on distal third of outer surface, length to width ratio of P4 and P5 propodus 2.3 and 3.6, respectively, distal margin fringed by sharp spines bracketing dactylus; dactylus claw-like, strongly incurved, extensor margin with median spine or absent, flexor margin with 2–4 spines. Thoracic sternite 7 with low transverse ridge from posterior

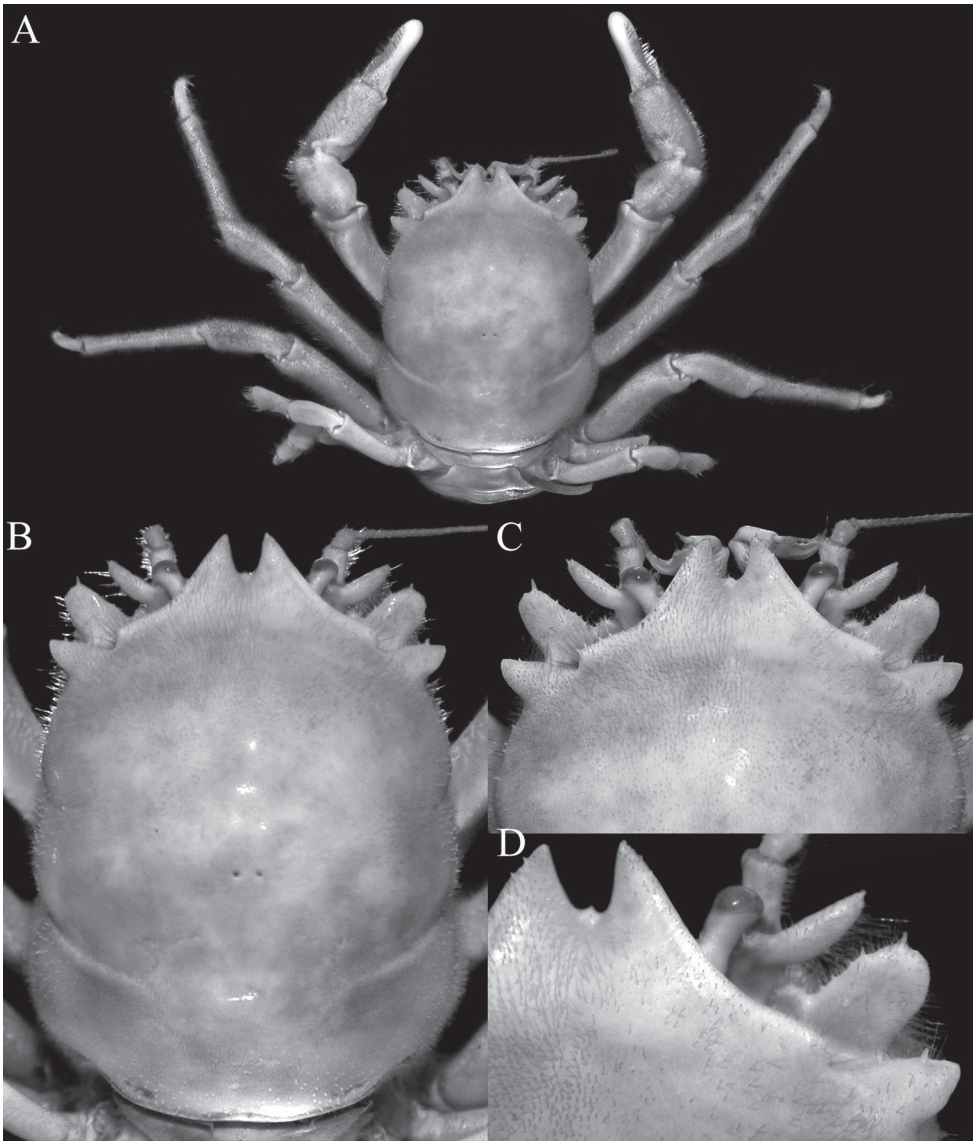

Figure 17. *Dicranodromia robusta* sp. nov., holotype ♀ (19.6 × 26.4 mm) (ZRC 2018.0161), Philippines **A** overall view **B** dorsal view of carapace **C** front and anterior part of carapace **D** right front, orbit and first anterolateral spine

inner part of female gonopore, lateral part high, forming triangular tubercle, curving posteriorly to join oblique ridge formed by posterior part of sternite 7, just before suture with sternite 8, groove between sternites 7 and 8 curve to join spermathecal aperture at base of triangular tubercle. Male and female pleons with 6 free somites and telson; male telson distinctly elongate, triangular with gently convex lateral margins; female telson triangular, with gently convex margins. G1 stout, endopod distally covered by dense

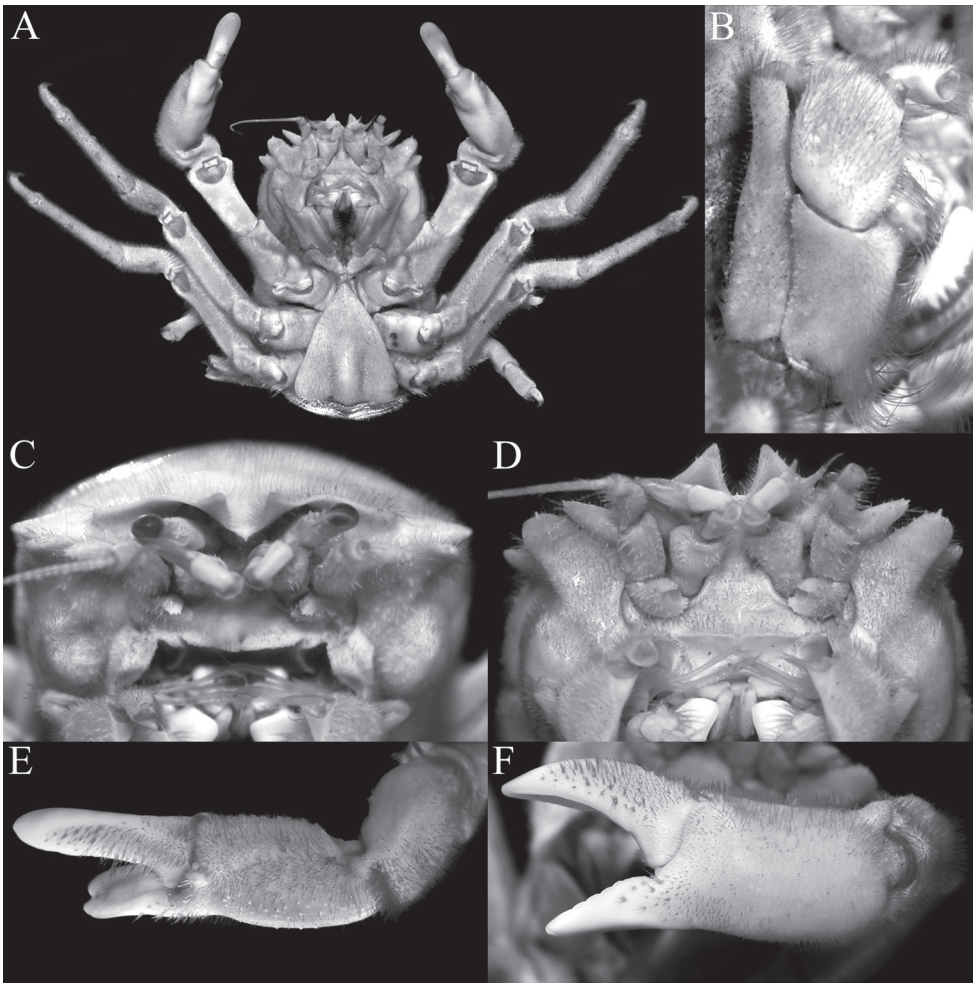

Figure 18. *Dicranodromia robusta* sp. nov., holotype ♀ (19.6 × 26.4 mm) (ZRC 2018.0161), Philippines **A** ventral view of cephalothorax **B** left third maxilliped **C** frontal view of cephalothorax **D** epistome, antennules, antennae and orbits **E** dorsal view of left chela **F** left chela.

long setae, subdistal part of outer margin with two lobes, the distal one being more prominent; G2 endopod gradually tapering to sharp tip.

Variation. In the holotype female, the left P5 dactylus has a prominent spine on the extensor margin (Fig. 21I), but there is none on the right side (Fig. 21H). The P5 dactyli of the paratype male are armed a spinule on the extensor margin. Both specimens possess the spine on the outer surface of the P5 propodus (Fig. 21H, I).

Etymology. The species is named after the Latin *robusta* for stout, alluding to the stocky appearance of the species.

Remarks. The most diagnostic character of *D. robusta* sp. nov. is the large dorsoventrally flattened infraorbital tooth, which is dentiform to linguiform, clearly visible

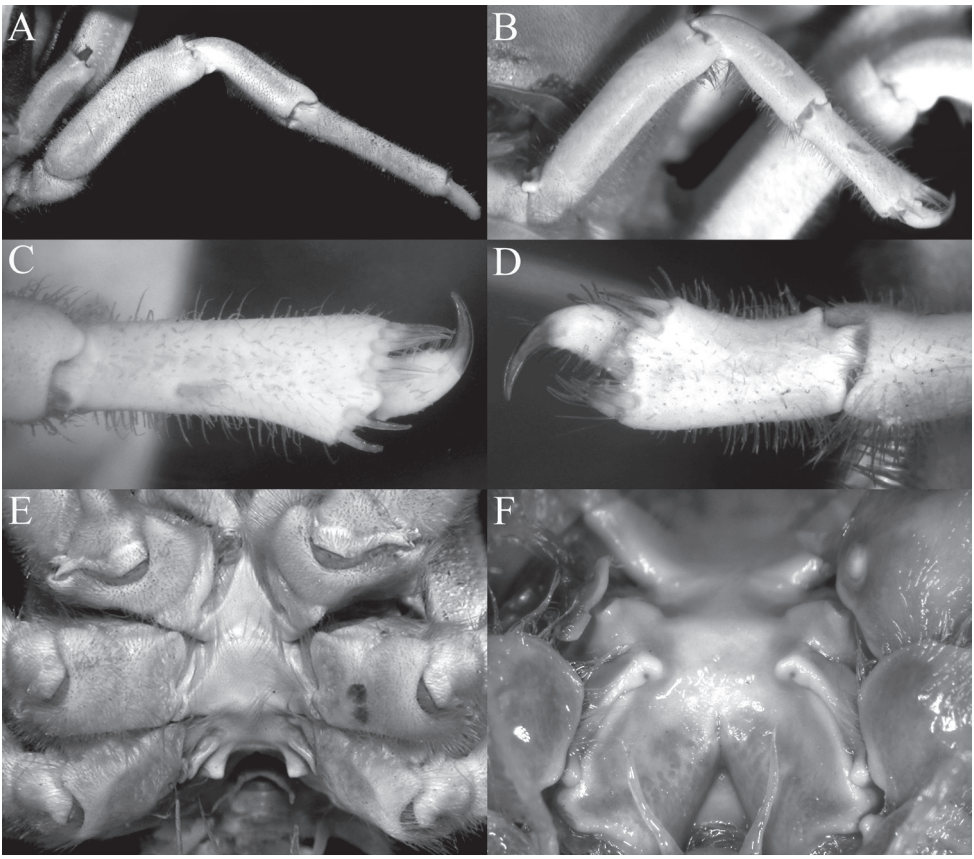

Figure 19. *Dicranodromia robusta* sp. nov., holotype ♀ (19.6 × 26.4 mm) (ZRC 2018.0161), Philippines **A** right P3 **B** right P5 **C** right P5 propodus and dactylus **D** left P4 propodus and dactylus **E** anterior thoracic sternum and spermatheca **F** posterior thoracic sternum showing spermatheca.

in dorsal view, and distinctly larger than the exorbital tooth (Figs 17B–D, 20B). No other Indo-West Pacific species of *Dicranodromia* has such a large and wide infraorbital tooth. The long anteroexternal tooth on the basal antennal article allies *D. robusta* with *D. martini* (cf. Guinot 1995: fig. 20B), *D. baffini* (cf. Alcock 1899: pl. 2 fig. 1a; Alcock 1901: pl. 1 fig. 1a), *D. danielae* (cf. Ng and McLay 2005: fig. 3A, B) and *D. chenae* (cf. Ng and Naruse 2007: fig. 5b) but the structure of the infraorbital tooth easily distinguishes it from them.

The carapace shape of *D. robusta* is distinctly more quadrate (Figs 17A, B, 20A, B) than the more pyriform *D. martini* described from the Philippines (cf. Figs 4A, C, 6A, B; Guinot 1995: fig. 19b; Ng and Naruse 2007: fig. 1a–c); the posterior margin of the epistome is entire (Fig. 18C) (versus margin gently crenulate in subventral view in *D. martini*, cf. Guinot 1995: fig. 20B); P2 and P3 are prominently shorter with the dactylus especially short (e.g., P3 merus 3.9× longer than broad, propodus 6.4× longer than broad, Fig. 19A) (versus P3 merus 7.0× longer than broad, propodus 7.2× longer

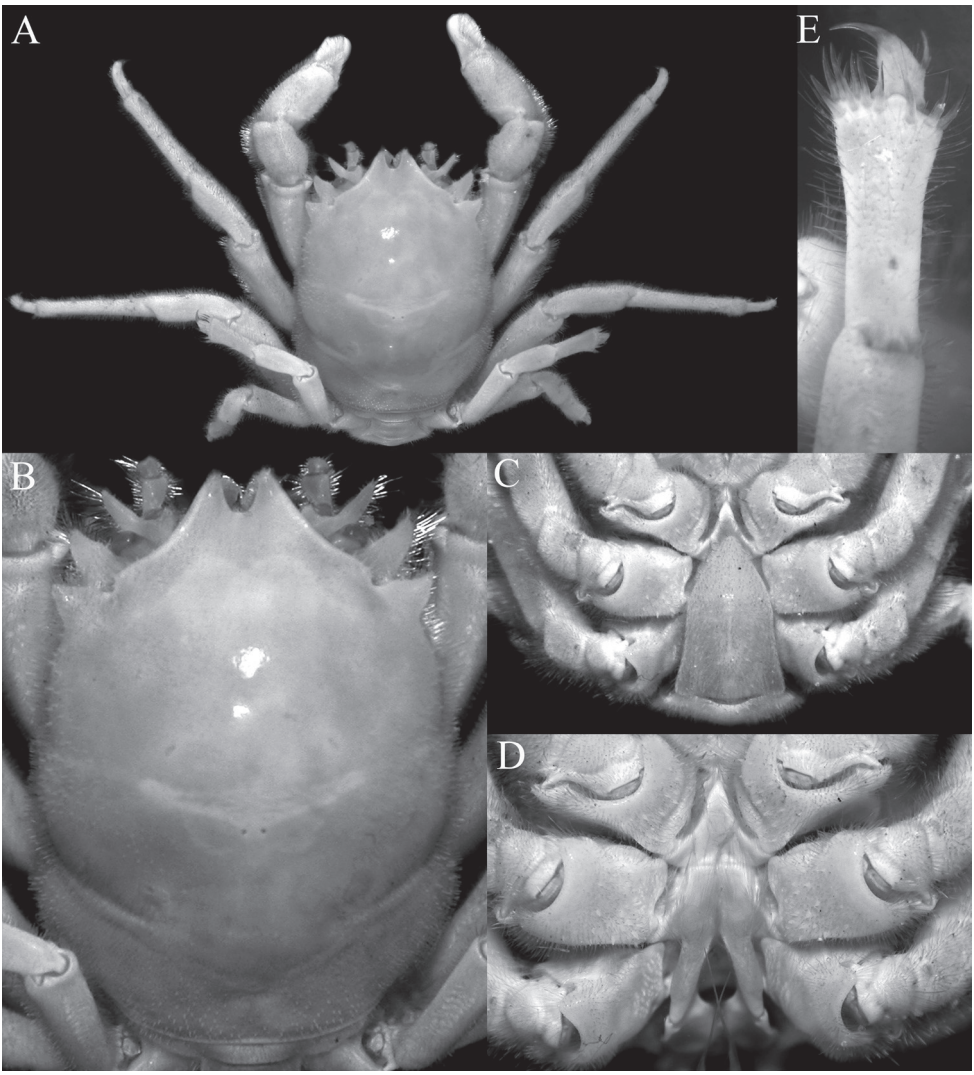

Figure 20. *Dicranodromia robusta* sp. nov., paratype ♂ (15.2 × 21.0 mm) (ZRC 2018.0095), Philippines **A** overall view **B** dorsal view of carapace **C** pleon **D** anterior thoracic sternum and G1s in situ.

than broad in *D. martini*, cf. Figs 4A, 5C, 6A; Guinot 1995: figs 19a, e, 20C); P4 and P5 are much shorter (e.g., P4 merus just reaching branchiocardiac groove when folded dorsally, Figs 17A, 19B, 20A) (versus P4 merus long, reaching beyond branchiocardiac groove when folded dorsally in *D. martini*, cf. Figs 4A, 5D, 6A; Guinot 1995: fig. 19a); and the male telson is lingulate (Fig. 20C) (versus more elongate in *D. martini*, cf. Fig. 6D; Guinot 1995: fig. 19c).

Compared to *D. baffini* from the Indian Ocean, *D. robusta* has a more quadrate carapace (Figs 17A, B, 20A, B) (versus more pyriform in *D. baffini*, cf. Alcock 1899: pl. 2 fig. 1a; Guinot 1995: fig. 13; Padate et al. 2020: fig. 2a); and the P2 and P3 dactylus

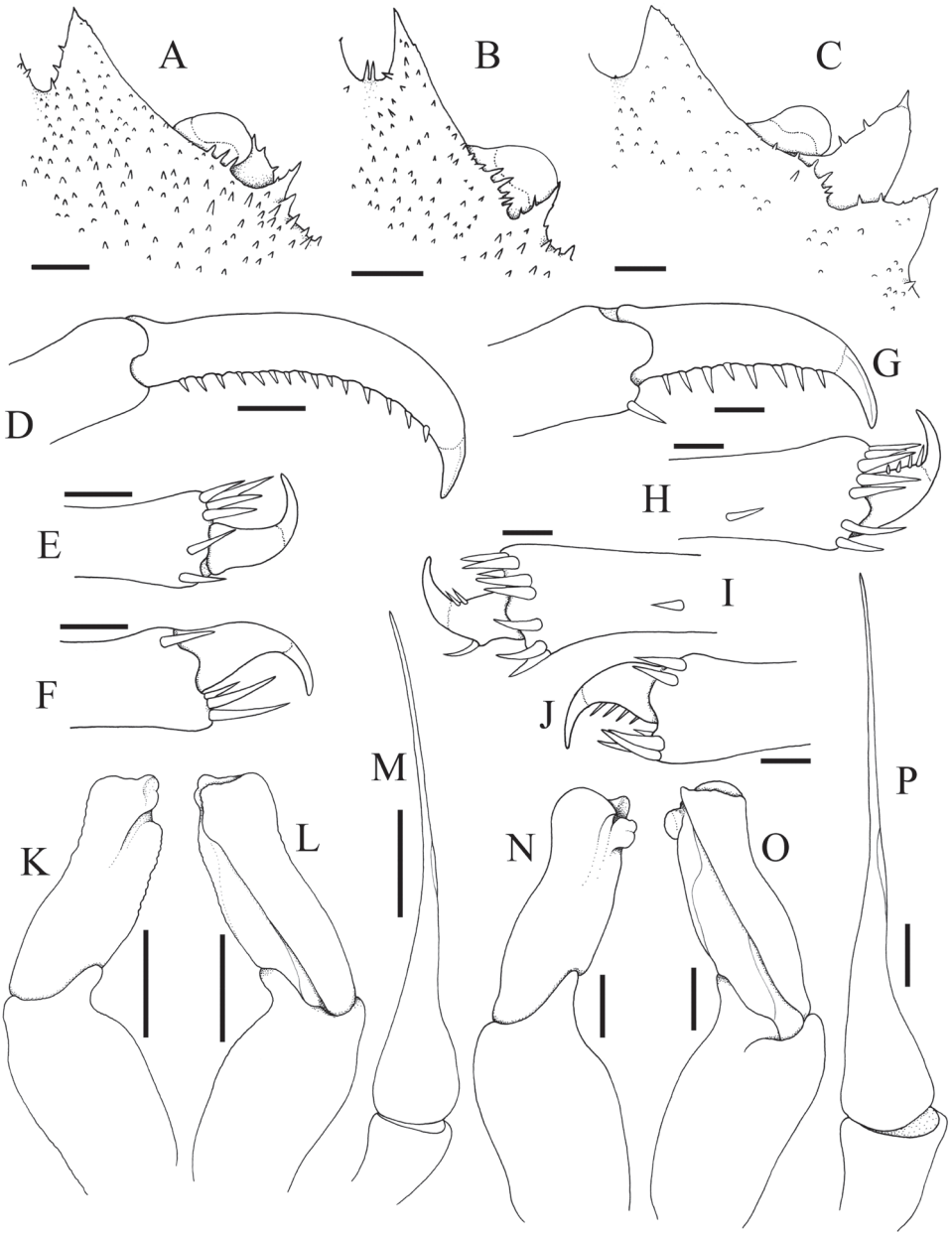

Figure 21. A *Dicranodromia erinaceus* sp. nov., holotype ♀ (14.0 × 18.0 mm) (NTOU B00126), Taiwan **B, D–F, K–M** *D. erinaceus* sp. nov., paratype ♂ (8.2 × 12.5 mm) (ZRC 2021.0085), Taiwan **C, G–J, N–P** *D. robusta* sp. nov., paratype ♂ (15.2 × 21.0 mm) (ZRC 2018.0095), Philippines **A–C** right anterior part of carapace (setae removed or not drawn) **D** right P3 propodus and dactylus **E** right P5 propodus and dactylus **F** right P4 propodus and dactylus **G** right P3 propodus and dactylus **H** right P5 propodus and dactylus **I** left P5 propodus and dactylus **J** left P4 propodus and dactylus **K, N** left G1 (ventral view) **L, O** left G1 (dorsal view) **M, P** left G2. Setae for all structures not figured. Scale bars: 1.0 mm.

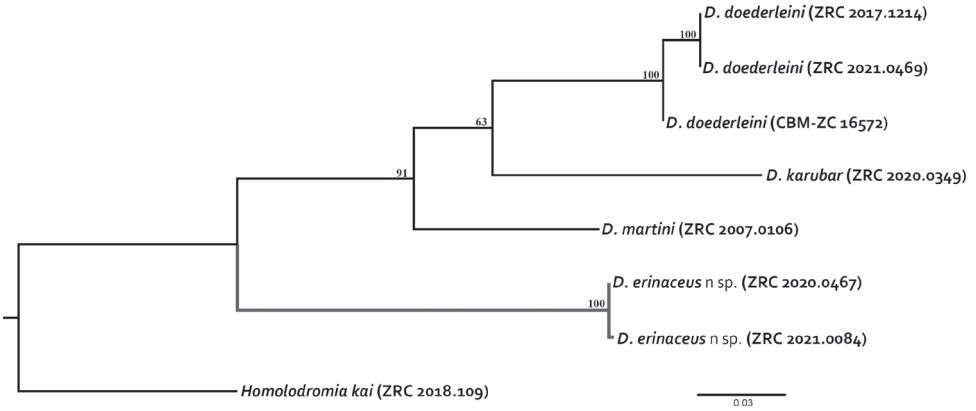

Figure 22. Maximum likelihood phylogenetic tree for *Dicranodromia erinaceus* sp. nov. based on the COI gene dataset. *Homolodromia kai* Guinot, 1993 was chosen as outgroup. Maximum likelihood bootstrap value is represented as above the branches. Values less than 50 are not shown.

is distinctly shorter (Figs 19A, 21G) (versus longer in *D. baffini*, cf. Alcock 1899: pl. 2 fig. 1a; Guinot 1995: fig. 13). With regards to the relatively shorter P2 and P3 dactyli, *D. robusta* resembles *D. chenae*, described from a single large ovigerous female from the central Philippines. *Dicranodromia robusta*, however, can easily be distinguished in having the outer margin of the pseudorostral lobe is almost straight and the structure is directed anteriorly (Figs 17B–D, 20B) (versus outer margin of the pseudorostral lobe is distinctly convex with the structure gradually curved inwards towards the median in *D. chenae*, cf. Ng and Naruse 2007: fig. 5A); the ischium of the third maxilliped is short and rectangular (Fig. 18B) (versus distinctly longer and more slender in *D. chenae*, cf. Ng and Naruse 2007: fig. 5b); the female telson is relatively more elongate (Fig. 18A) (versus proportionately wider and shorter in *D. chenae*, cf. Ng and Naruse 2007: fig. 2b); and the spermatheca is on the prominently raised part around the suture between sternites 7 and 8 and ends at the centre of the triangular tubercle on sternite 6 (Fig. 19F) (versus spermatheca is not prominently raised and ends at the base of the triangular tubercle in *D. chenae*, cf. Ng and Naruse 2007: fig. 8).

Dicranodromia robusta can be separated from *D. danielae* in having the exorbital tooth distinctly triangular to linguiform (Figs 17B–D, 21C) (versus subtrapezoidal in *D. danielae*, cf. Fig. 12A, B; Ng and McLay 2005: figs 1B, 4A); the posterior margin of the epistome is entire (Fig. 18C) (versus clearly serrate in *D. danielae*, cf. Fig. 12C; Ng and McLay 2005: fig. 4C); the median part of the outer surface of the chela is granular (Fig. 18E, F) (versus smooth in *D. danielae*, cf. Fig. 12D; Ng and McLay 2005: fig. 3A, B); and P2–P5 are all proportionately longer with the flexor margins of the meri not spinate (Figs 17A, 19A, 20A) (versus relatively shorter in *D. danielae* with the meri of P2 and P3 distinctly spinate, cf. Fig. 12E, F; Ng and McLay 2005: fig. 1A).

Discussion

Ng and Naruse (2007) discussed the value of the spine present on the extensor margin of P5 dactylus as a taxonomic character. They noted that it was sometimes present in *D. martini* (cf. comparative material examined above; Ng and Naruse 2007: fig. 3a, b) and was present on the holotype of *D. danielae* (cf. Ng and Naruse 2007: fig. 3c; Fig. 12F, G). In the specimens of *D. doederleini* examined, none of the P5 dactyli possess this spine (Fig. 3D, E). The presence and absence of this spine must therefore be used with caution. The setae on the P5 propodus are a mixture of setae and spines, but there are some setae which are intermediate in proportions, suggesting that the setae and spines are homologous structures, the "spines" on the distal edge and the outer surface of the P5 propodus, and "spines" on the flexor margin of the dactylus are almost certainly derived from the setae. They all have a clearly defined base and articulate with the cuticle. Normal spines and granules are part of the cuticle and there is no defined base. That being said, the extensor margin of the P5 dactylus in all the specimens of *D. doederleini* and *D. erinaceus* sp. nov. we examined are unarmed (Figs 3D, E, 15B, C). In the case of *D. karubar*, some of the P5 dactyli have spines while others do not (Figs 9G, 10D). For *D. robusta* sp. nov., the dactylar spine on the extensor margin is present in both specimens (but missing on the right leg in the holotype), and in addition, there is a prominent spine on the median outer surface of the P5 propodus which is always present (Fig. 21H, I). In *D. doederleini*, the P5 propodus has two or three spines on the outer surface (Fig. 3D, E); there are two spines in *D. martini*, with one or two spines in *D. karubar* (Fig. 9G), while in *D. erinaceus* sp. nov., the P5 propodus is unarmed (Fig. 15B, C).

The armature of the posterior margin of the epistome is a useful character but must be used carefully as well. In species like *D. danielae*, the margin is prominently spinose even when viewed frontally, with spines appearing more prominent when the margin is viewed subventrally (Fig. 12C). In *D. doederleini* and *D. karubar*, the posterior margin is almost entire or only weakly crenulate when viewed frontally or subventrally (Figs 2D, 8D, 9A). In *D. martini*, the margin appears almost entire in frontal view (Fig. 4E) but when viewed subventrally, it is weakly crenulated and uneven, as figured by Guinot (1995: fig. 20B). The structure of the proepistome, present in all the species examined, is relatively conservative, being separated from the epistome only by the lateral clefts, and for all the species, it is triangular in shape and slightly "sunken" into the distal margin of the epistome. In most species, the surface of the proepistome is covered with low granules and setae (Figs. 2E, 5A, 9A, 14D, 18D); but in *D. danielae*, the lateral parts have long spinules and the surface also has short spinules (Fig. 12C).

Guinot (1995: fig. 2C) noted that the actual rostrum of *Dicranodromia*, when visible, is present only as a small median tooth or spinule between the two pseudorostral teeth. It must be noted that this character is probably variable to some degree. In *D. martini*, there is no trace of a rostrum (Figs 4D, 6C). In *D. doederleini*, the rostrum is a distinct sharp granule (Fig. 2B; Guinot 1995: fig. 12B). When it is present as a spinule, the structure may be small, brittle and can easily be broken off. In one of the

paratype males of *D. erinaceus* sp. nov. (ZRC 2021.0085), the rostrum is composed of three small, slender spinules, which are very minute and delicate (Fig. 21B). The rostral spinules are not clearly visible on the large female specimens of *D. erinaceus* sp. nov. but it may simply have been lost. In *D. danielae*, there are three spinules (Fig. 12B). In *D. robusta* sp. nov., the rostrum is just a sharp but relatively low granule that is barely discernible (Figs 17C, D, 21C), as in the case of *D. karubar* (Fig. 8D). As such, this character should not be relied on to separate taxa.

In general, all species have spinules on some part of the carapace and these are often surrounded by stiff setae which partially obscure the spinules. Cleaning must be done with great care as the spinules (and even some of the spines) are brittle and break easily.

The structures of the G1 and G2 have not been used to separate species and Guinot (1995) only figured them for one American species (*D. maheuxii*). The G1 endopod is the main character and, while they all have a similar shape, the relative proportions differ and the subdistal part of the outer margin has two lobes of differing shapes and sizes. The G1 of the four species examined here show that there are differences between some taxa and can be used as a taxonomic character. The most distinctive is the G1 of *D. karubar*, in which the subdistal lobe on the outer margin of the endopod is curved and beak-like (Fig. 11D, E), distinct from the more rounded structure of its most similar species, *D. baffini*. The G1 endopods of *D. martini* and *D. karubar* (Fig. 11A, B, D, E) are also proportionately longer than those of *D. erinaceus* sp. nov. and *D. robusta* sp. nov. (Fig. 21K, L, N, O). In addition, the subdistal lobe on the outer margin of the G1 endopod in *D. robusta* (Fig. 21N, O) is distinctly more pronounced than either *D. martini* or *D. erinaceus* sp. nov. (Figs 11A, B, 21K, L). As such, G1 structures for *Dicranodromia* species should be described and figured as part of species descriptions.

Guinot (1995: 182) placed more emphasis on the structure of the spermathecal apertures and associated structures on thoracic sternites 7 and 8, pointing that there are clear differences between species. One of the characteristic features is that all the species have a pair of enlarged tubercles on each side of thoracic sternite 7 which are anterior or adjacent to the spermatheca. When viewed frontally, they appear as a pair of rounded or triangular tubercles (Figs 3G, 5H, 9J, 15E, 19F). In some species like *D. doederleini*, *D. martini*, *D. karubar* and *D. robusta* sp. nov., the two tubercles are separate (Figs 3G, 5H, 9J) but in *D. erinaceus* sp. nov., the two tubercles are connected by a clear ridge that bridges them (Fig. 15E). In *D. doederleini*, the tubercle is distinctively curved laterally outwards (Fig. 3G). In two species, *D. baffini* and *D. karubar*, the tubercle is distinctively comma-shaped, with the spermatheca positioned posteriorly to it (Fig. 9J). The suture between sternites 7 and 8, which joins the spermatheca is also differently structured. In most species, the suture is level with the rest of the sternal surface (Figs 3H, 5H, 9J, 19F). In most species, the spermatheca is posterior to the sternal tubercle (Figs 3H, 5H, 19F). In one species, *D. erinaceus* sp. nov., however, the suture is distinctly raised, on a prominent ridge and joins the spermatheca laterally (Fig. 15F).

The molecular analyses using COI sequences closely supported the morphological observations. There was some intraspecific divergence in the three individuals of *D. doederleini* tested (GenBank accession nos. OK351331-OK351333), ranging

from 0–1.2%, while that in two specimens of *D. erinaceus* sp. nov. (accession nos. OK351334-OK351335) was 0.2%. In *Dicranodromia*, the divergence at the species level was 9.6–14.0%, with *D. erinaceus* sp. nov. distinct from the tested species by 12.8–14.0%. The outgroup *H. kai* (accession no. OK351338) has a minimal divergence of 12.6–12.8% with *D. erinaceus* sp. nov., and a maximal value of 14.2% with *D. karubar*. The maximum likelihood tree also showed *D. erinaceus* sp. nov. to form an independent clade from other *Dicranodromia* species with an extremely high support (MLb = 100) (Fig. 22). The significance of this divergence will need to be re-appraised when more species of *Dicranodromia* (especially the American taxa) can be tested to see if the genus is monophyletic.

Noteworthy is that the Philippines has four species: *D. danielae*, *D. chenae*, *D. martini* and *D. robusta* sp. nov. Two of the species (*D. chenae* and *D. martini*) were collected by trawls, the substrate being more level and less rocky. Like *D. danielae*, *D. robusta* sp. nov. was collected by tangle nets set in deep-water, which may explain why it has not been collected until now. Deep-water habitats with steep rocky substrates are difficult to sample, and the fauna is often different from those occurring in flatter substrates (see Ng et al. 2009; Mendoza et al. 2010). Several other brachyuran taxa show the same pattern, notably in Majoidea (e.g., see Ng and Richer de Forges 2015; Richer de Forges and Ng 2008; Richer de Forges et al. 2021).

Acknowledgements

We thank T. Komai for his kind help with specimens. Paul Ng kindly passed us the specimen and shared the photographs of live *D. doederleini*. Thanks are due to Evelyn Antig (Palaone Trading) in the Philippines for help with and information on the two specimens from Mindanao. The SJADES cruise which obtained *D. karubar* was a joint Indonesian-Singapore expedition to southern Java funded by the National University of Singapore and the Research Center for Oceanography, Indonesian Institute of Sciences (LIPI), and supported by their respective Ministries of Foreign Affairs under the RISING 50 program to promote bilateral co-operation. We thank Bertrand Richer de Forges for his invaluable help with the cruise and trawling efforts, as well as Tin-Yam Chan and his team for their invaluable help in the trawling work and other support. We are also most grateful to Danièle Guinot, Tohru Naruse, and Shane Ahyong for their many suggestions which have improved the manuscript.

References

Ahyong ST (2008) Deepwater crabs from seamounts and chemosynthetic habitats off eastern New Zealand (Crustacea: Decapoda: Brachyura). Zootaxa 1708: 1–72. https://doi.org/10.11646/zootaxa.1708.1.1

Ahyong ST, Naruse T, Tan SH, Ng PKL (2009) Part II. Infraorder Brachyura: Sections Dromiacea, Raninoida, Cyclodorippoida. In: Chan T-Y, Ng PKL, Ahyong ST, Tan SH (Eds) Crustacean Fauna of Taiwan: Brachyuran Crabs, Volume I. Keelung, Taiwan, 27–180.

Alcock A (1899) An account of the Deep-Sea Brachyura collected by the Royal Indian marine survey ship INVESTIGATOR. Printed by order of the Trustees of the Indian Museum, Calcutta, 87 pp, pls 1-4. https://doi.org/10.5962/bhl.title.10330

Alcock A (1901) Catalogue of the Indian Decapod Crustacea in the collection of the Indian Museum. Part 1. Brachyura. Fasciculus 1. lntroduction and Dromides or Dromiacea (Brachyura Primigenia). Trustees of the Indian Museum, Calcutta. 1–80.

Alcock A, Anderson ARS (1899) Natural history notes from H. M. Royal Indian Marine Survey Ship 'Investigator,' Commander T. H. Heming, R. N., commanding. Series III, no. 2. An account of the deep-sea Crustacea dredged during the surveying-season of 1897-98. Annals and Magazine of Natural History (7) 3: 1–27. https://doi.org/10.1080/00222939908678071

Caustier E (1895) Sur le développement embryonnaire d'un Dromiacé du genre *Dicranodromia*. Comptus rendus Hebdomadaires des Séances de l'Académie des Sciences, Paris 120: 573–575.

Davie PJF, Guinot D, Ng PKL (2015) Anatomy and functional morphology of Brachyura. In: Castro P, Davie PJF, Guinot D, Schram FR, von Vaupel Klein JC (Eds) Treatise on Zoology – Anatomy, Taxonomy, Biology. The Crustacea (Vol. 9C–I): Decapoda: Brachyura (Part 1). Brill, Leiden, 11–163. https://doi.org/10.1163/9789004190832_004

Felsenstein J (1985) Confidence limits in phylogenies: an approach using the bootstrap. Evolution 39: 783–791. https://doi.org/10.1111/j.1558-5646.1985.tb00420.x

Folmer O, Black M, Hoeh W, Lutz R, Vrijenhoek R (1994) DNA primers for amplification of mitochondrial cytochrome c oxidase subunit I from diverse metazoan invertebrates. Molecular Marine Biology and Biotechnology 3: 294–299.

Gordon I (1950) Crustacea Dromiacea. Part I: Systematic account of the Dromiacea collected by the "John Murray" Expedition. Part II. The morphology of the spermatheca in certain Dromiacea. Scientific Reports of the John Murray Expedition 1933–34 9(3): 201–253, figs 1–26, pl. 1.

Guinot D (1993) Données nouvelles sur les crabes primitifs (Crustacea Decapoda Brachyura Podotremata). Comptes Rendus Hebdomadaires de Séances de l'Académie des Sciences, Paris 316 (10): 1225–1232.

Guinot D (1995) Crustacea Decapoda Brachyura: Révision de la famille des Homolodromiidae Alcock, 1900. In: Crosnier A (Ed) Résultats des Campagnes MUSORSTOM. Volume 13, Mémoires du Muséum national d'Histoire naturelle 163: 155–282.

Hall TA (1999) BioEdit: A user-friendly biological sequence alignment editor and analysis program for Windows 95/98/ NT. Nucleic Acids Symposium Series 41: 95–98.

Hebert PDN, Cywinska A, Ball SL, deWaard JR (2005) Biological identifications through DNA barcodes. Proceedings of the Royal Society of London B 270: 313–321. https://doi.org/10.1098/rspb.2002.2218

Ho P-H, Ng PKL, Chan T-Y, Lee D-A (2004) New records of 31 species of brachyuran crabs from the joint Taiwan-France Expeditions, "TAIWAN 2000" and "TAIWAN 2001", off deep waters in Taiwan. Crustaceana 77(6): 641–668. https://doi.org/10.1163/1568540041958617

Hosie AM, Hara A (2016) Description of a new species of brooding spider crab in the genus *Paranaxia* Rathbun, 1924 (Brachyura: Majoidea), from northern Australia and Indonesia. Zootaxa 4127(1): 121–134. https://doi.org/10.11646/zootaxa.4127.1.6

Ikeda H (1998) The deep-sea crabs of Sagami Bay. Hayama Shiosai Museum, Japan, 180 pp.

Kumar S, Stecher G, Tamura K (2016) MEGA7: Molecular evolutionary genetics analysis version 7.0 for bigger datasets. Molecular Biology and Evolution 33: 1870–1874. https://doi.org/10.1093/molbev/msw054

Martin JW (1991) Crabs of the family Homolodromiidae. III. First record of the larvae. Journal of Crustacean Biology 11(1): 156–161. https://doi.org/10.2307/1548553

Mendoza JCE, Naruse T, Tan SH, Chan T-Y, Richer De Forges B, Ng PKL (2010) Case studies on decapod crustaceans from the Philippines reveal deep, steep underwater slopes as prime habitats for 'rare' species. Biological Conservation 19: 575–586. https://doi.org/10.1007/s10531-009-9744-x

Mendoza JCE, Richer de Forges B, Safaruan MD, Ng PKL (2021) Checklist of the Brachyura (Crustacea: Decapoda) collected by the SJADES 2018 biodiversity cruise in the Sunda Strait and southwestern Java, Indonesia. Raffles Bulletin of Zoology, Supplement 36: 277–304.

Milne-Edwards A (1880) Etudes préliminaires sur les Crustacés, 1ère Partie. Reports on the Results of Dredging under the Supervision of Alexander Agassiz, in the Gulf of Mexico, and in the Caribbean Sea, 1877, '78, '79, by the U.S. Coast Survey Steamer "Blake", Lieut. Commander C. D. Sigsbee, U.S.N., and Commander J. R. Bartlett, U.S.N., Commanding, VIII. Bulletin of the Museum of Comparative Zoology, Harvard University 8(1): 1–68, pls 1, 2.

Morgan GJ (1987) Brooding of juveniles and observations on dispersal of young in the spider crab *Paranaxia serpulifera* (Guérin) (Decapoda, Brachyura, Majidae) from Western Australia. Records of the Western Australian Museum 13: 337–343.

Ng PKL, Guinot D, Davie PJF (2008) Systema Brachyurorum: Part I. An annotated checklist of extant brachyuran crabs of the world. Raffles Bulletin of Zoology, Supplement 17: 1–286.

Ng PKL, Ho P-H, Lin C-W, Yang C-H (2018) The first record of an eastern Pacific invasive crab in East Asian waters: *Amphithrax armatus* (Saussure, 1853) (Crustacea: Brachyura: Majoidea: Mithracidae) in Taiwan. Journal of Crustacean Biology 38(2): 198–205. https://doi.org/10.1093/jcbiol/rux109

Ng PKL, McLay CL (2005) *Dicranodromia danielae*, a new species of homolodromiid crab from the Philippines (Crustacea: Decapoda: Brachyura). Zootaxa 1029: 39–46. https://doi.org/10.11646/zootaxa.1029.1.3

Ng PKL, Mendoza JCE, Manuel-Santos M (2009) Tangle net fishing, an indigenous method used in Balicasag Island, central Philippines. Raffles Bulletin of Zoology, Supplement 20: 39–46.

Ng PKL, Naruse T (2007) On two species of deep sea homoloid crabs of the genus *Dicranodromia* (Crustacea: Decapoda: Brachyura: Homolodromiidae) from the Philippines, with description of a new species. Raffles Bulletin of Zoology, Supplement 16: 47–53.

Ng PKL, Richer de Forges B (2015) Revision of the spider crab genus *Maja* Lamarck, 1801 (Crustacea: Brachyura: Majoidea: Majidae), with descriptions of seven new genera and 17 new species from the Atlantic and Indo-West Pacific. Raffles Bulletin of Zoology 63: 110–225.

Ng PKL, Shih H-T, Ho P-H, Wang C-H (2017) An updated annotated checklist of brachyuran crabs from Taiwan (Crustacea: Decapoda). Journal of the National Taiwan Museum 70(3 & 4): 1–185.

Ortmann AE (1892) Die Abtheilungen Hippidea, Dromiidea und Oxystomata. Die Decapoden-Krebse des Strassburger Museums, mit besonderer Berücksichtigung der von Herrn Dr. Döderlein bei Japan und bei den Liu-Kiu-Inseln gesammelten und zur Zeit im Strassburger Museum aufbewahrten Formen. Theil V [= Part V]. Zoologische Jahrbücher, Abtheilung für Systematik Geographie und Biologie der Thiere 6(4): 532–588, pl. 26. https://doi.org/10.5962/bhl.part.26456

Padate VP, Amritha KM, Cubelio SS, Saravanane N, Sudhakar M, Ng PKL (2020) Deep-water Brachyura from the surveys of the FORV Sagar Sampada off the Andaman and Nicobar archipelagos, India. Regional Studies in Marine Science 35: e101117. https://doi.org/10.1016/j.rsma.2020.101117

Rathbun MJ (1914) Stalk-eyed crustaceans collected at the Monte Bello Islands. Proceedings of the Zoological Society of London 84(3): 653–664. https://doi.org/10.1111/j.1469-7998.1914.tb07055.x

Rathbun MJ (1924) Results of Dr. E. Mjöberg's Swedish scientific expeditions to Australia 1910–1913 37. Brachyura, Albuneidae and Porcellanidae. Arkiv för Zoologi 16: 1–33.

Richer de Forges B, Lee BY, Ng PKL (2021) Spider crabs from the SJADES 2018 biodiversity cruise in Indonesia, with descriptions of one new genus and five new species, including one from Western Australia (Crustacea: Brachyura: Majoidea). Raffles Bulletin of Zoology, Supplement 36: 211–257.

Richer de Forges B, Ng PKL (2008) New records of deep-sea spider crabs of the genus *Cyrtomaia* Miers, 1886, from the Pacific Ocean, with description of a new species (Crustacea: Decapoda: Brachyura: Majidae). Zootaxa 1861: 17–28. https://doi.org/10.11646/zootaxa.1861.1.2

Song H, Buhay JE, Whiting MF, Crandall KA (2008) Many species in one: DNA barcoding overestimates the number of species when nuclear mitochondrial pseudogenes are coamplified. Proceedings of the National Academy of Sciences of the United States of America 105: 13486–13491. https://doi.org/10.1073/pnas.0803076105

Stamatakis A (2006) RAxML-VI-HPC: maximum likelihood based phylogenetic analyses with thousands of taxa and mixed models. Bioinformatics 22: 2688–2690. https://doi.org/10.1093/bioinformatics/btl446

Tan LWH, Lim SSL, Ng PKL (1986) The complete larval development of the dromiid crab, *Cryptodromia pileifera* Alcock, 1899 (Decapoda: Dromiidae) in the laboratory. Journal of Crustacean Biology 6(1): 111–118. https://doi.org/10.2307/1547934

Tavares M, Lemaitre R (2014) New morphological and distributional information on Homolodromiidae and Homolidae (Decapoda: Brachyura) from the Americas, with description of a new species and comments on western Pacific species. Journal of Crustacean Biology 34(4): 504–524. https://doi.org/10.1163/1937240X-00002243

Wear RG (1967). Life history studies on New Zealand Brachyura 1. Embryonic and post embryonic development of *Pilumnus novaezealandiae* Filhol, 1886, and of *P. lumpinus* Bennett, 1964 (Xanthidae, Pilumninae). New Zealand Journal of Marine and Freshwater Research 1: 482–535. https://doi.org/10.1080/00288330.1967.9515221